



Oxidative degradation of organic contaminants using nanoscale zero-valent iron

Author:

Joo, Sung Hee

Publication Date:

2005

DOI:

<https://doi.org/10.26190/unsworks/8815>

License:

<https://creativecommons.org/licenses/by-nc-nd/3.0/au/>

Link to license to see what you are allowed to do with this resource.

Downloaded from <http://hdl.handle.net/1959.4/63410> in <https://unsworks.unsw.edu.au> on 2024-04-29

Oxidative Degradation of Organic Contaminants

Using Nanoscale Zero-Valent Iron

A thesis

Submitted in fulfillment of the requirements for the degree of

Doctor of Philosophy

at



The University of New South Wales

By

Sung Hee Joo

August 2004

Acknowledgements

I would like to express deeply my gratitude to my supervisor, Professor David Waite and co-supervisor, Dr. Andrew Feitz, for their guidance, support, valuable discussions, and insightful comments during my doctoral studies. Especially I wish to extend my appreciation to Professor David Sedlak for his invaluable suggestions, comments, scientific input, support, and encouragement.

I wish to thank Dr. Alice Lee who kindly provided me several pesticide ELISA kits with advice in ELISA analysis technique, Dr. Ervin Slansky for XRD analysis, and Professor Kennedy and his research group at the University of Sydney for their support on pesticide ELISA work.

During my Ph.D. studies, many people helped me and with my colleagues in our laboratory, I had a great time in studying and conducting research over the last three years. I especially wish to express my appreciation to Tredwell, Gautam, Hyungjin, Andrew R, Andrew B, San San, Jin, Olivier, Ervina, Jing, Shami, Nazli, Kaktien, Kate, Angelina, Christine, Sonya, and Iona for their support and friendship.

Funding support provided by the UNSW Faculty of Engineering with Supplementary Engineering Award as a Ph.D. research scholarship and other kinds of support from the Australian government funded Cooperative Research Center for Waste Management and Pollution Control through the project (03-6039) and Center for Water and Waste Technology is also greatly appreciated.

Finally, I would like to greatly acknowledge my parents and older sisters for their never-ending support, prayer, and love, which makes me stronger and gives a light to my life. This thesis is especially dedicated to my parents.

Thank you all!

Publications

The following is a list of papers arising from this Ph.D. thesis that have been published.

Journals and book

Sung Hee Joo; Andrew J Feitz; T David Waite (2004) Oxidative degradation of the carbothioate herbicide, molinate, using nanoscale zero-valent iron. *Environmental Science and Technology*, 38, pp. 2242-2247.

Sung Hee Joo; Andrew J Feitz; David L. Sedlak; T David Waite (2004) Quantification of the oxidizing ability of nanoparticulate zero-valent iron and assessment of possible environmental applications. *Environmental Science and Technology* (in press).

Andrew J Feitz; **Sung Hee Joo**; Jing Guan; David L. Sedlak; T David Waite (2004) Oxidative transformation of contaminants using colloidal zero-valent iron. *Journal of Colloid and Surfaces, A: Physicochemical and Engineering Aspects* (in press).

T David Waite; **Sung Hee Joo**; Andrew J Feitz; David L. Sedlak (2004) Oxidative transformation of contaminants using nanoscale zero-valent iron. In: *Chemical Water and Wastewater Treatment*, Hahn, Hermann H.; Hoffmann, Erhard; Ødegaard, Hallyard, eds., IWA Press, London.

Patent

Andrew J Feitz; T D Waite; **Sung Hee Joo**, "Method for Decontaminating Surfaces", Provisional patent application filed: 20th August 2003, Unisearch Ltd., Australia.

Conference papers

Sung Hee Joo; Andrew J Feitz; David L. Sedlak; T David Waite (2004) Reaction mechanism and yields for the oxidation of organic contaminants by nanoparticulate zero-valent iron in the presence of oxygen. *Preprints of Extended Abstracts* presented at the ACS National Meeting, American Chemical Society, Division of Environmental Chemistry, 44(2), 458-462, ISSN: 1524-6434.

Andrew J Feitz; **Sung Hee Joo**; David L. Sedlak; T David Waite (2004) Oxidative transformation of contaminants using colloidal zero-valent iron. *The Third International Conference "Interfaces Against Pollution"* under the auspices of IACIS, German Soil Science Society, German Colloid Society, RWTH Aachen, May 24-27, Jülich, Germany.

Sung Hee Joo; Andrew J Feitz; T David Waite (2004) Molinate degradation using nanoscale zero valent iron and its oxidative pathway. *Book of abstracts*, 227th American Chemical Society National Meeting, Anaheim California, USA, March 28 – April 1, AGRO-001. ISBN 0-8412-3924-X.

Sung Hee Joo; Andrew J Feitz; T David Waite (2003) Nanoscale zero-valent iron degradation of molinate and the role of the hydrogen peroxide intermediate. *Proc. 7th Annual Australian Environmental Engineering Research Event*, December 1-4; The Cumberland, Marysville, Victoria, Australia; CD-ROM; ISBN 0-9580158-2-1; EERE Organizing Committee. In *Environmental Sustainability Through Multidisciplinary Integration*, Mowlaei, M.J.; Rose, A.; Lamborn, J., eds., February, EERE, ISBN 0-9580158-3-X.

Jing G.; Simon L.; **Sung Hee Joo**; Andrew J Feitz; Gautam C. (2003) Application of solid-phase microextraction for chemical analysis in environmental engineering research. *Proc. of TechTrains2003 "Techniques and Procedures"*, July 3-4, UNSW, Sydney Australia.

Sung Hee Joo; Andrew J Feitz; T David Waite (2002) Agrochemical degradation using zero-valent iron. *Proc. of 6th Annual Australian Environmental Engineering Research Event*, December 3-6; Blackheath New South Wales Australia; CD-ROM; ISBN 0-9580158-1-3; EERE Organizing Committee.

Sung Hee Joo; Andrew J Feitz; T David Waite (2002) Agrochemical degradation using nano-scale zero valent iron, ZVI/H₂O₂, and Fenton's reagent. In: *Proc. of the Second International Conference on Oxidation and Reduction Technologies for In-Situ Treatment of Soil and Groundwater*, November 17-21, Toronto, Ontario, Canada.

Seminar and research report

(Seminar by) **Sung Hee Joo**, "Agrochemicals degradation using nano-sized zero valent iron particles", Department of Soil & Water, The Connecticut Agricultural Experiment Station, New Haven, Connecticut, USA, 11 Feb. 2003.

Andrew J Feitz; T David Waite; **Sung Hee Joo**; Jing Guan; Tapas Biswas (2002) Development of nano-sized zero valent iron particles for organic contaminant degradation. CRC WMPC report, Center for Water and Waste Technology, UNSW, Sydney, Australia.

UNSW media release/magazine publication

Media release on March 2, 2004, <http://www.unsw.edu.au>, entitled with "Researchers discover new treatment for pesticides"

UNIKEN (magazine published by Division of Institutional Advancement UNSW), April 2004/Issue 12 entitled with "An iron-clad weapon to break down pesticides"

Table of Contents

Acknowledgements	-----	ii
Publications	-----	iii
List of Figures	-----	x
List of Tables	-----	xvi
Abbreviations and Symbols	-----	xvii
Abstract	-----	xviii
Chapter 1. Introduction	-----	1
1.1. Objectives	-----	2
1.2. Outlines	-----	3
Chapter 2. Literature review	-----	5
2.1. Zero-valent iron (ZVI)	-----	5
2.1.1. Introduction	-----	5
2.1.2. Permeable reactive barrier (PRB) using granular ZVI	-----	8
2.1.3. PRB and ZVI colloids	-----	10
2.1.4. Use of ZVI, H ₂ O ₂ and complexants	-----	11
2.1.5. Nanosized ZVI	-----	13
2.2. Pesticides and contamination	-----	14
2.2.1. Introduction	-----	14
2.2.2. Characteristics of pesticides and their environmental effects	-----	16
2.2.3. Commonly used pesticides in Australia	-----	20
2.2.4. Pesticides treatment and management practices	-----	24
2.3. Summary	-----	31

Chapter 3. Nanoscale ZVI Particles Manufacture and	
Analytical Techniques	----- 33
3.1. Synthesized nano-scale zero-valent iron particles	----- 33
3.1.1. ZVI particle characterization	----- 34
3.2. Analytical techniques	----- 39
3.2.1. Solid-phase microextraction (SPME) GC/MSD	----- 39
3.2.1.1. SPME Process	----- 40
3.2.1.2. Extraction technique for hydrophobic compounds	----- 43
3.2.1.3. GC/MS analysis	----- 44
3.2.2. HPLC analysis of benzoic acid and p-hydroxybenzoic acid	----- 45
3.2.3. Measurement of ferrous iron concentrations	----- 46
3.2.4. Measurement of hydrogen peroxide (H ₂ O ₂) concentrations	----- 47
3.3. Procedures Used in nZVI-mediated Degradation Studies	----- 48
3.3.1. Molinate Degradation	----- 48
3.3.1.1. Reagents	----- 48
3.3.1.2. Experimental setup	----- 48
3.3.2. Benzoic Acid Degradation	----- 49
3.3.2.1. Reagents	----- 49
3.3.2.2. Experimental setup	----- 50
3.4. Determination of ZVI Surface Products by XRD	----- 51
3.4.1. Measurements in the Presence of Molinate	----- 52
3.4.2. Measurements in the Absence of Molinate	----- 52
Chapter 4. Oxidative degradation of the thiocarbamate	
herbicide, molinate, using nanoscale ZVI	----- 53
4.1. Introduction	----- 53
4.2. Results	----- 54
4.2.1. Effect of the Presence of Air/Oxygen	----- 54
4.2.2. Effect of Molinate and ZVI Concentration	----- 55
4.2.3. Effect of pH	----- 57
4.2.4. Ferrous Iron Generation	----- 60
4.2.4.1. Ferrous iron generation in pH ₀ 4 solution	----- 60
4.2.4.2. Effect of use of dried ZVI particles	----- 64

4.2.5. Effect of DO	-----	67
4.2.6. Hydrogen Peroxide Generation	-----	68
4.2.7. Catalase and butanol competition	-----	72
4.2.8. Degradation Byproducts	-----	74
4.3. Molinate degradation by combined ZVI and H₂O₂	-----	78
4.3.1. Effect of ZVI at fixed hydrogen peroxide concentration	-----	79
4.3.2. Effect of hydrogen peroxide at constant ZVI	-----	80
4.3.3. Degradation byproducts by combined ZVI and H ₂ O ₂	-----	82
4.3.4. Fe (II) generation from coupled ZVI/H ₂ O ₂		
in the presence of molinate	-----	84
4.3.4.1. Comparison of Fe(II) generation in the absence		
and presence of peroxide	-----	84
4.3.4.2. Fe ²⁺ release in the absence of molinate		
(online continuous measurement)	-----	85
4.4. Molinate degradation using Fenton's reagents	-----	86
4.4.1. Degradation byproducts of molinate using Fenton's reagents	-----	88
4.5. Comparison of ZVI, coupled ZVI/ H₂O₂		
and Fenton's process at high pH	-----	91
4.6. XRD and XPS analysis	-----	93
4.6.1. Results of X-ray diffraction (XRD) analysis	-----	93
4.6.1.1. Results of XRD analysis in the presence of molinate	-----	93
4.6.1.2. XRD results on ZVI particles		
in the absence of molinate	-----	94
4.6.2. X-ray photoelectron spectroscopy (XPS) result	-----	95
4.7. Discussion	-----	96
4.7.1. Evidence of oxidation pathway	-----	96
4.7.1.1. Keto-molinate byproducts	-----	96
4.7.1.2. Same byproducts for different oxidation process	-----	97
4.7.1.3. Effect of catalase	-----	99
4.7.1.4. Effect of SOD	-----	99
4.7.2. Reaction mechanism	-----	101
4.7.3. Kinetics of Fe(II) and H ₂ O ₂ generation	-----	103
4.7.4. Overview of the ZVI-mediated oxidative technology	-----	104
4.8. Conclusion	-----	105

Chapter 5. Quantification of the oxidizing capacity of nanoparticulate zero-valent iron and assessment of possible environmental applications	-----	107
5.1. Introduction	-----	107
5.2. Results	-----	108
5.2.1. p-Hydroxybenzoic acid (p-HBA) formation	-----	108
5.2.2. Cumulative hydroxyl radical formation over long-term	-----	110
5.2.3. Effect of Fe(II) as oxidant scavenger	-----	112
5.2.4. Effect of ZVI concentrations on oxidant yield	-----	114
5.2.5. Effect of pH	-----	115
5.2.6. Selectivity of oxidant	-----	116
5.2.7. Effect of ZVI type on oxidant yields	-----	123
5.2.8. Comparison study on standard Fenton oxidation of benzoic acid	-----	124
5.2.9. Effect of pure O ₂ on oxidant yield	-----	126
5.2.10. Discussion	-----	127
5.2.11. Conceptual kinetic modeling	-----	132
5.2.11.1. ZVI corrosion process	-----	132
5.2.11.2. Key reactions involved in the ZVI oxidation process	-----	134
5.2.12. Conclusion	-----	140
 Chapter 6. Conclusions and Future Research Needs	-----	142
6.1. Summary of results	-----	142
6.2. Possible applications of the ZVI-mediated oxidative process	-----	144
6.3. Overview of nZVI research and further research needs	-----	145
 Chapter 7. References	-----	148
 Appendix A: XRD analysis of ZVI collected from 4 different samples (in the presence of molinate)	-----	172

Appendix B: XRD analysis of ZVI collected from 4 different samples (in the absence of molinate)	-----	175
Appendix C: Enzyme –linked immunosolvent assays (ELISA) analysis methodology	-----	176
Appendix D: Oven programs for GC/MS analysis of pesticides	-----	180
Appendix E: Experimental conditions for pesticides and preliminary screening studies using nanoscale ZVI	-----	181

List of Figures

Figure 2.1a. Perchloroethylene (PCE) dechlorination.....	6
Figure 2.1b. A nanoscale bimetallic particles for chlorinated solvent removal.....	6
Figure 2.2. Typical configuration of a permeable reactive barrier (PRB), showing the source zone, plume of contamination, treatment zone, and plume of treated groundwater.....	9
Figure 2.3. Formation of chemically reactive barrier through coordinated use of injection and extraction wells.....	11
Figure 2.4. Schematic of in situ injection of nano-scale bimetallic particles.....	14
Figure 2.5. Chemical structure of compounds investigated in this research.....	18
Figure 3.1. Transmission Electron Microscope (TEM) images.....	35
Figure 3.2. ZVI identified by XRD analysis.....	36
Figure 3.3. Scanning Electron Microscope (SEM) images of freeze-dried ZVI aggregates manufactured using NaBH ₄	37
Figure 3.4. ZVI particle size distributions determined using the Malvern MasterSizerE.....	38
Figure 3.5. Zeta-potential of ZVI at different pH.....	39
Figure 3.6. A plot of extraction time vs. equilibrium for pesticides.....	43
Figure 3.7. Schematic of dissolved ferrous iron measurement.....	47
Figure 3.8. Schematic of total ferrous iron measurement.....	47
Figure 3.9. Typical system of GC/MS with solid-phase microextraction (SPME)....	49

Figure 4.1. Comparison of 100ppb molinate removal at pH ₀ 4, 10.7mM ZVI when sparging with N ₂ (◆), zero-grade air (●), 100% O ₂ (○) or shaking in the presence of air (□). Also shown is a control in which a ZVI-free solution containing 100ppb molinate is sparged with N ₂ (Δ).....	54
Figure 4.2. Molinate degradation in unbuffered solutions (pH _{initial} ≈ 6.4) for different ZVI concentrations and [Molinate] ₀ = 100ppb.....	55
Figure 4.3. Dependence of pseudo-first order rate constant (k) for molinate degradation on ZVI concentration (as quantified by total Fe ⁰ concentration) for initial molinate concentrations of 5 and 100ppb in unbuffered solutions (pH _{initial} ≈ 6.4).....	56
Figure 4.4. Ability of ZVI to maintain molinate degradation on continued addition of aliquots of molinate. Conditions: pH = 4, [ZVI] ₀ = 10.7 mM, addition of molinate at 0, 1, 3 and 5 hours resulted in increase in molinate concentration in reaction medium of 100ppb.....	57
Figure 4.5. Variation in pH and Eh on ZVI-mediated degradation of molinate in unbuffered solutions (pH ₀ 6.8, 1.8mM ZVI, 100ppb molinate).....	58
Figure 4.6. Comparison of molinate degradation at different starting pHs for [molinate] ₀ = 100 ppb and [ZVI] ₀ concentrations of 5.4 and 21.4mM	59
Figure 4.7. Molinate degradation in a 2mM bicarbonate buffered solution at various ZVI concentrations (100ppb molinate; pH ₀ 8.1).....	60
Figure 4.8. Dissolved ferrous iron concentrations in pH ₀ 4 solutions containing 0.89, 1.79 and 2.68 mM ZVI.....	61
Figure 4.9a. [Fe ²⁺] in the reaction mixture on addition of a ZVI solution and an equivalent volume of the ZVI supernatant. Conditions: pH ₀ = 4, [ZVI] ₀ = 1.8 mM.....	62
Figure 4.9b. [Fe ²⁺] in the reaction mixture after ZVI addition to a nitrogen-sparged suspension with subsequent air-sparging. Conditions: pH ₀ = 4, [ZVI] ₀ = 1.8 mM.....	63
Figure 4.10. Fe(II) generation on addition of colloidal ZVI to reaction medium in un-buffered solution (pH ₀ ~ 6.4).....	64

Figure 4.11. Fe(II) generation on addition of dried ZVI to reaction medium in un-buffered solutions ($pH_0 \sim 6.4$).....	65
Figure 4.12. Comparison of molinate degradation using ZVI concentrate and dried ZVI (100ppb molinate; $pH_0 \sim 6.4$).....	65
Figure 4.13. Dissolved Fe(II) generation from colloidal and dried ZVI at pH 8 in bicarbonate buffered system.....	67
Figure 4.14. DO variations during molinate degradation a. pH_0 4, b. pH_0 8.1.....	68
Figure 4.15. H_2O_2 generations on addition of various amounts of ZVI at pH_0 4 solutions (a) and pH_0 8 solutions (b).....	71
Figure 4.16. Instant (initial) generation of H_2O_2 as a function of ZVI at pH 4.....	71
Figure 4.17. Comparison of H_2O_2 concentrations in pH 4 (\circ) and pH 8.1 (\blacklozenge) solutions containing 1.79 mM ZVI; Possible H_2O_2 concentrations resulting from addition of stock solution is given for pH 4 (\triangle) and pH 8.1 (\bullet).....	72
Figure 4.18. Effect of ZVI-mediated degradation of molinate of 60ppm catalase. Conditions: $[Molinate]_0 = 100ppb$ and $[ZVI]_0 = 10.7mM$	73
Figure 4.19. Effect on ZVI-mediated degradation of molinate; 5mM 1-butanol. Conditions: $[Molinate]_0 = 100ppb$ and $[ZVI]_0 = 10.7mM$, butanol study undertaken at pH_0 4.....	73
Figure 4.20. GC/MSD-EI (TIC) obtained from ZVI extracted after the reaction time of 3.25hrs.....	75
Figure 4.21. Mass fragments for each peak on keto-molinate and molinate.....	77
Figure 4.22. The effect of ZVI dose at fixed hydrogen peroxide. Condition: unbuffered ($pH_0 \sim 6.4$), 5ppb molinate.....	80
Figure 4.23. The effect of peroxide at constant ZVI: Molinate (100ppb) degradation in the presence of Fe^0 and H_2O_2 ($pH_0 = 6.4 \pm 0.3$).....	81
Figure 4.24. (A). Disappearance of molinate and production of by-product by ZVI/ H_2O_2 (B) molinate degradation by ZVI (19.6mM) and coupled ZVI (19.6mM) and H_2O_2 (20mM).....	83

Figure 4.25. Molinate degradation and the formation of byproducts by ZVI/H ₂ O ₂	84
Figure 4.26. Dissolved Fe(II) variations during molinate degradation by H ₂ O ₂ /ZVI in pure water (pH ₀ ~ 6.4), molinate 100ppb.....	85
Figure 4.27. Fe ²⁺ release from ZVI in presence of H ₂ O ₂ (pH ₀ ~ 6.4).....	86
Figure 4.28. Degradation kinetics using Fenton's reagent under different pH for the removal of molinate (100ppb); A: pH ₀ = 6.4 ± 0.3, B: pH 4... 87	87
Figure 4.29. MS of the peak appeared in Fenton process at 17.6min (A) and 18.9min (B).....	89
Figure 4.30. Molinate and its byproducts after 3.25hrs by dark Fenton process (0.11mM Fe ²⁺ /20mM H ₂ O ₂).....	90
Figure 4.31. Molinate and its byproducts after 15min by dark Fenton process: Increased Fe ²⁺ (0.66mM) with 20mM H ₂ O ₂	90
Figure 4.32. Bicarbonate effect (pH 8) on the degradation of molinate (100ppb) by Fenton (A), H ₂ O ₂ /ZVI (B), and ZVI (C).....	93
Figure 4.33. GC Chromatogram: Disappeared keto-molinate peaks in the absence of oxygen.....	98
Figure 4.34. GC Chromatogram: Disappeared keto-molinate peaks in the presence of Catalase/O ₂	99
Figure 4.35. GC Chromatogram: keto-molinate peaks appeared in the presence of SOD/O ₂	100
Figure 4.36. Effect of presence/absence of oxygen and presence/absence of superoxide dismutase (SOD). Note: 5μg/mL of SOD was added over 2.75 hrs.....	100
Figure 4.37. MS fragments for molinate and keto-molinate isomers and proposed oxidation pathway.....	102
Figure 5.1. p-hydroxybenzoic acid (p-HBA) formation over time in pH 3 suspension and 30mM ionic strength containing 10mM benzoic acid (A) and p-HBA formation after two hours as a function of benzoic acid concentration (B).....	110

Figure 5.2. ▲ pH 3 ♦ pH 5 ■ pH 8, Cumulative hydroxyl radical formation and p-HBA concentration over time at pH 3,5 and 8. (Condition: 0.9mM Fe ⁰ , 30mM ionic strength and 10mM BA).....	112
Figure 5.3. Oxidant formation as a function of BA concentration and predicted oxidant formation in the absence and presence of Fe(II) scavenging OH radicals (Conditions: 0.9mM Fe ⁰ , pH 3, 30mM ionic strength, reaction time 2 hours). Solid and dashed lines show calculated [p-HBA] assuming competitive hydroxyl radical scavenging by 0.2 and 5mM Fe(II) respectively.....	113
Figure 5.4. Total Fe(II) in solution over time as a function of BA concentration at pH 3 and ionic strength of 0.03M.....	113
Figure 5.5. p-hydroxybenzoic acid formation as a function of ZVI concentration. Conditions. pH 3 solutions, 30 mM ionic strength, reaction time 1 hr and [benzoic acid] ₀ = 50μM in (A) and [benzoic acid] ₀ = 10 mM in (B).....	114
Figure 5.6. Effect of increase in mass of nZVI used on concentration of principal oxidised products (p-HBA). (Condition: 10mM BA, 30mM ionic strength, pH 3, reaction time 1hour).....	115
Figure 5.7. pH dependence of the formation of p-HBA. Conditions: pH 3, 0.9mM ZVI, ionic strength 30 mM and reaction time 1hr.....	116
Figure 5.8. Fraction (F) of p-HBA produced in the presence of a certain concentration of aniline to that produced in the absence of aniline (i.e. in the presence of BA only) with a) nZVI used as the oxidant source, and b) Fenton reagent used as the oxidant source.....	119
Figure 5.9. Fraction (F) of p-HBA produced in the presence of a certain concentration of phenol to that produced in the absence of phenol (i.e. in the presence of BA only) with a) nZVI used as the oxidant source, and b) Fenton reagent used as the oxidant source.....	120
Figure 5.10. Fraction (F) of p-HBA produced in the presence of a certain concentration of o-HBA to that produced in the absence of o-HBA (i.e. in the presence of BA only) with a) nZVI used as the oxidant source, and b) Fenton reagent used as the oxidant source.....	121
Figure 5.11. Fraction (F) of p-HBA produced in the presence of a certain concentration of humic acid to that produced in the absence of humic acid (i.e. in the presence of BA only) with a) nZVI used as the oxidant source, and b) Fenton reagent used as the oxidant source.....	122

Figure 5.12. Concentration of p-HBA produced after one hour reaction of commercial granular Fe, ZVI powders, and synthesized nZVI with benzoic acid. Conditions: pH 3, 0.9 mM Fe ⁰ , ionic strength 30 mM, 10 mM BA, reaction time 1 hour.....	123
Figure 5.13. BA oxidation by Fenton's reagents (A) and ZVI (0.9mM) (B) at pH 3.....	125
Figure 5.14. Oxidant formation in Fenton oxidation system.....	126
Figure 5.15. Kinetics of oxidant formation in nZVI system under O ₂ and air sparging. Condition: 10mM BA, 0.9mM ZVI, pH 3, 30mM ionic strength.....	127

List of Tables

Table 2.1. Chemical and physical properties of commonly used pesticides in Australia and banned pesticides still routinely found in contaminated soils.....	17
Table 2.2. Example of highly contaminated irrigation channel water.....	19
Table 2.3. Summary on the extent of degradation for pesticides by ZVI.....	30
Table 3.1. Properties of various ZVI particles.....	35
Table 4.1. Interpretation of mass fragments of molinate and molinate degradation product (keto-molinate isomers).....	78
Table 4.2. XRD results from four different samples.....	95
Table 4.3. XPS results (in the presence of molinate) and atomic concentration [AT]%	96
Table 4.4. GC-MS-EI retention times (RT) and spectral characteristics of molinate identified byproducts in both ZVI, ZVI/H ₂ O ₂ , and Standard Fenton processes.....	98
Table 5.1. Rate constants for reaction of probe molecules with hydroxyl radicals generated at pH 3 using both nZVI and Fenton reagent relative to that of benzoic acid ($k_{C/BA}$). Literature values for reaction of benzoic acid and probe compounds (C) with hydroxyl radicals are also shown.....	117
Table 5.2. Characteristics of ZVI particles used in this study.....	124
Table 5.3. Model reactions and rate constants (example of compound: benzoic acid).....	139

Abbreviations and Symbols

ZVI	Zero Valent Iron
PRB	Permeable Reactive Barrier
SPME	Solid-Phase MicroExtraction
GC	Gas Chromatography
MS	Mass Spectrometer
HPLC	High Performance Liquid Chromatography
ELISA	Enzyme Linked Immuno Sorbent Assays
SOD	Superoxide Dismutase
SEM	Scanning Electron Microscope
TEM	Transmission Electron Microscope
XRD	X-Ray Diffraction
XPS	X-ray Photoelectron Spectroscopy

Abstract

This thesis describes the results of studies into the degradation of organic contaminants by nanosized particulate zero valent iron (nZVI). Molinate (a thiocarbamate herbicide) was chosen for detailed investigation because of its particular susceptibility to degradation by nZVI and found to be degraded by an oxidative pathway. Both ferrous iron and superoxide (or, at pH < 4.8, hydroperoxy) radicals appear to be generated on corrosion of the ZVI with resultant production of strongly oxidizing entities capable of degrading the trace contaminant. Fenton oxidation and oxidative by-products were observed during nZVI-mediated degradation of molinate under aerobic conditions. To assess the potential application of nZVI for oxidative transformation of organic contaminants, the conversion of benzoic acid (BA) to *p*-hydroxybenzoic acid (p-HBA) was used as a probe reaction. When nZVI was added to BA-containing water, an initial pulse of p-HBA was detected during the first 30 minutes, followed by the slow generation of additional p-HBA over periods of at least 24 hours. The yield of p-HBA increased with increasing BA concentration, presumably due to the increasing ability of BA to compete with alternate oxidant sinks, such as ferrous iron. At pH 3, maximum yields of p-HBA during the initial phase of the reaction of up to 25% were observed. The initial rate of nZVI-mediated oxidation of BA exhibited a marked reduction at pH values above 3. Despite the decrease in oxidant production rate, p-HBA was observed during the initial reaction phase at pH values up to 8. Competition experiments with probe compounds expected to exhibit different affinities for the nZVI surface (phenol, aniline, *o*-hydroxybenzoic acid and synthetic humic acids) indicated relative rates of reaction that were similar to those observed in competition experiments in which hydroxyl radicals were generated in solution. The ZVI-mediated oxidation may be useful for in situ applications of nZVI particles and may also provide a means of oxidizing organic contaminants in granular ZVI-containing permeable reactive barriers.

Chapter 1: Introduction

Organic compounds such as herbicides, pesticides and insecticides are of considerable concern with respect to contamination of waters and sediments in the environment and, where inappropriate deposition has occurred, must be removed or degraded. One of the most interesting, and potentially least costly, methods for their degradation involves the use of elemental iron (Fe(0)). While Fe(0) or zero valent iron (ZVI) has been used principally to degrade contaminants in subsurface environments by placing ZVI barriers across the groundwater flowpath, the possibility also exists of using particulate ZVI which could be either pumped into a contaminated aquifer or dispersed through contaminated sediments. There have been suggestions recently that use of nanosized ZVI (denoted here as nZVI) could render such an approach particularly attractive due to the high degradation rates that might ensue. Given that many agrochemicals are strongly hydrophobic, use of nanosized ZVI could also facilitate degradation of contaminants sorbed to natural particulate matter.

While the use of nZVI appears attractive, many questions remain concerning the mode of degradation of dissolved or sorbed contaminants, the effect of solution and surface conditions and the overall viability of the method. The purpose of the research work reported in this thesis is the resolution (at least in part) of some of these issues.

1.1 Objectives

The first objective of the work reported here is the examination of the suitability of nanoscale zero-valent iron (ZVI) to degradation of organic contaminants for the purpose of development of a cost-effective treatment technology. A focus of the work reported here is on the degradation of agrochemicals, which are widely used worldwide and yet for which low cost treatment methods are scarce.

A second objective of this study is the identification of by-products produced from the ZVI-mediated degradation process of particular contaminants. Any process which generates byproducts that are potentially more harmful than the starting material is clearly of limited value. Additionally, identification of any byproducts formed may provide insight into the reaction mechanism and suggest approaches by which the technology can be further refined.

The third objective is to clarify the reaction mechanism by which ZVI degrades a chosen contaminant. As noted above, identification of specific byproducts may assist in elucidating mechanism. Other methods, including use of specific probe molecules, examination of the degradation process under varying reaction conditions and measurement of any reactive transient involved in the degradation process may assist in this task.

The fourth objective is to assess how the ZVI-based technology may be applied in complex, natural systems and to assess limitations to implementation and possible avenues for further research which might improve the viability of the process.

1.2 Outlines

A review of literature relevant to the subject area (zero-valent iron, pesticides contamination and treatment, management practices) is presented in Chapter 2. Firstly, the degradation of organic compounds by granular zero-valent iron (ZVI) in permeable reactive barriers (PRBs), by ZVI colloids and by nanosized ZVI is described. Secondly, chemical characteristics and environmental impacts of pesticides are described and common treatment techniques (e.g., incineration, photochemical processes, bioremediation.) presented and compared with the ZVI technology. Thirdly, preliminary results of screening studies used to assess the applicability of nanoscale ZVI for treatment of organochlorine insecticides, herbicides, and organophosphate insecticides are presented.

In Chapter 3, materials and analytical techniques that were used in the experimental program are described. In particular, the method for synthesizing nanoscale ZVI particles is presented as are the techniques used to characterize the material produced. The methods used to quantify both the starting material as well as organic and inorganic intermediates and products are also outlined including Solid-Phase MicroExtraction (SPME) GC/MS, High-Performance Liquid Chromatography (HPLC), and colorimetric methods for Fe(II) and H₂O₂ analysis.

Results of screening studies showed that the thiocarbamate herbicide S-ethyl perhydroazepin-1-carbothioate commonly known as molinate is particularly susceptible to degradation by ZVI. This compound is widely used in rice growing areas of New South

Wales, Australia and represents a significant water quality problem. In light of these factors, detailed studies of the degradation of molinate by nanosized ZVI have been undertaken and results are presented in Chapter 4. The results of these studies suggest that molinate is degraded by ZVI via an oxidative process if oxygen is present. The effect of oxygen, pH, and the effect of systems conditions on generation of key intermediates (ferrous iron and hydrogen peroxide) are reported in this chapter.

The mode of oxidative degradation of organic compounds by nZVI is investigated in more detail in Chapter 5 where results of studies into the degradation of benzoic acid by nZVI are reported. Quantification of the oxidative capacity of the technique under specific system conditions is provided in this chapter as is the importance (or lack thereof) of heterogeneous versus homogeneous processes.

In Chapter 6, the experimental results reported in the previous chapters are summarized and conclusions of this research presented. Further research needs are described as are the possibilities for application of nanosized zero valent iron-based technologies.

Chapter 2. Literature Review

2.1. Zero-valent iron

2.1.1. Introduction

Zero-valence state metals (such as Fe^0 , Zn^0 , Sn^0 , and Al^0) are surprisingly effective agents for the remediation of contaminated groundwaters (Powell *et al.*, 1995; Warren *et al.*, 1995). Zero-valent iron (ZVI or Fe^0) in particular has been the subject of numerous studies over the last 10 years. ZVI is effective for the reduction of a diverse range of contaminants including dechlorination of chlorinated solvents in contaminated groundwater (Matheson and Tratnyek, 1994; Powell *et al.*, 1995), reduction of nitrate to atmosphere N_2 (Rahman and Agrawal, 1997; Chew and Zhang, 1999; Choe *et al.*, 2000), immobilization of numerous inorganic cations and anions (Powell *et al.*, 1995; Puls *et al.*, 1999; Pratt *et al.*, 1997; Su and Puls, 2001; Morrison *et al.*, 2002; Lackovic *et al.*, 2000; Charlet *et al.*, 1998), reduction of metallic elements (Morrison *et al.*, 2002), and the reduction of aromatic azo dye compounds (Nam and Tratnyek, 2000; Cao *et al.*, 1999) and, other organics such as pentachlorophenol (Kim and Carraway, 2000) and haloacetic acids (Hozalski *et al.*, 2001). ZVI is the preferred and most widely used zero-valent metal because it is readily available, inexpensive, and nontoxic (Liang *et al.*, 2000; Gillham and O'Hannesin, 1994). The reduction process in ZVI systems is an abiotic redox reaction where the metal serves as an electron donor for the reduction of oxidized species. Under anaerobic conditions, and in the absence of any competitors, iron can slowly reduce water resulting in the formation of hydrogen gas (Tratnyek *et al.*, 2003), i.e.



Other reactants, even if present at trace concentrations, may also be reduced by iron.

For example, the overall surface-controlled hydrogenolysis of alkyl chlorides (R-Cl) by Fe⁰ is likely to occur as follows (Kaplan *et al.*, 1996; Matheson and Tratnyek, 1994; Tratnyek *et al.*, 2003):

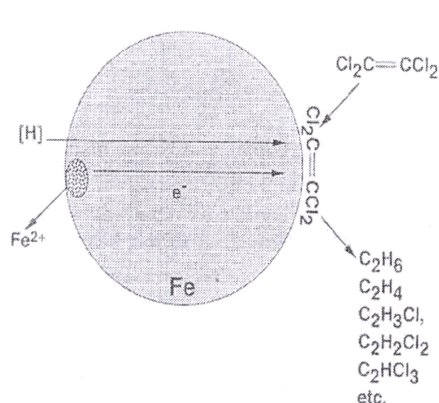


Figure 2.1a. Perchloroethylene dechlorination. (Zhang *et al.*, 1998)

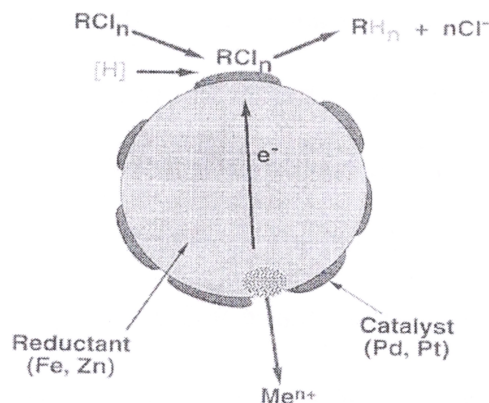


Figure 2.1b. A nanoscale bimetallic particles for chlorinated solvent removal. (Zhang *et al.*, 1998)

A schematic of the reduction of tetrachloroethylene is given in Figure 2.1a and 2.1b. Figure 2.1a shows perchloroethylene (PCE) reacting on the surface of ZVI (Zhang *et al.*, 1998), where ZVI is oxidized to Fe(II) while PCE is dechlorinated. Figure 2.1b gives an example of the reaction of a chlorinated organic with a bimetallic particle. In this system one metal (Fe, Zn) serves primarily as electron donor while the other (Pd, Pt) serves as a catalyst (Zhang *et al.*, 1998). Electrochemical effects, catalytic hydrogenation, or intercalation of H₂ are considered to be responsible for the enhanced reactivity of these bimetallic systems (Tratnyek *et al.*, 2003).

Boronina *et al.* (1995) studied organohalides removal using metal particles such as magnesium, tin, and zinc and observed that the ability of Zn and Sn particles to decompose the chlorocarbons depends on the quantity of metal and its surface properties and increased in the order: Sn (mossy) < Sn (granular) < Sn (cryo-particles) < Zn (dust) < Zn (cryo-particles).

The destruction of pesticides using ZVI is also possible. The reductive dechlorination of alachlor and metolachlor (Eykholt and Davenport, 1998) and reductive dechlorination and dealkylation of s-triazine (Ghauch and Suptil, 2000) was observed in laboratory studies. Ghauch (2001) even found rapid removal of some pesticides (benomyl, picloram, and dicamba) under aerobic conditions (8ppm DO) ($\tau_{1/2}$ of a few minutes) and proposed that degradation continued via the dechlorination and dealkylation pathways. The disappearance of carbaryl under phosphate buffer in deionized non-deoxygenated water (pH 6.6) was also observed by Ghauch *et al.* (2001). In an earlier study, Sayles *et al.* (1997) demonstrated the dechlorination of the highly recalcitrant pesticides DDT, DDD, DDE using ZVI under anaerobic conditions at pH₀ of 7.

ZVI may be used to treat higher contaminant loads that are resistant to biodegradation (Bell *et al.*, 2003) as the technology is not susceptible to inhibition that microorganism sometimes encounter with chlorinated compounds. Even polyhalogenated pollutants can be destroyed via reductive dehalogenation using ZVI in contrast to many advanced oxidation processes (AOPs) such as H₂O₂+UV, Fenton, photolysis, O₃, O₃+UV (Pera-Titus *et al.*, 2004), UV, UV/H₂O₂, Photo-Fenton (Al Momani *et al.*, 2004).

The presence of oxygen is generally assumed to lower the efficiency of the reduction process as a result of competition with the target contaminants, e.g. organics or metals with the reduction of oxygen by ZVI generally envisaged as a four-electron step with water as the major product:



Additionally, further oxidation of Fe^{2+} to Fe(III) species is likely with subsequent precipitation of particulate iron oxyhydroxides which may coat the Fe^0 surface and lower reaction rate. Consistent with such an effect, Tratnyek *et al.* (1995) found that the half-time for dechlorination of 180 μM carbon tetrachloride by 16.7 g/L of 325 mesh Fe^0 granules increased from 3.5 hr when reaction mixtures were purged with nitrogen to 111 hr when purged with oxygen. Surprisingly, Tratnyek *et al.* (1995) observed a higher rate of degradation of CCl_4 in an air-purged system ($\tau_{1/2} = 48$ min) than in the nitrogen purged case ($\tau_{1/2} = 3.5$ hr). It would thus appear that the impact of oxygen in ZVI-mediated degradation of organic compounds is worthy of further investigation.

2.1.2. Permeable reactive barrier (PRB) using granular zero-valent iron

Permeable chemical barriers (PRBs) are an emerging alternative technology to traditional pump and treat systems for the *in-situ* remediation of groundwater. Reactive materials are chosen for their ability to remain sufficiently reactive for periods of years to decades (Benner *et al.*, 1997). The field evidence provided by O'Hannesin and Gillham (1998) indicates that granular iron could serve as an effective medium for the *in situ* treatment of chlorinated organic compounds in groundwater. The iron was placed in the ground as a permeable reactive barrier (Figure 2.2); other configurations place the iron within the

reaction cells of funnel and gate systems, around the exterior of a pumped well or at treatment points in an impermeable encasement around hazardous waste (Reeter, 1997).

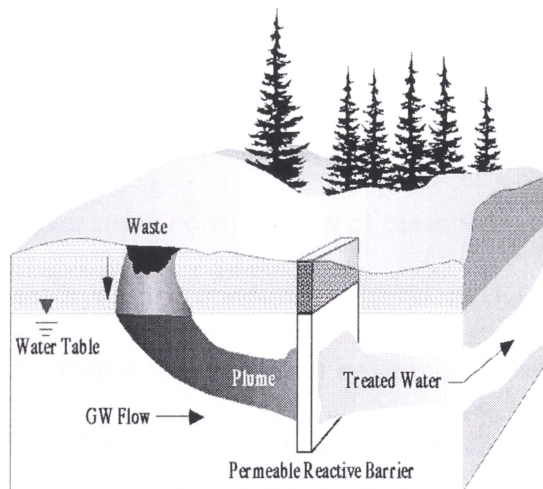


Figure 2.2. Typical configuration of a permeable reactive barrier (PRB), showing the source zone, plume of contamination, treatment zone, and plume of treated groundwater (Powell *et al.*, 1998).

The most common methods of installation include constructing a trench across the contaminated groundwater flow path by using either a funnel-and-gate system or a continuous reactive barrier (NFESC, 2004). The gate or reactive cell portion is typically filled with granular zero-valent iron. Several methods for emplacing PRBs include trench and fill, injection or grouting (USDEGJO, 1989).

There are many advantages of using passive reactive barriers compared to existing ex-situ treatment technologies. PRBs require no external energy source and it is possible that iron fillings may last for 10 to 20 years before requiring maintenance or replacement (NFESC, 2004). Studies have shown that iron barriers are more cost-effective than pump-and-treat systems (USDEGJO, 1989). For instance, although the installation for PRB requires a

higher initial capital investment, operating and maintenance (O&M) costs are significantly lower, provided that the PRB does not show an unexpected breakdown before costs are recovered (Birke *et al.*, 2003; Powell *et al.*, 2002). While the advantages of ZVI barriers are compelling, the long term problems are not well understood and may include chemical and/or biological precipitate formation at the barrier, changes in contaminant removal efficiency over time, consumption of dissolved oxygen, higher pH, and modification to the groundwater hydraulic conductivity (USDEGJO, 1989). The life-time of PRBs using Fe⁰ as a reactive media is expected to be primarily limited by precipitation at the barrier (Liang *et al.*, 2003). There are also concerns regarding the maintenance, life-time and costs of this technology (Felsot *et al.*, 2003). Nevertheless, PRBs have the potential to gain broad acceptance that is still lacking (Birke *et al.*, 2003).

2.1.3. PRB and ZVI colloids

Another approach to the installation of passive reactive barriers involves injection of ZVI colloids into porous media (e.g., the subsurface environment). In such systems, colloidal barriers are placed in the subsurface environment, perpendicular to groundwater flow, and selectively remove targeted groundwater contaminants as water and other non-targeted constituents pass through the barrier as shown in the Figure 2.3 (Kaplan *et al.*, 1996). As illustrated in the figure, the movement of colloidal ZVI can be controlled to some extent by injecting the colloids in one well and withdrawing groundwater from a nearby second well, thereby drawing colloids in the desired direction.

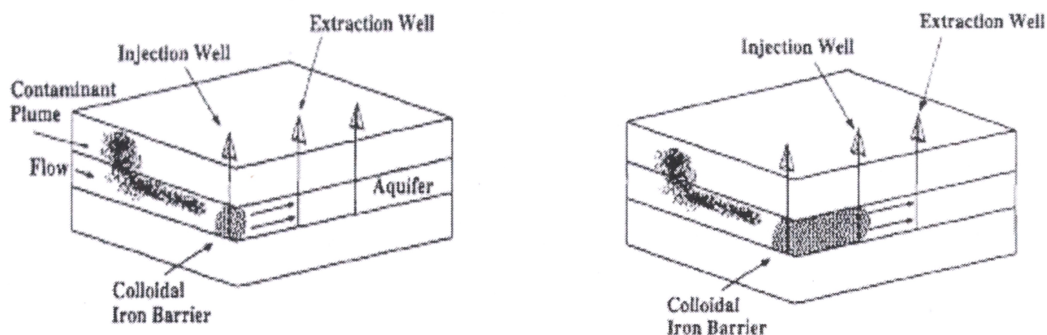


Figure 2.3. Formation of chemically reactive barrier through coordinated use of injection and extraction wells (Cantrell and Kaplan, 1997).

The effectiveness of the chemical barrier depends on the distribution and uniformity of the colloidal ZVI injection and the longevity of the ZVI materials. Cantrell and Kaplan (1997) observed in column experiments that as the injection rate was increased, the Fe^0 concentration became more uniform. They predicted that the life span of the barrier would be 32 years based on groundwater flow rate, effective porosity, and barrier thickness. The reported advantages of colloidal barriers are that there are no requirements for above-ground treatment facilities, installation is relatively simple, capital costs are moderate and there are no additional waste disposal requirements. However, for long-term performance, the total mass of reactive material, rate of reaction within the barrier and physical changes such as decreases in porosity and permeability may limit the life-time of the barrier. Performance will also depend on the nature of contaminants, groundwater flux, subsurface geology, and chemistry (Kamolpornwijit *et al.*, 2003).

2.1.4. Use of ZVI, H_2O_2 and complexants

There are several reports of using a combination of ZVI and peroxide/complexants to promote remediation of water and soil highly contaminated with organics. Hundal *et al.*

(1997) showed that ZVI combined with H_2O_2 destroyed 2,4,6-trinitrotoluene (TNT) and hexahydro-1,3,5-trinitro-1,3,5-triazine (RDX) in contaminated soil slurries more efficiently than ZVI alone. Less iron was required to achieve the same level of remediation. For example, sequential treatment of a TNT-contaminated solution (70mg TNT/L spiked with ^{14}C -TNT) with ZVI (5% w/v) followed by H_2O_2 (1% v/v) completely destroyed TNT and removed about 94% of the ^{14}C from solution, 48% of which was mineralized to $^{14}CO_2$ within 8h. It was shown that adding ethylenediaminetetraacetic acid (EDTA) or glucose to a Fe(0)-amended TNT solution resulted in 6% mineralization, while only 0.5% mineralization of untreated TNT was observed. Similar improvements were observed by Noradoun *et al.* (2003), who demonstrated the complete destruction of 4-chlorophenol and pentachlorophenol in the presence of Fe(0) and EDTA.

The feasibility of Fenton's oxidation of MTBE using zero-valent iron as the source of catalytic ferrous iron was assessed in a study by Bergendahl and Thies (2004). Over 99% of methyl *tert*-butyl ether (MTBE)-contaminated water was removed at pHs 4 and 7 using a H_2O_2 :MTBE molar ratio of 220:1. Similarly, Lücking *et al.* (1998) investigated the oxidation of 4-chlorophenol in aqueous solution by hydrogen peroxide in the presence of a variety of additional substrates including iron powder. H_2O_2 oxidation of 4-chlorophenol in the presence of iron powder proceeded much faster when iron powder was used instead of graphite or activated carbon, presumably via Fenton's oxidation of the 4-chlorophenol. Studies by Tang and Chen (1996) showed the degradation of azo dyes was faster using the H_2O_2 /iron powder system than the Fenton's reagent system, e.g., H_2O_2 /Fe(II). The difference was attributed to the continuous dissolution of Fe(II) from the iron powder and the dye adsorption on the powder.

Another system using peroxide involves the combination of hydrogen peroxide and electrochemically-amended iron, which has been found to successfully degrade the two organophosphorous insecticides, malathion and methyl parathion (Roe and Lemley, 1997). In this system, Fe(II) is generated electrochemically at the Fe(0) electrode while H₂O₂ can either be added from an external source or can be generated by reduction of oxygen at a mercury or graphite. It appears that the addition of H₂O₂ in these studies initiates the Fenton reaction and results in oxidation of organic contaminants. Hundal *et al.* (1997) notes that the Fe(0)-treated contaminants could be more susceptible to biological mineralization than would otherwise be the case.

2.1.5. Nanosized ZVI

Zhang and coworkers (1998) at Lehigh University investigated the application of nanosized (1 to 100nm) ZVI particles for the removal of organic contaminants and found that not only is the reactivity higher due to an elevated surface area (average of 33.5m²/g for the nanosized particles compared to 0.9m²/g for the commonly used microscaled particles) but the reaction rate was also significantly higher (by up to 100 times) on a surface area normalized basis. In one such system, 1.7kg of nanosized ZVI particles were fed into a 14m³ groundwater plume over a 2-day period as illustrated in Figure 2.4 (Elliot and Zhang, 2001). Despite the low particle dosage, trichloroethylene reduction efficiencies of up to 96% were observed over a 4-week monitoring period with the highest values observed at the injection well and at adjacent piezometers in the well field. The critical factors that influence degradation kinetics appear to be the ZVI condition and available surface area (Chen *et al.*, 2001; Choe *et al.*, 2000).

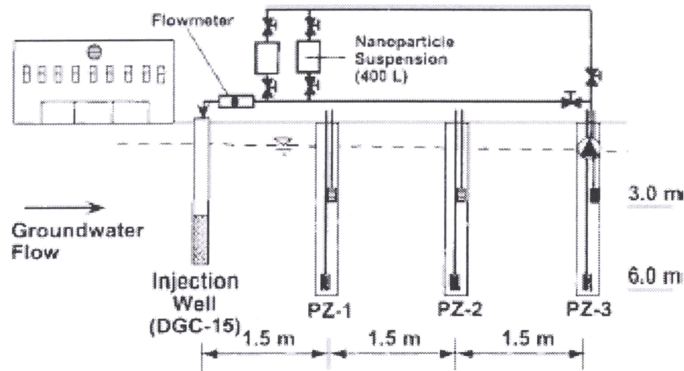


Figure 2.4 Schematic of in situ injection of nano-scale bimetallic particles (Elliott and Zhang, 2001).

Nanoparticles may provide an effective, flexible, and portable remedial technique for suitable groundwater contaminants such as chlorinated hydrocarbons (Elliott and Zhang, 2001). Other possibilities include remediation of on-farm irrigation channels or dams (for pesticide contamination) or remediation of contaminated sites where surface application with subsequent infiltration would appear feasible (Feitz *et al.*, 2002). The particles could also be attached to activated carbon, zeolite or silica with the added advantage of the adsorptive removal of polycyclic aromatic hydrocarbons (PAHs) and other highly persistent contaminants such as chlorinated hydrocarbons (CHCs) (Birke *et al.*, 2003).

2.2. Pesticides and contamination

2.2.1. Introduction

Pesticides are used extensively in agricultural production throughout the world to protect plants against pests, fungi, and weeds. For example, world pesticide usage exceeded 5.6 billion pounds and expenditures totalled more than \$US 33.5 billion in 1998 and 1999

(Donaldson *et al.*, 2002). Pesticide usage during grain production is particularly high, and in the grain belt of south-west Western Australia, central and southern Queensland and north-east New South Wales, total expenditure on crop chemicals was estimated at over \$50,000 in 1998-99. In contrast, the expenditure in the rest of the mixed farming regions ranges from \$5,000 to \$30,000 (Australia State of Environment, 2001).

The Indian pesticides industry is the largest in Asia and twelfth largest in the world with a value of US \$0.6 billion, which is 1.6% of the global market (IPISMIS, 2001; Mindbranch, 2001). The continuous growth of the pesticide industry in India has contributed to the worsening problems of air, water, and soil pollution in this country (Mall *et al.*, 2003). China is also a large producer and consumer of pesticides (Qui *et al.*, 2004). From 1949 on, the consumption of pesticides in China increased rapidly from 1920 tons in 1952 to 537,000 tons in 1980, and then decreased to 271,000 tons in 1989 after the manufacture of organic chlorinated pesticides ceased at the beginning of 1980s (Li and Zhang, 1999).

In Australia, cotton production has been particularly successful and is currently worth approximately \$1.5 billion per year (Raupach *et al.*, 2001). The substantial growth in the cotton industry, however, has resulted in environmental contamination. For example, in the irrigated cotton region of central and northern New South Wales, the presence of several pesticides has been detected in rivers near and downstream of cotton-growing areas during the growing season (Raupach *et al.*, 2001). In particular, spot-sampled riverine concentrations of the insecticide endosulfan were found to range from 0.02 to 0.2 ppb, which significantly exceeds environmental guidelines for protection of ecosystems

(currently 0.01 ppb; Australian and New Zealand Environment and Conservation Council, 1992).

The extensive use of pesticides affects the wider ecology and there are links with birth defects in birds and fish (Nowell *et al.*, 1999; Oliver, 1985; Ferraro *et al.*, 1991; McKim, 1994). High deposition of pesticides in sediment can inhibit the microbial activity in the sediment (Redshaw, 1995) and certain pesticides such as α -BHC, γ -BHC, isodrine, dieldrin and *p-p'*-DDT accumulate in fish (Amaraneni, 2002). Pesticides also have cumulative effects on the human body and lead to several diseases, ranging from chronic common cough and cold to bronchitis and cancer of the skin, eye, kidney and prostate gland (Paldy *et al.*, 1988; Gupta and Salunkhe, 1985).

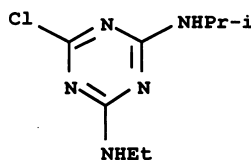
2.2.2. Characteristics of pesticides and their environmental effects

The recalcitrance of a pesticide is largely determined by its chemical structure. Some herbicides (such as 2,4-D) are susceptible to environmental degradation while others (including most chlorinated insecticides such as endosulfan, heptachlor and dieldrin) are considerably more resistant. Solubility will not only affect transport, but also pesticide degradation since degradation is believed to occur mainly in the solution phase. The characteristics and structures of pesticides investigated in this research are presented as shown in the Table 2.1 and Figure 2.5. Ionizability, water solubility, volatility, soil retention, and longevity are key properties.

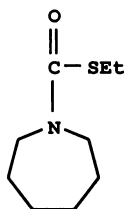
Table 2.1. Chemical and physical properties of commonly used pesticides in Australia and banned pesticides still routinely found in contaminated soils (Hartley and Kidd, 1983).

Compound	Formula (molecular weight)	T _{1/2} (days)	Solubility in water (mg/L)	Log octanol/water partition coefficient	Vapor pressure (mbar)
Atrazine	C ₈ H ₁₄ ClN ₅ (216)	60 ^a	33	2.7	4×10 ⁻⁷ (20 °C)
Aldrin	C ₁₂ H ₈ Cl ₆ (365)	>30, <100 ^b	< 0.05	5.11	3×10 ⁻⁵ (20°C)
Dieldrin	C ₁₂ H ₈ Cl ₆ O (381)	1460-2555 ^c	< 0.1	3.7 - 6.2	10 ⁻⁶ (20 °C)
Diuron	C ₉ H ₁₀ Cl ₂ N ₂ O (233)	90 ^a	42	2.8	4×10 ⁻⁶ (50 °C)
Molinate	C ₉ H ₁₇ NOS (187)	21 ^a	880	2.9	7×10 ⁻³ (25 °C)
Chlorpyrifos	C ₈ H ₁₁ Cl ₃ NO ₃ PS (351)	30 ^a	2	5.0	2×10 ⁻⁵ (25 °C)
Heptachlor	C ₁₀ H ₅ Cl ₇ (373)	>30, <100 ^b	0.056	5.44	4×10 ⁻⁴ (25 °C)
Chlordane	C ₁₀ H ₆ Cl ₈ (410)	>100 ^b	0.056	2.78	1×10 ⁻⁵ (25 °C)
Diazinon	C ₁₂ H ₂₁ N ₂ O ₃ PS (304)	40 ^a	40	3.3	2×10 ⁻⁴ (20 °C)
Endosulfan	C ₉ H ₆ Cl ₆ O ₃ S (407)	50 ^a	0.32	N/A	1×10 ⁻² (80 °C)

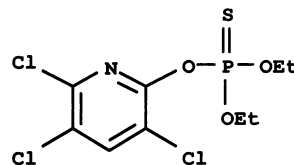
^a adapted from Weber (1994), ^b PMEP (2003), ^c WHO (1989)



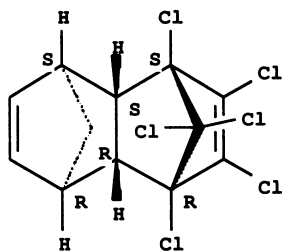
Atrazine



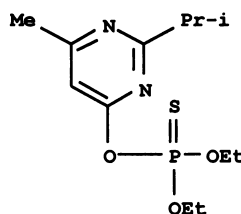
Molinate



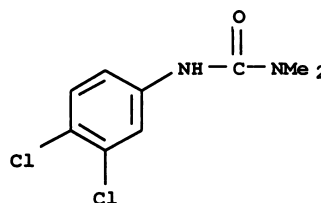
Chlorpyrifos



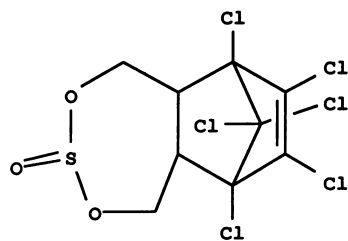
Aldrin



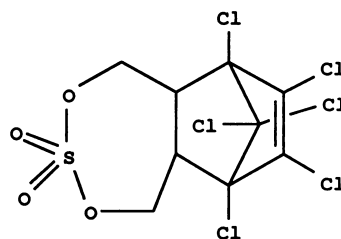
Diazinon



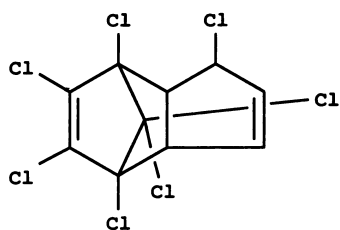
Diuron



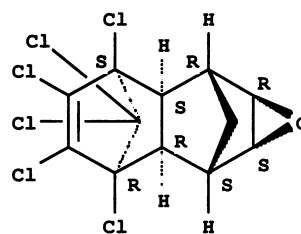
Endosulfan



Endosulfan sulfate



Heptachlor



Dieldrin

Figure 2.5. Chemical structure of compounds investigated in this research.

Pesticides are widely distributed in drinking waters, groundwaters and soils. There are various routes for pesticide contamination in the environment including runoff from agricultural land, direct entry from spray, industrial effluents and dust. Pesticide contamination of soils, water and other matrices may also be caused by accidental spills during manufacture, formulation and shipment, or at local agrochemical dealerships. Although many current pesticides are designed to break down quickly in sunlight or in soil, they are more likely to persist if they reach groundwater because of reduced microbial activity, absence of light and lower temperatures in the sub-surface zone (National Center for Toxic and Persistent Substances, 1995).

Residues of pesticides have significant environmental impacts on aquatic ecosystems and mammals. For example, in the drainage and irrigation canals in southern New South Wales, high concentrations of pesticides (e.g., molinate) have been regularly detected (Australia State of Environment, 2001). Such pesticides (particularly endosulfan) have been linked to large fish kills in several rivers throughout Australia. Freshwater crustaceans are particularly at risk (Australia State of Environment, 2001). Besides the detrimental effect on natural ecosystems, there are negative economic and social impacts associated with agrochemical contamination of both irrigation networks and the wider aquatic environment. There are instances where it is simply not possible to hold water or where uncontrolled releases result in a severe reduction in the quality of irrigation waters as shown in the Table 2.2. A major economic concern of elevated pesticide levels in irrigation channels is that the water may contain pesticides that are incompatible and harm crops for users downstream of uncontrolled releases. For example, atrazine used by citrus and sorghum growers is toxic to soybeans.

Table 2.2. Example of highly contaminated irrigation channel water.
(Data courtesy of CSIRO Land and Water, 2001).

Pesticides	Concentration found in irrigation channel ($\mu\text{g/L}$)	EPA Limit ($\mu\text{g/L}$)		Toxicity ratings (Q value)
		Notification	Action	
Chlorpyrifos	25	0.001	0.005	9520
Endosulfan	0.58	0.05	0.1	4700
Molinate	30	12.5	25	12
Malathion	30	0.07	0.35	340
Diuron	700	8	40	9
Atrazine	79	2	10	3

Current best practice requires landholders to hold discharge water until the levels of pesticides and herbicides meet the prescribed limits through natural photolysis or biodegradation. However, this can place severe restrictions on farm operation since the water must be held within the drainage network on the farm until concentrations have fallen below the regulated levels. In such cases, an inexpensive but highly effective treatment technology which could remove the pesticides before they are released and thus prevent detrimental downstream effects would be useful.

2.2.3. Commonly used pesticides in Australia

Organochlorine insecticides

Organochlorine insecticides are compounds that are highly lipid soluble and toxic. The organochlorine insecticides endosulfan, aldrin, and their metabolites, are often detected in natural environment (Guerin *et al.*, 1992; Hung and Thiemann, 2002; Smith and Gangoll, 2002; Matin *et al.*, 1998). Exposure to these compounds has resulted in the death of freshwater species (Naqvi and Vaishnavi, 1993; Mishra and Shukla, 1997) and bioaccumulation in organisms, which may produce adverse effects on ecosystems (Hutson and Roberts, 1990). Of the organochlorine insecticides, endosulfan is the most widely used in Australia, the USA, and elsewhere and has been used widely in cotton farming in Australia (Brooks *et al.*, 1996). The cotton industry is very much dependent on three pesticide groups (endosulfan; synthetic pyrethroids; and certain organophosphates and carbamates) to prevent damage by *Heliothis* species (Brooks *et al.*, 1996). Endosulfan, which is hydrophobic, and a highly toxic and hazardous pesticide, has been the dominant

insecticide detected in agricultural areas (natural waterways in these regions) of the central north west of NSW (Brooks *et al.*, 1996).

Aldrin and dieldrin, which is aldrin epoxide, are quickly adsorbed on soils where they remain for years. Due to their high persistence and toxicity, the use of aldrin and dieldrin, which were used in soil treatment after harvest (grape vines, bananas) (INCHEM, 1989) and for termite controls (Stevenson *et al.*, 1999), was banned in 1995. They are still detected in the environment, however, because of their persistence and previous wide use as insecticides for the control of pests on crops such as corn and cotton. Aldrin and dieldrin are structurally similar synthetic compounds, highly toxic and hazardous for humans (e.g., toxic by mouth, skin contact, inhalation of dust), aquatic and terrestrial life. Aldrin is readily converted to dieldrin under normal environmental conditions (Ramamoorthy, 1997) and, as a result, dieldrin residues in soil are higher than aldrin. Dieldrin is one of the most persistent of the chlorinated hydrocarbons, and is highly resistant to biodegradation (UNEP, 1989). Abiotic processes play a limited role in the degradation of aldrin and dieldrin in the environment (WHO, 1989).

Heptachlor and chlordane, the use of which has now been banned, were used in termite control and ants (ATSDR, 1992, 1993), as well as pest control on cotton crops (ATSDR, 1990). Heptachlor was used primarily as an insecticide in seed grains and on crops during the 1960s and 1970s before it was banned in 1995. The microbial and photochemical transformation products, heptachlor epoxide and photoheptachlor remain in soil for long periods of time (>15 years) and are equally or more toxic than the parent compound (Ramamoorthy, 1997). Heptachlor is fairly stable to light and moisture and it is not readily

dehydrochlorinated. Its half-life in the soil in temperate regions ranges between $\frac{3}{4}$ - 2 years. It is not likely to penetrate into groundwater but contamination of surface water and sludge can occur (WHO, 1989). Chlordane is another toxic organochlorine pesticide that was used routinely from 1948 to 1988. Chlordane is not a single compound, but a mixture of about ten major compounds (Ramamoorthy, 1997), and is highly persistent in the environment (see Table 2.1).

Herbicides

Atrazine is one of the most widely used herbicides in the US, Europe and Australia and is still used for control of annual broadleaf weeds and certain annual grasses, particularly in corn production (KDARFC, 2004). Atrazine is the most commonly detected pesticide in the river systems in Australia (Harris and Kennedy, 1996). Atrazine is moderately soluble and, because of its persistence in water and mobility in soil, is among the most frequently detected pesticide in groundwater (Ghauch and Suptil, 2000).

Diuron is a widely used herbicide, because of its ability to inhibit photosynthesis (Mazellier *et al.*, 1997). Diuron is also used for control of a wide variety of annual and perennial broadleaf and grassy weeds and is used on many agricultural crops such as fruit, cotton, sugar cane, alfalfa, and wheat (Gooddy *et al.*, 2002; Råberg *et al.*, 2003; Macounová *et al.*, 2003). Diuron is stable in neutral media at normal temperatures, but is hydrolyzed by acids and alkalis and at elevated temperatures (diuron decomposes at 180-190°C). The degradation of diuron through chemical (hydrolysis) or biological processes is very slow at

neutral pH. Because of its chemical stability and moderate solubility, diuron is often detected in surface waters and groundwaters (Mazellier and Sulzberger, 2001).

Molinate is one of five thiocarbamate herbicides; a class of compounds that possess low volatility and are slowly degraded by hydrolysis over a period of months (WHO, 1988). Molinate is a moderately toxic herbicide used extensively worldwide in the rice industry for the control of germinating broad-leaved and grass weeds, particularly *Echinochloa spp.* (Hsieh *et al.*, 1998). Molinate is only weakly bound to soils, is soluble in water, mobile and presents a significant contamination risk to groundwaters.

Organophosphorus insecticides

Chlorpyrifos is an organophosphorus pesticide which is widely used in the home to control cockroaches, fleas, termites, and in some pet flea and tick collars. Chlorpyrifos is also used on grain, cotton, field, nut, vegetable crops (Cochran *et al.*, 1995), and on the farm, as a dip or spray to control ticks on cattle, and as dust or spray to control pests in crops such as rice, fruit, vineyards, sugar-cane, corn, tobacco, potatoes, and other horticultural crops (Ramamoorthy, 1997; WHO, 1998). Typical field dissipation half-lives at the soil-surface is 1 to 2 weeks and, for soil incorporated applications (when applied to high organic matter soil), 4 to 8 weeks. The half-life of chlorpyrifos in water is relatively short, from a few days to two weeks (US EPA, 2000).

Diazinon is another organophosphorus insecticide with a wide range of insecticidal activity. Diazinon has been widely used with applications in agriculture and horticulture for

controlling insects in crops, lawns, fruit and vegetables and as a pesticide in domestic, agricultural and public building (NRA, 2000; Worthing and Hance, 1991). It is stable in neutral media, but slowly hydrolyses in alkaline media and more rapidly in acid media. In natural water diazinon has a half-life of the order of 5-15 days (WHO, 1998).

2.2.4. Pesticides treatment and management practices

Pesticides play a critical role in worldwide agriculture, but uncontrolled releases are a major environmental concern. Remediation of soil and water contaminated with pesticides range from conventional treatment techniques (e.g. incineration, thermal desorption, soil flushing/washing, bioremediation, land-farming, phytoremediation, photochemical processes, and direct oxidative processes) to innovative remediation technologies such as ultrasound-promoted remediation and other advanced oxidation technologies. The properties of pesticides in soil and water strongly influences disposal options, as does treatment costs, public health, and technical feasibility. The major techniques for the remediation of contaminated soils, surface waters, and groundwaters are described in more detail below.

Incineration & thermal desorption: Treatment by incineration reduces the volume and destroys toxic materials in contaminated soils that may otherwise remain for hundreds of years. Incineration affects treatment of a contaminated soil through two mechanisms: desorption, which removes the pesticide from the soil and liberates it to the gas phase; and combustion, which destroys the target compound (Steverson, 1998). Most pesticides are thermally fragile and therefore amenable to incineration. Thermal desorption is the most widely used treatment for cleaning up contaminated soil from large-scale sites (Troxler,

1998). Pesticide removal efficiencies from soil are greater than 99% for most pesticides using a typical thermal desorption system (Troxler, 1998). Both techniques, however, are expensive options for soil remediation and generally lack public acceptance because of the health concerns of nearby residents.

Soil flushing/washing: Soil flushing and washing are processes that employ water, co-solvents, surfactants or supercritical fluids to remove organic contaminants from soils.

Supercritical Fluid Extraction (SFE) using carbon dioxide alone, or in combination with a modifier, has been shown to be an effective extraction method for pesticides in several matrices although the cost was estimated as about twice the cost of incineration (Rock *et al.*, 1998). Pesticides commonly degraded by SFE are 2,4-D (Rochette *et al.*, 1993), and organochlorine pesticides (Nerín *et al.*, 2002; Barnabas *et al.*, 1994).

Phytoremediation and bioremediation: Phytoremediation, which uses plants to clean up contaminated environments such as soil, water or sediments, is potentially more cost effective and less environmentally disruptive than conventional *ex situ* remediation technologies (Schnoor *et al.*, 1995; Wenzel *et al.*, 1999). Nevertheless, recalcitrant halogenated organic chemicals such as DDT, dieldrin, and PCBs are bound tightly to the soil and have low water solubility, resulting in very little of the residue being taken up into plants. Bioremediation is an uncontrolled process that can be stimulated with selective nutrients or fortified by bio-augmentation and involves inoculating sites lacking the appropriate strain(s) with non-indigenous pesticide-degrading microorganisms (Van Veen *et al.*, 1997).

The feasibility of bioremediation depends on the specific contaminant, and its suitability as a substrate for microbial degradation. The planned future use of the site is also an important consideration (Arthur and Coats, 1998). Detailed site characterization and preliminary feasibility studies are required for the design and optimization of any biostimulation approach. Remediation also depends on the site-specific nature of each contaminated matrix (Zablotowicz *et al.*, 1998). A bio-active soil barrier technique, known as the FILTER technique, which combines the use of contaminated water with filtration through the soil to a subsurface drainage has been found to reduce pesticide loads up to 99% (Jayawardane *et al.*, 2001). However, field studies have shown that the concentration of pesticides in the discharge, particularly mobile ones such as molinate, are often found above accepted environmental limits (Biswas *et al.*, 2000).

Land-farming: Land farming involves mixing or dispersing wastes into the upper zone of the soil-plant system with the objective of microbial stabilization, adsorption, immobilization, selective dispersion or crop recovery. Land farming is an older, proven bioremediation technology that can be applied to pesticide waste. Land farming is commercially applied for the remediation of pesticide waste at agrochemical retail facilities under special state permits (Andrews Environmental Engineering, 1994).

Advanced Oxidation Processes:

Advanced oxidation processes (AOPs) appear suited to the treatment of pesticide-containing waste. Indeed, many hundreds of laboratory studies have shown that pesticides may be oxidized using AOPs such as UV/H₂O₂, photocatalysis, ozonation and Fenton-based processes. The efficiency of the oxidation process however is a function of the type

and nature of the waste and the structural properties of the pesticides (Larson and Weber, 1994).

AOPs are based on hydroxyl radical generation and subsequent oxidation of the organic substrate. The efficiency of AOPs strongly depends on operating parameters such as pH, initial pesticide concentration, solubility and light intensity for photochemical processes. For example, the degradation rate of a pollutant in the UV/H₂O₂ system is affected by the H₂O₂ concentration, UV light intensity and, to a lesser extent, by solution pH. As one of modifications of Fenton's reagent, Sun and Pignatello (1992) observed complete mineralization of phenoxyacetic herbicides in a Fe³⁺/H₂O₂ system where reaction rate is depended on the concentrations of H₂O₂, chelators, and pH. However, in practice, oxidation has been limited to waste containing low organic matter as other constituents can act as radical scavengers and lower the effectiveness toward trace contaminant degradation.

Photochemical AOPs often induce rapid degradation through homogeneous (e.g., UV-H₂O₂ (Muszkat, 1998), Fe³⁺/UV) or heterogeneous processes (e.g., TiO₂/UV, ZnO/UV) (Legrini *et al.*, 1993). Although photochemical AOPs have definite advantages over other AOP methods, further development of more active, less costly photocatalysts and increase in the efficiency of sunlight/UV lamp utilization is required before widespread adoption of the technology is likely.

Ozonation processes and chemical oxidation processes appear to be especially suitable for industrial applications. The degradation products formed during AOPs of hydrophobic pesticides are often more polar and more bioavailable than the parent compounds.

Complete mineralization can often be enhanced by coupling AOPs to biodegradation (Chiron *et al.*, 2000).

High power ultrasound can promote both oxidation and reduction through the formation of OH^\bullet radicals (powerful oxidizing agents) and H^\bullet radicals (effective reducing agents) during the thermal dissociation of water ($\text{H}_2\text{O} \rightarrow \text{H}^\bullet + \text{OH}^\bullet$). This process is one of the most intriguing and least obvious advanced treatment methods for chemical wastes. However, practical application of sonochemistry to chemical waste treatment has proven challenging and limited its application. For example, the energy efficiency and economics of sonochemical treatment need to be better defined and practical production-scale reactors need to be developed (Sivakumar and Gedanken, 2004). The design of reactors and maintenance of treatment efficiency under practical conditions are likely to be difficult. Also, the fundamental physical and chemical processes occurring in sonochemical treatment remain less well defined than for most other advanced treatment processes (Rock *et al.*, 1998).

Zero-valent metal remediation:

Initial screening studies using nanoscale zero-valent iron particles found that cyclodiene insecticides (e.g., chlordane, heptachlor, aldrin, dieldrin, endosulfan sulfate, α , β -endosulfan) are generally very resistant to degradation by ZVI (Table 2.3). The hydrophobic nature of organic pollutants, particularly halogenated organic compounds, seems to limit the efficient electron transfer due to their immiscibility with water.

While ZVI was not effective in degrading endosulfan, it did prove effective for other pesticide and herbicides. These include compounds containing nitrogen heteroatoms such as atrazine, molinate, chlorpyrifos and to a limited extent, diazinon and diuron (Table 2.3). Chemicals with seemingly similar structures reacted differently. This is especially true for aldrin and dieldrin where the chemical structure is quite similar but the extent of degradation is significantly different. A similar, although less pronounced, effect was observed for α - and β -endosulfan compared to endosulfan sulfate.

Agrawal and Tratnyek (1996) observed that nitro-substituted entities were reduced by ZVI significantly faster than dechlorination. Some researchers have noted that the treatment of strongly surface-active organic chemicals such as PCBs, dioxin, DDT, toxaphene, mirex, lindane, hexachlorobenzene may not be practicable using ZVI (Weber, 1996). The results of the screening study undertaken here suggest that molinate is particularly well suited to ZVI-mediated degradation. Molinate is an indicator chemical used by the New South Wales EPA for flagging likely pesticide contamination in irrigation channels. Molinate is highly soluble and has an environmental half-life of 21 days (Hartley and Kidd, 1983). It is one of the most heavily used herbicides in Australia and routinely detected in waterways in Australia (Australia State of Environment, 2001). Because molinate undergoes slow hydrolysis, it may also leach into and persist in groundwaters. Additional details of the screening studies into degradation of different pesticides and herbicides using nanoscale ZVI are given in Appendix E.

Table 2.3. Summary on the extent of degradation for pesticides by ZVI.

Compound	Chemical formula	Condition	Initial concentration ($\mu\text{g/L}$)	Total reaction time (hrs)	Fe^0 (mM)	pH	Analysis technique	Percent removal
Atrazine	$\text{C}_8\text{H}_{14}\text{ClN}_5$	Anaerobic	1000	7	36	6.8 ¹	GC/MS	84
Aldrin	$\text{C}_{12}\text{H}_8\text{Cl}_6$	Aerobic	20(10)	6(29)	5.4 (8.9)	6.8	ELISA	50(70)
Dieldrin	$\text{C}_{12}\text{H}_8\text{Cl}_6\text{O}$	Aerobic	10	5	8.9	6.8	ELISA	0
Diuron	$\text{C}_9\text{H}_{10}\text{Cl}_2\text{N}_2\text{O}$	Aerobic	100	5	18	6.8	ELISA	12
Molinate	$\text{C}_9\text{H}_{17}\text{NOS}$	Aerobic	100	3	11	NB ²	GC/MS	>99
Chlorpyrifos	$\text{C}_8\text{H}_{11}\text{Cl}_3\text{NO}_3\text{PS}$	Aerobic	10	0.25	25	NB	ELISA	98
Heptachlor	$\text{C}_{10}\text{H}_5\text{Cl}_7$	Aerobic	10	5	8.9	6.8	ELISA	0
Chlordane	$\text{C}_{10}\text{H}_6\text{Cl}_8$	Aerobic	10	5	8.9	6.8	ELISA	0
Diazinon	$\text{C}_{12}\text{H}_{21}\text{N}_2\text{O}_3\text{PS}$	Aerobic	0.1	3	11	NB	ELISA	27
Endosulfan sulfate	$\text{C}_9\text{H}_6\text{Cl}_6\text{O}_4\text{S}$	Aerobic	10	27	8.9	6.8	ELISA	25
α -endosulfan	$\text{C}_9\text{H}_6\text{Cl}_6\text{O}_3\text{S}$	Aerobic	10	5	8.9	6.8	ELISA	0
β -endosulfan	$\text{C}_9\text{H}_6\text{Cl}_6\text{O}_3\text{S}$	Aerobic	10	5	8.9	6.8	ELISA	0

¹ pH 6.8 set using a 0.02M phosphate buffer; ² pH not buffered in these cases due to interference

2.3. Summary

Fe^0 has been reported to be very effective for the reduction of various organic and inorganic contaminants. Granular ZVI incorporated into permeable reactive barriers (PRBs) has proven to be a cost-effective in-situ remediation method for groundwaters contaminated with chlorinated organics and appears to be a particularly promising alternative technology to traditional pump and treat systems. Nanosized ZVI has a greater reactivity than granular ZVI and its application is more versatile. Rather than building large trenches and installing iron walls, initial field trials have shown that nanosized ZVI can be injected directly into the groundwater plume. This minimizes installation costs, which are a major cost component of ZVI PRBs. Little is known about the long-term performance of these nanoparticle/colloidal systems however with particular uncertainty surrounding the effect of formation of passivating ferric oxide layers on the outer iron surface.

Pesticides contamination of surface waters, groundwaters and soils due to their extensive application in agriculture is a growing worldwide concern. Pesticides affect aquatic ecosystems as well as accumulate in the human body. Approaches to the treatment of pesticide contaminated soils and waters ranges from conventional methods such as incineration, phytoremediation and photochemical processes to innovative methods such as ultrasound-promoted remediation and other advanced oxidation processes. Recent studies have shown that many pesticides are susceptible to degradation using ZVI. Preliminary studies in this work on the susceptibility of pesticide degradation using nZVI found that several compounds such as atrazine, molinate, and chlorpyrifos were effectively degraded. Cyclodiene insecticides such as endosulfan, however, were generally very resistant.

Molinate appears to be particularly susceptible to degradation by nZVI and results of more detailed studies on this compound are reported in Chapter 4.

Chapter 3.

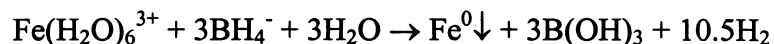
Nanoscale ZVI Particles Manufacture and Analytical Techniques

The experimental techniques used in this work are described in this chapter with examination firstly of the method of manufacture of the nanoscale ZVI particles used throughout the study. This is followed by a description of the methods of analysis of both organic compounds (agrochemicals and their degradation products by SPME GC/MS and benzoic acid and p-hydroxybenzoic acid by HPLC) and inorganic compounds (ferrous iron and hydrogen peroxide using colorimetric techniques). A description of the experimental approaches used in detailed studies of molinate and benzoic acid degradation are given as is a summary of the XRD approach to determining the nature of inorganic products formed on the surface of the ZVI particles.

3.1. Synthesis of nano-scale zero-valent iron particles

Nanoscale ZVI particles were prepared freshly each day by adding 0.16M NaBH₄ (98%, Aldrich) aqueous solution dropwise to a 0.1M FeCl₃·6H₂O (98%, Aldrich) aqueous solution at ambient temperature as described by Wang and Zhang (1997). The synthesis of nZVI was performed under atmospheric conditions. The preparation of solutions involved the following steps: sodium borohydride (NaBH₄, 0.6053g) solids were dissolved in 100mL of 0.1M NaOH solution (0.16M NaBH₄ in 0.1M NaOH solution) and 2.7030g of FeCl₃·6H₂O dissolved into 100mL pure water (0.1M FeCl₃·6H₂O). NaBH₄ solution can be made either in water or NaOH solution, although NaBH₄ is unstable in water and can

quickly result in a loss of reduction power. Addition of the NaBH₄ to the FeCl₃ solution in the presence of vigorous magnetic stirring resulted in the rapid formation of fine black precipitates as the ferric iron reduced to Fe⁰ and precipitated according to the following reaction:



The particles were washed 3 to 4 times with a 10⁻⁴M (pH 4) HCl solution and stored as a 5mg Fe/mL concentrate at pH 4 and kept in a cooling room (< 4°C). The total amounts of ZVI particles produced were 0.2g assuming all the soluble Fe(III) is reduced to Fe⁰. Although the total amount of iron by estimation of mass balance is 0.2g, there were likely to be iron losses during the acid washing step. A series of control tests indicated that the mass of Fe⁰ lost due to this process was approximately 5% (Agrawal and Tratnyek, 1996).

3.1.1. ZVI particle characterization

Dry particles for particle characterization were obtained by washing the wet precipitates with 10⁻⁴M HCl 3 to 4 times, followed by rinsing with pure water, and then separating using a centrifuge at 3000rpm for 5min to remove the remaining moisture. The ZVI particles were then quickly frozen using liquid nitrogen and freeze dried under vacuum over 20hrs. Compared with freeze-drying under vacuum, drying under air resulted in the color of Fe particles changing from black to reddish-brown within a few hours, indicating significant surface oxidation. Analysis of the freeze-dried particles by Scanning Electron Microscope (SEM) and by Transmission Electron Microscope (TEM) revealed that the primary particle size ranged from 1 – 200nm with an average size of approximately 50nm (Figure 3.1a). The presence of a strong diffraction pattern during TEM analysis confirmed

that the particles were crystalline (Figure 3.1b). The dried ZVI particles were identified as elemental iron by XRD analysis using a Philip PW 1830 X-ray diffractometer with X'pert system (Figure 3.2). No other minerals, such as magnetite or maghemite, were identified in the freshly prepared, freeze-dried samples. Single point BET analysis by N₂ adsorption (Micromeritics ASAP 2000, GA) determined that the surface area of the particle was 32 m²/g. The results of the particle sizing and surface area measurements are similar to results found by other researchers for nano-sized ZVI as shown in Table 3.1.

Table 3.1. Properties of various ZVI particles

Surface area (m ² /g)	Size (nm)	References
33.5	1-100	Zhang <i>et al.</i> , 1998
31.4	1-200	Choe <i>et al.</i> , 2001
27.8-31.8	1-200	This work
0.063	75,000 – 150,000	Choe <i>et al.</i> , 2000 (Commercial grade)
0.038	425,000 – 850,000	Agrawal and Ttratnyek, 1996 (Commercial grade)

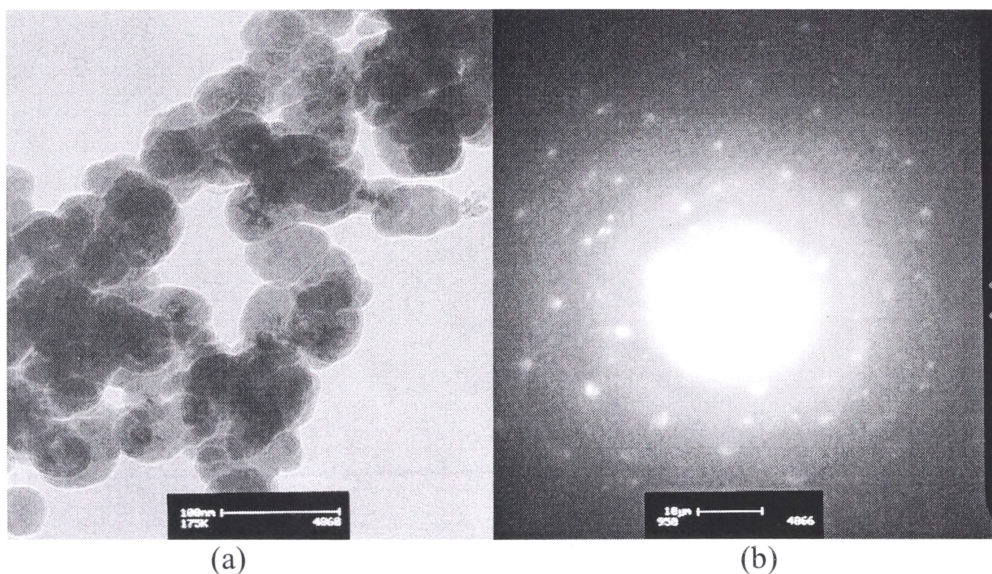


Figure 3.1. Transmission Electron Microscope (TEM) images of: (a) primary ZVI particles (scale bar = 100nm) and (b) the diffraction pattern (scale bar = 10μm).

Figure 3.2. ZVI identification by XRD analysis.

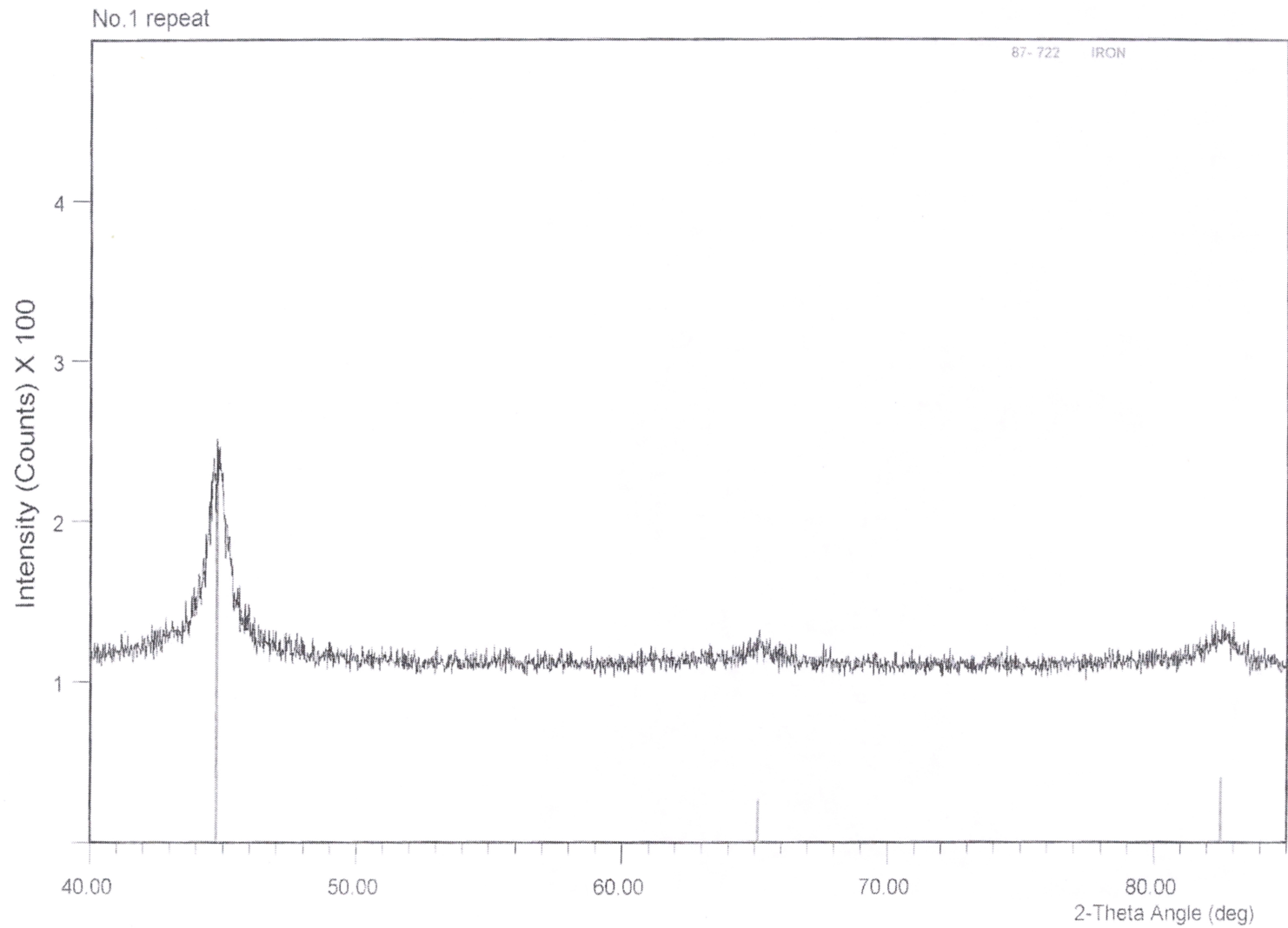
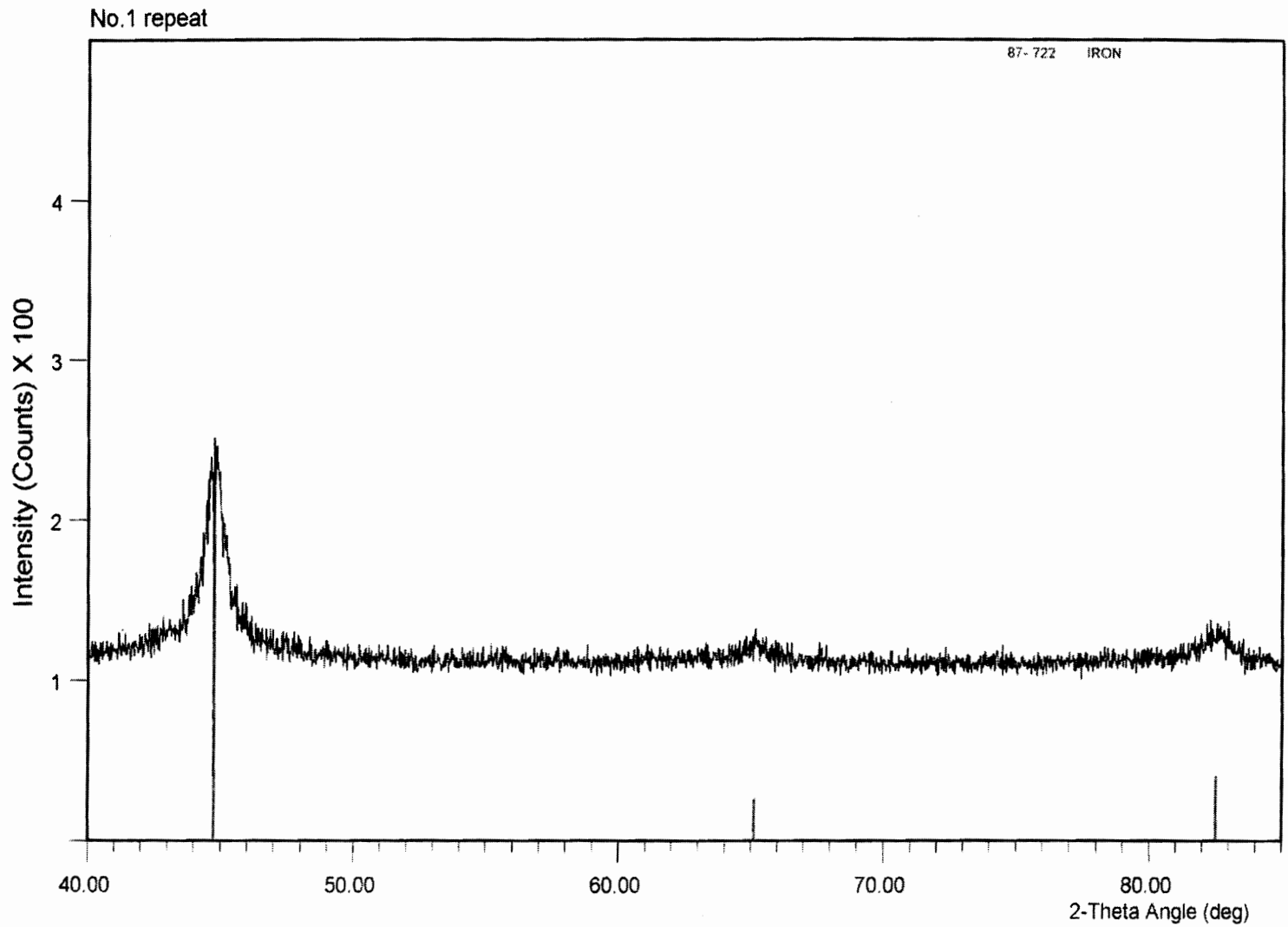


Figure 3.2. ZVI identification by XRD analysis.



File Name: a:\020616rr.rd

The ZVI particles, however, tend to form larger aggregates and these may reduce the tendency for the particles to remain in suspension (Figure 3.3).

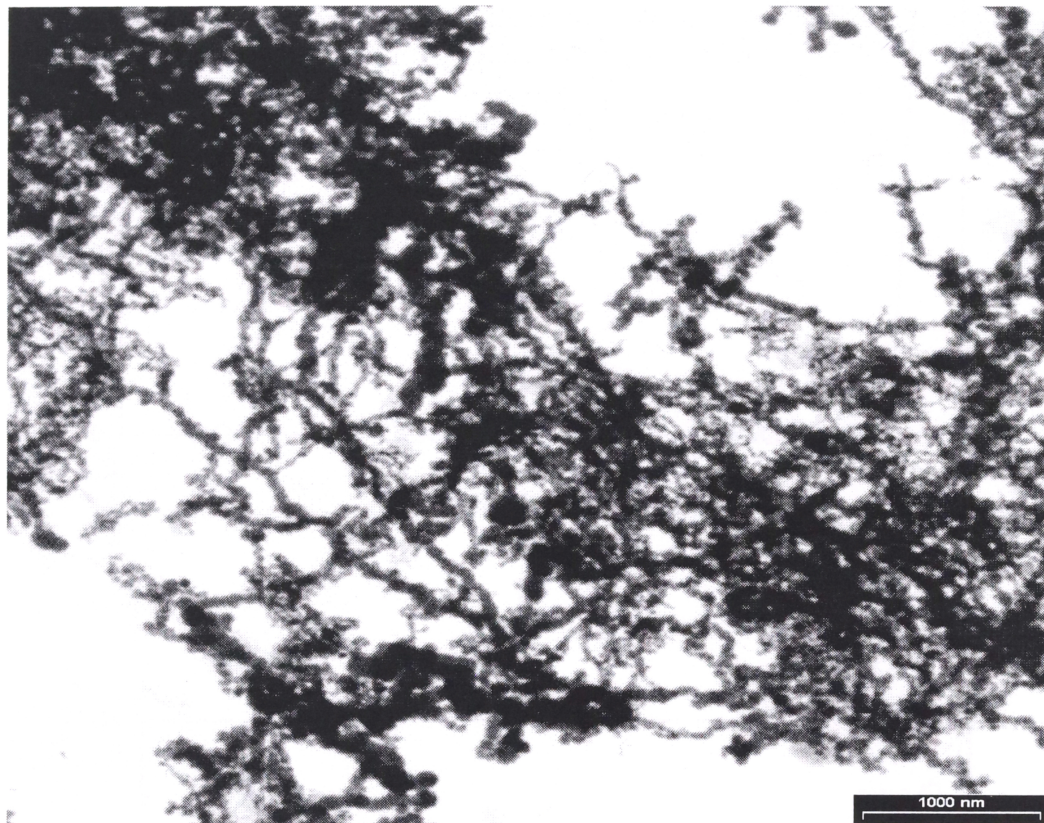


Figure 3.3. Scanning Electron Microscope (SEM) images of freeze-dried ZVI aggregates manufactured using NaBH_4 (scale bar 1000nm).

Malvern MasterSizerE was used to determine the particle size distribution of wet aggregates. Results are shown in Figure 3.4 and indicate the presence of a population of aggregates of around 200 nm mean size and a population of larger aggregates of size $> 30\text{-}40\ \mu\text{m}$.

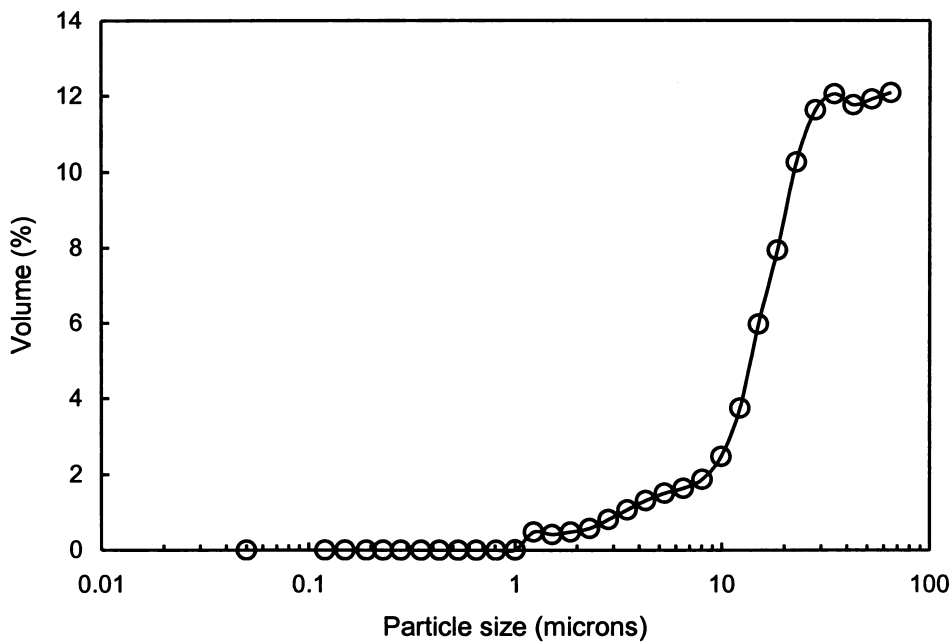
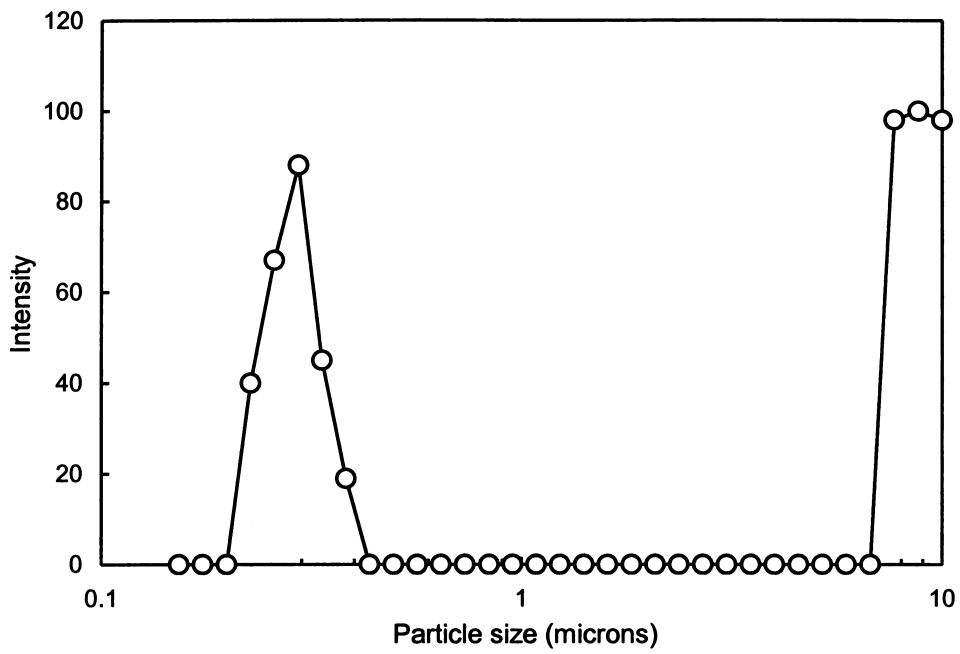


Figure 3.4. ZVI particle size distributions determined using the Malvern MasterSizerE.

In addition to surface area, primary particle size and aggregate particle size measurements, the zeta potential was measured (using a Brookhaven ZetaPlus particle charge analyser) to assess the surface charge of the particles at different pH (Figure 3.5). The results indicate that at low pH, the particles have a net positive charge and at higher pH a net negative charge.

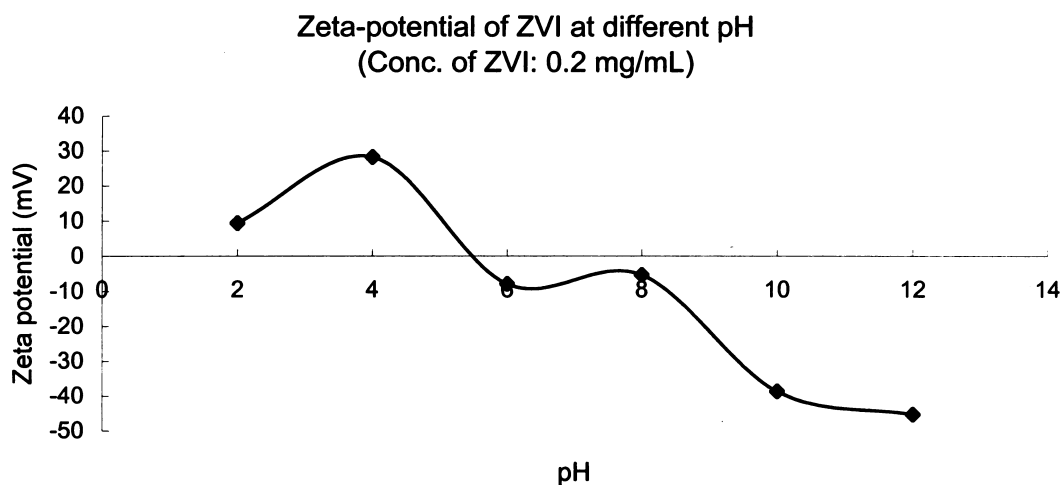


Figure 3.5. Zeta-potential of ZVI at different pH.

3.2. Analytical techniques

3.2.1. Solid-phase microextraction (SPME) GC/MSD

Pesticides are difficult to analyze due to the wide range of chemical characteristics, structures and properties. For example, organochlorine pesticides are classified as nonpolar while herbicides are generally very polar semivolatiles. This range of polarities creates challenges for effective preconcentration and analysis. The approach to preconcentration used here is that of solid-phase microextraction (SPME). The SPME method has been successfully applied in the analysis of some mid-polar pesticides in water and food samples

(Natangelo *et al.*, 2002), to a variety of volatile compounds (Bouaid *et al.*, 2001), and in the analysis of both polar and non-polar analytes from solid, liquid and gas phases (Matisová *et al.*, 2002; Vereen *et al.*, 2000; Boyd-Boland and Pawliszyn, 1996). The preconcentration of nitrogen-containing pesticides has also been successfully accomplished using SPME (Magdic and Pawliszyn, 1996). SPME is typically used prior to GC analysis and is being increasingly adopted because of its simplicity, low cost, rapidity and sensitivity when combined with GC (Bouaid *et al.*, 2001). Problems may be encountered, however, when environmental samples contain too many unknown components that compete with the target analytes for absorption by the polymer fibre (Eisert and Levsen, 1995).

3.2.1.1. SPME Process

The SPME process has two steps: 1) partitioning of the analytes between the sample matrix and a stationary phase which is coated on a fused-silica fibre: and 2) desorption of trapped analytes into the analytical instrument (Beltran *et al.*, 2000; Dugay *et al.*, 1998). Sampling, extraction, and concentration are focused into a single step. In this first step, the coated fiber is exposed to the sample and the target analytes partition from the sample matrix into the coating. Partitioning onto the fiber can be conducted in the sample liquid or head-space. After absorption equilibrium is achieved or after exposure for some defined time, the fibre containing the concentrated analytes is injected into a preheated injector port in a gas chromatography system. The fibre is left in the hot injector port for a given period of time (typically 3mins) to provide sufficient time for the analytes to desorb from the fibre. After desorption, the now gaseous compounds are released into the GC column where they are separated and quantified.

A microextraction fibre coated with 100 μm polydimethylsiloxane(PDMS) was used in all experiments described here since this material has been reported to have a satisfactory extraction efficiency for a variety of compounds including atrazine (Hernandez *et al.*, 2000), several organophosphorus pesticides (Beltran *et al.*, 1998) and organochlorine pesticides (Dugay *et al.*, 1998). High recoveries have been reported (Santos *et al.*, 1996) although the 85 μm polyacrylic acid fibre is better for polar compounds (Buchholz and Pawliszyn, 1993; Magdic *et al.*, 1996). In addition, the PDMS fiber is capable of being used over a high temperature range of 220-320 $^{\circ}\text{C}$, which allows for desorption of higher boiling point semi-volatile compounds (Barnabas *et al.*, 1995) and non-polar compounds (Agilar *et al.*, 1998).

The general SPME procedure used for all experiments in this research was as follows:

1. The coated fibers were conditioned according to the manufacturers' instructions to ensure that any contaminants, which might be present and cause high baseline noise or ghost peaks, were removed prior to use (Boyd-Boland *et al.*, 1996). Preconditioning involved heating the fibre in a GC injector port for 3hrs at 260 $^{\circ}\text{C}$. The highest recommended temperature for the PDMS fiber is 260 $^{\circ}\text{C}$ (Young and Lopez-Avila, 1996).
2. 1mL of sample and a small teflon coated magnetic stirring bar was placed in a 2mL glass vial before being sealed with a PTFE-lined septa. The sorption on the Teflon coating of the magnetic stir bar is negligible based on blank and adsorption experiments. While the sample was stirred, the septum was pierced using a stainless-steel needle and the PDMS fiber exposed to the sample for 15min.

Constant rapid stirring was maintained, as the rate at which the extraction process reaches equilibrium is primarily dependent on the rate of mass transfer in the aqueous phase. Although 15 minutes is insufficient for most pesticides to reach equilibrium concentrations (Figure 3.6), a precise quantification was possible, as this extraction time was kept exactly constant for all experiments conducted. All nZVI batch experiments conducted were reproducible with the relative standard deviations of less than 10%.

The fibre was again withdrawn into the needle and the syringe removed from the vial. The injector port septum of the GC/MS was pierced with the stainless steel syringe and the fiber is directly exposed in the hot injector port.

3. Thermal desorption was carried out for 3 or 5 min at 260°C (considered to be the optimum desorption time for quantification (Ramesh and Ravi, 2001)) and the heating program initiated. Finally, the fibre was removed from the injector port. Separate vials were used for each experiment as consecutive experiments lead to non-reproducible results.

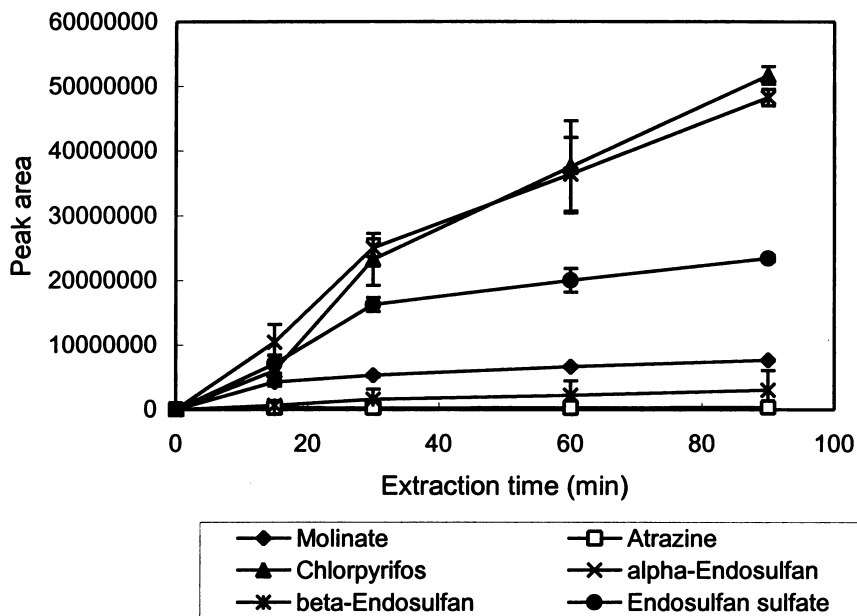


Figure 3.6 A plot of extraction time vs. equilibrium for pesticides.

3.2.1.2. Extraction technique for hydrophobic compounds

The analysis of highly hydrophobic compounds in contaminated soils is challenging because pesticide residues tend to strongly adsorb to soil particles and there is interference from non-target compounds. The problem has yet to be overcome by many extraction methods. Of the different methods used for extraction of hydrophobic organics from soils (e.g., tumbling, soxhlet, blending, ultrasonic, and supercritical fluid extraction) (Green, J.M. 1996; Capangpangan and Suffet, 1996, 1997; Lopez-Avila *et al.*, 1994; Noordkamp *et al.*, 1997), ultrasonic extraction was examined in greater detail as it is quick, comparatively easy to do and typically yields satisfactory extraction efficiency (Schneider, 1995). Among solvents such as methanol, acetone, dichloromethane, and hexane, which are commonly used for extraction, *n*-hexane was chosen as hexane and methanol are the most used solvent

for extracting organochlorine pesticide (e.g., endosulfan) residues from environmental samples (Kanatharana *et al.*, 1993).

Using ultrasonic/hexane extraction, centrifugation and direct injection into GC/MS gave a recovery rate of 70% for endosulfan from a contaminated sand mixture. In this study SPME GC/MSD was only used for solution measurement while GC/MSD was employed for the extraction of water/sand mixture into n-hexane. This is because the 100 μ m PDMS non-bonded fibre cannot be used with non-polar organic solvents. Only fibres that are indicated as bonded can withstand most organic solvents. In addition, glass was used in all the apparatus to reduce poor recovery as organics are readily absorbed to plastic tubes. It was found that without the SPME step (e.g., by direct injection using solvents), the sensitive was too low for the dilute levels (e.g., 10ppb) typically found in waterways.

3.2.1.3. GC/MS analysis

As indicated in Section 3.2.1.1, the fiber was removed from the sample and introduced into the GC/MS injector where the analytes were thermally desorbed for 3 min and injected onto a (HP-5MS) column in splitless mode with the injector held isothermally at 260°C. For quantification of molinate, the GC/MS was operated in the SIM (Selected Ion Monitoring), by monitoring the base peak of molinate (m/z 126, 55, 187, 83). The MS was tuned to m/z 126, 55, 187, 83 for EI corresponding to perfluorobutylamine (PFBTA). In some experiments, by-products were analyzed using a full-scan between 50 and 500 m/z.

The temperature program in SIM mode was as follows: the initial temperature was 80°C (1min), which was increased to 178°C (3min) at 30°C/min, and then to 250°C (5min) at 30°C/min, giving total run time of 14.7min. In the full scan mode the initial temperature was 80°C, which was increased to 200°C at 5°C/min, and then to 210°C (3min) at 5°C/min, followed by to 270°C (3min) at 20°C/min, giving a total run time of 35min. For both analytical methods the detector was set at 280°C, helium (pure carrier gas grade) was used as the carrier gas at a flow-rate of 1.0mL/min and the electron impact (EI) ionization energy was set to 70eV. All standard curves involved use of five concentrations and were linear with regression coefficients greater than 0.9995 in all cases. The method provided a limit of detection for molinate of 10 ng/L. In order to prevent carryover, blanks were run before the next sample extraction. To account for the filter recovery (95%), initial samples (before adding ZVI) were also filtered.

3.2.2 HPLC analysis of benzoic acid and p-hydroxybenzoic acid

Benzoic acid and para-hydroxybenzoic acid concentrations were quantified by HPLC using a Hewlett-Packard 1100 series HPLC system equipped with a 250 × 4.6mm Waters Spherisorb ODS-2 5μ column (Alltech, IL). A two-solvent gradient elution consisting of pH 3 water (adjusted with 85% ortho-phosphoric acid) and acetonitrile (85:15, v/v %) at a flow rate of 1.0mL/min was used to separate benzoic acid and isomers of hydroxybenzoic acid. The p-HBA isomer was quantified at 255 nm and benzoic acid (BA) was quantified at 270 nm. All standard curves were linear with regression coefficients of >0.9990 in all cases. The method detection limit for BA and p-HBA were 2.5μM, and 0.1μM.

3.2.3. Measurement of ferrous iron concentrations

Ferrous ion generation for both the molinate and benzoic acid experiments was quantified by monitoring the absorbance of a Fe(II)-bipyridine complex at 522nm in a manner similar to that described by Voelker (1994). Samples were filtered through a 0.22 μ m Millex-GS syringe filter before analysis. The procedure consisted of premixing 0.4mL of a pH 6 phosphate buffer (0.5M) and 0.1mL of bipyridine solution (0.01M) in a 5-cm spectrometer cell and adding 2mL of the filtered sample, followed by 0.02mL of EDTA stock (0.01M Na₂EDTA). After 60 seconds, the absorbance was measured at 522nm.

Ferrous ion generation for the molinate experiments was also quantified by continuously monitoring the absorbance of a ferrozine-Fe(II) complex at 562nm in a flow-injection apparatus similar to that described by Rose and Waite (2002). Analysis of Fe²⁺ evolution from the 1.79mM ZVI suspension required 1mM ferrozine while 4mM ferrozine was used to measure total Fe²⁺ released from 5.36mM ZVI. The higher 4mM ferrozine was not necessary for the 1.79mM ZVI and did not affect Fe²⁺ measurement. Samples were continuously pumped through a 0.45 μ m GF (glass fibre) filter before injection. For dissolved ferrous measurement, the ZVI samples were filtered using GF before combining with ferrozine while total ferrous iron (adsorbed and dissolved Fe(II)) was measured by mixing with ZVI samples and ferrozine before filtering using GF.

Schematics of the approaches to dissolved and total ferrous iron analysis are shown in Figures 3.7 and 3.8.

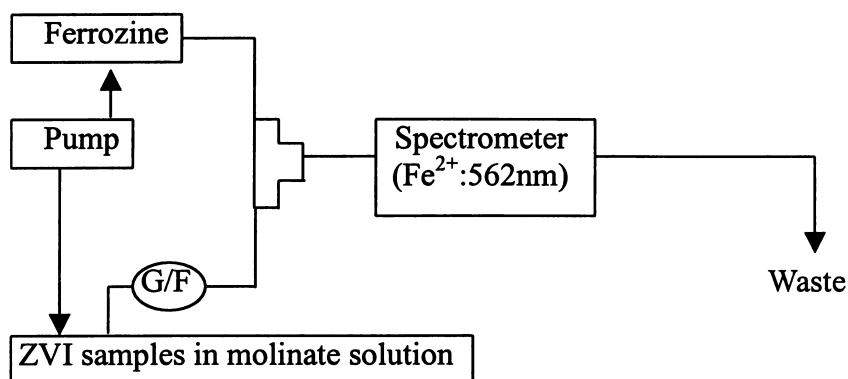


Figure 3.7. Schematic of dissolved ferrous iron measurement.

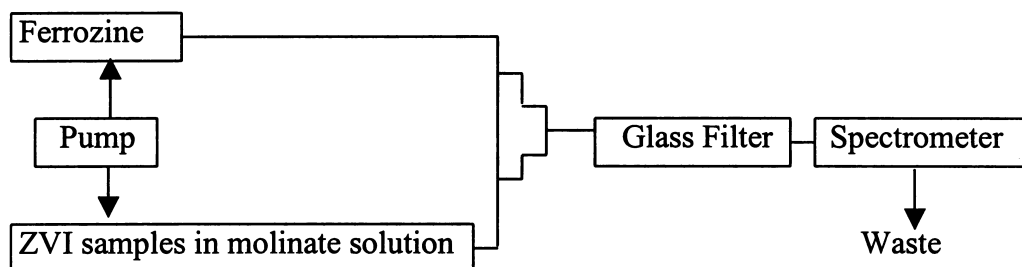


Figure 3.8. Schematic of total ferrous iron measurement.

3.2.4 Measurement of hydrogen peroxide (H₂O₂) concentrations

The concentration of hydrogen peroxide was measured in the absence of organic compounds (e.g. molinate) in these studies. The method used is similar to that developed by Balmer and Sulzberger (1999) and involves the use of the reagent DPD (*N,N*-diethyl-*p*-phenylenediamine). 0.4mL of phosphate buffer solution (pH 6.0, 0.5 M phosphate) and 0.1mL of pure water were premixed in a 1 cm quartz cell. 2mL of sample solution from which ZVI particles had been removed by filtration was added followed by the addition of 0.02mL EDTA solution (0.01 M Na₂EDTA). 0.03 mL of DPD reagent (1% in 0.1M H₂SO₄)

was then added followed by the addition of 0.03mL POD (horseradish peroxidase) reagent (about 0.8mg/mL). The absorbance was then measured at 551nm.

3.3. Procedures Used in nZVI-mediated Degradation Studies

3.3.1. Molinate Degradation

3.3.1.1. Reagents

Molinate (S-ethyl perhydro-azepin-1-carbothioate; 99% purity) was purchased from Alltech Associates (Aust) Pty Ltd. All chemicals used in this work were analytical reagent grade and solutions were prepared in ultra-pure water (Milli-Q water, Millipore). Molinate solutions were prepared from a 100ppm stock solution (water solubility of molinate is 880 ppm at room temperature; Hartley and Kidd, 1983).

3.3.1.2. Experimental setup

Experiments were carried out at room temperature ($20 \pm 2^\circ\text{C}$) under both air and nitrogen atmospheres without pH control (pH $\sim 6 - 7$) as well as at fixed pHs of 4 (obtained by HCl addition) and 8.1 (obtained using a 2 mM bicarbonate buffer). Experiments were conducted in 100mL serum bottles using a total suspension volume of 50mL under aerobic conditions while the vials were completely filled (i.e. no headspace) for studies under deoxygenated conditions. ZVI suspensions were prepared from the 5mg Fe/mL stock suspensions and molinate was added using a micropipette. Each bottle was either continuously shaken using an orbital shaker at 175rpm (Hybritech Incorporated) or continuously sparged with the indicated gas/mixture and samples were taken at regular time intervals using a syringe and

filtered through a 0.45 μ m GF filter before SPME GC/MS analysis. Typical system of GC/MS with solid-phase microextraction (SPME) is shown in the Figure 3.9.

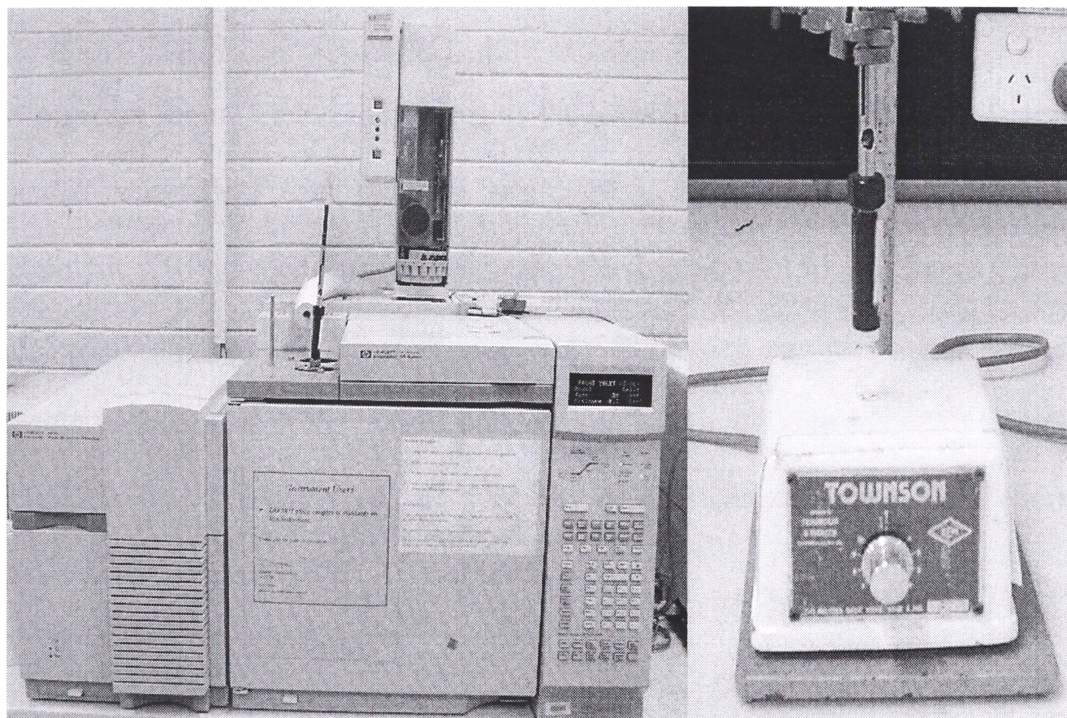


Figure 3.9. Typical system of GC/MS with solid-phase microextraction (SPME).

3.3.2. Benzoic Acid Degradation

3.3.2.1. Reagents

All chemicals were high purity and were used as received. Reagents were prepared using 18 M Ω Milli-Q water. The reactions of nZVI were studied in pH-buffered solutions with an ionic strength adjusted to 0.03 M with NaCl. Benzoic acid served as the buffer at pH 3 and 5. 2 mM bicarbonate buffer served as the buffer at pH 8. When necessary, the pH of the solutions was adjusted using 0.1 N HCl or 1N NaOH. Synthetic humic acid and

commercial ZVI powder (>97% purity, particle size: 4.5-5.5 μm) were obtained from Aldrich. Benzoic acid, hydroxybenzoic acid, and phenol were obtained from Sigma-Aldrich and aniline was obtained Ajax FineChem Ltd. Nanoscale ZVI was synthesized as described in Section 3.1.

To compare the nZVI to other forms of $\text{Fe}^0_{(s)}$ the following were used: Master Builders granular zero-valent iron (particle size: 750 - 1200 μm ; Orica Chem., Australia), electrolytic ZVI powder (purity: >98%, particle size: 100 – 150 μm ; Kanto Chemical Co., Inc, Japan), and Aldrich fine ZVI powder (>97% purity, particle size: 4.5-5.5 μm). The specific surface areas of the Master Builders iron, Aldrich, Kanto and nZVI were 0.71, 0.38, 0.60, 32 m^2/g , respectively, as determined by BET (Brunauer, Emmet and Teller) analysis using a Micromeritics ASAP 2000 instrument.

3.3.2.2. Experimental setup

All experiments were carried out at room temperature ($20 \pm 2^\circ\text{C}$) in 100 mL serum bottles using a total volume of 50 mL. The nZVI particles were kept in suspension by placing the bottles on an orbital shaker table at 175 rotations per minute. To ensure gas exchange, the serum bottles were open to the atmosphere. The solution pH was continuously monitored with a pH electrode throughout each experiment and adding nZVI usually resulted in an increase during the initial phase of the reaction. To maintain a constant pH value, HCl was added with a 1000 μL Eppendorf pipette as needed during the first hour of the experiments.

After the first hour the pH remained constant. The pH of the suspensions was maintained within ± 0.2 unit from the initial values during the reaction runs.

To initiate a reaction, nZVI was added from the stock suspensions to buffered solutions containing benzoic acid. Samples were collected at different time intervals in a 5 mL glass syringe and filtered immediately through a 0.45 μ L Millipore (Millex AP 20) glass syringe to stop the reaction. Loss of p-HBA on the filter was less than 5%, as determined by comparison of filtered and unfiltered samples collected prior to addition of nZVI. p-HBA was analyzed within 24 h of sample collection.

Experiments also were performed to assess the relative rates of hydroxyl radical oxidation of several probe compounds. These experiments were performed using Fenton's reagent as a source of hydroxyl radical. Experiments were conducted in serum bottles by adding an excess of Fe(II) (i.e., 200 μ M) to H_2O_2 (20 μ M) at pH 3 with an ionic strength of 0.03 M and 10 mM BA. Samples collected after 10 min were analyzed for p-HBA by HPLC.

3.4. Determination of ZVI Surface Products by XRD

In addition to confirmation of the identity of the primary reactant (ZVI), X-ray diffraction analysis was also used to examine the nature of mineral products formed on the ZVI surface during degradation studies. Details of the procedures used are given below.

3.4.1. Measurements in the Presence of Molinate

XRD analysis was performed using a Philip PW 1830 X-ray diffractometer with X'pert system. Samples of ZVI particles (from studies containing 1.79mM ZVI) were collected after reaction with molinate (100ppb) over 3hrs in both un-buffered and buffered systems (i.e. 2mM NaHCO₃; 20mM NaCl; pH 8.1). All the ZVI particles were separated after reaction time of 3.25hrs and then moisture removed by centrifugation (3000rpm for 10min, at 15°C), freezing at -84°C using liquid nitrogen, followed by freeze drying for 20hours.

3.4.2. Measurements in the Absence of Molinate

Four samples in the absence of molinate were obtained for XRD analysis as follows. Sample nos. 1 and 3 were collected from 10.7mM ZVI suspensions in both Milli-Q water and pH 8.1 2mM NaHCO₃ /20mM NaCl solutions after 3hours of reaction while sample nos. 2 and 4 were collected after 3 hours of reaction from 10.7mM suspensions in both Milli-Q water and pH 8.1 2mM NaHCO₃ /20mM NaCl solutions to which H₂O₂ (0.33mM) had been added. After 3hrs, all the ZVI particles were collected and rinsed with Milli-Q water two times. Dried ZVI was obtained as described above.

Chapter 4.

Oxidative degradation of the thiocarbamate herbicide, molinate, using nanoscale ZVI

4.1. Introduction

The herbicide molinate [S-ethyl hexahydro-1H-azepine-1-carbothioate] is used extensively to control germinating broad-leaved and grass weeds during rice production. It is a moderately persistent ($\tau_{1/2} = 21$ days) (Weber, 1994) and highly soluble (solubility = 880ppm (Hartley and Kidd, 1983)) herbicide that is often detected as a contaminant in rainwater (Suzuki *et al.*, 2003; Sakai, 2003; Charizopoulos and Papadopoulou-Mourkidou, 1999), lakes (Sudo *et al.*, 2002; Nohara *et al.*, 1997), rivers (Crepeau and Kuivila, 2000; Coupe *et al.*, 1998; Cerejeira *et al.*, 2003; Paune *et al.*, 1998) and estuaries (Oros *et al.*, 2003) worldwide. Molinate is one of the most frequently detected pesticides/herbicides exceeding drinking water guidelines and guidelines for the protection of aquatic ecosystems in southern Australian irrigation networks and rivers (Australian State of the Environment Committee, 2001). Molinate has a high cancer hazard factor (Gunier *et al.*, 2001; Kelly and Reed, 1996) – primarily as a consequence of possible exposure to contaminated air and dust (Lee *et al.*, 2002) - the long term effects of its presence in aquatic ecosystems is of concern (Crepeau and Kuivila, 2000; Coupe *et al.*, 1998).

As noted in Chapter 2, molinate was found to be especially susceptible to degradation by ZVI in screening studies conducted on a range of agrochemicals (Joo *et al.*, 2002). Therefore, molinate was selected for detailed investigation in order to examine the

degradation mechanism and improve our understanding of how the removal rate could be enhanced, particularly in field situations.

4.2. Results

4.2.1. Effect of the Presence of Air/Oxygen

The degradation of 100 ppb molinate was examined both under deoxygenated conditions and in the presence of air and 100% oxygen. As shown in the Figure 4.1, molinate showed little removal in pH 4 solutions in the absence of oxygen while 70% removal was observed over 3 hours when the sample was sparged with air. Removal was further enhanced when the suspension was sparged with pure oxygen. Vigorous shaking of the vials under atmospheric conditions achieved a similar degree of removal as sparging with zero-grade air. A control with N₂ sparging showed no removal by volatilization over 3 hours (Figure 4.1).

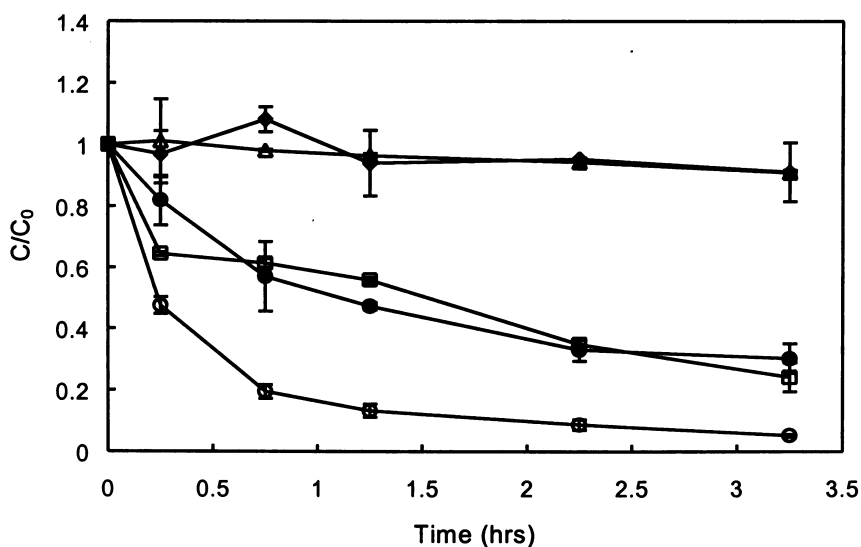


Figure 4.1. Comparison of 100 ppb molinate removal at pH₀ 4, 10.7 mM ZVI when sparging with N₂ (◆), zero-grade air (●), 100% O₂ (○) or shaking in the presence of air

(). Also shown is a control in which a ZVI-free solution containing 100 ppb molinate is sparged with N₂ (Δ).

4.2.2. Effect of Molinate and ZVI Concentration

For any particular ZVI concentration, molinate degradation under oxic conditions exhibits pseudo-first order decay with both a linear dependence of ln(C/C₀) on time and an independence of the observed pseudo-first order rate constant (k) on initial molinate concentration (Figures 4.2 and 4.3). As can be seen from Figure 4.3, a linear dependence of rate of molinate degradation on ZVI concentration (measured as total Fe⁰) is observed, suggesting an overall rate expression of the form:

$$\frac{d[\text{molinate}]}{dt} = -k[\text{molinate}][\text{ZVI}] \quad [4.1]$$

where the second order rate constant $k = 1.8 \times 10^{-2} \text{ M}^{-1} \text{ s}^{-1}$.

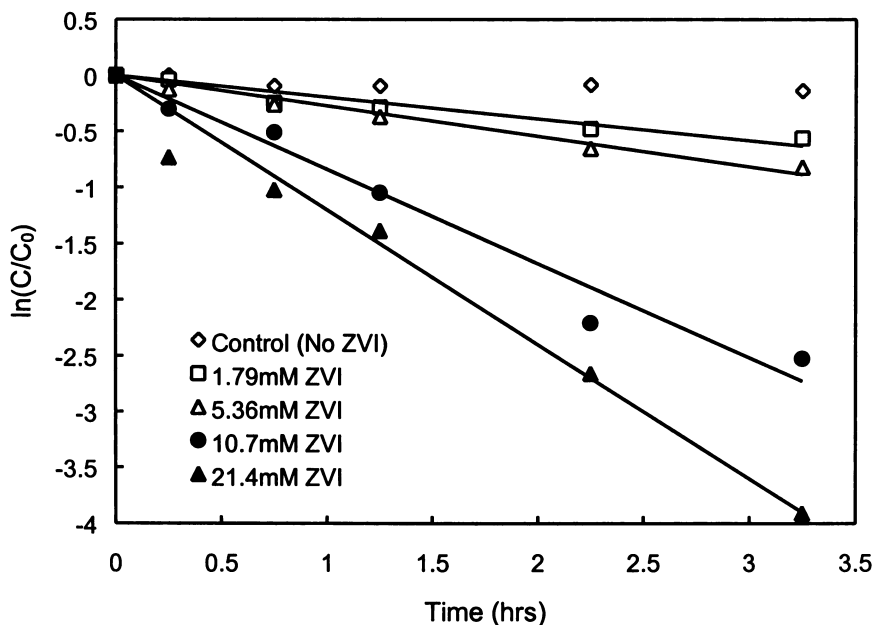


Figure 4.2. Molinate degradation in unbuffered solutions ($\text{pH}_{\text{initial}} \approx 6.4$) for different ZVI concentrations and $[\text{Molinate}]_0 = 100 \text{ ppb}$.

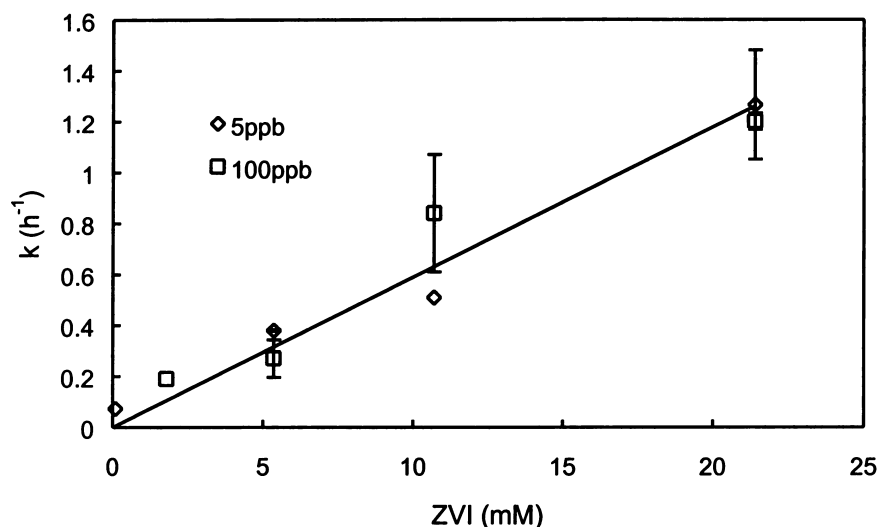


Figure 4.3. Dependence of pseudo–first order rate constant (k) for molinate degradation on ZVI concentration (as quantified by total Fe^0 concentration) for initial molinate concentrations of 5 and 100 ppb in unbuffered solutions ($\text{pH}_{\text{initial}} \approx 6.4$).

The effect of different ZVI concentrations on the degradation of molinate at two different concentrations (5 and 100ppb) is shown in Figure 4.3. As can be seen in this figure, the molinate disappearance rate was strongly dependent on ZVI concentration. As the concentration of ZVI increases, the degradation rate increases for both high and low initial molinate concentrations. The results of control runs (no ZVI) also shown in Figure 4.2 reveal that molinate removal by hydrolysis at neutral pH is negligible. The capacity of ZVI to maintain the degradation of molinate was examined and is shown in Figure 4.4. As can be seen, a second addition of 100 ppb of molinate after 1 hour is rapidly degraded but the rate and extent of degradation of further additions of 100 ppb molinate at 3 and 5 hours is observed to be significantly less than that observed initially.

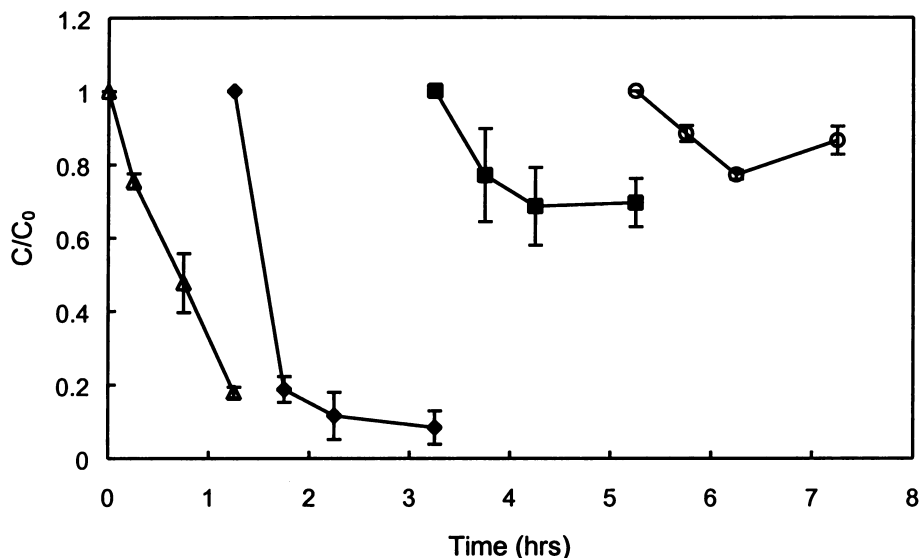
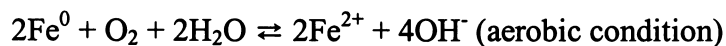


Figure 4.4. Ability of ZVI to maintain molinate degradation on continued addition of aliquots of molinate. Conditions: pH = 4, [ZVI]₀ = 10.7 mM, addition of molinate at 0, 1, 3 and 5 hours resulted in increase in molinate concentration in reaction medium of 100 ppb.

4.2.3. Effect of pH

As observed in other studies, adding ZVI to water resulted in an increase in pH and a concurrent decrease in Eh over the experimental runs (Figure 4.5). This behaviour is indicative of a standard reduction process (Orth and Gillham, 1996; Elliott and Zhang, 2001). In un-buffered Fe-H₂O systems, pH rise is expected under both aerobic and anaerobic conditions due to aqueous corrosion of the metal (Agrawal and Tratnyek, 1996) as shown in the following reactions:



In reaction runs with 1.8mM ZVI, the pH rose from an initial value of 4 to 7.4 after three hours of reaction. In solutions buffered to around pH 8 with 2 mM NaHCO₃, little change in pH was observed over a 3 hour reaction time.

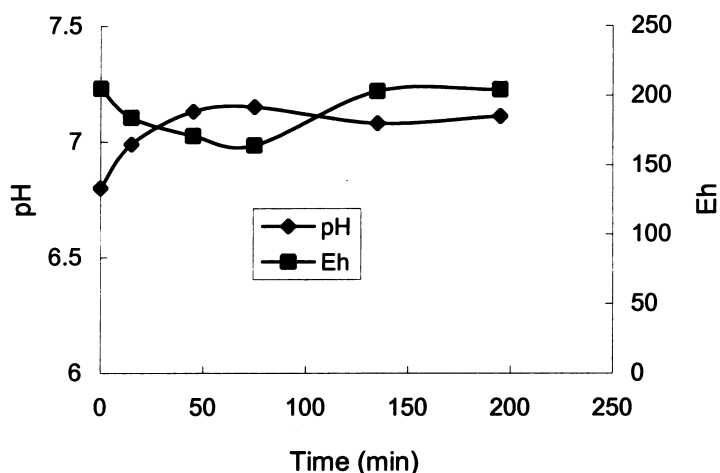


Figure 4.5. Variation in pH and Eh on ZVI-mediated degradation of molinate in unbuffered solutions (pH₀ 6.8, 1.8mM ZVI, 100ppb molinate).

As can be seen from the comparative results in Figure 4.6, molinate degradation occurs at a slower rate in a pH₀ 8.1 (adjusted with 2mM NaHCO₃) carbonate buffered solution than observed from an initial pH₀ 4 solution. Significant degradation is still observed at pH 8.1, however, with approximately 60% of 100 ppb molinate degraded after 150 minutes reaction with 21.4 mM ZVI (Figure 4.6) (c.f. approximately 65% removal at pH 4 for similar reactant concentrations). The rate of molinate removal appears to slow down markedly at times greater than 150 minutes while continued degradation is apparent at pH 4.

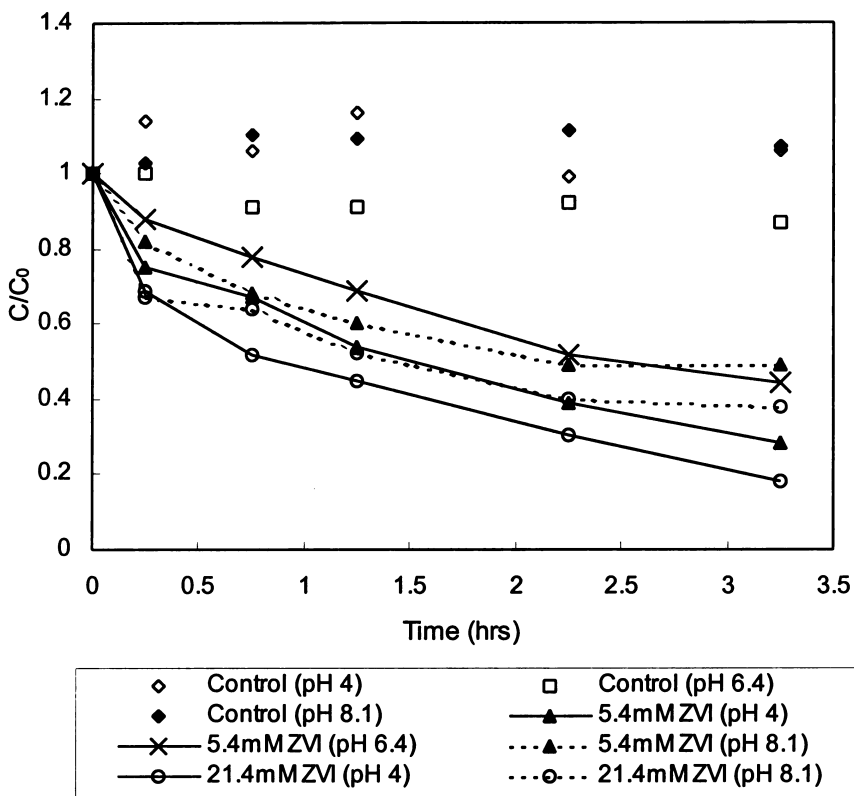


Figure 4.6. Comparison of molinate degradation at different starting pHs for $[\text{molinate}]_0 = 100$ ppb and $[\text{ZVI}]_0$ concentrations of 5.4 and 21.4 mM.

Increasing the concentration of the ZVI at pH 8.1 does not appear to significantly improve the degradation rate (Figure 4.7). At these higher pH values, oxide and hydroxide coatings will develop which hinders access to the Fe^0 surface (Dombek *et al.*, 2001). The influence of pH on the degradation rate is probably the result of both the available iron surface area for reaction and the competition by other solution components (such as carbonate) for reactive species. According to MacKenzie *et al.* (1995), a ten-fold increase in aqueous alkalinity reduced the reaction rate by three fold.

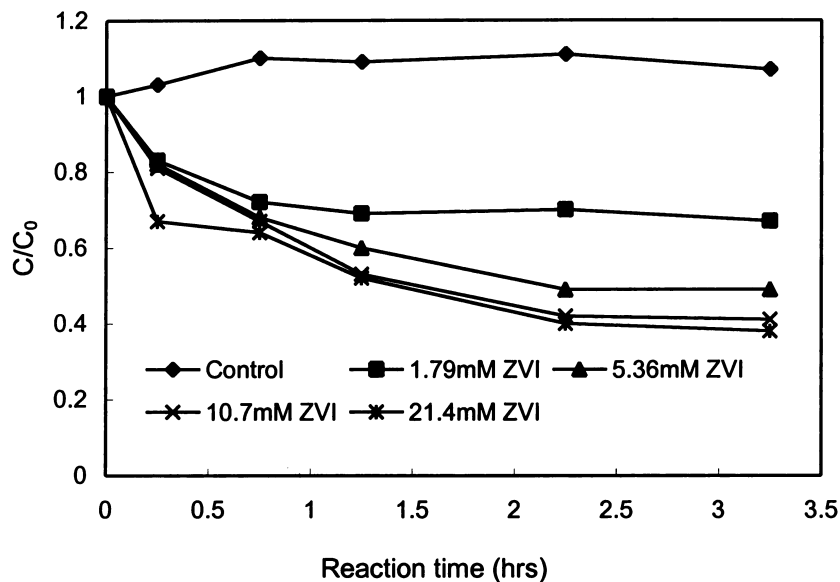


Figure 4.7. Molinate degradation in a 2mM bicarbonate buffered solution at various ZVI concentrations (100ppb molinate; pH₀ 8.1).

4.2.4. Ferrous Iron Generation.

4.2.4.1. Ferrous iron generation in pH₀ 4 solution

The initial product of ZVI oxidation is ferrous iron. Results of ferrous iron concentration measurement immediately after adding the ZVI particles to pH 4 solutions are shown in Figure 4.8. Immediately after addition of ZVI to water, concentrations of Fe(II) ranging from 0.07 to 0.14 mM are detected depending on the amount of ZVI added, and these concentrations subsequently decrease over time. The initial concentrations of Fe(II) observed in solution increase with increasing ZVI concentration with 72 μM Fe(II) produced on addition of 0.89 mM ZVI, 120 μM produced on addition of 1.79 mM ZVI and 140 μM produced on addition of 2.68 mM ZVI. An Fe(II) concentration of 140 μM appears to be the maximum achievable as higher concentrations of ZVI do not lead to a greater concentration of Fe(II) in solution.

The subsequent loss of Fe(II) from solution occurs over the ensuing 60-90 minutes and may result from adsorptive or oxidative processes though the rate of oxygen-mediated oxidation of ferrous iron at pH 4 ($\tau_{1/2} \approx 2$ years) is substantially slower than the rate of removal observed (Stumm and Morgan, 1996).

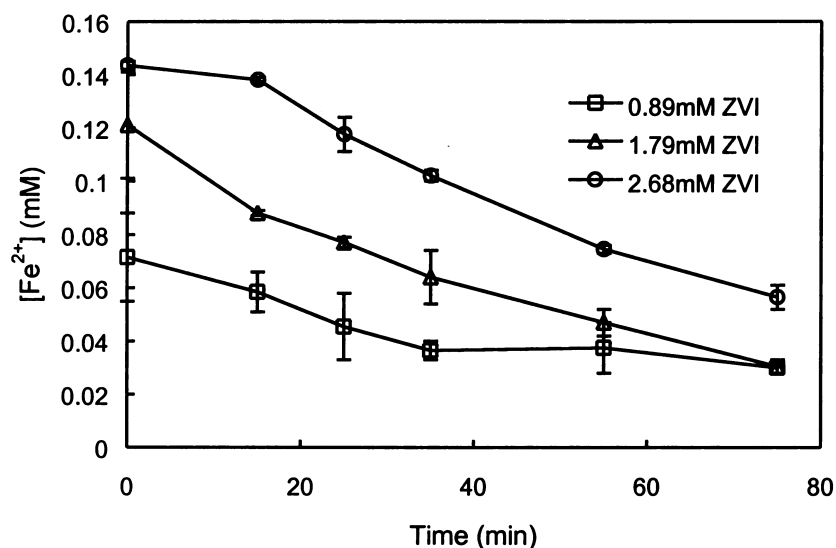


Figure 4.8. Dissolved ferrous iron concentrations in pH₀ 4 solutions containing 0.89, 1.79 and 2.68 mM ZVI.

While the concentration of ferrous iron in solution at pH 8.1 has not been measured, much lower concentrations than observed at pH 4 are to be expected as a result of both the relatively rapid rate of Fe(II) oxidation at pH 8.1 ($\tau_{1/2} \approx 3-4$ minutes) and the likely adsorption of Fe(II) species to Fe⁰ and/or Fe(III) iron oxyhydroxides formed as a result of Fe(II) oxidation.

The possibility exists that the rapid appearance of Fe(II) in the reaction mixtures can be attributed to ferrous iron present in the stock ZVI suspension and added to the reaction

mixture on addition of Fe^0 . This possibility was checked and, indeed, a portion of the Fe(II) present in the reaction mixture appears to be present initially in the reaction mixture. As can be seen from Figure 4.9a, addition of an identical volume of supernatant from the ZVI stock results in a measurable (ca. $25 \mu\text{M}$) concentration of ferrous iron though this is significantly less than the ferrous iron concentration (ca. $120 \mu\text{M}$) generated on addition of ZVI to the oxygenated reaction mixture. This issue was further investigated by examining the extent of release of ferrous iron on addition of ZVI to a deoxygenated reaction mixture and, once steady-state conditions had been reached, sparging with zero-grade air. As can be seen in Figure 4.9b, air sparging resulted in a sudden dramatic increase in dissolved ferrous iron concentration consistent with rapid corrosion of the ZVI.

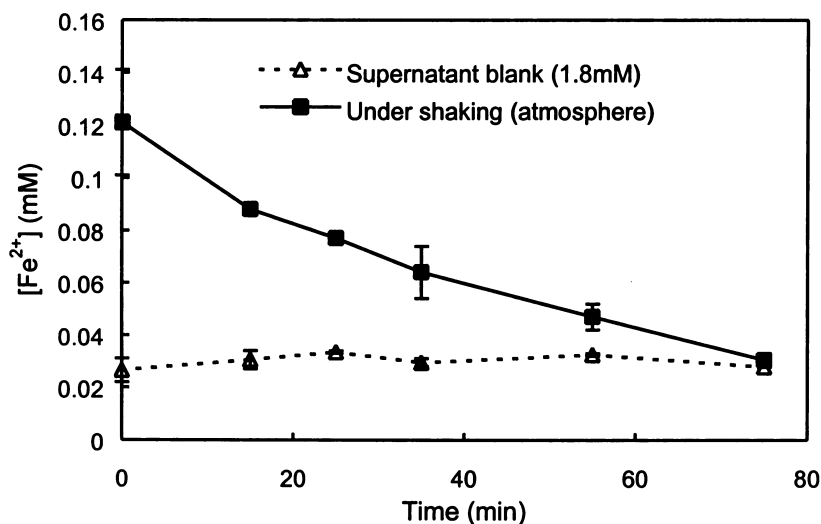


Figure 4.9 a. $[\text{Fe}^{2+}]$ in the reaction mixture on addition of a ZVI solution and an equivalent volume of the ZVI supernatant. Conditions: $\text{pH}_0 = 4$, $[\text{ZVI}]_0 = 1.8 \text{ mM}$.

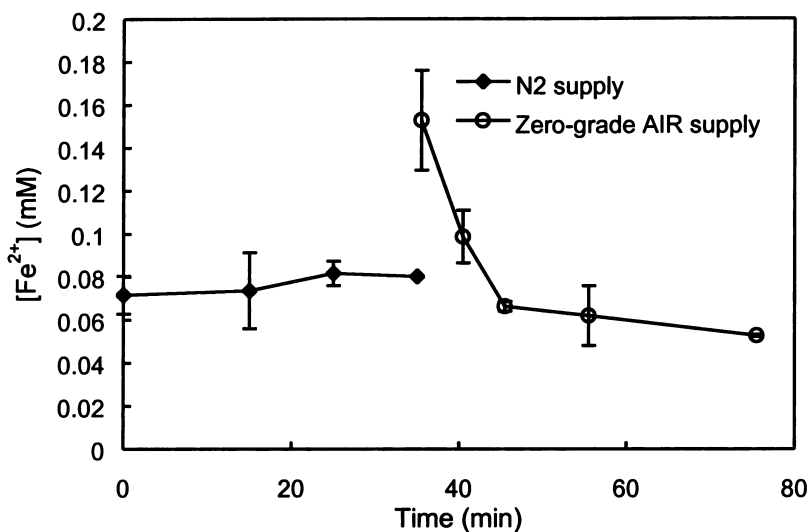


Figure 4.9b. $[\text{Fe}^{2+}]$ in the reaction mixture after ZVI addition to a nitrogen-sparged suspension with subsequent air-sparging. Conditions: $\text{pH}_0 = 4$, $[\text{ZVI}]_0 = 1.8 \text{ mM}$.

Interestingly, the concentration of ferrous iron released to solution in the presence of ZVI but under N_2 sparging is significantly greater than observed when adding ZVI supernatant alone to the reaction mixture (approximately $70 \mu\text{M}$ compared to $30 \mu\text{M}$ from Figures 4.9a and b). It is thus apparent that the ZVI does release some ferrous iron to the reaction mixture that was present in adsorbed form in the ZVI stock. However, at least a doubling in ferrous iron concentration is observed on introduction of oxygen, presumably as a result of rapid corrosion of the ZVI.

Confirmation that a portion of ferrous iron was retained on the ZVI surface (presumably as a result of adsorptive effects) was obtained by continuously monitoring the concentration of both dissolved and adsorbed Fe(II). As shown in Figure 4.10, total Fe(II) (adsorbed plus dissolved) remains constant over the 60min duration of the study. The dissolved fraction is observed to attain concentrations somewhat lower than the total concentration.

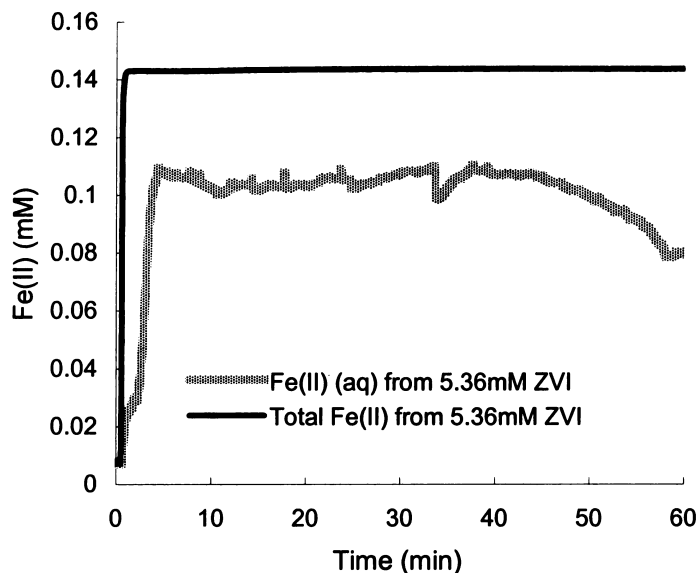


Figure 4.10. Fe(II) generation on addition of colloidal ZVI to reaction medium in unbuffered solution ($\text{pH}_0 \sim 6.4$).

4.2.4.2. Effect of use of dried ZVI particles

Dried ZVI particles were obtained by twice washing the ZVI stock solution (pH 4) with Milli-Q water, centrifuging the wet particles, decanting and discarding the supernatant, immersing the centrifuge tube containing the remaining solids into liquid nitrogen to limit oxidation, followed by drying under vacuum over 20hours using a freeze drier. Dried ZVI particles were dispersed into solution using sonication for 10min before adding molinate. Continuous on-line monitoring over 60min was undertaken in order to observe the extent of ferrous iron release from the particles.

The total ferrous iron generated from the dried samples (Figure 4.11) is similar to that observed from colloidal ZVI although the fraction of dissolved ferrous iron from dried ZVI is significantly less than observed for the particles that had been maintained wet. Possibly

consistent with the lower extent of ferrous iron release from dried ZVI particles is a smaller increase in pH on addition of the particles to solution compared to that observed for the wet particles.

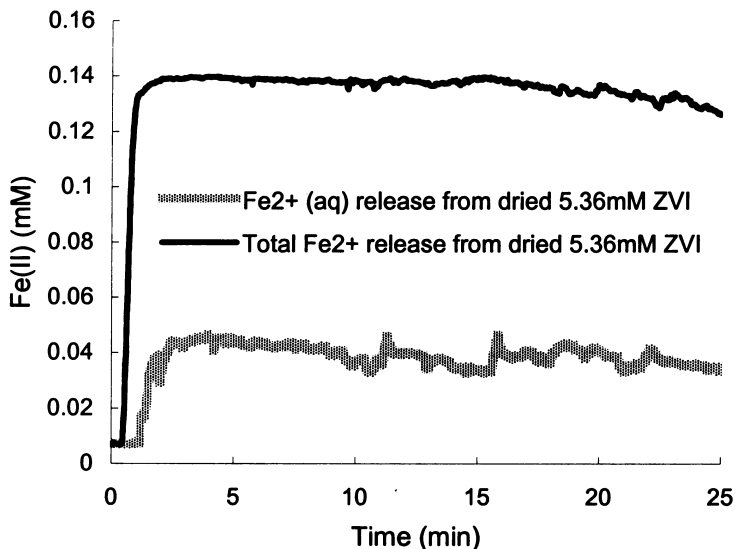


Figure 4.11. Fe(II) generation on addition of dried ZVI to reaction medium in un-buffered solutions ($pH_0 \sim 6.4$).

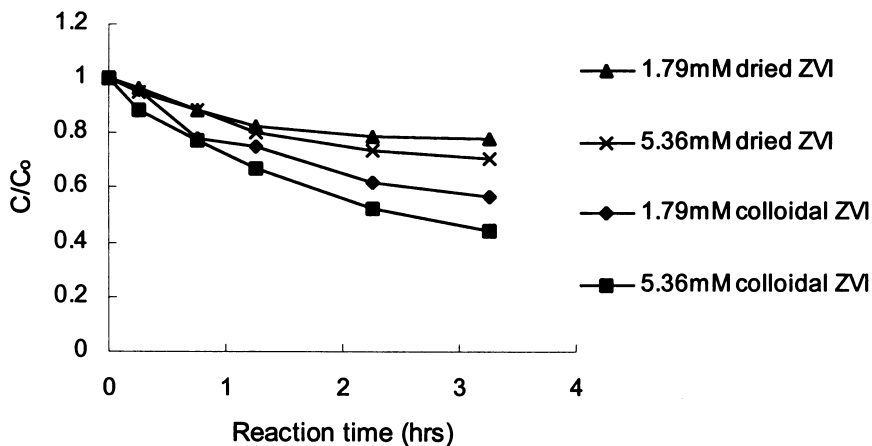


Figure 4.12. Comparison of molinate degradation using ZVI concentrate and dried ZVI (100ppb molinate; $pH_0 \sim 6.4$).

The results in Figure 4.12 indicate that there is a somewhat lower rate of molinate degradation for both 1.8 and 5.4mM ZVI using the dried particles compared to the colloidal particles, presumably because of the increased tendency for formation of an outer oxidized layer that inhibits the rate of molinate degradation. While the dried particle results suggest that the overall oxidation process is retarded by surface oxidation, residual oxidizing capacity remains in the particles despite oxidation of the outer surface. The formation of a passivating layer of iron oxide on oxidation of Fe^0 has been described by Davenport *et al.* (2000) who showed that a layer with properties similar to $\gamma\text{-Fe}_2\text{O}_3$ and Fe_3O_4 formed on the particle surface on exposure to oxygen.

Ferrous iron released from ZVI in the presence of 2mM bicarbonate (pH 8.1) was monitored using the on-line continuous system. It was observed that the Fe^{2+} concentrations released from ZVI were much less than for the unbuffered suspensions for both dried and colloidal ZVI with concentrations for dried and colloidal 5.4mM ZVI of around 20 μM and 35 μM respectively (Figure 4.11 and 4.13). The dried ZVI revealed much less Fe(II) release at pH 8.1 than that at pH 6.4 (40 μM Fe(II) at pH 6.4. vs 20 μM Fe(II) at pH 8.1) and presumably reflects both an increased tendency for formation of an iron oxide surface coating and an increased affinity of Fe(II) for this coating at higher pH.

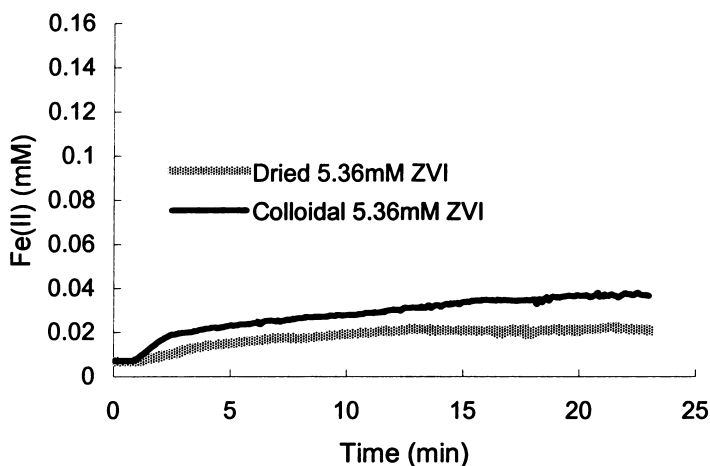


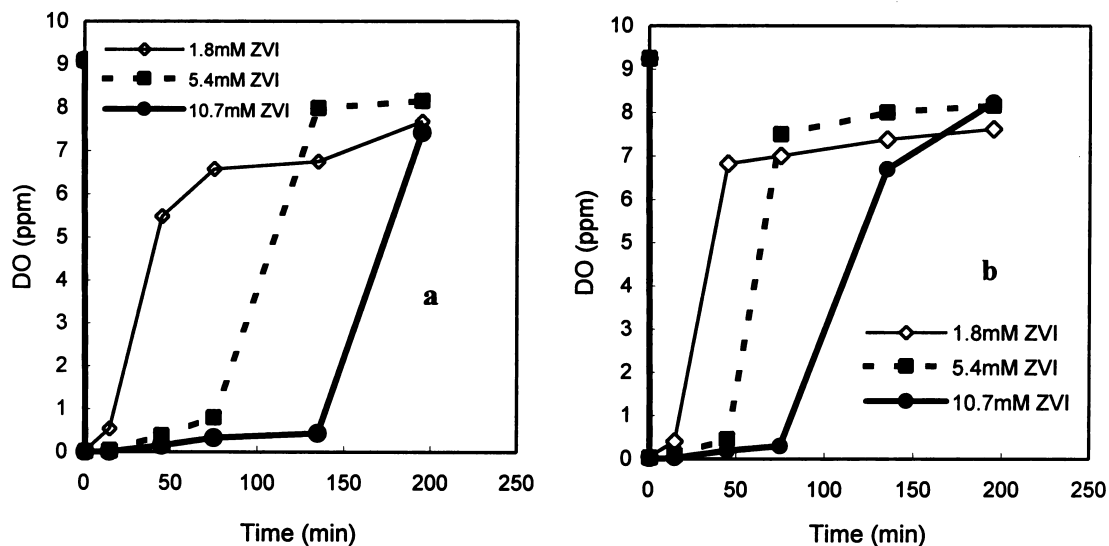
Figure 4.13. Dissolved Fe(II) generation from colloidal and dried ZVI at pH 8 in bicarbonate buffered system.

As indicated earlier, there is a general slowing down in the reaction rate at higher pH in the bicarbonate buffered system although little difference in the initial removal rates for pH_0 s ranging from 4 to 8.1 was observed (Figure 4.6). Note that for every mole of oxygen initially consumed (0.26mM at saturation) – assuming that Fe^0 is in excess – between 2 and 4 moles of H^+ ions are consumed leading to a large rise in pH. The rise in pH is tempered by diffusion of atmospheric CO_2 into the suspension and the ensuing carbonate buffering ensures that the maximum pH does not exceed pH 8.1. Within 15 minutes, the pH reaches approximately pH 7 regardless of whether the initial pH is 4 or 6.4 and reaches pH 7.4 for both experiments after 3 hours. There is no change in pH when the initial pH of the suspension is pH 8.1. The rapid alignment of pHs, independent of the starting pH over the range studied, is the most likely explanation for the similarities in degradation rates (Figure 4.6).

4.2.5. Effect of DO

The DO concentrations during ZVI corrosion were measured. Solutions with initial pHs of 4 (obtained by HCl addition) and 8.1 (obtained using 2mM bicarbonate) were saturated with

air for 10min and then spiked to give 100ppb molinate in a total volume of 50mL. After adding different concentrations of ZVI, DO changes were monitored using an Au/Ag DO probe with teflon membrane. As can be seen in Figure 4.14, the dissolved oxygen concentration decreased to zero immediately after adding ZVI and then increased to >70% saturation within 40-200 minutes depending on the ZVI concentration and initial pH. The increase in DO is a result of oxygen influx from the atmosphere. Long lag times are observed for higher ZVI doses due to a greater capacity for the ZVI surface to consume O₂ (Figure 4.14a, b). These effects are more distinctive at low pH.



< Figure 4.14. DO variations during molinate degradation a. pH₀ 4, b. pH₀ 8.1 >

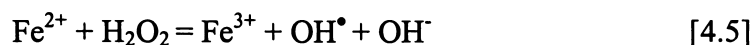
4.2.6. Hydrogen Peroxide Generation

Hydrogen peroxide was monitored since it is considered to be a possible product of the reduction of oxygen. The method used is similar to that developed by Balmer and Sulzberger (1999) and involves the use of the reagent DPD (*N,N*-diethyl-*p*-phenylenediamine). In the data presented here, no attempt was made to minimize the interaction of Fe(II) with peroxide as was done by Bader *et al.* (1988). Later attempts to

assess the potential for artifacts associated with the presence of Fe(II) indicated some interference from Fe(II) which could be controlled by adding bipyridine and EDTA. However, the concentrations and trends were not significantly different from those observed in the absence of the complexing agents. Samples were filtered through 0.22 μ m filters prior to analysis. At different initial pHs (e.g., pH₀ 4 and pH₀ 8.1) and constant time intervals, H₂O₂ was measured as a function of ZVI concentrations (Figure 4.15). Figure 4.15a shows the hydrogen peroxide generation on addition of ZVI to aerobic pH 4 solutions with 5 - 6 μ M H₂O₂ produced over extended times of about one hour or more over a range of ZVI concentrations. Although H₂O₂ was not measured under anaerobic condition almost no H₂O₂ is expected as indicated by Zečević *et al.* (1989), who observed that on the oxide-free surface, very little H₂O₂ is formed (less than 0.5% of the total reduction current). Interestingly, steady state concentrations of this magnitude were reached at lower Fe⁰ doses more quickly than at higher doses of iron. As the dosage of zero valent iron was increased, a distinct lag was observed before H₂O₂ could be detected but with concentrations subsequently increasing to the 5 - 6 μ M level. The detection of μ M concentrations of H₂O₂ suggests that superoxide is the likely intermediate or the formation of H₂O₂ could be from the protonation of O₂²⁻, which is the reduction of O₂, i.e.



The initial absence of H₂O₂ at higher ZVI doses at pH₀ = 4 is consistent with rapid reaction of H₂O₂ with Fe²⁺ released during the corrosion process, i.e. the Fenton reaction:



$$k \text{ (at pH 4)} = 586 \text{ M}^{-1}\text{s}^{-1} \text{ (Wells and Salam, 1968a)}$$

which results in the production of ferric iron and highly oxidative hydroxyl radicals.

The initial (at time 10s) peroxide measured (at pH 4) as a function of ZVI revealed that peroxide concentration increased with ZVI dose at relatively low concentrations (a maximum of 5.3 μM H_2O_2 was generated from 70 μM ZVI) followed by decrease at comparatively higher ZVI (Figure 4.16). The maximum initial behaviour could be due to the surface total oxygen concentration and the initial Fe(II) concentration in the suspension. Small but significant concentrations of hydrogen peroxide (1 - 2 μM) were detected at pH 8.1. The initial concentrations were slightly higher than those at pH 4 (Figure 4.15b) and again inversely proportional to the ZVI concentration. Unlike at $\text{pH}_0 = 4$ where H_2O_2 was not detected initially except at very low ZVI concentrations, small amounts of H_2O_2 were measured at 10s for ZVI concentrations ranging from 0.54 to 2.7mM at $\text{pH}_0 = 8.1$ (Figure 4.15b). The difference is probably due to the rapid oxidation of ferrous to ferric by O_2 at higher pH (Scherer *et al.*, 1998), out competing reaction via the Fenton reaction (Equation 4.5).

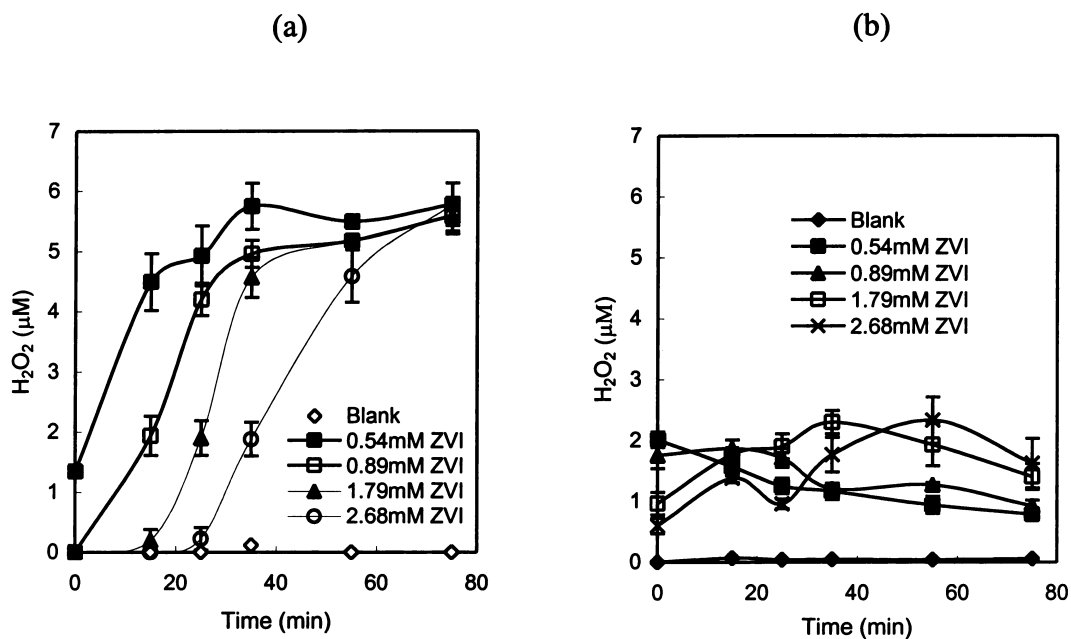


Figure 4.15. H_2O_2 generations on addition of various amounts of ZVI at pH_0 4 solutions (a) and pH_0 8 solutions (b).

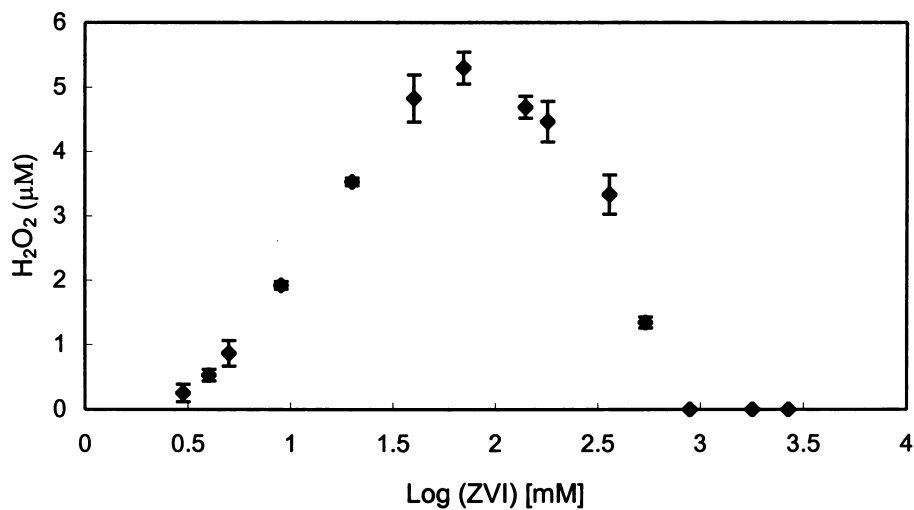


Figure 4.16. Instant (initial) generation of H_2O_2 as a function of ZVI at pH 4.

Figure 4.17 shows the results of kinetic experiments conducted at pHs of 4 and 8.1 over longer reaction times. As can be seen, the hydrogen peroxide concentration in pH 4

solutions was quite stable for extended periods of time once a plateau had been reached. In comparison, at pH 8.1, while hydrogen peroxide was certainly still detectable, its concentration peaked (at about 2 μM) within about 30 minutes of adding the ZVI to the solution and then decreased to immeasurable concentrations in the ensuing 2-3 hours.

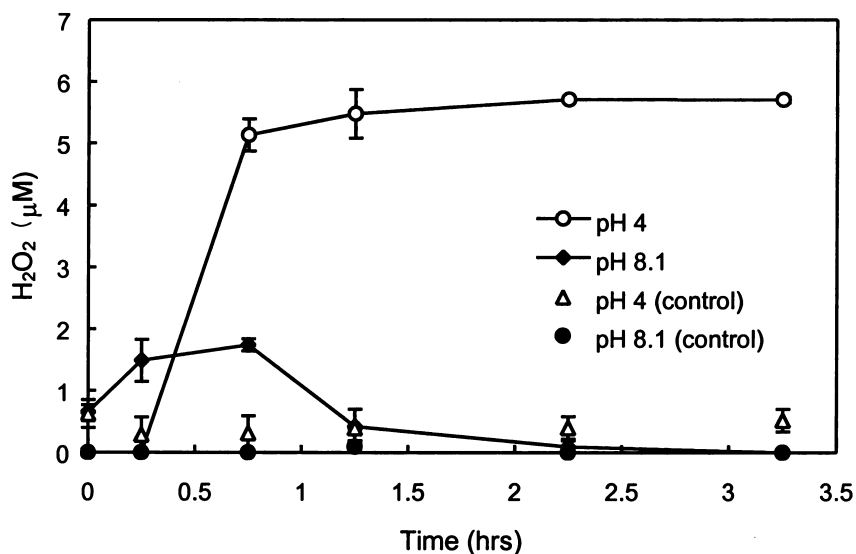


Figure 4.17. Comparison of H_2O_2 concentrations in pH 4 (\circ) and pH 8.1 (\blacklozenge) solutions containing 1.79 mM ZVI.; Possible H_2O_2 concentrations resulting from addition of stock solution is given for pH 4 (\triangle) and pH 8.1 (\bullet).

4.2.7. Catalase and butanol competition

That hydrogen peroxide plays a key role in degradation of molinate is suggested by examination of the effect of addition of catalase, an enzyme that induces the rapid degradation of hydrogen peroxide, to the experimental system. As can be seen in Figure 4.18, no degradation was observed in the presence of catalase. While this result is suggestive, it is not definitive of a key role for hydrogen peroxide. Other oxidants such as the powerful hydroxyl radical could be involved which may well be scavenged by

compounds such as catalase. Indeed, as can be seen from the results shown in Figure 4.19, little degradation of molinate is observed in the presence of 1-butanol, an effective hydroxyl radical scavenger.

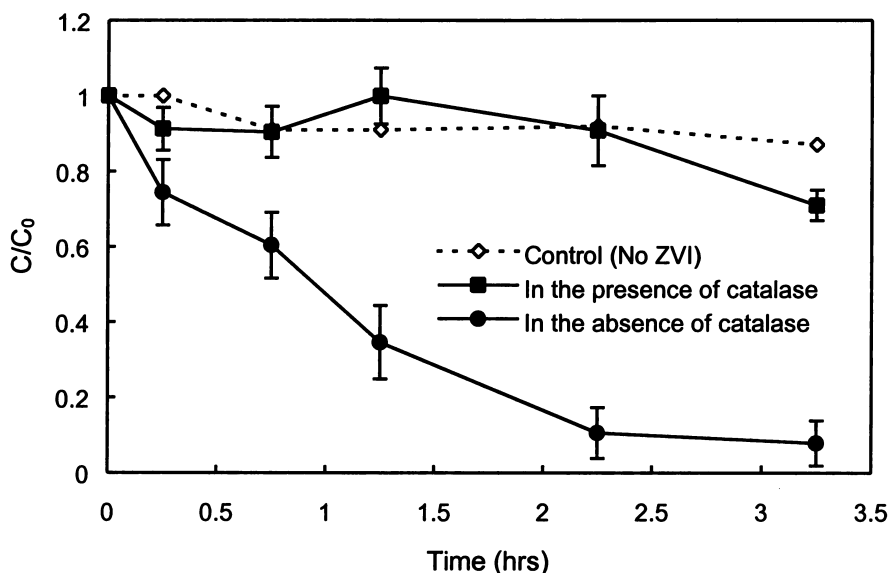


Figure 4.18. Effect of ZVI-mediated degradation of molinate of 60ppm catalase. Conditions: [Molinate]₀ = 100ppb and [ZVI]₀ = 10.7mM.

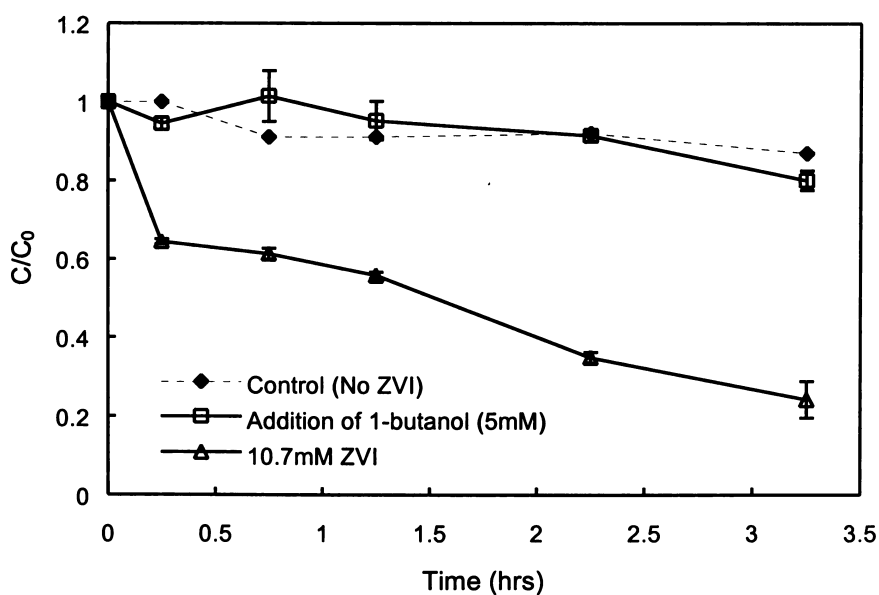


Figure 4.19. Effect on ZVI-mediated degradation of molinate; 5mM 1-butanol. Conditions: [Molinate]₀ = 100ppb and [ZVI]₀ = 10.7mM, butanol study undertaken at pH₀ 4.

4.2.8. Degradation Byproducts

Reaction intermediates are usually of low stability and undergo fast degradation, making detailed study of intermediate species a difficult task. Moreover, they occur at low quantities, sometimes only in trace amounts, and are difficult to isolate and identify. As indicated by Pichat (1997) most intermediates can be identified only when the initial substrate concentration is raised by about two orders of magnitude (Pichat, 1997). High concentrations (10 mg/L) of molinate were degraded using ZVI in order to isolate and identify the intermediate products. Byproducts were identified using GC/MS analysis. Since the byproduct peaks were relatively small compared with that from molinate, all the ZVI particles in suspension containing molinate (10ppm) after the final reaction time (3.25hrs) were removed in order to clearly identify the intermediate peaks. ZVI particles were separated from the suspension using magnetic separation. 2mL of hexane was then added to the wet ZVI particles which were sonicated for 20min and using centrifugation at 2000rpm for 5min. The extracted supernatant was analyzed using GC/MS-EI (TIC). An example chromatogram for ZVI/O₂ showing molinate and keto-molinate peaks as a function of retention time is given in Figure 4.20.

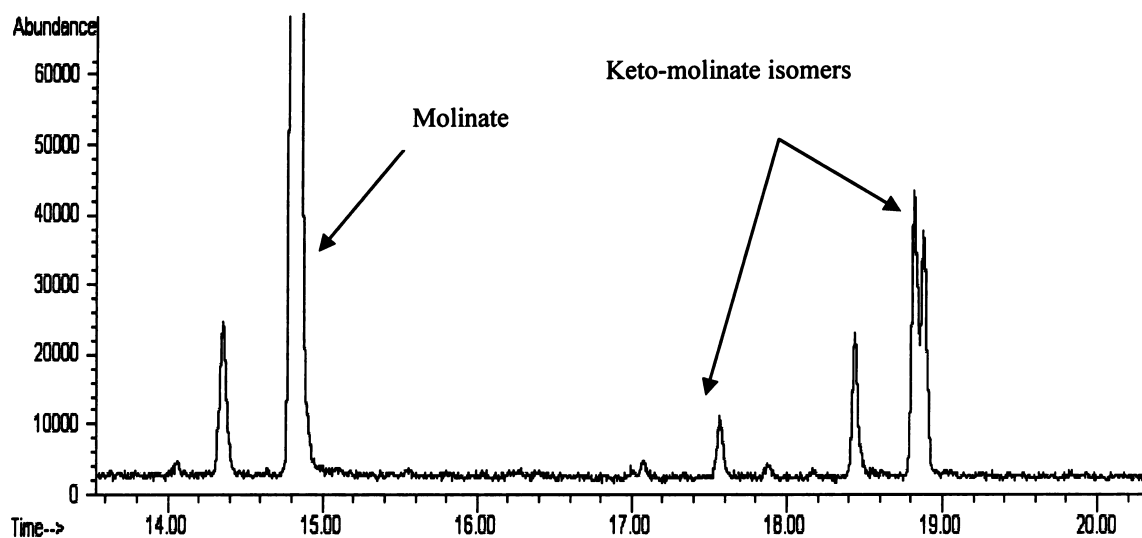


Figure 4.20. GC/MSD-EI (TIC) obtained from ZVI extracted after the reaction time of 3.25hrs.

Qualitative analysis using SCAN mode (total run time: 35min) was performed and mass spectra were collected in the total ion current (TIC) mode to characterize each fragment. Two peaks, which exhibited retention times of 17.6 and 18.8 min, were closely investigated since these peak areas increased as molinate concentration decreased during the reaction. The mass fragments of these peaks were different from the molinate mass fragments and had different retention times:

m/z and abundance (%) at 17.6min:

112 (100), 69 (44), 140 (25), 201 (45), 56 (17)

m/z and abundance (%) at 18.8min:

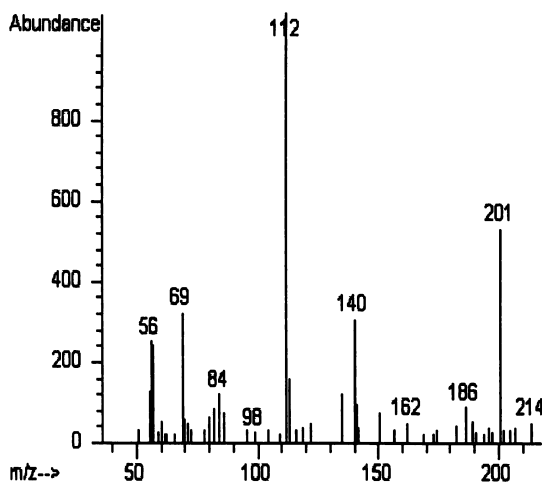
112 (100), 69 (22), 140 (65), 201 (35), 56 (17)

m/z and abundance (%) at 14.9min (molinate):

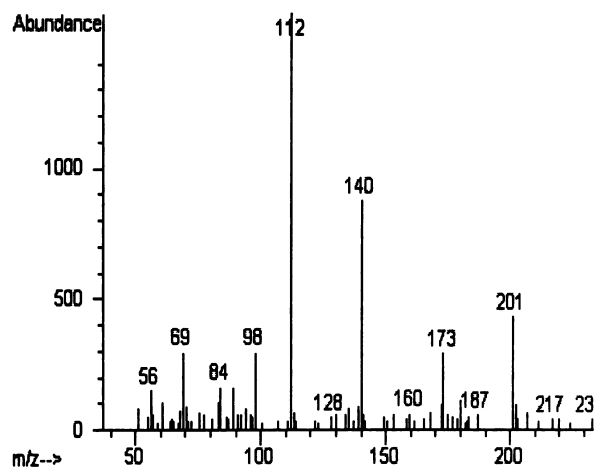
126 (100), 55 (39), 187(37), 83(16), 98(14)

GC/MS results obtained on samples after 3.25 hours of reaction time are shown in Figure 4.21 and reveal the presence of both the starting material (molinate) and the major products, keto-molinate isomers. By interpretation of the mass fragmentation patterns, keto-molinate isomers presumably arise from attack at the N-alkyl chain (azepine ring) of molinate.

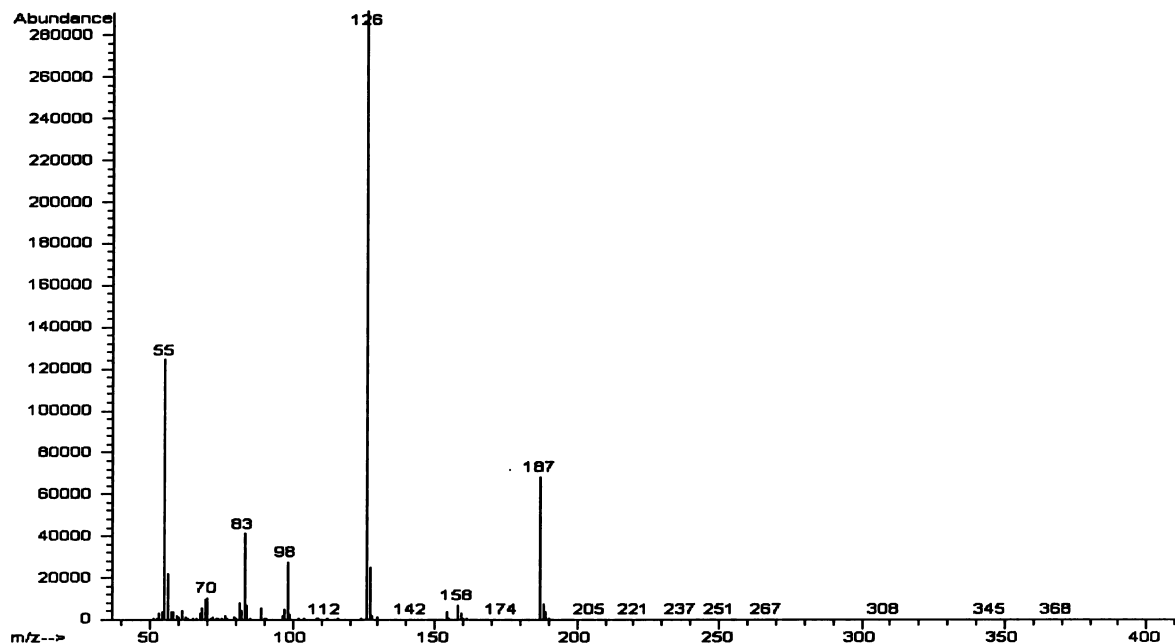
The mass spectra of these peaks do not have the hexahydroazepine isocyanate ion (m/z : 126), the base peak of molinate, and yield oxygenated hexahydroazepine isocyanate ions (m/z : 140) and weak molecular ions (m/z : 201). The major products, keto-molinate isomers are formed by oxygen addition to partially oxidized molinate. This observation was consistent with the findings of Konstantinou *et al.*, 2001 who identified keto-molinate isomers from the photocatalytic degradation of molinate over aqueous TiO_2 suspensions. The process is rationalized as hydrogen abstraction by surface-bound hydroxyl radicals occurring preferentially on the N-alkyl chain, resulting in rapid decomposition, particularly in the case of aliphatic thiocarbamates (Konstantinou *et al.*, 2001).



Keto-molinate isomers (a) RT (17.6min)



(b) RT (18.8min)

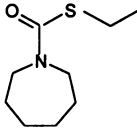
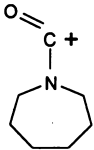
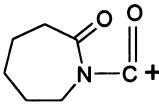
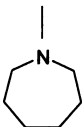
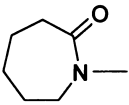


(c) RT (14.9min): molinate

Figure 4.21. Mass fragments for each peak on keto-molinate and molinate.

The likely fragmentation processes leading to the molinate and keto-molinate mass/charge patterns are summarized in Table 4.1, which illustrates the structure of the main mass fragments of molinate and intermediates (keto-molinate isomers) with functional group lost. As can be seen in Table 4.1, the [C=O] group is lost twice in keto-molinate isomers (but not in the parent compound), confirming that the keto-molinate structure has a functional group of [C=O] that is generated from oxidation.

Table 4.1. Interpretation of mass fragments of molinate and molinate degradation product (keto-molinate isomers).

Molinate	Keto-molinate isomers	Functional group lost
$M^+ = 187$ 	$M^+ = 201$	
$m/z = 126$ 	$m/z = 140$ 	- [S-CH ₂ -CH ₃]
$m/z = 98$ 	$m/z = 112$ 	- [C=O]
$m/z = 83$ (C ₆ H ₁₁)	No ion	- [N-H]
No ion	$m/z = 84$ 	- [C=O]
No ion	$m/z = 69$ (C ₅ H ₉)	- [N-H]

4.3 Molinate degradation by combined ZVI and H₂O₂

The possibility of enhancing ZVI oxidative degradation through the addition of hydrogen peroxide was investigated. Hydrogen peroxide is decomposed to hydroxide and hydroxyl radical in the presence of transition-element catalysts such as iron. Hydroxyl radicals are strong, nonselective oxidants that react with most organic compounds at rates near the diffusion-controlled limit of $10^{10} \text{ M}^{-1}\text{s}^{-1}$. Dowling and Lemley (1995) found that organophosphate insecticides and their breakdown products are susceptible to degradation via hydroxyl radical attack and preliminary studies showed that the addition of peroxide to

nanoscale ZVI (using a 1.6:1 ratio of Fe(0) and H₂O₂) significantly increased the removal rate of organophosphorus insecticides such as chlorpyrifos (>90% degraded within 15min).

4.3.1 Effect of ZVI at fixed hydrogen peroxide concentration

Investigations of the effect of ZVI concentration on molinate degradation in the presence of hydrogen peroxide (H₂O₂) were undertaken. As shown in the Figure 4.22, addition of 50mM H₂O₂ to different concentrations of ZVI significantly enhanced the degradation rate of molinate. Approximately 40% of the molinate is removed over 3 hours in the presence of 50mM H₂O₂ and the rate is further enhanced upon addition of ZVI. Depending on the initial ZVI doses and the ratios, there is an initial sharp fall in concentration followed by slower degradation that results in the removal of between 70-100% of molinate over 3 hours (Figure 4.22). The biphasic shape of the degradation curves suggests that Fe(II) is rapidly consumed upon addition of H₂O₂ but there is slower continued degradation following the initial high activity.

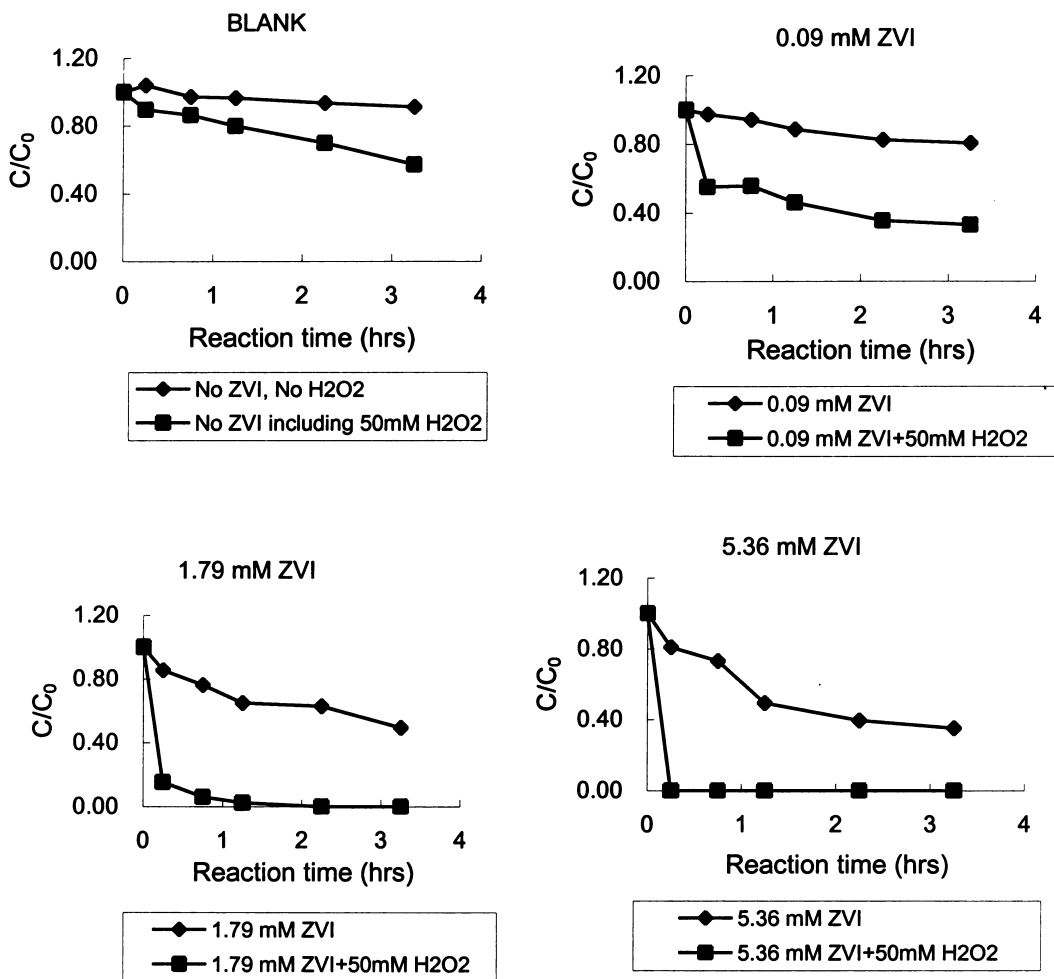


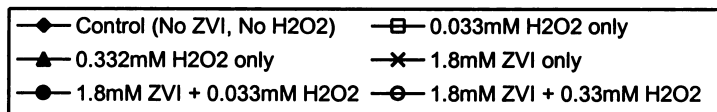
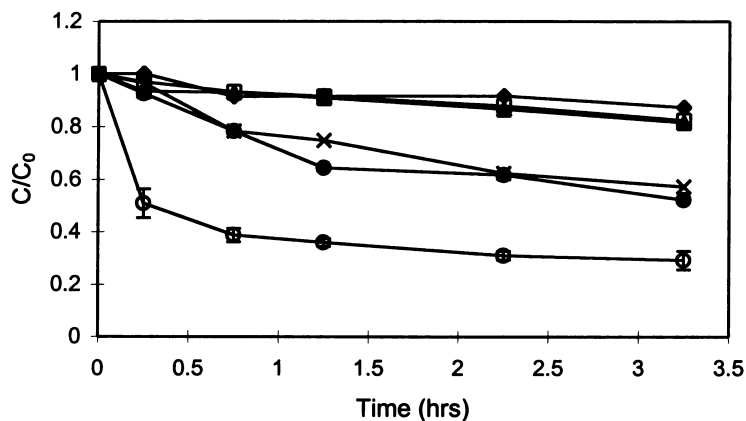
Figure 4.22. The effect of ZVI dose at fixed hydrogen peroxide. Condition: unbuffered (pH₀ ~ 6.4), 5ppb molinate.

4.3.2. Effect of hydrogen peroxide at constant ZVI

The effect of low levels of peroxide at constant ZVI was examined and the results are given in Figure 4.23. The results indicate that while low levels of hydrogen peroxide (e.g. 0.033mM and 0.33mM H₂O₂) have little ability to degrade molinate, its use in combination with 1.8mM ZVI significantly enhanced the rate of degradation. The degradation results indicate that there is no additional enhanced in degradation if only 33μM of H₂O₂ is added

to 1.8mM of ZVI. This level of H₂O₂ can therefore be considered a lower limit for enhanced degradation and may be similar to the transient levels of H₂O₂ initially generated upon addition of ZVI to the molinate solution.

A.



B.

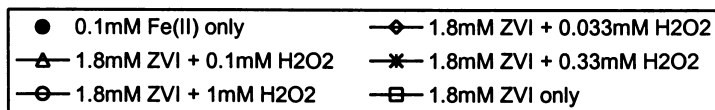
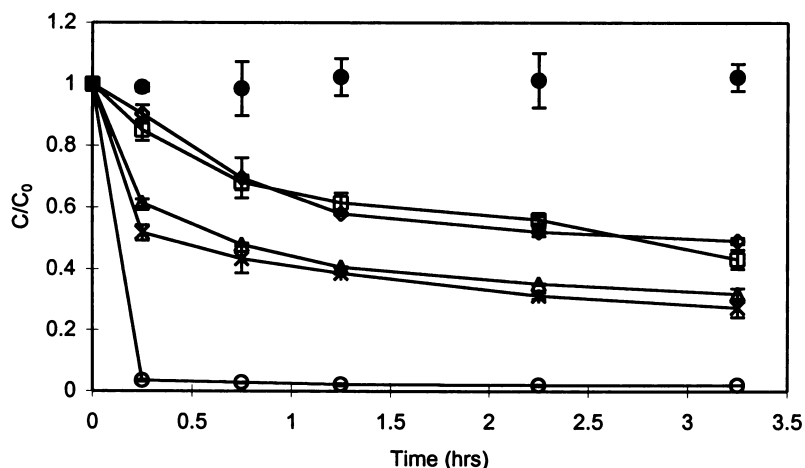


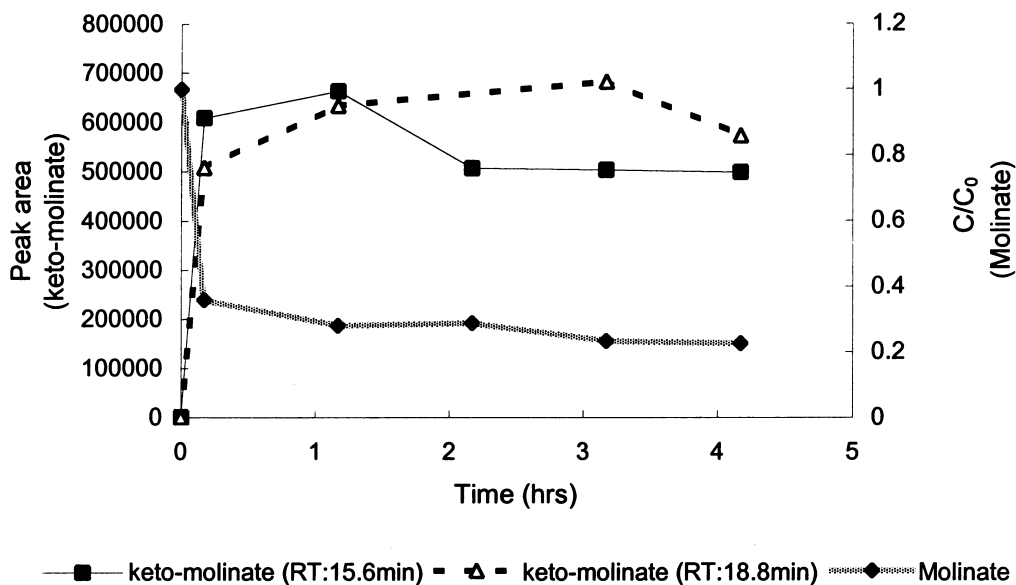
Figure 4.23. The effect of peroxide at constant ZVI: Molinate (100ppb) degradation in the presence of Fe⁰ and H₂O₂ (pH₀ = 6.4 ± 0.3).

Molinate degradation efficiency was increased with increasing H_2O_2 dose. The effect of ferrous iron only in the absence of ZVI was also investigated to assess whether there is any effect of the oxygenation of Fe(II) to Fe(III) on molinate degradation. When ferrous iron alone is added to molinate, no degradation is observed (Figure 4.23).

4.3.3. Degradation byproducts by combined ZVI and H_2O_2

Since similar molinate degradation behaviour was observed with both ZVI and coupled ZVI/ H_2O_2 , extraction experiments were conducted to examine whether there was any difference in the byproducts generated for both processes. Byproduct experiments were conducted using 10ppm molinate, 19.6mM ZVI and 20mM of H_2O_2 for the coupled system. After 15min reaction for the ZVI only system and 10min for the coupled system, all ZVI particles were extracted using 2mL hexane, followed by sonication for 20min, centrifugation and direct injection into the GC/MS. The extent of molinate degradation was 33% for the ZVI only system and 64% for the coupled ZVI/ H_2O_2 system (Figure 4.24). The major byproducts in both cases were identified to be keto-molinate isomers (Figure 4.25).

A.



B.

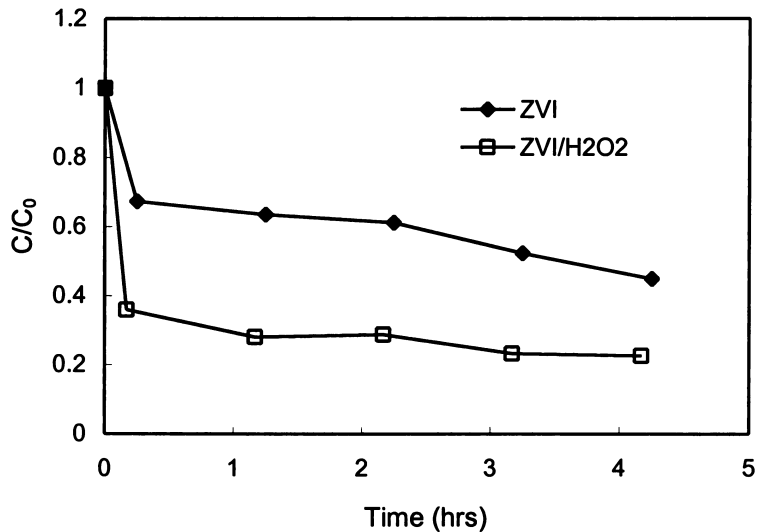


Figure 4.24. (A). Disappearance of molinate and production of by-product by ZVI/H₂O₂ (B) molinate degradation by ZVI (19.6mM) and coupled ZVI (19.6mM) and H₂O₂ (20mM).

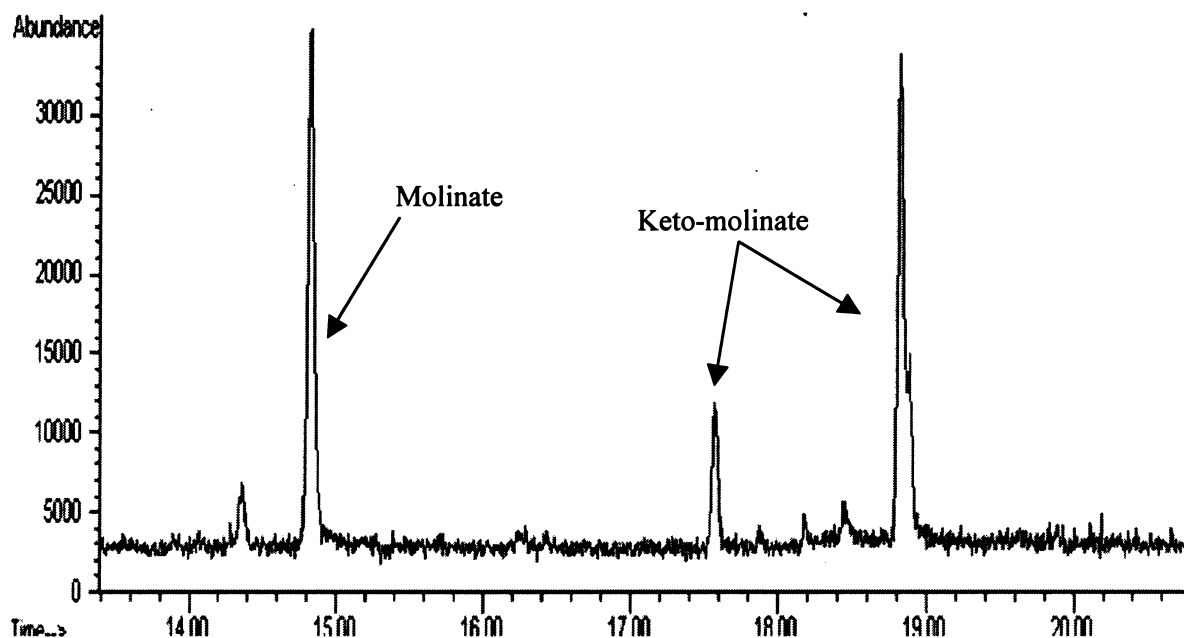


Figure 4.25. Molinate degradation and the formation of byproducts by ZVI/H₂O₂.

4.3.4. Fe(II) generation from coupled ZVI/H₂O₂ in the presence of molinate

4.3.4.1. Comparison of Fe(II) generation in the absence and presence of peroxide

Dissolved Fe(II) was quantified by monitoring the absorbance of an Fe(II)-bipyridine complex at 522nm (Voelker, 1994) both in the absence and presence of molinate. As can be seen in Figure 4.26, the initial concentrations of Fe(II) observed in solution increases with increasing ZVI with a subsequent loss of Fe(II) from solution occurring over time. There was no substantial difference in Fe²⁺ evolution and disappearance between ZVI only and ZVI/H₂O₂ systems, given the low levels of H₂O₂ used in the coupled system. The results are consistent with the similar rates of molinate degradation observed for the two systems (Figure 4.23b).

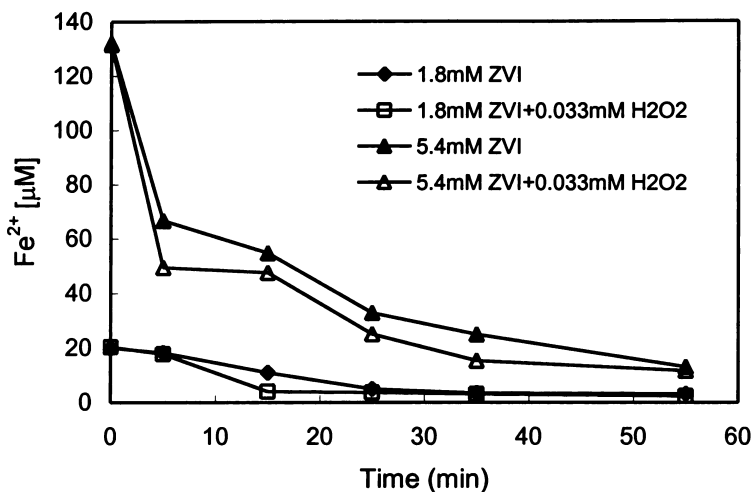


Figure 4.26. Dissolved Fe(II) variations during molinate degradation by H₂O₂/ZVI in pure water (pH₀ ~ 6.4), molinate 100ppb.

4.3.4.2. Fe²⁺ release in the absence of molinate (online continuous measurement)

Both adsorbed and dissolved Fe²⁺ generated during the ZVI/H₂O₂ process was measured using the continuous analytical system. In the ZVI/H₂O₂ (0.33mM H₂O₂) case, both the total and dissolved Fe²⁺ fractions decrease after 30min (Figure 4.27). At higher H₂O₂ concentrations (3.3mM), the total Fe²⁺ is considerably lower and very little dissolved Fe²⁺ is observed.

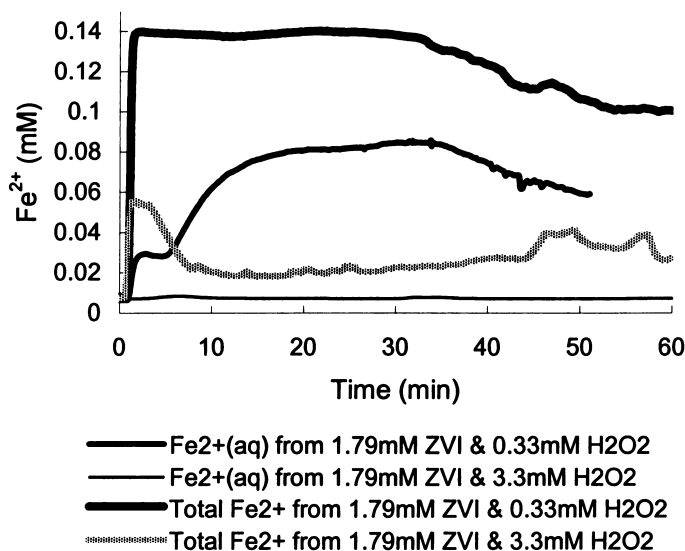


Figure 4.27. Fe^{2+} release from ZVI in presence of H_2O_2 ($\text{pH}_0 \sim 6.4$).

4.4 Molinate degradation using Fenton's reagent

Fenton's reagent is a mixture of ferrous iron and hydrogen peroxide which leads to the generation of hydroxyl radical (OH^\bullet) through the iron-catalyzed decomposition of hydrogen peroxide in acidic solution:



pHs of <3.5 are optimal as this ensures high solubility of iron as well as a higher reducing potential. At higher pH, hydrogen peroxide decomposes to water and oxygen resulting in excessive consumption of H_2O_2 :



As can be seen in Figure 4.28A, the extent of molinate degradation is dependent on ferrous iron availability when H_2O_2 is in excess. The removal kinetics of molinate is initiated by rapid decay followed by much slower degradation. The slow removal is likely to be due to

the slow regeneration of Fe(II) from the oxidized Fe(III). When Fe(II) rather than H₂O₂ is in excess (Figure 4.28B), the reaction ceases after 15minutes as there is insufficient H₂O₂ for further degradation.

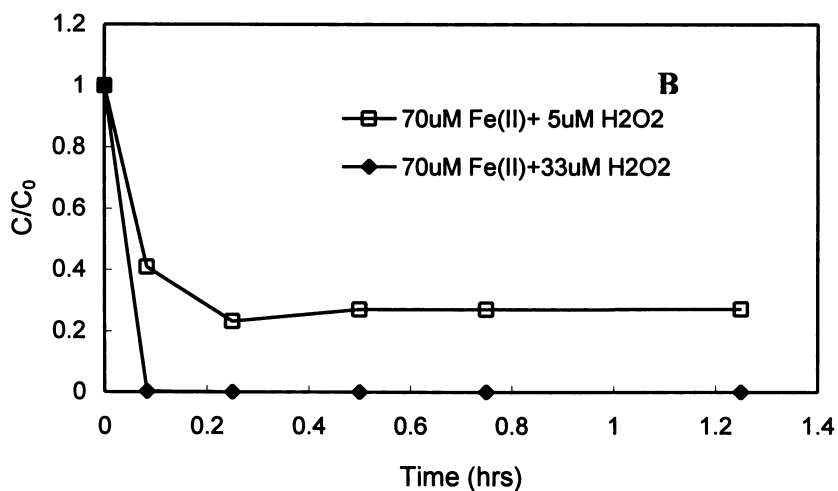
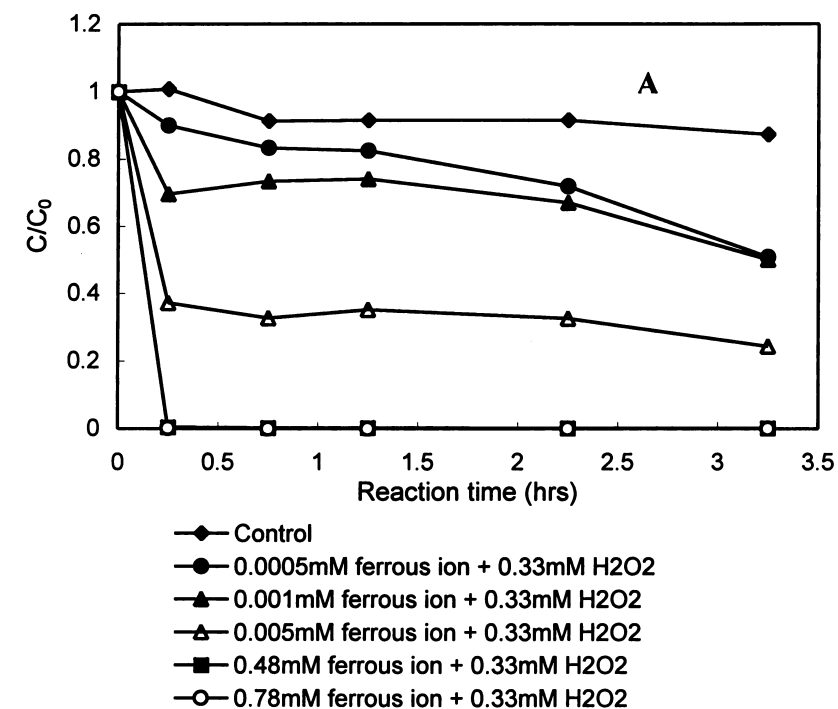
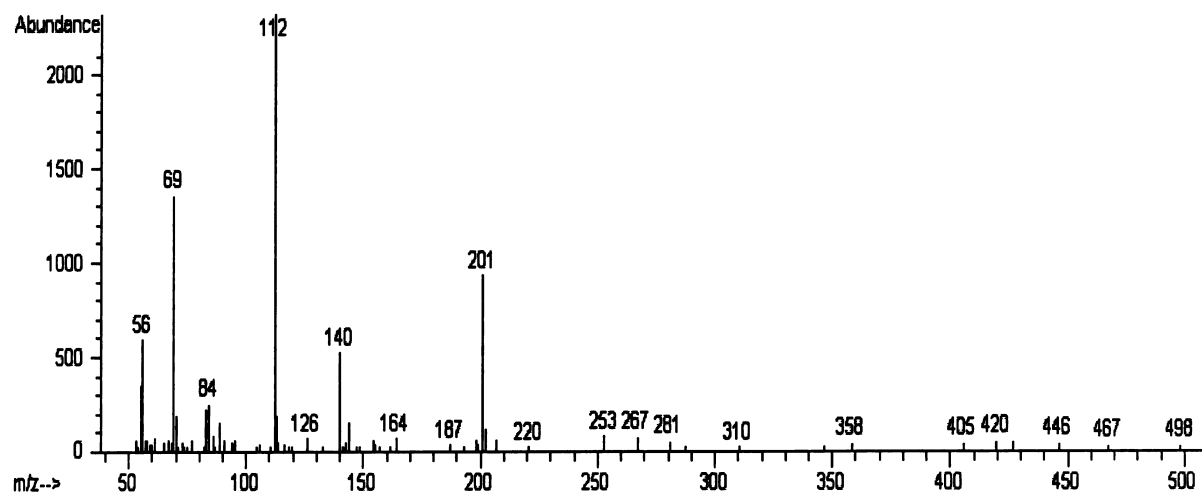


Figure 4.28. Degradation kinetics using Fenton's reagent under different pH for the removal of molinate (100ppb); A: pH₀ = 6.4 ± 0.3, B: pH 4.

4.4.1. Degradation byproducts of molinate using Fenton's reagents

As can be seen in the Figure 4.29, 4.30, and 4.31, the keto-molinate isomers, which were also found in ZVI and ZVI/H₂O₂, were identified as byproducts during degradation using Fenton's reagent. The finding strongly suggests that when using ZVI or the coupled H₂O₂/ZVI system, molinate is oxidized by radical species through a Fenton-like reaction. However, one of the isomers (exhibiting a retention time of 18.8min) was not seen in the standard Fenton treatment. The retention times of the characteristic ions of the intermediates are summarized in the Table 4.4. The two GC chromatograms (Figure 4.30 and 4.31) indicate that in the Fenton process, the concentrations of the byproducts are lower than in the ZVI-mediated processes suggesting that the byproducts are susceptible to oxidation. Hydroxyl radical reactions with the thiocarbamates (e.g., EPTC, vernolate, buytlate, cycloate, molinate) are expected to proceed by H-atom abstraction from C-H bonds of the alkyl substituent groups or by addition to the N or S atoms of the NC(O)S groups. OH, CHO and C=O group containing thiocarbamate derivatives are the primary intermediates of thiocarbamates (Vidal *et al.*, 1999), which is consistent with the observation of keto-molinate isomers during the degradation of molinate with ZVI, ZVI/H₂O₂ and dark Fenton process.

A.



B.

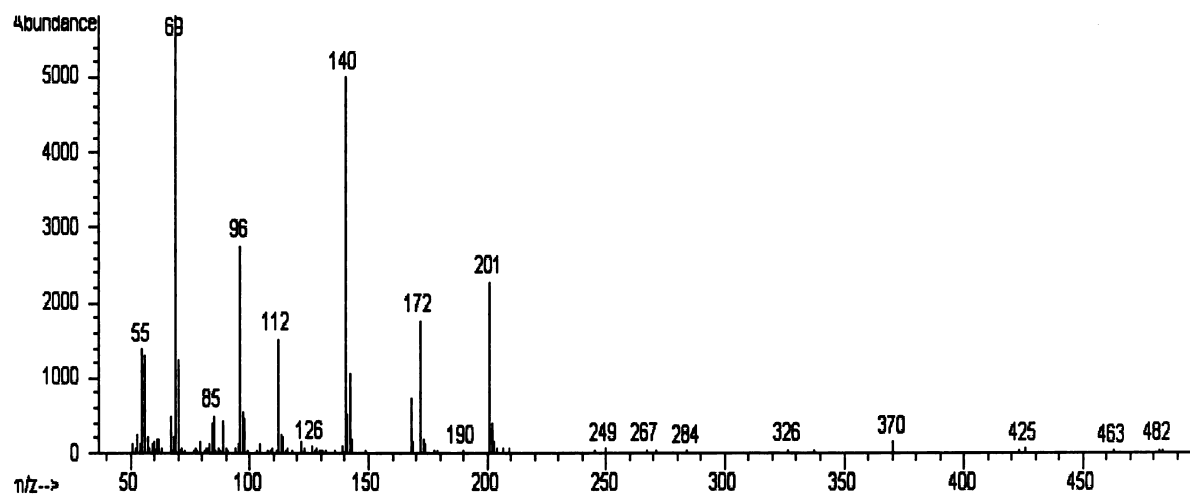


Figure 4.29. MS of the peak appeared in Fenton process at 17.6min (A) and 18.9min (B).

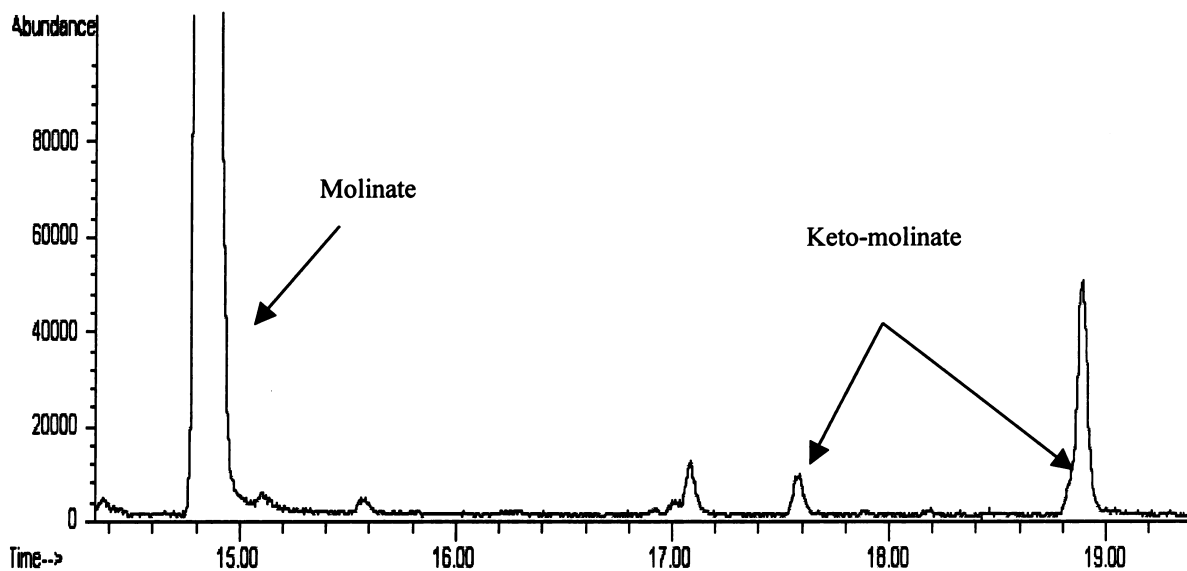


Figure 4.30. Molinate and its byproducts after 3.25hrs by dark Fenton process (0.11mM Fe^{2+} /20mM H_2O_2).

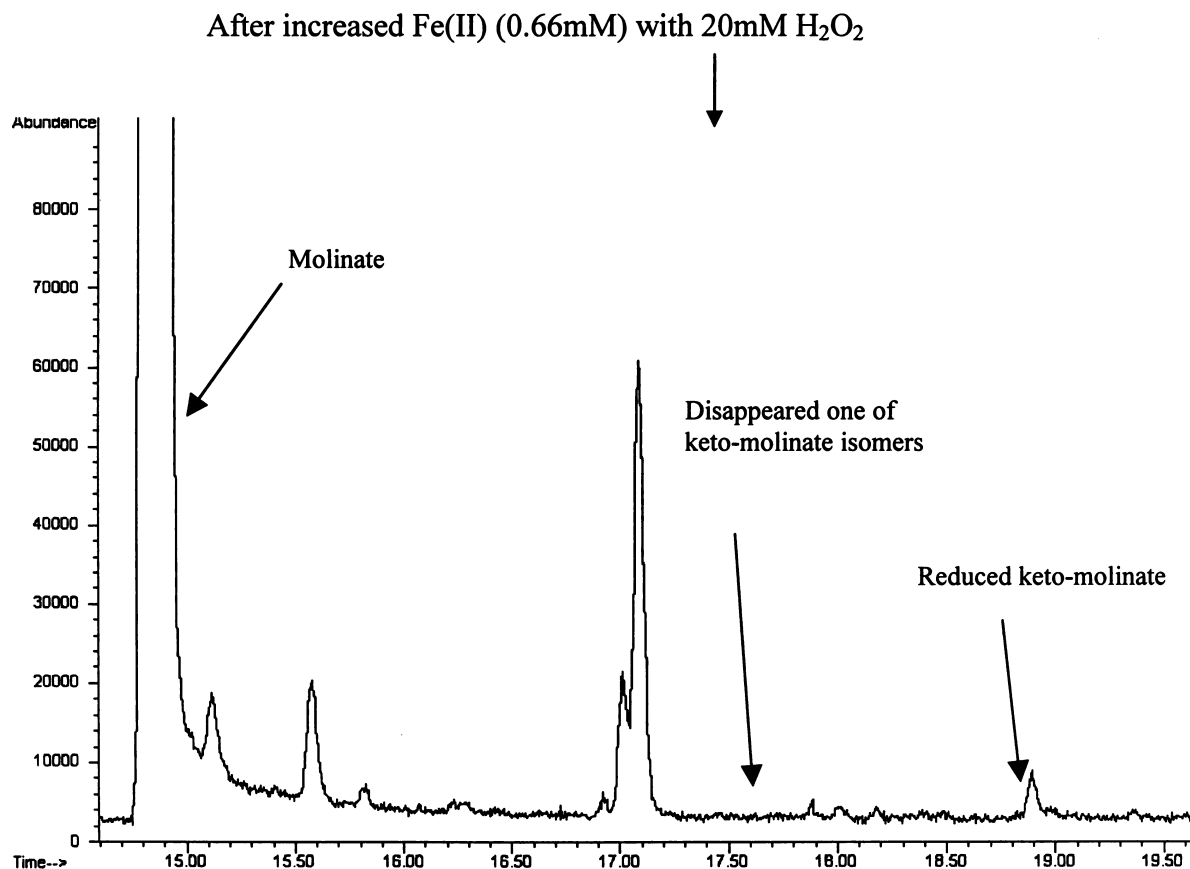
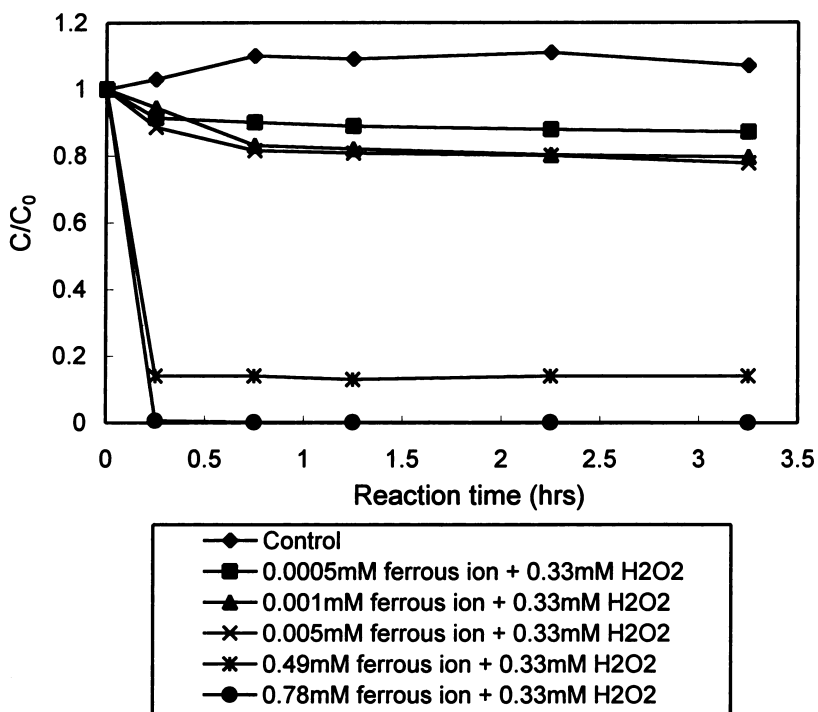


Figure 4.31. Molinate and its byproducts after 15min by dark Fenton process: Increased Fe^{2+} (0.66mM) with 20mM H_2O_2 .

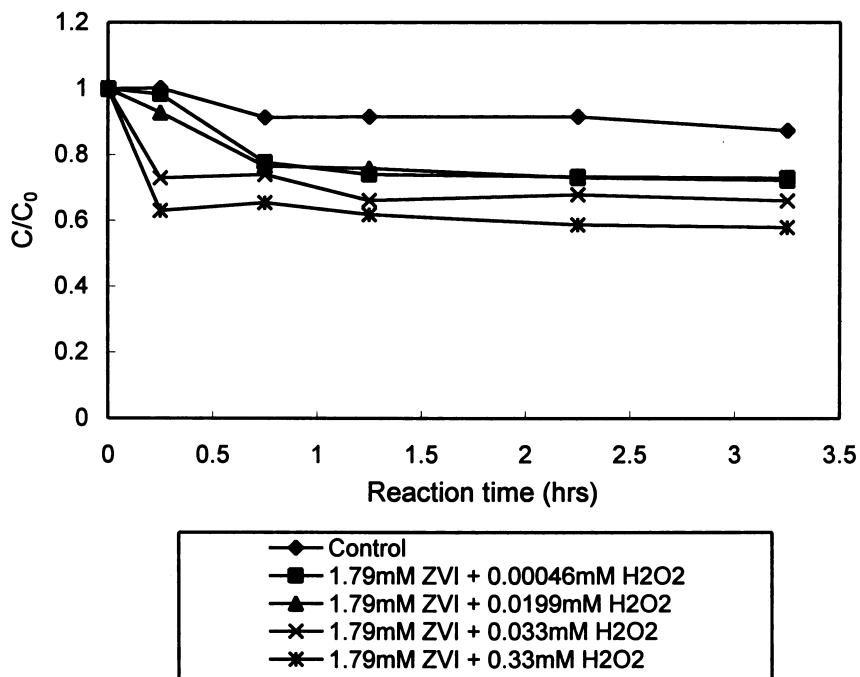
4.5. Comparison of ZVI, coupled ZVI/H₂O₂ and Fenton's process at high pH

Molinate degradation in a carbonate buffered solution was investigated for the H₂O₂/ZVI system and dark Fenton process and compared with the ZVI only case. In all cases the degradation rate containing 2mM NaHCO₃ (pH 8.1) was considerably slower (Figure 4.32 A-C) than observed when starting with a lower initial pH (Figure 4.6), especially for the H₂O₂/ZVI and dark Fenton processes. For these two processes molinate degradation ceased completely after 1 hour. In contrast, continuous ZVI degradation was observed during the ZVI process, especially for higher initial ZVI concentrations, although the degradation rate began to plateau after 2 hours. Increasing concentrations of the ZVI, however, did not significantly improve the degradation rate (Figure 4.32 C) unlike at lower pH (Figure 4.6). The reduction in degradation of molinate in the bicarbonate buffered system is most likely due to the formation of a deactivating oxide layer on the surface of the particles, competitive adsorption from excess carbonate species for surface sites, faster oxidation of ferrous to ferric iron at the higher pH and bicarbonate scavenging of hydroxyl radicals.

A. Fenton



B. H₂O₂/ZVI



C. ZVI

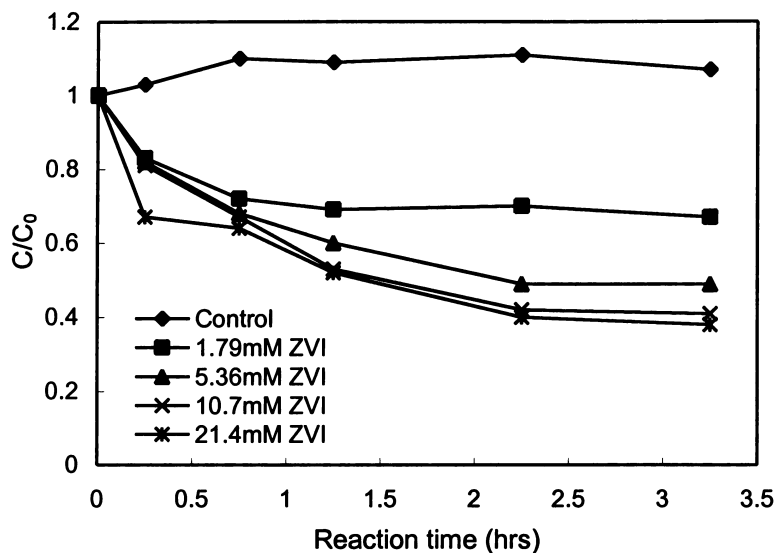


Figure 4.32. Bicarbonate effect (pH 8) on the degradation of molinate (100ppb) by Fenton (A), H₂O₂/ZVI (B), and ZVI (C).

4.6. XRD and XPS analysis

Since the morphology of a solid controls its dissolution and growth and the atomic structure on various crystal faces determines preference for adsorption of contaminants (Stipp *et al.*, 2002), XPS analysis would be a useful tool for determining the surface chemical structure information and XRD for determining the bulk composition of the particles.

4.6.1. Results of X-ray diffraction (XRD) analysis

4.6.1.1. Results of XRD analysis in the presence of molinate

In general, corrosion products of iron consist of ferric oxyhydroxides (α -, β - and γ -FeOOH), magnetite (Fe₃O₄) and amorphous iron oxide (Ishikawa *et al.*, 1998). Corrosion products formed during molinate degradation in pure water and in bicarbonate buffered solution

were characterized in order to assess their likely impact on molinate degradation kinetics. Samples were collected after 3h reaction time and the results are summarized in the Table 4.2 (See Appendix A for XRD). As can be seen, corrosion products collected from H₂O₂/ZVI and ZVI in pure water were identified as magnetite (Fe₃O₄), a black or brownish – red iron oxide, and maghemite-C or maghemite-Q (γ -Fe^{III}₂O₃). In comparison, the XRD peaks from the bicarbonate-buffered samples were consistent with ferric hydroxide, Fe(OH)₃.

4.6.1.2. XRD results on ZVI particles in the absence of molinate

In the absence of molinate, all four ZVI samples collected from each of the different reaction systems (after 3 hrs) were identified as a combination of iron and maghemite-C (γ -Fe^{III}₂O₃). It is known that the first corrosion product of Fe⁰ under anaerobic conditions is Fe(OH)₂, which may be further oxidized to magnetite Fe₃O₄. Prior to the formation of magnetite, mixed valent Fe(II) + Fe(III) salts, known as green rusts, may form under neutral pH conditions. The oxidation of mixed-valent salts commonly leads to the formation of maghemite (γ -Fe₂O₃) (Ishikawa *et al.*, 1998). Charlet *et al.* (1998) revealed by detailed analysis that the corrosion products adhering to iron after oxidation by dissolved oxygen are hematite (α -Fe₂O₃), nonstoichiometric magnetite (Fe₃O₄), and lepidocrocite (γ -FeOOH). Odziemkowski (2000) showed that the electron-conducting magnetite layer could be oxidized to maghemite (γ -Fe₂O₃) at near neutral pH, thereby stopping electron transfer from the Fe⁰ core and halting the redox reaction. However, when aqueous Fe²⁺ ions were adsorbed and incorporated into the maghemite lattice, maghemite could be locally

converted to magnetite, enhancing the conductivity of the oxide layer and allowing transfer of electrons from Fe^0 to the contaminant at the oxide-water interface.

Table 4.2. XRD results from four different samples.

XRD	In the presence of molinate				In the absence of molinate			
	Pure water		Bicarbonate		Pure water		Bicarbonate	
	ZVI	ZVI/ H_2O_2	ZVI	ZVI/ H_2O_2	ZVI	ZVI/ H_2O_2	ZVI	ZVI/ H_2O_2
Products	Fe_3O_4 and $\gamma\text{-Fe}^{\text{III}}_2\text{O}_3$	Fe_3O_4 and $\gamma\text{-Fe}^{\text{III}}_2\text{O}_3$	$\text{Fe}(\text{OH})_3$	$\text{Fe}(\text{OH})_3$	$\gamma\text{-Fe}^{\text{III}}_2\text{O}_3$	$\gamma\text{-Fe}^{\text{III}}_2\text{O}_3$	$\gamma\text{-Fe}^{\text{III}}_2\text{O}_3$	$\gamma\text{-Fe}^{\text{III}}_2\text{O}_3$

(Note that ZVI concentration was 1.8mM and H_2O_2 was 0.33mM in all cases)

4.6.2. X-ray photoelectron spectroscopy (XPS) result

The surfaces of the ZVI particles were analysed using XPS. All the ZVI particles were collected after 3.25hour reaction time and dried under nitrogen. Since the drying temperature under nitrogen may result in rapid surface oxidation, drying conditions were changed by using liquid nitrogen to minimize rapid oxidation in air, followed by drying over 20hrs using a vacuum drier. Results are reported in Table 4.3 and indicate that there is little difference on the particle surface regardless of whether degradation occurs using ZVI or ZVI/ H_2O_2 . The majority of the surface after reaction with molinate consists of iron-oxide forms that have been oxidized to Fe(III). The high C-C/C-H ratio is indicative of hydrocarbon surface contamination from samples exposed to air. In the high vacuum used for the analysis, molinate presumably volatilises as no N or S is seen in the samples.

Table 4.3. XPS results (in the presence of molinate) and atomic concentration [AT]%.

Samples	1.79 mM ZVI/ H ₂ O ₂		1.79 mM ZVI	
	[AT]%	Identity	[AT]%	Identity
O 1s	5.6	Organic	4.5	Organic
O 1s	22.4	Fe-hydroxide	22.4	Fe-hydroxide
O 1s	30.0	Fe-oxide	29.6	Fe-oxide
C 1s	2.1	O=C-OH	1.6	O=C-OH
C 1s	0.6	O=C	0.6	O=C
C 1s	2.4	C-O	1.7	C-O
C 1s	18.0	C-C / C-H	20.3	C-C / C-H
Fe 3p	18.9	Fe(III)	19.4	Fe(III)

The observations from XPS analysis are consistent with those of Devlin *et al.* (1998).

4.7. Discussion

4.7.1. Evidence of oxidation pathway

4.7.1.1. Keto-molinate byproducts

The nature of the reaction end product (the keto-molinate isomer) indicates that ZVI is initiating an oxidation rather than a reduction process. Indeed, the keto-molinate isomer has previously been reported in molinate degradation studies using light and TiO₂ semiconductor particles to result from hydrogen abstraction as a result of hydroxyl radicals preferentially attacking the N-alkyl chain (Konstantinou *et al.*, 2001). Although the reduction of oxygen by Fe⁰ is generally envisaged as a four electron step with water as the major product (equation [4.8]) a two electron reduction of oxygen to hydrogen peroxide would also appear possible (equation [4.9]).



Hydroxyl radicals (or possibly ferryl species (Bossmann *et al.*, 1998 and Kremer, 1999) may well be generated in these systems as a result of Fenton's reagent processes arising from the presence of both ferrous iron and hydrogen peroxide (equation [4.10])



Whether this process occurs principally in solution or at the surface of the ZVI particles is unclear at this stage but it is highly likely that many of the key steps occur at the surface of the zero valent iron particles. The proposed oxidation mechanism was further confirmed with the following results:

4.7.1.2. Same byproducts for different oxidation processes

The same byproducts (keto-molinate isomers) were found in all three processes (ZVI, ZVI/H₂O₂, standard Fenton) (Table 4.4). The result indicates that the attack of $\bullet\text{OH}$ represents the major initiation step in the degradation pathway of molinate. It has been suggested that $\bullet\text{OH}$ can react via hydrogen-atom abstraction, electron transfer or addition to the N atom, leading to carbon-centered and (or) nitrogen-centered radicals (Hayon *et al.*, 1970; Simic *et al.*, 1971; Rao and Hayon, 1975; Das *et al.*, 1987). In this reaction, hydroxyl radical react via the addition to the N-atom, leading to carbon-centered radical and in the presence of dissolved oxygen, the R \bullet radical lead to the production of ROO \bullet and subsequent reactions lead to the end product, keto-molinate isomers. Addition of butanol, a hydroxyl radical scavenger, prevented the degradation of molinate (Figure 4.19).

Table 4.4. GC-MS-EI retention times (RT) and spectral characteristics of molinate identified byproducts in both ZVI, ZVI/H₂O₂, and Standard Fenton processes

Byproducts	Retention time (min)	Characteristic ions, m/z (abundance %)
Keto-molinate isomer (H ₂ O ₂ /ZVI, dark Fenton, ZVI)	17.57	112(100), 69(44), 140(25), 201(45), 56(17)
Keto-molinate isomer (H ₂ O ₂ /ZVI, ZVI)	18.82	112(100), 69(22), 140(65), 201(35), 56(17)
Unknown (in ZVI)	18.435	128(100), 62(37), 85(32), 57(30)
Unknown (in H ₂ O ₂ /ZVI)	18.435	128(100), 57(88), 89(32)

Under anaerobic conditions, achieved by bubbling nitrogen gas through a reactor containing 10ppm molinate and ZVI, no degradation or keto-molinate isomers were found (Figure 4.33 and 4.36). This suggests that the presence of oxygen plays an important role in molinate degradation.

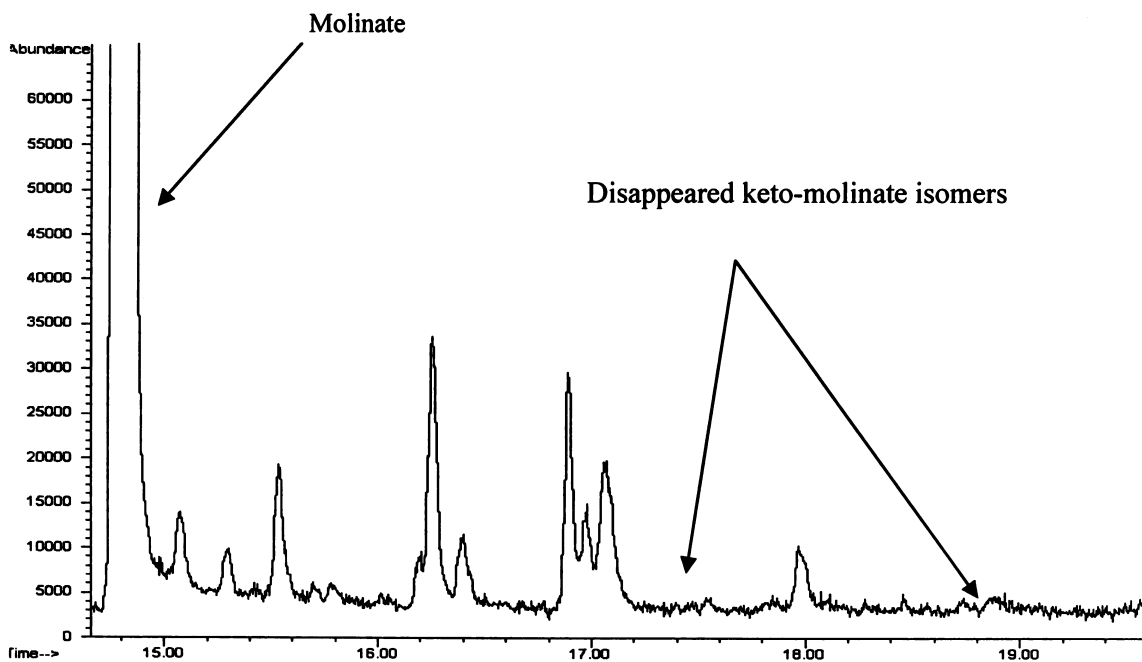


Figure 4.33. GC Chromatogram: Disappeared keto-molinate peaks in the **absence of oxygen**.

4.7.1.3. Effect of catalase

The addition of catalase, which induces the rapid breakdown of hydrogen peroxide, prevented the formation of keto-molinate isomers (Figure 4.34) and degradation of molinate (Figure 4.18). This suggests that the presence of hydrogen peroxide, an intermediate product formed from the disproportionation of superoxide, is critical for degradation. The catalase results support the hypothesis that ferrous iron formed from iron corrosion reacts with hydrogen peroxide, resulting in the formation of hydroxyl radicals, the primary oxidant in the system.

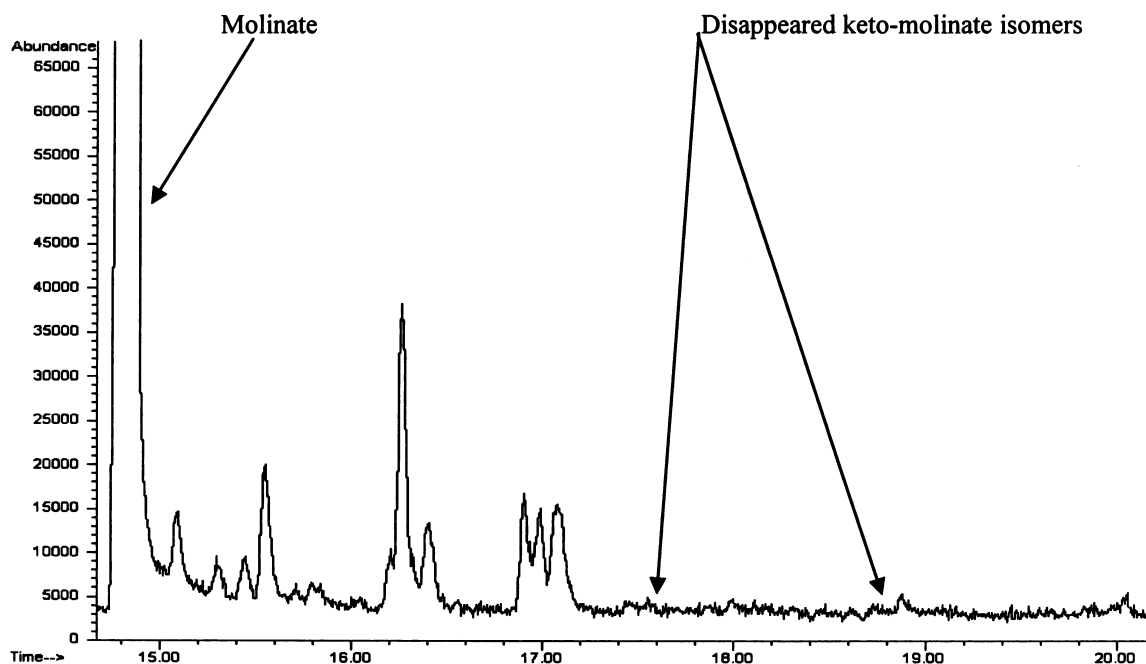


Figure 4.34. GC Chromatogram: Disappeared keto-molinate peaks in the **presence of Catalase/O₂**.

4.7.1.4. Effect of SOD

Addition of the enzyme superoxide dismutase (SOD), which catalyzes the disproportionation of the superoxide radical, O₂^{•-}, to H₂O₂ (Fee and DiCorleto, 1973), accelerates the formation of hydrogen peroxide and leads to a slight improvement in the

removal rate (Figure 4.36). Addition of SOD also resulted in the formation of keto-molinate isomers as shown in Figure 4.35.

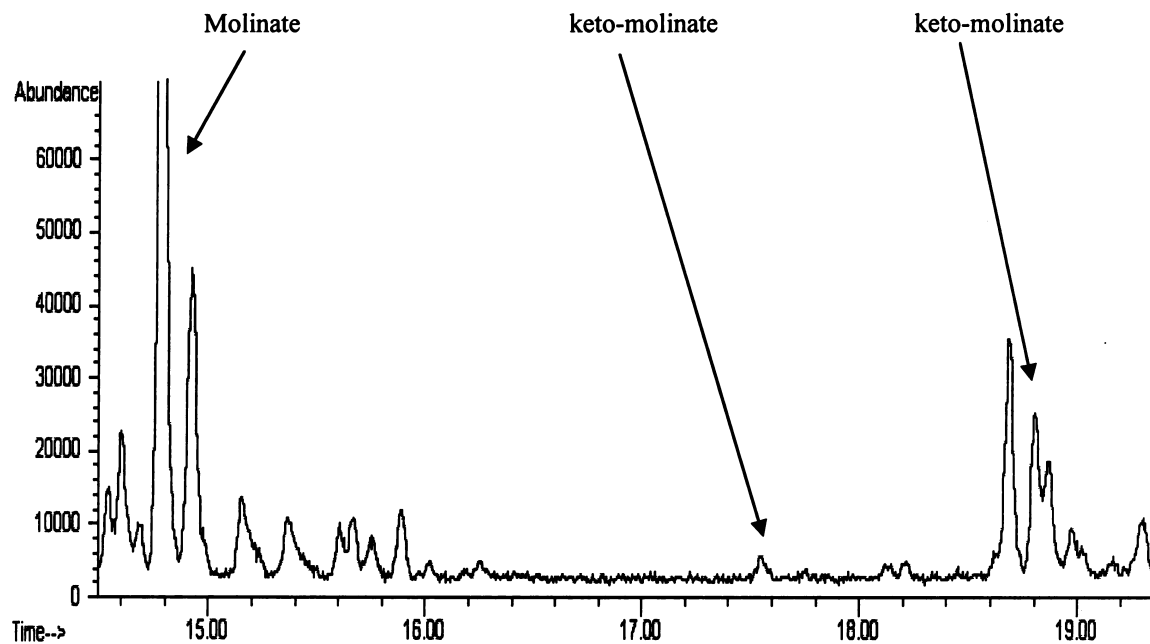


Figure 4.35. GC Chromatogram: keto-molinate peaks appeared in the presence of SOD/O₂.

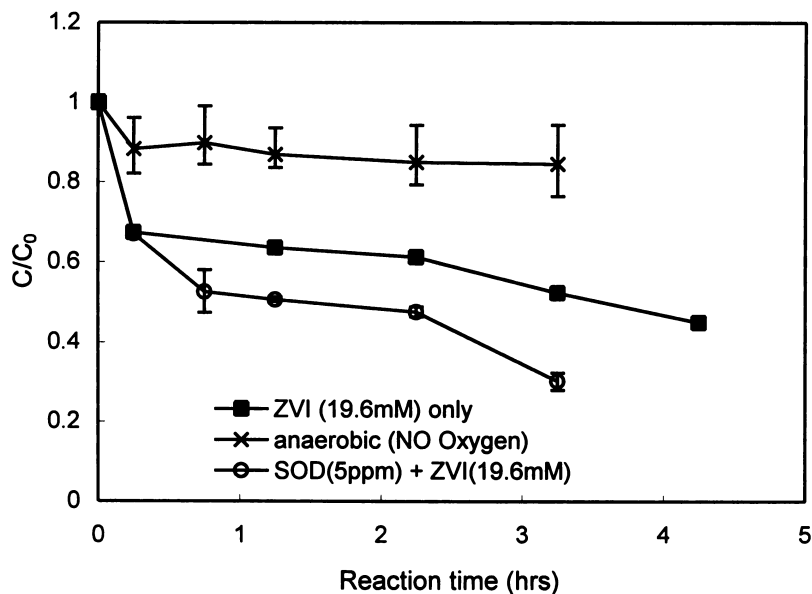


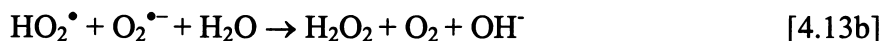
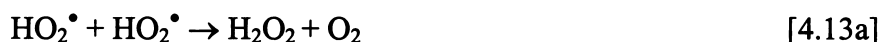
Figure 4.36. Effect of presence/absence of oxygen and presence/absence of superoxide dismutase (SOD). Note: 5µg/mL of SOD was added over 2.75 hrs.

4.7.2. Reaction mechanism

All these experimental results provide confirmative evidence for the proposed oxidation mechanism. For example, electrons produced on the oxidation of Fe^0 are likely to react with molecular O_2 adsorbed to the Fe^0 surface, possibly reducing it to the superoxide radical anion $\text{O}_2^{\bullet-}$ (or to the hydroperoxy radical HO_2^\bullet at $\text{pH} < 4.8$) as shown below.

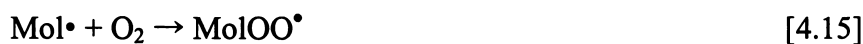


Disproportionation of these free radicals is likely to occur relatively rapidly at low pH ($k_{12a} = 9.7 \times 10^7 \text{ M}^{-1}\text{s}^{-1}$ (Bielski *et al.*, 1985)) (slower at higher pH; at pH 8, $k_{4.13b} = 6.1 \times 10^4 \text{ M}^{-1}\text{s}^{-1}$), resulting in formation of hydrogen peroxide at or near the ZVI surface (equation [4.13]):



The hydrogen peroxide generated in this manner may react with the ferrous iron released during the ZVI corrosion process to produce highly reactive hydroxyl radicals.

Molinate is degraded by the attack of hydroxyl radical then reacts with oxygen to form an organoperoxy radical (MolOO^\bullet) before forming the reaction end product, keto-molinate isomers, i.e.,



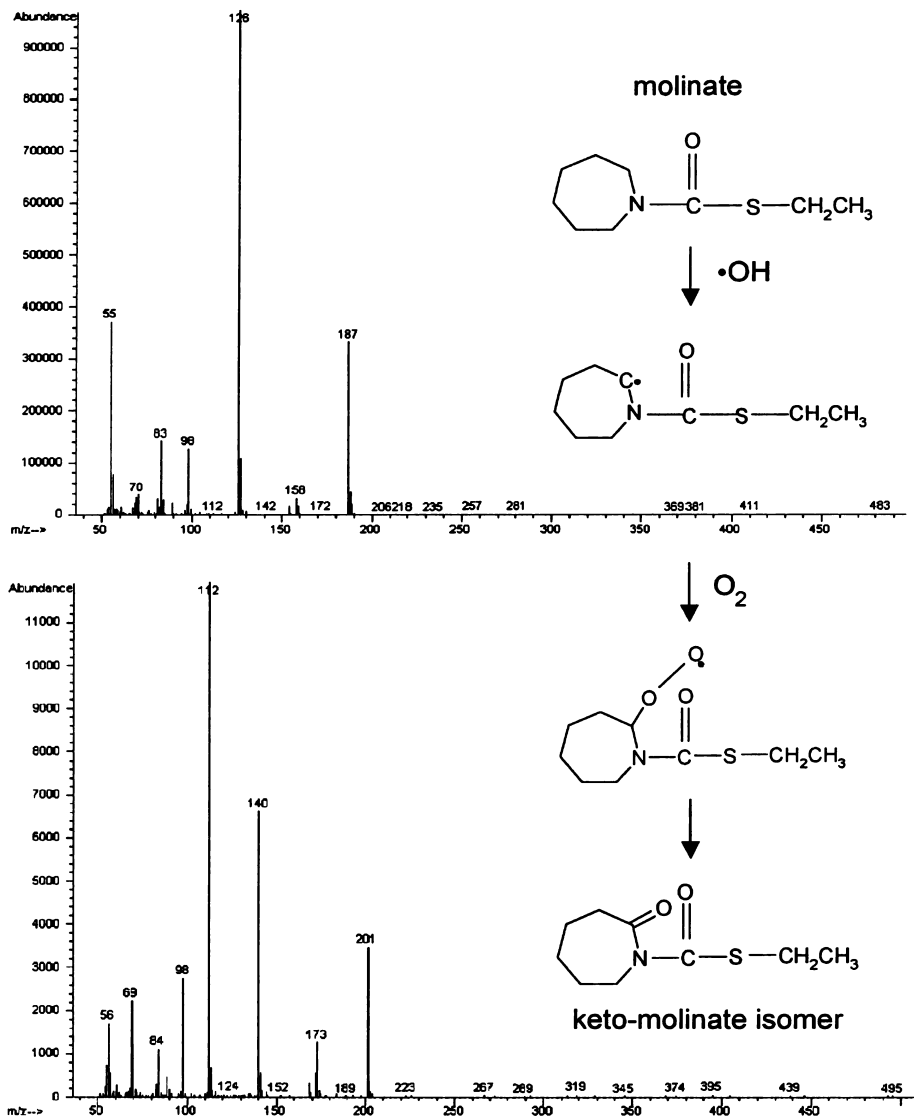


Figure 4.37. MS fragments for molinate and keto-molinate isomers and proposed oxidation pathway.

The presence and absence of keto-molinate byproducts under different reaction conditions strongly suggests that ZVI in the presence of O_2 is oxidatively rather than reductively degrading molinate. The rapid consumption of DO and production of hydrogen peroxide, the enhancement in molinate degradation when supersaturating the reaction solution with O_2 , and the absence on any appreciable degradation in the absence of O_2 further supports an oxidative mechanism. There are still many unknown, however; in particular, whether the

oxidation occurs on the surface of the particles or in the bulk solution. These issues are further investigated in the next chapter using specific model organics.

4.7.3. Kinetics of Fe(II) and H₂O₂ generation

The proposed pathway would appear to qualitatively account for the observed kinetics of Fe(II) and H₂O₂. For example, the slow decrease in ferrous iron concentrations in pH 4 solutions most likely represents a balance between Fe²⁺ release from the oxidizing Fe⁰ surface and subsequent oxidation of this ferrous iron by hydrogen peroxide to ferric species. Hydrogen peroxide concentrations reach a steady state at pH 4 but only after initial rapid reaction with released ferrous iron. It is presumably because of this initial consumption of hydrogen peroxide by ferrous iron that a lag in accumulation of H₂O₂, particularly at the higher ZVI loadings, is observed. The kinetic rate can be affected by concentrations of Fe²⁺ as well as reactive ZVI surface area available. The significant dependence of degradation rate on ZVI concentrations is mainly due to a greater accumulation of Fe(II) (aq) in the suspension. As the reaction proceeds, the concentration of Fe(II) (aq) decreases with this effect more pronounced in the bicarbonate system, where iron corrosion is inhibited by the formation of an oxide layer on the particles.

At higher pH (8.1), oxidation of Fe²⁺ by oxygen will proceed more rapidly resulting in very little accumulation of Fe²⁺ in solution. In addition, the tendency for Fe²⁺ to remain adsorbed to the surface of either Fe⁰ or to iron oxyhydroxide particles (formed on hydrolysis of ferric species present as a result of Fe²⁺ oxidation) would also be expected to lower the measurable concentration of Fe²⁺ in solution.

4.7.4. Overview of the ZVI-mediated oxidative technology

The results of the molinate study indicate that nanoscale zero-valent iron particles are capable of oxidising and thus degrading certain organic contaminants in the presence of oxygen. The reaction is abiotic and pH dependent (slower at higher pH levels). The formation of iron oxyhydroxide particles at alkaline pH might also be expected to lower the reactivity of the ZVI as a result of surface accumulation however relatively similar rates of molinate degradation are observed at pH 4 and 8.1, at least over the first hour or so. In such high carbonate content (2mM NaHCO₃) solutions used in this study, it is also possible that siderite (FeCO₃(s)) could initially form (thereby lowering the ferrous iron activity). Its occurrence would only be transitory, however, in view of the continual oxidation of Fe(II) to Fe(III) species.

Passivation of the Fe⁰ metal surface by these precipitates is one of the most likely limitations to effective long-term performance of permeable reactive barriers. In a traditional equilibrium analysis of corrosion potentials (Pourbaix, 1966), conditions that favor the formation of FeCO₃(s), Fe(OH)₂(s), and Fe(OH)₃(s), should passivate Fe⁰, whereas sustained corrosion is expected only below pH 6 where the oxidation product is aqueous Fe²⁺.

The continued degradation of molinate for two hours or more at pH 8.1 is confirmation of the continuing release of ferrous iron, formation of reduced oxygen species and the subsequent generation of strongly oxidizing substrates (such as the hydroxyl radical, or possibly ferryl species). Any ferrous iron initially present in the reaction medium (derived from the original ZVI stock) would expect to be oxidized in a few minutes with the resultant cessation of oxidant generation.

While the eventual reduction in extent of molinate degradation at higher pH may reflect the effect of surface coatings, it is intriguing to observe such a high degree of degradation as most Fenton reagent mediated processes are relatively ineffective at higher pH. The difference in this case is the continuing generation of fresh reactants (Fe^{2+} and H_2O_2) with the effectiveness of the process at high pH limited by Fe^0 availability.

The slow release/formation of the key reactants and their continuing effectiveness at degrading the contaminant of interest even at high pH suggests a range of possible applications for ZVI-mediated oxidative processes ranging from in-situ degradation of contaminants in oxic groundwaters, degradation of contaminants on surface sediments (or, indeed, surfaces in general) and degradation of contaminants in water treatment by periodic placement of nanosized ZVI particles on sand or anthracite components of deep bed filters. Such processes could be initiated by the simple emplacement of ZVI particles in oxic environments with the ensuing degradation of contaminants achieved without the need for continuous dosing of wet chemicals.

4.8. Conclusion

Degradation of the carbothiolate herbicide, molinate, has been investigated in oxic solutions containing nanoscale zero valent iron particles and found to be effectively degraded by an oxidative pathway. Both ferrous iron and superoxide (or, at $\text{pH} < 4.8$, hydroperoxy) radicals appear to be generated on corrosion of the zero valent iron with resultant production of strongly oxidizing entities capable of degrading the trace contaminant. While researchers have found the reductive degradation pathways in anoxic

Fe^0 - H_2O systems, which involves either direct electron transfer from ZVI at the surface of the iron metal or reaction with dissolved Fe^{2+} or H_2 , molinate degradation studies under aerobic condition showed the presence of oxidized degradation byproducts. These results suggest that molinate degradation occurs through an oxidative mechanism even though the ZVI process is normally considered highly reductive. At the trace levels of organics being used in this study, oxygen is expected to be the primary electron acceptor and superoxide the primary radical intermediate.

Investigation of degradation pathway indicates the important role of radical species in treating molinate by ZVI. Studies on Fe^{2+} and Fe^{3+} generation during ZVI and ZVI/ H_2O_2 treatment suggest that Fe^{2+} availability and surface dissolution kinetics may play a role in the degradation of molinate. The combined H_2O_2 /ZVI system was found to be highly effective and reduces the quantity of ZVI necessary for rapid removal of molinate for comparatively low H_2O_2 doses. However, in the presence of bicarbonate the removal of molinate was retarded, possibly due to the rapid oxidation of Fe(II) to Fe(III) and the inhibiting role of carbonates toward free radical reactions. Preventing the formation of surface oxide films at high pH and maintain ferrous iron availability would improve the applicability for treatment of pesticides in alkaline waters.

The ZVI-mediated oxidation process is promising although further research is required to understand the reaction mechanism, the particles lifetime, and factors that affect ZVI reactivity. Thus, the following chapter investigates the particles in greater detail by using specific organic probes to assess the oxidation mechanism and determine oxidizing capacity of ZVI.

Chapter 5

Quantification of the oxidizing capacity of nanoparticulate zero-valent iron and assessment of possible environmental applications

5.1 Introduction

In Chapter 4, it was shown that nanoscale zero-valent iron (nZVI) oxidizes the herbicide molinate when it is used in the presence of oxygen. Analysis of byproducts observed during ZVI-mediated oxidative degradation of the herbicide is consistent with the action of a non-specific oxidant such as the hydroxyl radical (OH^\bullet). The reactions that result in oxidant production are initiated when Fe^0 is oxidized by oxygen, which likely forms a reactive oxygen species either on the particle surface or in solution. The oxidation of Fe^0 by oxygen also results in the formation of a layer on the particle surface with properties similar to $\gamma\text{-Fe}_2\text{O}_3$ and Fe_3O_4 , which eventually leads to passivation of the surface accompanied by a decrease in the rate of Fe^0 oxidation (Davenport *et al.*, 2000). Passivation of the surface also appears to be responsible for the decreased rate of Fe^0 -mediated oxidation of molinate that is observed over extended time. For a system involving granular $\text{Fe}^0_{(s)}$, the diminution of reactivity can be counteracted by addition of a chelating agent (such as EDTA) that keeps the oxidized iron in solution (Noradoun *et al.*, 2003). However, addition of chelating agents limits the utility of the technique for *in situ* treatment. The high surface area of nZVI may allow for more efficient generation of oxidants, but a decrease in reactivity associated with the build-up of iron oxides on the surface eventually slows the reaction. The corrosion of the Fe^0 particles is accompanied by observation of release of

ferrous ions to solution and generation of hydrogen peroxide suggesting the possibility of a Fenton-like reaction at or near the particle surface. If the nZVI particles continue to produce oxidants after a surface coating forms, the continued slow release of oxidants may result in degradation of contaminants present in soil and contaminated aquifers. The high surface area of the nZVI particles could also provide a means for selective oxidation of surface-active compounds.

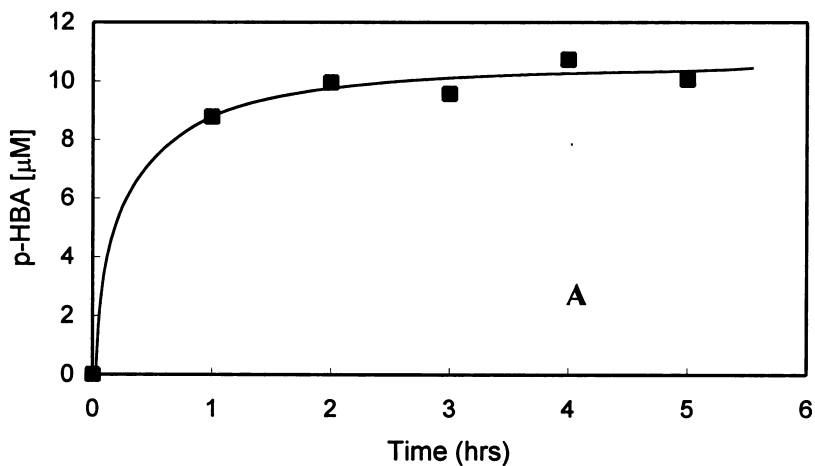
To assess the potential applicability of nZVI for the oxidative treatment of organic contaminants, and to investigate the reaction mechanism and yields of the oxidizing species further, experiments were performed using the oxidation of benzoic acid (BA) to para-hydroxybenzoic acid (p-HBA) as a probe reaction for oxidant production. Analysis of oxidative nZVI reactions under well-defined conditions provides insight into the effect of environmental conditions (e.g., pH) on oxidation rates, the selectivity of the oxidant and the overall efficiency of the process. Additionally, insights gained from the laboratory investigations under controlled conditions are used to assess the potential applications of this technology and to identify areas for further research. The results of the benzoic acid studies are presented in this chapter as is an assessment of future practical application of the oxidative use of nanoscale ZVI.

5.2 Results

5.2.1 p-Hydroxybenzoic acid (p-HBA) formation

The *p*-isomer is the dominant oxidation product formed on oxidation of benzoic acid and concentrations of this product generated as a function of time of reaction between benzoic

acid and 0.9 mM nanosized Fe^0 are shown in Figure 5.1A. Concentrations of *p*-HBA formed for different initial concentrations of benzoic acid after a 2-hour reaction time with 0.9 mM Fe^0 are shown in Figure 5.1B. The reaction goes to completion within the first hour with very little increase (at least at $[\text{benzoic acid}]_0 = 10\text{mM}$) in concentration of the reaction product *p*-HBA over the $10\mu\text{M}$ (or 0.1% of the initial benzoic acid concentration) achieved in the first hour. Increasing the initial concentration of benzoic acid results in an increase in concentration of *p*-HBA produced though the increase is less than proportional with the concentration of *p*-HBA plateauing at around 10mM at the higher benzoic acid concentrations examined.



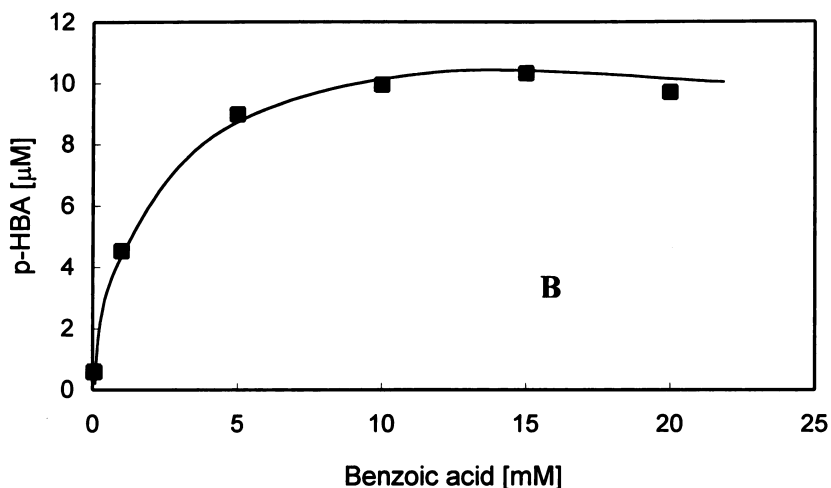


Figure 5.1. p-hydroxybenzoic acid (p-HBA) formation over time in pH 3 suspension and 30mM ionic strength containing 10mM benzoic acid (A) and p-HBA formation after two hours as a function of benzoic acid concentration (B).

5.2.2 Cumulative hydroxyl radical formation over long- term

Results of longer term (1 day) studies of hydroxyl radical production are shown in Figure 5.2 and suggest that, whilst a little slow initially, nZVI-mediated oxidation will continue for some time, particularly in the mid-pH range. The production of p-HBA from BA exhibited biphasic kinetics, with rapid initial production of p-HBA followed by a slow increase over periods of at least one day (Figure 5.2). The concentration of p-HBA produced after 1 hour was used in all subsequent experiments to compare the rates of oxidation under different conditions. Under the conditions used in these experiments (i.e., 10 mM BA; 0.9 mM nZVI), less than 5% of the BA initially present was transformed and therefore it served as the main sink for oxidants with the result that oxidation of p-HBA was negligible. Thus, the concentration of p-HBA formed is related to the concentration of oxidizing species that could be used to transform a contaminant.

BA is transformed into three isomers of hydroxybenzoic acid. Although it was not possible to quantify each of the isomers due to difficulty resolving the ortho and meta forms, the three isomers appeared to be present at similar concentrations. The three isomers of hydroxybenzoic acid account for $90 \pm 5\%$ of the products of OH^\bullet reactions with BA with the ratio of o-HBA, m-HBA, and p-HBA products reported to be in the proportion 1.7 : 2.3 : 1.2 (Klein *et al.*, 1975). For the oxidation of BA by solution phase OH^\bullet , the concentration of p-HBA has been used to estimate cumulative OH^\bullet production using Eq 5.1 (Zhou and Mopper, 1990):

$$\text{Cumulative OH}^\bullet \text{ produced} = [\text{p-HBA}] \times 5.87 \quad [5.1]$$

A similar approach is adopted with results from all nZVI experiments expressed in terms of both p-HBA concentration and cumulative OH^\bullet production with the latter quantity estimated using Eq 5.1.

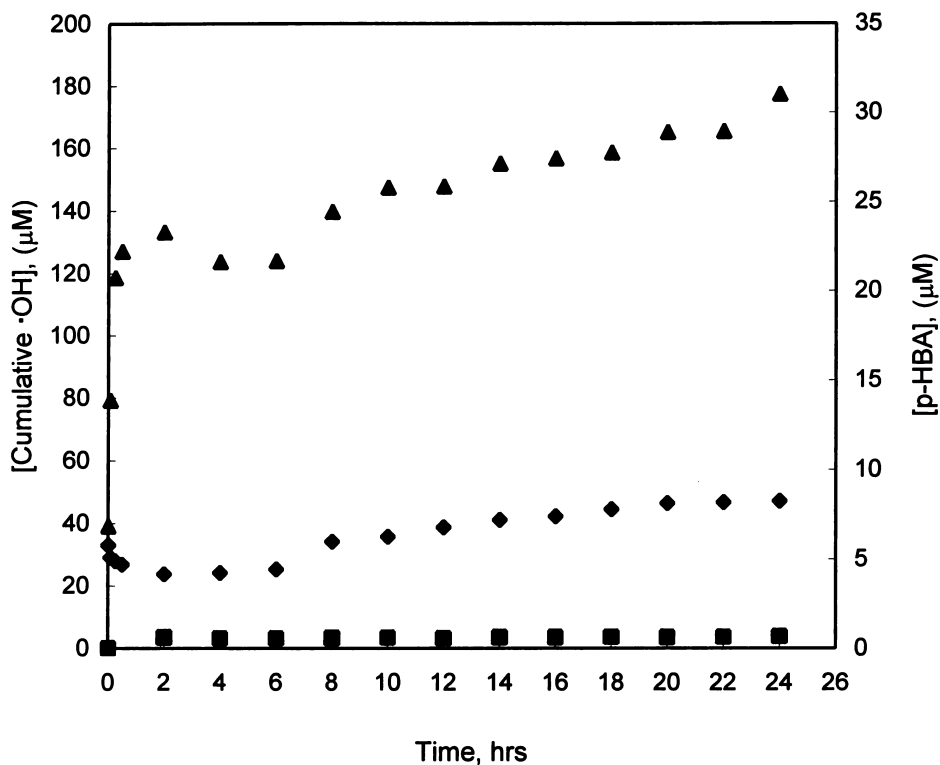


Figure 5.2. ▲ pH 3 ◆ pH 5 ■ pH 8, Cumulative hydroxyl radical formation and p-HBA concentration over time at pH 3,5 and 8. (Condition: 0.9mM Fe⁰, 30mM ionic strength and 10mM BA).

5.2.3 Effect of Fe(II) as oxidant scavenger

To assess competition for oxidants between BA and other oxidant scavengers, such as Fe(II), experiments were conducted at pH 3 over a range of BA concentrations. The yield of p-HBA increased as BA concentrations increased from 50 μM to 5 mM and then remained approximately constant up to 20 mM (Figure 5.3). Simultaneous measurements of ferrous iron indicated that total Fe(II) ranged from 190 - 200μM (Figure 5.4) in almost all cases and was relatively constant over the duration of the experiment.

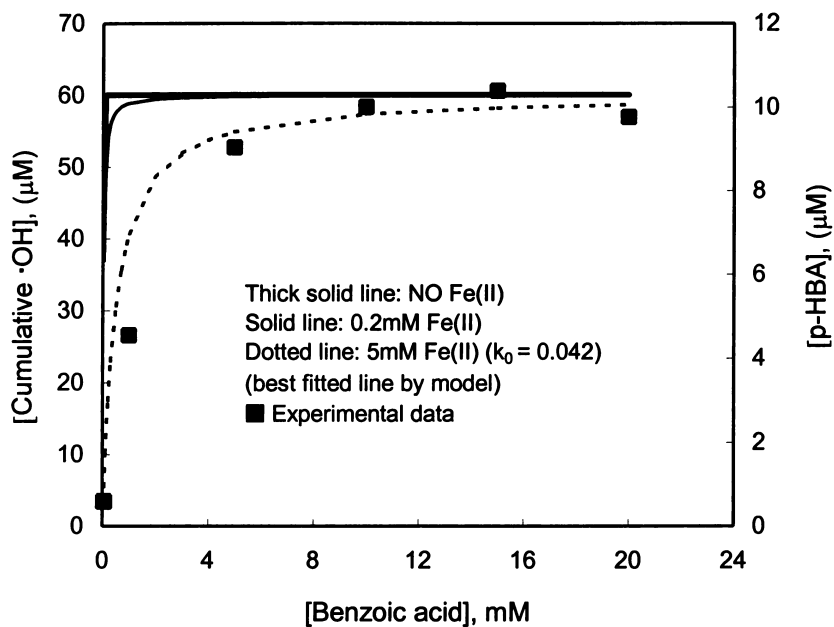


Figure 5.3. Oxidant formation as a function of BA concentration and predicted oxidant formation in the absence and presence of Fe(II) scavenging OH radicals (Conditions: 0.9mM Fe⁰, pH 3, 30mM ionic strength, reaction time 2 hours). Solid and dashed lines shows calculated [p-HBA] assuming competitive hydroxyl radical scavenging by 0.2 and 5mM Fe(II) respectively.

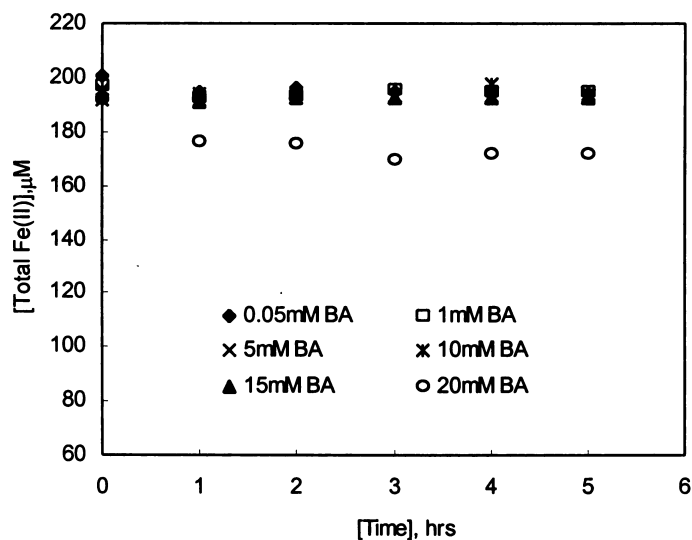


Figure 5.4. Total Fe(II) in suspension over time as a function of BA concentration at pH 3 and ionic strength of 0.03M.

5.2.4 Effect of ZVI concentrations on oxidant yield

Altering the relative concentrations of the target compound (benzoic acid) to ZVI can affect the extent of oxidation product formation (Figure 5.5). At low initial concentrations of benzoic acid ($50\mu\text{M}$), the dependence is not strong and an increase in the concentration of ZVI does not substantially influence the quantity of *p*-HBA formed. A 9-fold increase in ZVI concentration from 0.2 mM to 1.8 mM results in slightly less than a doubling in *p*-HBA concentration produced (Figure 5.5 A). At even higher ZVI concentrations, the concentration of *p*-HBA produced is observed to decrease, possibly as a result of scavenging of oxidant by ZVI. Experiments with higher BA concentrations (10mM) show a substantial increase in *p*-HBA production as nZVI increased (Figure 5.5 B). The difference in *p*-HBA production for 0.2 to 5mM ZVI is some 700%.

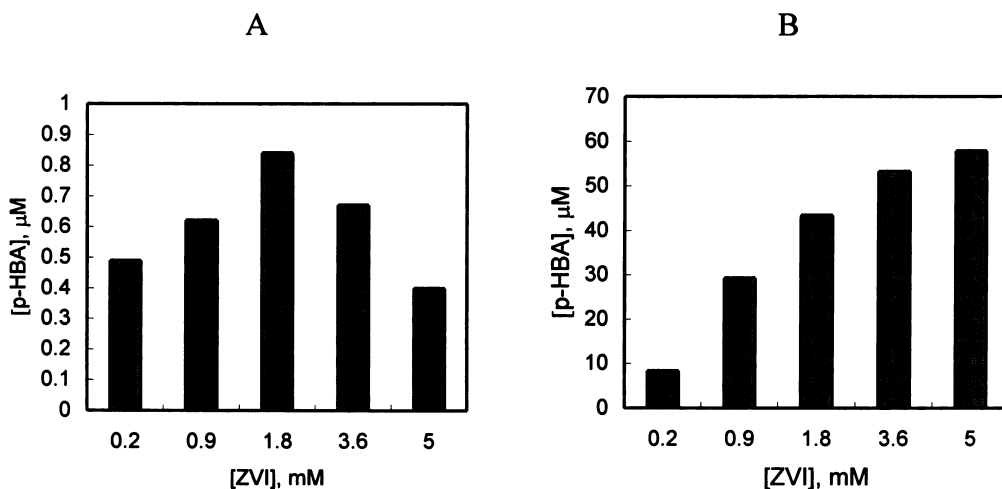


Figure 5.5. *p*-hydroxybenzoic acid formation as a function of ZVI concentration. Conditions. pH 3 solutions, 30 mM ionic strength, reaction time 1 hr and $[\text{benzoic acid}]_0 = 50\mu\text{M}$ in (A) and $[\text{benzoic acid}]_0 = 10\text{ mM}$ in (B).

Assuming the same distribution of HBA isomers in the nZVI system, the results can be used to estimate the efficiency of the initial fast reaction (i.e., the yield of oxidants per mole of nZVI added). The reaction efficiency ranged from approximately 5 to 25% with higher

values at the lowest ZVI concentration (Figure 5.6). The effectiveness of the nZVI as an oxidant generator decreases on increasing nZVI loading suggesting the need to use a low dose of nZVI for maximum efficiency.

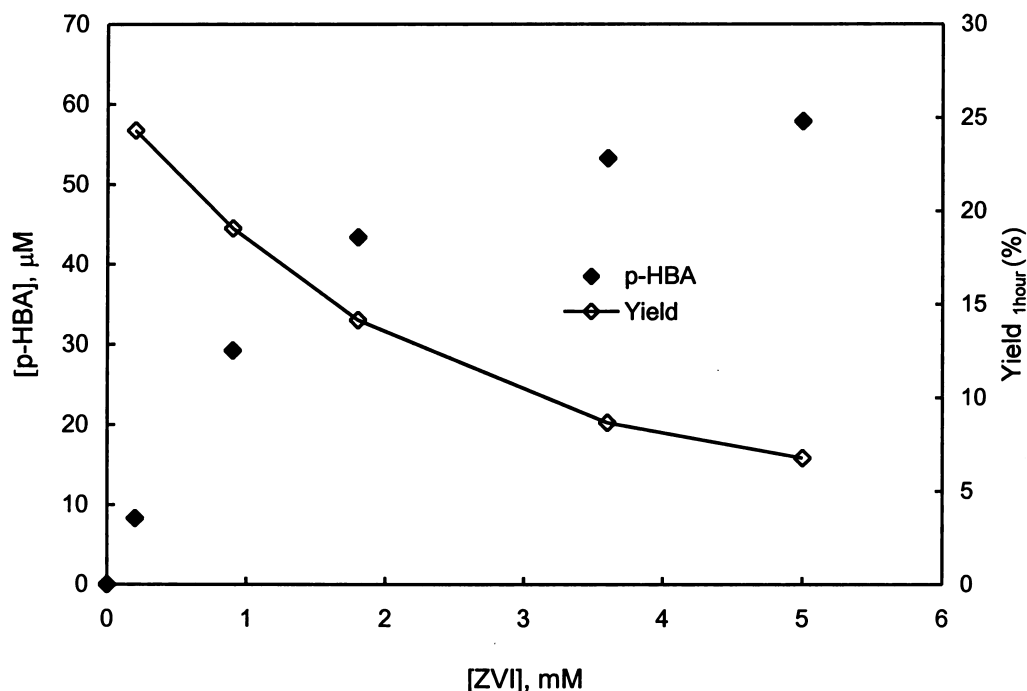


Figure 5.6. Effect of increase in mass of nZVI used on concentration of principal oxidised products (p-HBA). (Condition: 10mM BA, 30mM ionic strength, pH 3, reaction time 1hour).

5.2.5 Effect of pH

The oxidizing ability of nZVI (as measured by the extent of p-HBA production up to one hour) as a function of pH and relative to oxidizing ability at pH 3 is given in Figure 5.7 for two concentrations of BA, 50 μM and 10 mM. pH is observed to significantly influence the oxidizing ability of nanosized ZVI with a marked decrease in concentration of oxidized product (p-HBA) with increasing pH. This effect of pH could be related to passivation of

the ZVI surface at higher pH or could be related to the presence of more effective hydroxyl radical deactivation pathways at the higher pH. Despite the decrease in oxidant production rate as pH increased, oxidation was observed at pH values up to 8.

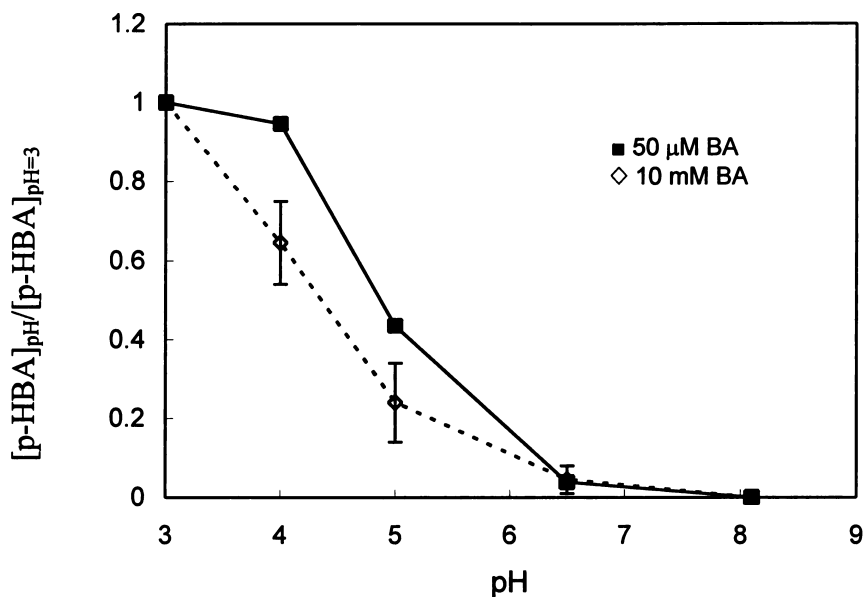


Figure 5.7. pH dependence of the formation of *p*-HBA. Conditions: pH 3, 0.9mM ZVI, ionic strength 30 mM and reaction time 1hr.

5.2.6 Selectivity of oxidant

To elucidate the selectivity of the oxidant, and the importance of surface versus solution-phase reactions, competition experiments were conducted with aniline, *o*-hydroxybenzoic acid, phenol and humic acid at pH 3 and 10 mM BA. In all cases, the yield of *p*-HBA decreased as the concentration of the competitor increased (Figure 5.8 - 5.11). The relative rate constant (i.e., the rate constant for each probe compound relative to the rate constant for BA) was estimated by least squares fit of the data to Eq 5.2:

$$F = \frac{k_{BA}[BA]}{k_{BA}[BA]+k_C[C]} = \frac{1}{1+\frac{k_C}{k_{BA}}\frac{[C]}{[BA]}} = \frac{1}{1+k_{C/BA}\frac{[C]}{[BA]}} \quad [5.2]$$

where F is the fraction of the p-HBA produced in the presence of a certain concentration of the competitor (C) to that in the absence of C and $k_{C/BA}$ is the relative rate constant. Relative rate constants were also determined for the compounds in a similar manner but using Fenton's Reagent as a source of OH^\bullet (Figures 5.8b - 5.11b). Experimentally determined relative rate constants for the four probe compounds are given in Table 5.1 as are literature values for the absolute rate constants for reaction of the probe compounds with hydroxyl radicals.

Table 5.1.

Rate constants for reaction of probe molecules with hydroxyl radicals generated at pH 3 using both nZVI and Fenton reagent relative to that of benzoic acid ($k_{C/BA}$). Literature values for reaction of benzoic acid and probe compounds (C) with hydroxyl radicals are also shown.

Compound	pK _a	Relative rate constant ($k_{C/BA}$)		Reported rate constant for reaction with OH^\bullet (k_C) ($\text{M}^{-1}\text{s}^{-1}$) (ref)
		nZVI	Fenton	
BA	4.2	1.00	1.00	4.3×10^9 (k_{BA} ; 1)
Aniline	4.6	1.33	1.28	8.6×10^9 - 1.7×10^{10} (2)
Phenol	10.0	4.65	2.28	6.6×10^9 - 1.8×10^{10} (2)
o-HBA	3.0	2.62	0.32	1.1×10^{10} - 1.8×10^{10} (2,3)
Humic acid	>3.6	2.74*	9.02*	-

*Units of $\text{L.M.s}^2.\text{mg}^{-1}$, #Units of L/mg/s

(Reference cited in the Table 5.1)

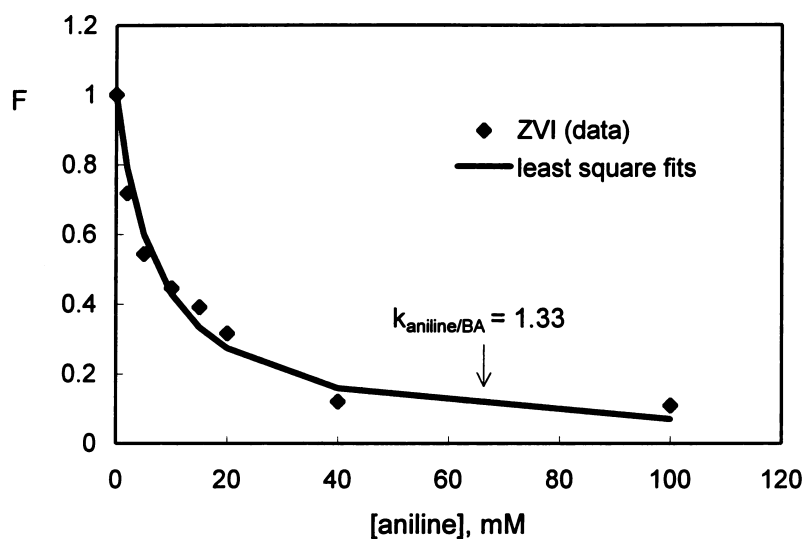
(1) Buxton, G.V.; Greenstock, C.L.; Helman, W.P.; Ross, A.B., *J. Phys. Chem. Ref. Data* **1988**, 17(2), 513-886.

(2) Rivas, F.J.; Beltrán, F.J.; Frades, J.; Buxeda, P., *Water Research* **2001**, 35, 387-396.

(3) Zečević S., Drazic D.M., Gojkovic S., *J. Electrochem. Soc.* **1989**, 265 (1-2), 179-193.

The relative rate constants for aniline, a positively charged molecule at pH 3, are similar in both the nZVI and Fenton systems suggesting no effect of the nZVI surface on reaction rate. For phenol, the relative rate constant obtained with nZVI is twice as high as that obtained with hydroxyl radicals generated in the solution phase while the relative rate constant for humic acid with nZVI-mediated oxidation is about one third of that found with Fenton reagent. Some uncertainty surrounds the quality of the relative rate data for o-HBA since the BA/o-HBA solution turned purple on adding Fe(II), presumably because of complexation between BA or o-HBA and Fe(II). Consistent with the low relative rate constant obtained in the Fenton case, this complexation might be expected to retard the rate of reaction of Fe(II) with H₂O₂ and therefore prevent the generation of OH[•].

A.



B.

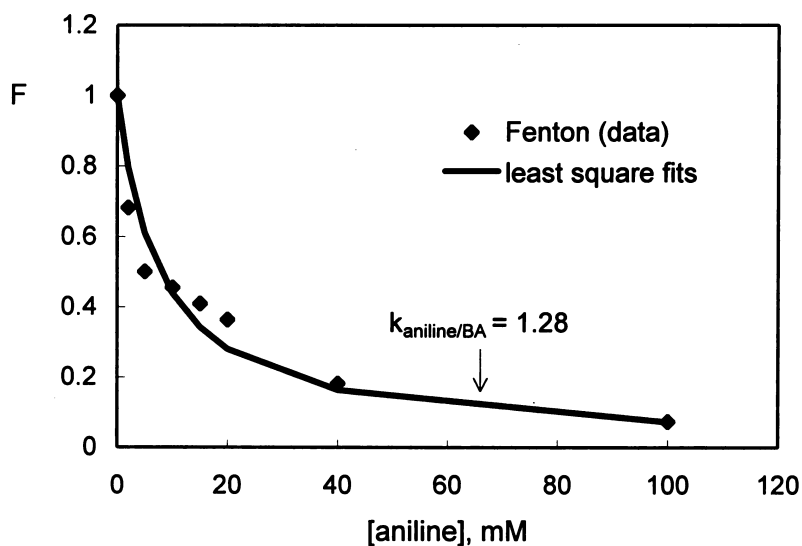
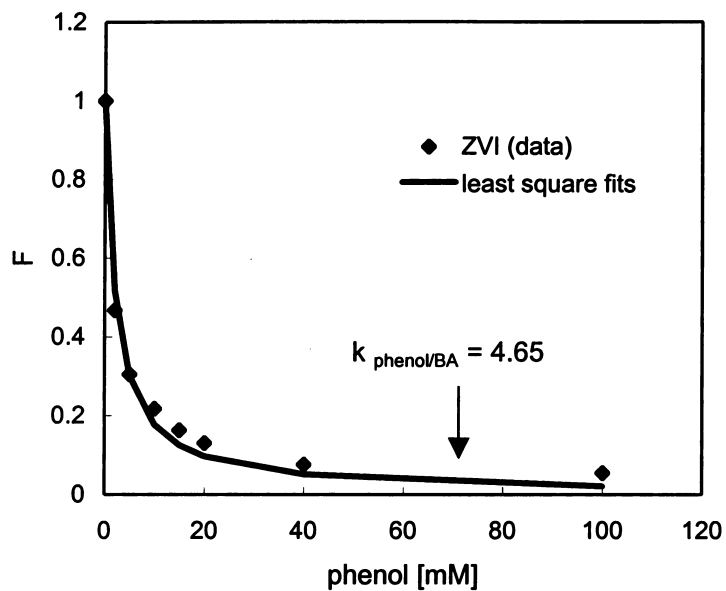


Figure 5.8. Fraction (F) of p-HBA produced in the presence of a certain concentration of aniline to that produced in the absence of aniline (i.e. in the presence of BA only) with a) nZVI used as the oxidant source, and b) Fenton reagent used as the oxidant source.

A.



B.

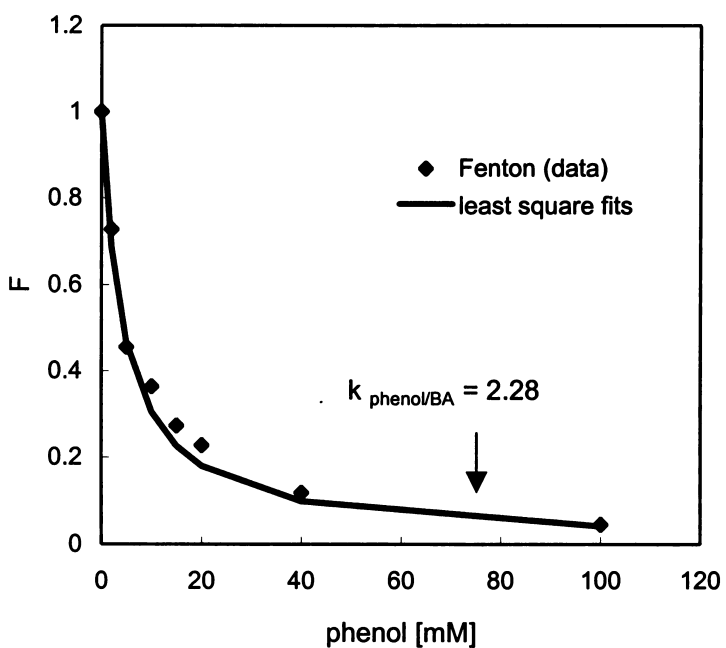
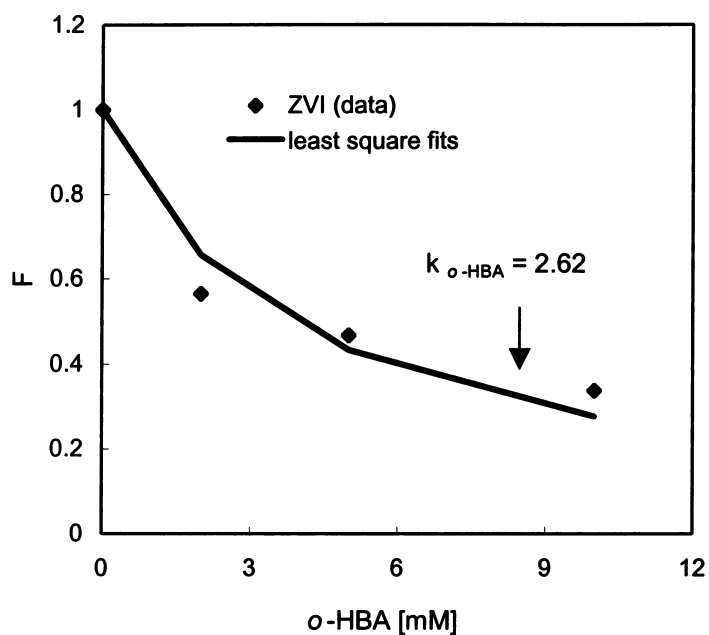


Figure 5.9. Fraction (F) of p-HBA produced in the presence of a certain concentration of phenol to that produced in the absence of phenol (i.e. in the presence of BA only) with a) nZVI used as the oxidant source, and b) Fenton reagent used as the oxidant source.

A.



B.

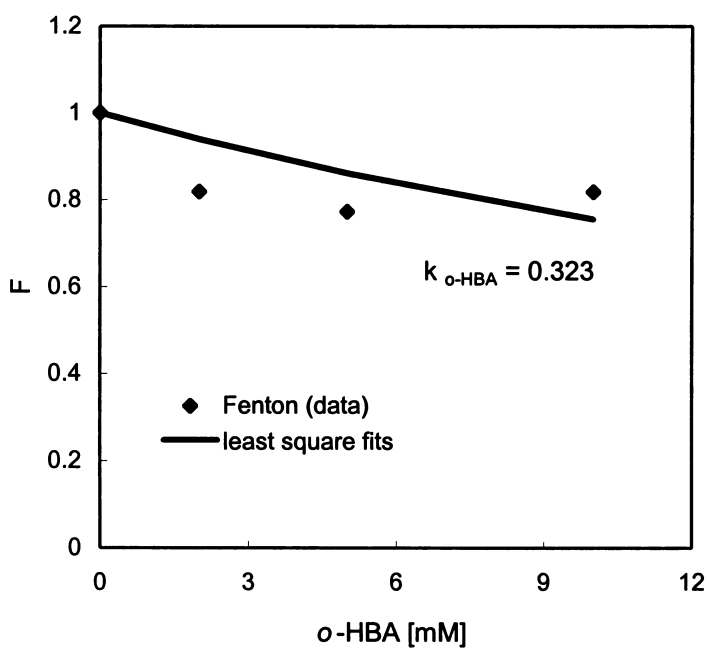
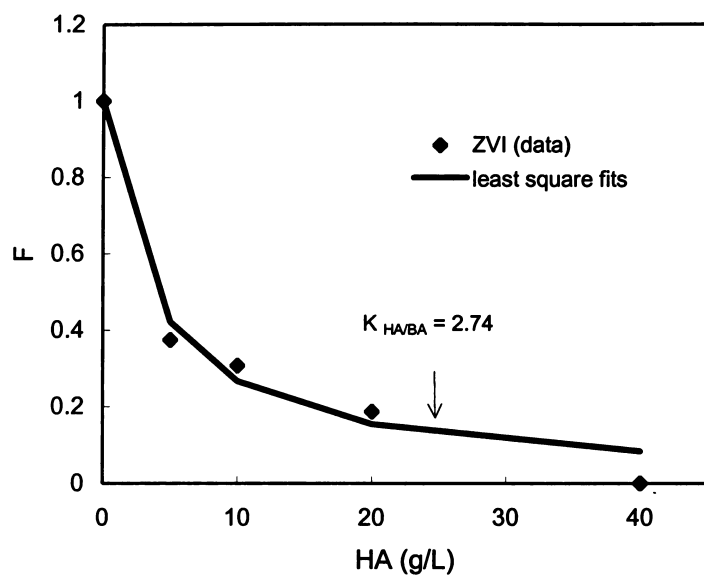


Figure 5.10. Fraction (F) of p-HBA produced in the presence of a certain concentration of o-HBA to that produced in the absence of o-HBA (i.e. in the presence of BA only) with a) nZVI used as the oxidant source, and b) Fenton reagent used as the oxidant source.

A.



B.

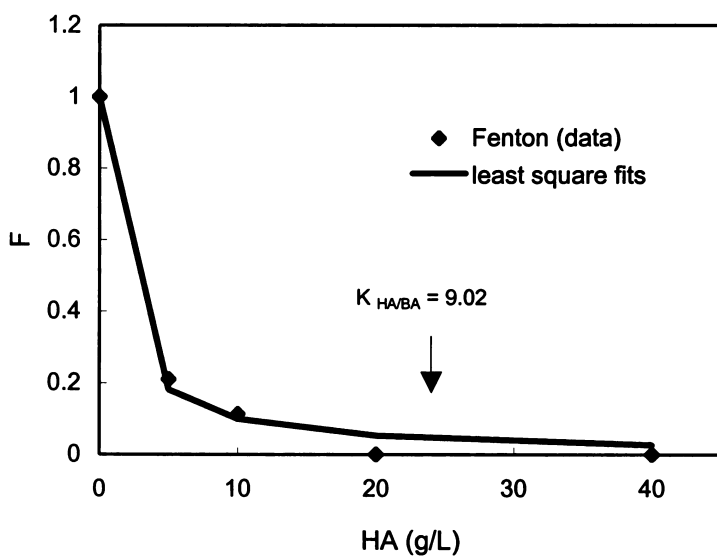


Figure 5.11. Fraction (F) of p-HBA produced in the presence of a certain concentration of humic acid to that produced in the absence of humic acid (i.e. in the presence of BA only) with a) nZVI used as the oxidant source, and b) Fenton reagent used as the oxidant source.

5.2.7 Effect of ZVI type on oxidant yields

The effect of the type of ZVI was evaluated at pH 3 with 10 mM BA. All four types of ZVI particles were capable of oxidizing BA and p-HBA production increased as the total ZVI concentration increased (Figure 5.12). While the nanosized ZVI produced more p-HBA than the other forms of Fe⁰, the rates of production for the other forms of Fe⁰ were very significant, particularly in light of their comparative surface areas (Table 5.2).

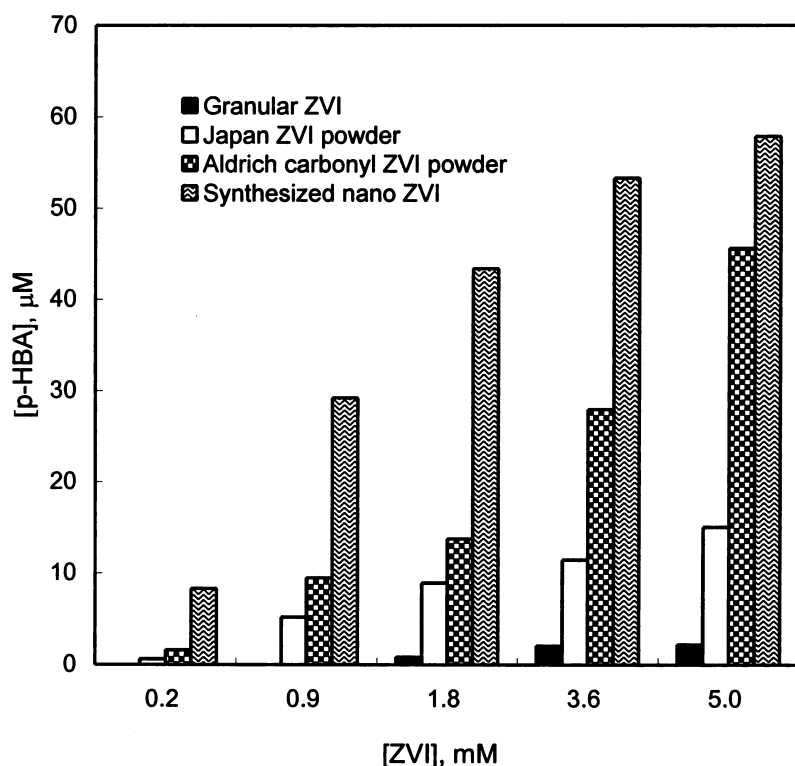


Figure 5.12. Concentration of p-HBA produced after one hour reaction of commercial granular Fe, ZVI powders, and synthesized nZVI with benzoic acid. (Conditions: pH 3, 0.9 mM Fe⁰, ionic strength 30 mM, 10 mM BA, reaction time 1 hour).

Table 5.2. Characteristics of ZVI particles used in this study.

Zero Valent Iron	Measured BET Surface Area (m ² /g) ¹	Literature Surface Area (m ² /g) (ref)	Particle size (μm)
Master Builders	0.71	1.3 ± 0.7 (1)	750 - 1200
Aldrich	0.38	0.9 ± 1.1 (1)	4.5 – 5.5
Kanto	0.60	-	100 – 150
nZVI ²	32	31.4 (2)	0.001 – 0.2

¹BET analyses performed on ZVI as received

²nZVI prepared by NaBH₄ reduction of FeCl₃ in this study

(Reference cited in the Table 5.2)

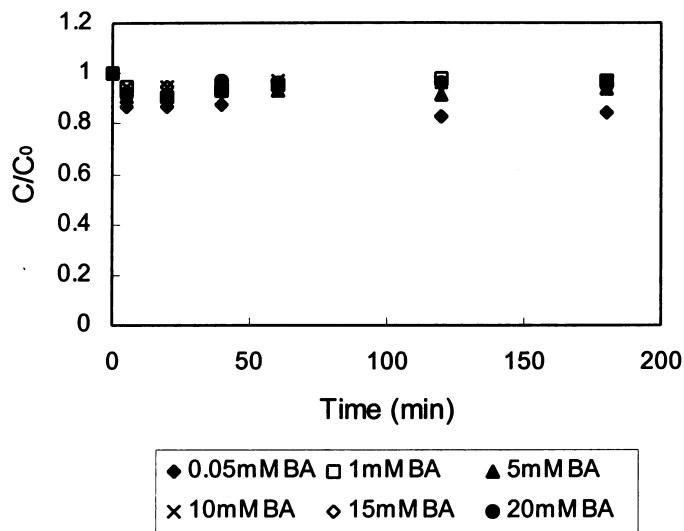
(1) Alowitz, M.J.; Scherer, M.M., *Environ. Sci. Technol.* **2002**, *36*, 299-306.

(2) Choe, S.; Lee, S-H.; Chang, Y-Y.; Hwang, K-Y.; Khim, J., *Chemosphere* **2001**, *42*, 367-372.

5.2.8 Comparison study on standard Fenton oxidation of benzoic acid

To compare with the nZVI system and to assess the oxidant yield by the Fenton process, the oxidation of benzoic acid using Fenton's reagents (e.g., 200 μM Fe(II) and 20 μM H₂O₂) was examined.

A.



B.

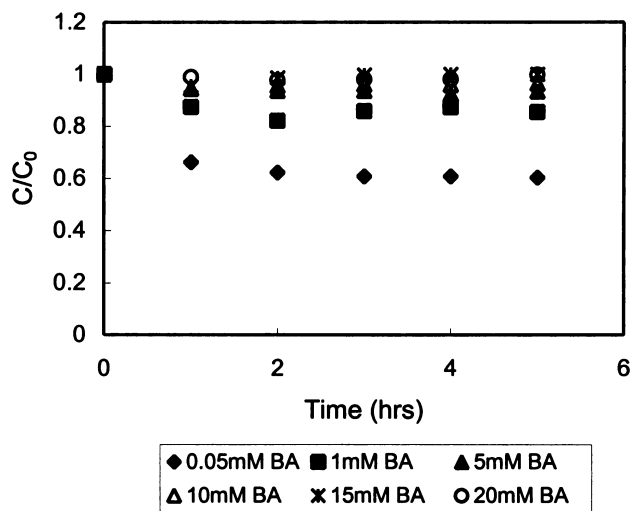


Figure 5.13. BA oxidation by Fenton's reagents (A) and ZVI (0.9mM) (B) at pH 3.

As can be seen in the Figure 5.13A-B, a similar oxidation trend was seen in the range of 0.05 – 20mM BA for both nZVI and Fenton's processes. Nevertheless, more oxidation at lower BA (e.g. 0.05mM BA) was seen in the nZVI system (Figure 5.13B) compared to the

Fenton system although this depends on the amount of iron used. As shown in Figure 5.14, the cumulative oxidant yield by Fenton was around $14\mu\text{M}$, which is lower than the expected oxidant yield of $20\mu\text{M}$ based on the amount of Fe(II) added to the system. Since *o*-HBA was not detected during the reaction, but *p*- and *m*-hydroxybenzoic acid were, the Fe(II) might be complexing the *o*-HBA and inhibiting the Fenton reaction, consequently lowering its efficiency.

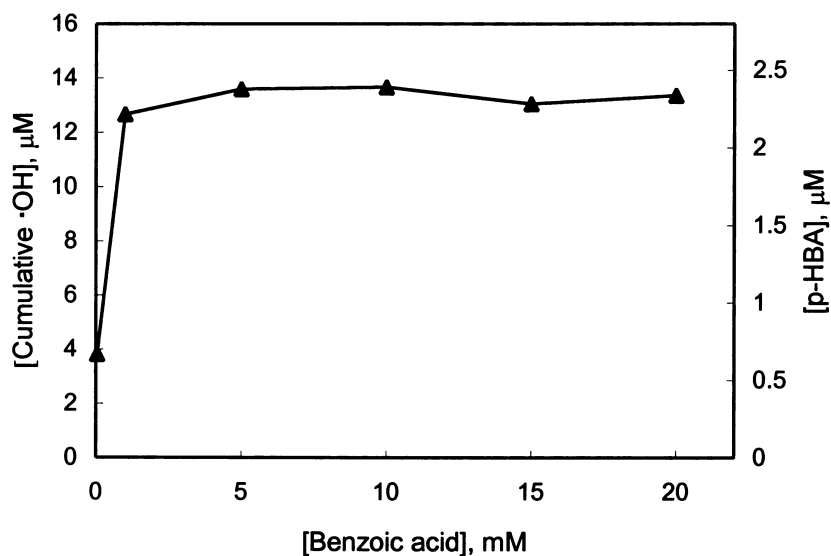


Figure 5.14. Oxidant formation in Fenton oxidation system.

5.2.9 Effect of pure O_2 on oxidant yield

The effect of replacing air with pure oxygen was investigated by sparging the ZVI suspension with oxygen gas and the kinetics of oxidant yield then assessed. As can be seen in Figure 5.15, the cumulative formation of hydroxyl radicals was greater under O_2 compared to an air sparged system. Within 1 minute, $88\mu\text{M}$ compared with $40\mu\text{M}$ of

cumulative hydroxyl radicals are formed when sparging with O₂ compared to air. The rate of oxidant formation slowed considerably for the O₂ system after 1min and there was little difference in yield for the O₂ and air sparged systems after 10mins. The results indicate that O₂ supersaturation accelerates corrosion, producing high amounts of oxidant within a short period of time, but also resulted in the rapid formation of a surface oxidation layer that hinders the continuous generation of oxidant by the nZVI.

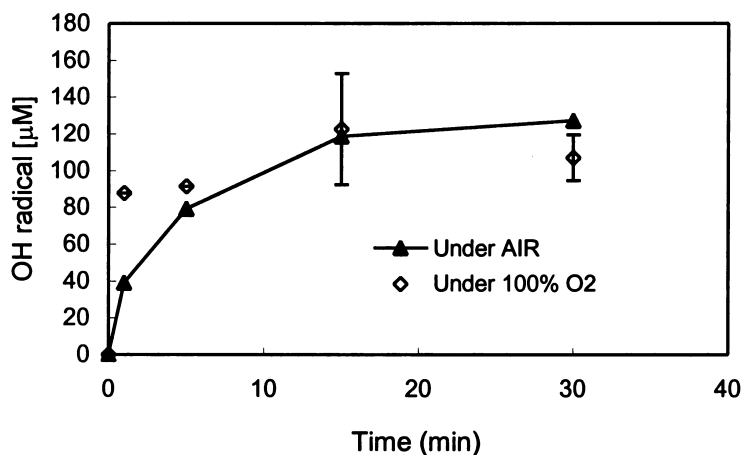
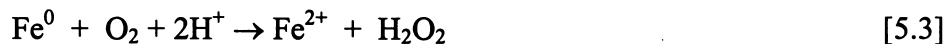


Figure 5.15. Kinetics of oxidant formation in nZVI system under O₂ and air sparging. Condition: 10mM BA, 0.9mM ZVI, pH 3, 30mM ionic strength.

5.2.10 Discussion

The first step in the oxidation of BA by nZVI involves the oxidation of Fe⁰ by O₂. Chemists and material scientists have studied this process, which is referred to as corrosion, for many years. One interpretation of corrosion posits the initial oxidation of Fe⁰ as a 2-electron process (Zečević *et al.*, 1989; Zečević *et al.*, 1991; Bozec *et al.*, 2001):



H₂O₂ produced in Eq 5.3 could oxidize another Fe⁰:



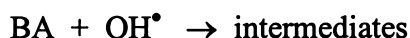
This process results in a 4-electron transfer and an overall stoichiometry of 2 moles of Fe^0 oxidized per mole of O_2 . Alternatively, H_2O_2 could react with species such as Fe(II) :



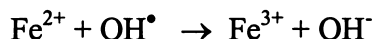
These reactions could occur on the Fe^0 surface or could involve transfer of electrons through an iron oxide layer (Zečević *et al.*, 1989), depending upon the reaction rates and affinity of the species for surfaces. Although the 4-electron transfer process is usually the dominant mechanism of O_2 -mediated corrosion, the 2-electron transfer process can result in production of significant amounts of O_2^{2-} or H_2O_2 , especially after an oxide coating has been formed on the surface. For example, in studies conducted on stainless steel rotating disc electrodes, 10 to 20% of the oxygen reduced during corrosion was converted into O_2^{2-} or H_2O_2 (Bozec *et al.*, 2001).

On Fe^0 surfaces, the initial rate of the reaction is fast. However, a surface oxide layer consisting of $\gamma\text{-Fe}_2\text{O}_3$ and Fe_3O_4 -like oxides forms as the surface is oxidized (Davenport *et al.*, 2000). This passive layer protects the remaining Fe^0 from attack by oxygen by serving as a barrier between the Fe^0 and O_2 . The initial pulse of oxidants produced in the nZVI system is consistent with oxidation of the surface Fe^0 serving as the source of oxidant. For example, assuming that each Fe^0 occupies an area equal to $1.6 \times 10^{-19} \text{ m}^2$ (i.e., assuming an atomic radius of 1.4 \AA and a Fe-Fe bond distance of 2.5 \AA), a monolayer would correspond to approximately 1.8% of the total ZVI. Therefore, the maximum reaction efficiency for the initial fast part of the reaction at pH 3 (Figure 5.6) would correspond to a corrosion layer that was about 14 molecules in thickness.

Reaction 5.4 provides a possible explanation for the observed oxidation of BA and other organic compounds that occurs when nZVI is exposed to O₂. The simplest model for this process would involve the production of OH[•] in solution followed by a homogeneous reaction between BA and OH[•]. In this case, the rate at which BA is oxidized would depend upon the relative concentrations of different OH[•] sinks. Under the conditions in this system, the dominant sinks are expected to be:



$$k = 4.3 \times 10^9 \text{ M}^{-1} \text{ s}^{-1} \text{ (Andreozzi and Marotta, 2004) [5.6]}$$



$$k = 4.0 \times 10^8 \text{ M}^{-1} \text{ s}^{-1} \text{ (Sychev et al., 1979) [5.7]}$$

When an aromatic compound reacts with OH[•], a cyclohexadienyl radical is formed that reacts with oxygen, eventually resulting in the production of hydroxylated products (Dorfman *et al.*, 1962; Eberhard and Yoshida, 1973). At the total Fe(II) concentrations measured in the experiments described in Figure 5.3 (approximately 0.2 mM), benzoic acid should be a dominant sink for OH[•] if the reaction occurs in the bulk solution. As indicated by the calculated fit depicted in Figure 5.3, OH[•] is scavenged more effectively than predicted by only Fe(II). Under the conditions used in these experiments, the pseudo-first order rate constant for other unknown sinks would have to be equal to $2 \times 10^6 \text{ s}^{-1}$ (dashed line in Figure 5.3). If the sink is dissolved Fe(II), this would correspond to 5 mM Fe²⁺.

An alternative explanation for the results depicted in Figure 5.3 is that hydroxyl radical is generated on or adjacent to the surface. Under such conditions, Fe(II) adsorbed on the nZVI surface or concentrated in the area immediately adjacent to the surface could more

effectively compete with BA for OH^\bullet . If this were the case, we would expect organic compounds with a higher tendency to adsorb to the surface to be oxidized more quickly than those compounds with a low affinity for surfaces. At pH 3, the surface of the nZVI is positively charged (Figure 3.5). Therefore, positively charged solutes such as aniline should have a lower affinity for the surface than neutral solutes and solutes that can form surface complexes (e.g., BA or phenol). Despite the tendency for BA to exhibit a higher surface affinity than aniline, the relative rate constant for the aniline (relative to BA) is nearly identical for the nZVI system and the Fenton's reagent system in which OH^\bullet is generated in solution (Figure 5.8 - 5.11; Table 5.1). The relative rates for the other solutes also do not exhibit strong selectivity for species that are expected to have a higher affinity for the surfaces.

The apparent low selectivity observed for nZVI contrasts with the high selectivity observed in TiO_2 photocatalysis, in which the oxidant is produced at the surface. For example, the trichloroacetate anion is preferentially degraded at low pH when the TiO_2 surface ($\text{pH}_{\text{zpc}} = 6.25$) is positively charged whereas the positively charged cation chloroethylammonium is degraded preferentially at high pH when the TiO_2 surface has a net negative charge (Kormann *et al.*, 1991). The absence of a relationship between the charge of the compound and relative rates of oxidation in the nZVI system suggests that a direct interaction between the surface and the solute is not important. As indicated earlier, the dependence of the yield on [BA] suggests that the oxidant is not produced in the bulk solution. Therefore, it is possible that the initial oxidation occurs close to the surface in a region in which [Fe(II)] is higher than the concentrations measured in the bulk solution. The detection of mixed

Fe(II)/(III) oxides such as maghemite at the nZVI surface is consistent with oxidation of Fe²⁺ to Fe(III) in these systems.

Irrespective of the identity of the oxidant or the location in which it is generated, these results indicate that oxidation of ZVI by oxygen results in the production of an oxidant that is capable of transforming organic contaminants. The initial pulse of oxidants might be useful in remediation of contaminated soils and groundwater and might serve as an alternative to other in situ treatment oxidation processes, such as the addition of H₂O₂. The slower release of oxidants that occurs after 30 minutes, which likely corresponds to the continued corrosion of the nZVI particle, might be useful for remediation of difficult-to-reach groundwater, provided that oxygen was not depleted from the groundwater. Additional research is needed to assess the kinetics of oxidant production from nZVI particles on the time scale of days to months.

The production of oxidants during Fe⁰ oxidation is not a phenomenon that is limited to nZVI particles (Figure 5.12). Although researchers studying nZVI have noted the disappearance of O₂ as oxic water enters a Fe⁰_(s) permeable reactive barrier (O'Hannesin and Gillham, 1998; Yabusaki *et al.*, 2001), the potential for transformation of contaminants in this zone has not been appreciated previously. The Fe-mediated production of oxidants on Fe⁰_(s) might provide new applications for ZVI reactive permeable barriers. For example, consider the leading edge of a groundwater plume that is contaminated with a highly mobile contaminant, such as MTBE or NDMA. Assuming the plume initially is saturated with oxygen (i.e., 0.26 mM) and that the plume contains 1 µg/L (i.e., ≈ 10⁻⁸ M) of the

contaminant, 2 mg/L of natural organic matter (i.e., $\approx 2 \cdot 10^{-6}$ M or less) and 1 mM of HCO_3^- . If all of the oxygen is consumed in the barrier by reaction with Fe^0 and 10% of the O_2 undergoes the 2-electron transfer pathway to form the oxidant, 26 μM of oxidant will be produced. Assuming that the oxidant exhibits the same reactivity as OH^\bullet , almost all of the contaminants would be removed in the reactive barrier via oxidative processes.

5.2.11 Conceptual kinetic modeling

5.2.11.1 ZVI corrosion process

Since the diffusion rate at steady state is proportional to oxygen concentration, it follows that the corrosion rate of iron is also proportional to oxygen concentration (Uhlig and Revie, 1985). Although an increase in oxygen concentration at first accelerates corrosion of iron, the corrosion rate drops again to a low value due to the formation of an oxide layer (Crow, 1984). The corrosion in the presence of oxygen is therefore initially very high and is largely dependent on the rate of diffusion of oxygen to the metal surface. The increased corrosion rate of iron as pH decreases is not caused only by increased hydrogen evolution; in fact, greater accessibility of oxygen to the metal surface on dissolution of the surface oxide favors oxygen depolarization, which is often the more important reason (Uhlig and Revie, 1985).

Rapid corrosion may produce the initial pulse of peroxide through the $2e^-$ pathway in the presence of oxygen. However, such corrosion decreases as the reaction proceeds due to an oxide layer developing, which is from $4e^-$ pathway. The continuous oxidant yield, degradation of molybdate even at high pH, and increasing trend of oxidants at mid-pH over

24hrs suggests that the $2e^-$ pathway though transient could continue through the corrosion reaction.

For processes that involve heterogeneous reactions, the apparent rate is usually dominated by either the rate of intrinsic chemical reactions on the surface or the rate of diffusion of the solutes to the surface (Uhlig and Revie, 1985). The average rate of reaction of H_2O_2 on the iron oxide surface is far slower than its diffusion rate to the surface through either the external film or internal pores (Lin and Gurol, 1998). Therefore, the intrinsic reactions on the oxide surface are expected to be the rate-limiting steps for this process. In general, the model for surface reactions consists of the following steps.

- Mass transport of the reactant to the Fe^0 surface from the bulk solution
- Adsorption of the reactant to the surface
- Chemical reaction at the surface
- Desorption of the products
- Mass transport of the products to the bulk solution.

It is proposed that the reactions occur at or near the Fe surface rather than in aqueous phase. However, probe compounds (aniline, phenol, o-hydroxybenzoic acid) showed similar relative rates of reaction, suggesting the key oxidation occurs in solution-phase but near the iron surface.

Contaminant molecules in the aqueous phase have access to the iron surface where they can either adsorb to non-reactive sites or reach reactive sites where the reactions can take place. It is postulated that iron sorbed to the non-reactive sites cannot leave the surface and there

is continuous regeneration of reactive sites as compounds degrade. Kitajima *et al.* (1978) proposed a possible mechanism for the heterogeneous goethite-catalyzed reaction (in the presence of peroxide) as described by.



where S is the mineral surface and S⁺ is an oxidized region of the surface. Consumption of peroxide increased as a function of its initial concentration and the treatment is most economical at low H₂O₂ concentrations because of minimal quenching and more efficient stoichiometry. Based on homogeneous rate constants, the oxidation rate of ferrous sites by H₂O₂ (reaction 5.8) is expected to be ~700 times faster than the oxidation rate of ferrous sites by oxygen (reaction 5.9).



5.2.11.2 Key reactions involved in the ZVI oxidation process

The reduction of oxygen plays a key role in the corrosion of iron in aerated environments, and H₂O₂ has been found to be a reduction product (Bozec *et al.*, 2001). The reduction of oxygen and the peroxide formation as an intermediate occur on the oxidized surface (Zečević *et al.*, 1991). On the oxide-free surface the 4e⁻ reduction was found although the kinetics of the O₂ reduction reaction is slower on more oxidized surfaces, with little hydrogen peroxide as an intermediate (less than 0.5% of the total reduction current, Zečević *et al.*, 1989; Jovancicevic and Bockris, 1986) and formation of superoxide radical while on passive iron, oxygen reduction proceeds through a 2e⁻ pathway with the formation of hydrogen peroxide as a reaction product (Zečević *et al.*, 1989; Jovancicevic and Bockris,

1986). The $4e^-$ pathway appears to proceed via formation of adsorbed peroxide or superoxide where these adsorbates do not lead to a solution phase species (Jovancicevic and Bockris, 1986).

Oxygen adsorption occurs on iron with the rate of adsorption of oxygen expected to be low. Ferro *et al.* (2004) showed that the O_2 molecule only slightly physisorbs to a graphite surface and induces very little charge transfers. The rate constant for Eq 5.10 is unknown.



The rate of oxidation of ZVI surface groups to $>Fe(II)$ is also unknown.



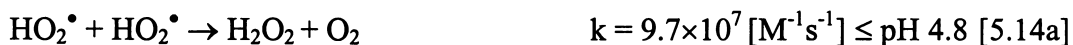
The reduction of $>O_2$ occurs rapidly as indicated by Bielski *et al* (1985).



Desorption of superoxide into solution occurs with a rate constant of $k = 10^{-4} [M^{-1}s^{-1}]$ estimated from modeling by Feitz and Waite (2003) although it was not measured experimentally.

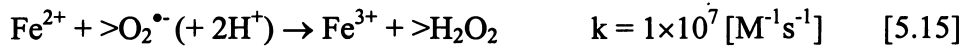


The superoxide in solution results in the formation of H_2O_2 via the following reaction with rate constants at different pHs (Bielski *et al.*, 1985):



Reaction 5.14a is likely to occur relatively rapidly at low pH but to occur more slowly at higher pH, resulting in formation of hydrogen peroxide at or near the ZVI surface.

Ferrous iron released from ZVI might also react with superoxide formed on the ZVI surface (Chen and Pignatello, 1997),



And might also be scavenged by hydroxyl radicals (Buxton *et al.*, 1988) and superoxide in solution (Keene, 1964).



Ferrous iron is regenerated by the reaction between Fe(III) and $\text{O}_2^{\bullet-}$ (Nadezhdin *et al.*, 1976)



Ferrous oxidation and deactivation of superoxide are likely to be important factors affecting organic contaminants removal rate. It is likely that ZVI will be regenerated by the release of $>\text{Fe}(\text{II})$ to solution (as Fe(II)) though this is expected to occur relatively slowly with rate constant estimated to be between 10^{-1} and 10^{-5} (s^{-1}) based modeling studies by Feitz and Waite (2003) for desorption from TiO_2 surface.



Since surface area concentrations of ZVI change with time, the surface area concentration is estimated assuming the ZVI particles are spherical and the size uniform as indicated by Chen *et al.* (2001).

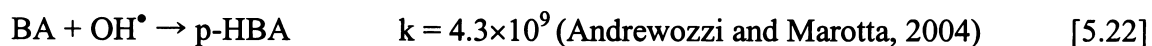
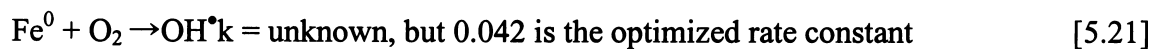
$$\rho_{a(t)} = \rho_{a(o)} \left[\frac{M_t}{M_o} \right]^{2/3} \quad [5.20]$$

where $\rho_{a(o)}$ is the initial surface concentration, M_o the initial ZVI mass and M_t is the ZVI mass at time t . M_t is calculated by subtracting the mass of total dissolved iron (i.e. ferrous iron concentration times the solution volume) from the initial iron loading. Chemical

reactions occur on reactive sites, which are those where the breaking of bonds in the reactant molecules takes place, while on nonreactive sites only sorption interactions occur and the solute molecule remains intact (Burriss *et al.*, 1995).

Due to several unknown rate constants, the exact reactions are not drawn, however, it was possible to estimate hydroxyl radical production in the presence of oxygen using the data presented in Figure 5.3. The following reactions were used to assess the effect of Fe(II) presence on the cumulative generation of OH radicals as the function of model compound (BA). The reactants and their concentrations used in the model using the ACHUCHEM kinetics program are as follows: ZVI, 0.9mM; O₂, saturated 0.26mM; BA, 50μM – 20mM; Fe²⁺, verified.

Reaction 5.21 is a simplification but represents the rate of generation of hydroxyl radicals at the ZVI surface from the interaction of ZVI surface sites and O₂.



The fitted rate constants for reaction 5.21 range from 0.04 – 0.042 [M⁻¹s⁻¹] with the Fe(II) concentration of 4 - 5mM. The optimized rate constant of the reaction [5.21] is 0.042 [M⁻¹s⁻¹] and the best fit scavenger concentration of Fe(II) with the rate constant is found to be 5mM. As an example with benzoic acid, the peroxide formed through 2e⁻ oxygen reduction pathway reacts with ferrous iron via the Fenton reaction, producing hydroxy radical that can indiscriminately react with most organics in solution-phase (Wells and Salam, 1968a).



On the iron surface, adsorbed benzoic acid competes for hydroxyl radical formed on surface and/or interface near surface layer (Eq 5.23). Although the Fenton reaction occurs in solution it is likely that most primary reactions arises near the iron surface.

Hydroxyl radicals formed react with H_2O_2 (Sychev *et al.*, 1995) and the decomposition of H_2O_2 (Bielski and Cabelli, 1995), speciation rate constants (Bielski and Cabelli, 1995) are as follows.



In the system containing bicarbonate, the rate constant is slower than that from most organic reaction with hydroxyl radical as follows (Buxton *et al.*, 1988; Bielski *et al.*, 1985).



The rate of catalytic decomposition of H_2O_2 on passive iron is very low, less than 8×10^{-11} mol $\text{cm}^{-2}\text{s}^{-1}$ (Calvo and Schiffrin, 1984). The oxygen reduction is controlled by the properties of the surface and significantly influenced by the surface oxides (Bozec *et al.*, 2001). In the four-electron pathway, O_2 reduction is limited by mass transport in the

solution. It may be due to a limited access of oxygen to the metal surface while on passivated surfaces, O₂ reduction occurs simultaneously with the reduction of ferric oxide. O₂ reduction rate is lower on oxide-covered surfaces than on bare metal electrode (Bozec *et al.*, 2001).

A summary of the reactions that may be involved in the ZVI-mediated oxidation process, with rate constants from literature values, is given in Table 5.3.

Table 5.3. Model reactions and rate constants (example of compound: benzoic acid).

Reactions	Constants (M ⁻¹ s ⁻¹)	References
1. Fe ⁰ + O ₂ → >O ₂	unknown	-
2. Fe ⁰ + >O ₂ → >Fe ²⁺ + 2>e ⁻	unknown	-
3. >O ₂ + >e ⁻ → >O ₂ ⁻	2×10 ¹⁰	Bielski <i>et al.</i> (1985)
4. >O ₂ ⁻ → O ₂ ⁻	1×10 ⁴	Feitz and Waite (2003)
5a. HO ₂ [•] + HO ₂ [•] → H ₂ O ₂ + O ₂	9.7×10 ⁷ (≤ pH 4.8)	Bielski <i>et al.</i> (1985)
5b. HO ₂ [•] + O ₂ ⁻ + H ₂ O → H ₂ O ₂ + O ₂ + OH ⁻	6.1×10 ⁴ (pH 8)	Bielski <i>et al.</i> (1985)
6. Fe ²⁺ + O ₂ ⁻ → Fe ³⁺ + H ₂ O ₂	1×10 ⁷	Chen and Pignatello (1997)
7. Fe ²⁺ + OH [•] → Fe ³⁺ + OH ⁻	4.3×10 ⁸	Buxton <i>et al.</i> (1988)
8. Fe ²⁺ + O ₂ ⁻ → Fe ³⁺ + HO ₂ ⁻	7.3×10 ⁵	Keene (1964)
9. Fe ³⁺ + O ₂ ⁻ → Fe ²⁺ + O ₂	1.9×10 ⁹	Nadezhdin <i>et al.</i> (1976)
10. >Fe ²⁺ → Fe ²⁺ + regenerated ZVI	unknown	-
11. Benzoic acid + OH [•] → intermediates	4.3×10 ⁹	Andreozzi and Marotta (2004)
12. Fe ²⁺ + H ₂ O ₂ → Fe ³⁺ + OH [•] + OH ⁻	586 (pH ≥ 4)	Wells and Salam (1968a)
13. OH [•] + H ₂ O ₂ → HO ₂ [•] + H ₂ O	3×10 ⁷	Sychev <i>et al.</i> (1995)
14. H ₂ O ₂ → HO ₂ [•] + H ⁺	5×10 ⁻² (s ⁻¹)	Bielski and Cabelli (1995)
15. O ₂ ⁻ + H ⁺ → HO ₂ [•]	5×10 ¹⁰	Bielski and Cabelli (1995)
16. HO ₂ [•] → O ₂ ⁻ + H ⁺	5×10 ⁵ (s ⁻¹)	Bielski and Cabelli (1995)
17. HO ₂ ⁻ + H ⁺ → H ₂ O ₂	5×10 ¹⁰	Bielski and Cabelli (1995)
18. HCO ₃ ⁻ + OH [•] → CO ₃ ^{•-} + H ₂ O	8.5×10 ⁶	Buxton <i>et al.</i> (1988)
19. CO ₃ ^{•-} + O ₂ ⁻ → CO ₃ ²⁻ + O ₂	6.5×10 ⁸	Bielski <i>et al.</i> (1985)

Note that some rate constants were drawn from homogeneous studies. Therefore, caution must be exercised because the heterogeneous rate constants may be different.

5.2.12 Conclusion

Addition of nanoparticulate zero-valent iron (nZVI) to oxygen-containing water results in oxidation of organic compounds. Additional studies on the oxidation of benzoic acid suggest that the oxidation involves the production of hydroxyl radicals through the reaction of ferrous iron and hydrogen peroxide. When nZVI was added to BA-containing water, an initial pulse of p-HBA was detected during the first 30 minutes, followed by the slow generation of additional p-HBA over periods of at least 24 hours. The yield of p-HBA increased with increasing BA concentration, presumably due to the increasing ability of BA to compete with alternate oxidant sinks, such as ferrous iron. At pH 3, maximum hydroxyl radical yields during the initial phase of the reaction were as high as 25% based on p-HBA measurements.

The initial rate of nZVI-mediated oxidation of BA exhibited a marked reduction at pH values above 3. Despite the decrease in oxidant production rate, p-HBA was observed during the initial reaction phase at pH values up to 8. Competition experiments with probe compounds expected to exhibit different affinities for the nZVI surface (phenol, aniline, o-hydroxybenzoic acid and synthetic humic acids) indicated relative rates of reaction that were similar to those observed in competition experiments in which hydroxyl radicals were generated in solution. A number of key findings, which have implications to the potential applications of this technology are summarised below:

- Nanoscale zero valent iron (nZVI) particles are capable of producing highly reactive and unselective hydroxyl radicals in the presence of oxygen. This newly discovered

advanced oxidation technology therefore has the potential to oxidize almost all organic contaminants.

- As is the case for hydroxyl radicals, the presence of compounds other than the contaminant being targeted may reduce the efficiency of the process as a result of competition for the oxidant produced
- While the process appears to exhibit high, short term activity (especially at low pH), the process does appear to continue to be an effective oxidant generator over longer time periods and over a range of pH.
- The findings on competition study suggest that, whilst the key reagents leading to generation of the powerful oxidants are sourced from the nZVI particles, the key oxidation step occurs in solution but in close proximity to the particle surface. The results of these studies will suggest possible applications of nanosized Fe^0 particles in oxidatively degrading chemicals of concern.
- The possibility that nano iron particles can induce oxidative degradation of contaminants in the presence of oxygen markedly broadens the applicability of ZVI as a potentially useful reagent for the degradation of contaminants in waters and wastewaters.
- The non-specificity of the nZVI oxidative process would appear to limit its application to scenarios involving high contaminant concentrations in systems where oxygen supply can be maintained.
- Consideration should be given to the possibility that ZVI-mediated oxidative processes are occurring at the surface of Fe^0 reactive barriers.
- Further investigations are required to both clarify the reaction mechanism and optimize operating conditions.

Chapter 6. Conclusions and Future Research Needs

6.1. Summary of results

Contamination of water and soil with agrochemicals is a global environmental problem.

Pesticide residues have been detected in various natural waters in many countries and the presence of agrochemicals in drinking water supplies is of particular concern. It is an emerging problem in developing countries and there is a genuine need for efficient and cost-effective remedial technologies. Thus, the investigation of remediation technology for polluted waters containing trace amounts of herbicides is of environmental interest.

The effectiveness of nanoscale zero-valent iron (nZVI) in degrading selected organic contaminants was found to vary widely. Extensive degradation was observed for aldrin, molinate, chlorpyrifos, and atrazine while dieldrin, heptachlor, chlordane and endosulfan were not degraded significantly under the experimental conditions used. Of the contaminants investigated, molinate was found to degrade effectively in oxic solutions containing nZVI, but removal ceased in the absence of oxygen. Molinate was subsequently chosen as the subject of further investigations into the kinetics and mechanism of nZVI particle facilitated degradation under oxic conditions.

The degradation rate of molinate was dependent on a number of physical conditions including ZVI concentration and pH. Additional studies using a ZVI/H₂O₂ process were highly effective, reducing the quantity of ZVI necessary for rapid removal of molinate. The degradation by-products were found to be the same for ZVI alone, ZVI/H₂O₂ and the

Fenton process (Fe(II)/H₂O₂), suggesting that molinate may be oxidized by the same pathway in each case.

The primary degradation products of the nZVI-mediated degradation process, keto-molinate isomers, have been previously found to be generated by hydroxyl-radical attack on molinate. That hydroxyl radicals or hydroxyl radical-like entities were involved in the degradation process is supported by findings that the hydroxyl radical scavenger, 1-butanol, was capable of completely limiting the oxidation of molinate. In addition, results of the reaction of molinate and nZVI in the presence of catalase (which removes H₂O₂) and in the presence of superoxide dismutase (which enhances the rate of formation of H₂O₂) lends further support to an oxidative mechanism involving hydrogen peroxide as an intermediate in the degradation pathway. Both hydrogen peroxide and Fe(II) were identified as reaction products.

The primary oxidant is therefore consistent with hydroxyl radicals. The radicals are likely to be formed as a result of reduction of oxygen to superoxide at the particle surface, disproportionation of the superoxide to hydrogen peroxide and a Fenton reaction between the hydrogen peroxide and Fe(II) released during the corrosion process.

To identify the reaction mechanism and the factors that affect nZVI reactivity, a series of experiments were conducted using the formation of hydroxybenzoic acid (HBA) from benzoic acid (BA) as a probe for measuring the oxidizing capacity of nZVI. The p-isomer is the dominant product formed on oxidation of benzoic acid. The reaction went to completion within the first hour with little increase in reaction product concentration thereafter.

Increasing the initial concentration of BA results in an increase in the concentration of p-HBA produced. In contrast, the radical production efficiency of the nZVI as an oxidant generator decreases with increased nZVI loading, which suggests the need to use a low dose of nZVI for maximum efficiency. It was observed that almost 25% of the ZVI at low loading is converted to oxidant using the hydroxyl radical conversion factor noted by Zhou and Mopper (1990). The rate and overall yield of the reaction decreased with increasing pH, presumably due to either changes in the corrosion process or increasingly effective passivation effects.

Results of longer-term (1 day) studies of hydroxyl radical production indicate that, while slow, nZVI-mediated oxidation will continue for some time, particularly in the low to mid-pH range. The findings using competing probe molecules (phenol, aniline, and o-hydroxybenzoic acid) to ascertain the importance of surface versus solution-phase reactions suggest that, whilst the key reagents leading to generation of the powerful oxidants are sourced from the nZVI particles, the key oxidation step occurs in solution but presumably in close proximity to the particle surface given the highly reactive nature of hydroxyl radicals.

6.2. Possible applications of the ZVI-mediated oxidative process

The nanoscale iron particles may be useful for a wide range of environmental applications. There are more flexible emplacement options for nanoscale iron compared to granular iron and its use in permeable reactive barriers. For surface and groundwater remediation, the particles could remain suspended under very gentle agitation in an aqueous solution or

could be injected into contaminated soils, sediments, and aquifers for in situ remediation of contaminants. Alternatively they could be anchored onto a solid matrix to enhance the treatment of water, wastewater, or gaseous process streams.

While the standard Fenton process has been reported to be relatively ineffective at higher pH, a high degree of degradation of contaminants was observed at alkaline pH in the radical-mediated process that is initiated by nZVI in the presence of dissolved oxygen. Degradation is possible at high pH and there is ongoing, although slower, decontamination after an initial rapid pulse of degradation activity. The process is effective as long as Fe^0 is available. This ongoing activity could enable the degradation of contaminants present in oxygen-rich groundwaters.

6.3. Overview of nZVI research and further research needs

The use of nanoscale ZVI for remediation provides fundamental research opportunities and technological applications in environmental engineering and science. ZVI has proven to be useful for reductively transforming or degrading numerous types of organic and inorganic environmental contaminants. Few studies, however, have investigated the oxidation potential of ZVI. Contaminants investigated so far include molinate, atrazine, aldrin, chlorpyrifos from this study, methyl *tert*-butyl ether (MTBE) (by coupled ZVI/ H_2O_2) from the finding by Bergendahl and Thies (2004), chlorinated phenols by Noradoun *et al.* (2003) and possibly many nitrogen containing NDMA precursors, including dimethylamine and trimethylamine, which might be suitable for oxidative degradation.

ZVI would be very useful for widespread remediation of organic contaminants due to the relative simplicity of the technology and the potential ready availability of key reactants. Since nanoscale iron particles have high surface reactivity with high surface areas, nZVI provides a new option in environmental remediation technologies, and may provide cost-effective treatment to some of the most challenging environmental problems.

While such nanoscale ZVI technology appears interesting, some issues need to be addressed and require further research. These issues are listed below:

1. It was suggested that a pH increase will favor the formation of iron hydroxide $\text{Fe}(\text{OH})_3$, which may eventually form a surface layer that inhibits iron dissolution. Formation of other mineral phases can also occur depending on the ions available in solution. The formation of surface films may cause long-term problems by reducing the activity of the metal surfaces or clogging pores;
2. Long-term efficiency of nZVI colloidal barriers is unclear.
3. Nanoscale ZVI particles tend to aggregate, limiting their dispersability and potential reactivity;
4. Microbiological effects are likely to occur during extended application of in-ground reactive barriers.

Additional research in the following areas is needed if nZVI-mediated treatment technology is to become established:

1. Minimization of the surface passivation with respect to the contaminant degradation reaction:

2. Investigate of combined treatment with biodegradation since biodegradation by microorganisms may be important in meeting remediation targets if effluent from the iron-bearing zone contains partial degradation products that are still considered hazardous;
3. Improvement of effective treatment over longer time periods, and the determination of the efficiency of continuous removal with a cleaner surface under certain groundwater conditions;
4. An accurate means of predicting the interactions in nZVI colloidal barriers to improve the efficiency of application and to predict longevity so that reliable cost assessments can be made;
5. Understanding the chemical interactions over long time periods;
6. Understanding of both contaminant and major ion chemistry for cost-effective designs;
7. Methods of provision of oxygen in systems where this key reactant is limiting;
8. Development of efficient nZVI emplacement methods.

Decontamination of polluted groundwater is always problematic since the technological facilities used for flow through treatment systems must be designed for a high capacity and long-term operation. Thus, economic considerations, and concern about effective long-term treatment are contributing to a shift away from the established “pump and treat” treatment remediation systems towards in situ methods (Janda *et al.*, 2004). Within this context, nZVI oxidative technologies, which do not require the use of expensive oxidants, are likely to be particularly attractive.

Chapter 7. References

Agency for Toxic Substances and Disease Registry (ATSDR) (1990) *Toxicological profile for toxaphene*. US Public Health Service, US Department of Health and Human Services, Atlanta, GA.

Agency for Toxic Substances and Disease Registry (ATSDR) (1992) *Toxicological profile for chlordane*. US Public Health Service, US Department of Health and Human Services, Atlanta, GA.

Agency for Toxic Substances and Disease Registry (ATSDR) (1993) *Toxicological profile for heptachlor/heptachlor epoxide*. US Public Health Service, US Department of Health and Human Services, Atlanta, GA.

Agilar, C.; Peñalver, S.; Pocurull, E.; Borrull, F.; Marcé, R.M. (1998) Solid-phase microextraction and gas chromatography with mass spectrometric detection for the determination of pesticides in aqueous samples. *Journal of Chromatography A*, 795, pp. 105-115.

Agrawal, A.; Tratnyek, P.G. (1996) Reduction of nitro aromatic compounds by zero-valent iron metal. *Environmental Science and Technology*, 30(1), pp. 153-160.

Al Momani, F.; Sans, C.; Esplugas, S. (2004) A comparative study of the advanced oxidation of 2,4-dichlorophenol. *Journal of Hazardous Materials*, 107(3), pp. 123-129.

Alowitz, M.J.; Scherer, M.M. (2002) Kinetics of nitrate, nitrite, and Cr(VI) reduction by iron metal. *Environmental Science and Technology*, 36, pp. 299-306.

Amaraneni, S.R. (2002) Persistence of pesticides in water, sediment and fish from fish farms in Kolleru Lake, India. *Journal of the Science of Food and Agriculture*, 82, pp. 918-923.

Andreozzi, R.; Marotta, R. (2004) Removal of benzoic acid in aqueous solution by Fe(III) homogeneous photocatalysis. *Water Research*, 38, pp. 1225-1236.

Andrews Environmental Engineering, Inc. (1994) *Use of landfarming to remediate soil contaminated by pesticides*, HWRIC TR-019 Final Report, Illinois Hazardous Waste Research and Information Center, Champaign, IL, 42pp.

Arthur, E.L.; Coats, J.R. (1998) Phytoremediation. *Pesticide remediation in soils and water*, Kearney, P. C.; Roberts, T., eds, John Wiley & Sons Ltd., NY, pp. 251-283.

Australia State of the Environment Committee, Australia State of the Environment Report 2001, CSIRO Publishing: Collingwood, Vic., 2001.

Australian and New Zealand Environment and Conservation Council (1992) *Australian water quality guidelines for fresh and marine waters*. Australian and New Zealand Environment and Conservation Council, Environment Priorities and Coordination Group, Environment Australia, Canberra, Australia.

Bader, H.; Sturzenegger, V.; Hoigné, J. (1988) Photometric method for the determination of low concentrations of hydrogen peroxide by the peroxidase catalyzed oxidation of N,N-Diethyl-p-phenylenediamine (DPD). *Water Research*, 2(9), pp. 1109-1115.

Balmer M.E.; Sulzberger B. (1999) Atrazine degradation in irradiated iron/oxalate systems: effects of pH and oxalate. *Environmental Science and Technology*, 33, pp. 2418-2424.

Barnabas, I.J.; Dean, J.R.; Hitchen, S.M.; Owen, S.P. (1994) Supercritical fluid extraction of organochlorine pesticides from an aqueous matrix. *Journal of Chromatography A*, 665(2), pp. 307-315.

Barnabas, I.L.; Dean, J.R.; Fowles, I.A.; Owen, S.P. (1995) Automated determination of s-triazine herbicides using solid-phase microextraction. *Journal of Chromatography A*, 705, pp. 305-312.

Bell, L.S.; Devlin, J.F.; Gillham, R.W.; Binning, P.J. (2003) A sequential zero-valent iron and aerobic biodegradation treatment system for nitrobenzene. *Journal of Contaminant Hydrology*, 66, pp. 201-217.

Beltran, J.; Lopez, F.J.; Cepria, O.; Hernandez, F. (1998) Solid-phase microextraction for quantitative analysis of organophosphorus pesticides in environmental water samples. *Journal of Chromatography A*, 808, pp. 257-263.

Beltran, J.; López, F.J.; Hernández, F. (2000) Solid-phase micro-extraction in pesticide residue analysis. *Journal of Chromatography A*, 885, pp. 389-404.

Benner, S.G.; Blowes, D.W.; Ptacek, C.J. (1997) A full-scale porous reactive wall for prevention of acid mine drainage. *Ground Water Monitoring and Remediation*, 17(4), pp. 99-107.

Bergendahl, J.A.; Thies, T.P. (2004) Fenton's oxidation of MTBE with zero-valent iron. *Water Research*, 38, pp. 327-334.

Bielski, B.H.J.; Cabelli, D.E.; Arudi, R.L.; Ross, A.B. (1985) Reactivity of HO₂/O₂⁻ radicals in aqueous solution. *Journal of Physical and Chemical Reference Data*, 14(4), pp. 1041-1100.

Bielski, B.H.J.; Cabelli, D.E. (1995) *Active oxygen in chemistry*. Foote, C.S.; Valentine, J.S.; Greenberg, A.; Liebrnan, J.F., eds., Blackie Academic & Professional: New York, p. 66.

Birke, V.; Burmeier, H.; Rosenau, D. (2003) Design, construction, and operation of tailored permeable reactive barriers. *Practice periodical of hazardous, toxic, and radioactive waste management*, 7(4), pp. 264-280.

Biswas, T.K.; Naismith, A.N.; Jayawardane, N.S. (2000) Performance of a land FILTER technique for pesticide removal from contaminated water. pp. 23-24. *In Proc. Soil 2000: New Horizons for a new Century*, Adams, J.A.; Metherell, A.K., eds, Lincoln University, Canterbury Christchurch, New Zealand.

Boronina, T.; Klabunde, K.J.; Sergeev, G. (1995) Destruction of organohalides in water using metal particles: Carbon tetrachloride/water reactions with magnesium, tin, zinc. *Environmental Science and Technology*, 29(6), pp. 1511-1517.

Bossmann, S.H.; Oliveros, E.; Göb, S.; Siegwart, S.; Dahlen, E.P.; Payawan, L. (Jr.); Straub, M.; Wörner, M.; Braum, A.M. (1998) New evidence against hydroxyl radicals as reactive intermediates in the thermal and photochemically enhanced Fenton reactions. *Journal of Physical Chemistry A*, 102, pp. 5542-5550.

Bouaid, A.; Ramos, L.; Gonzalez, M.J.; Fernandez, P.; Camara, C. (2001) Solid-phase microextraction method for the determination of atrazine and four organophosphorus

pesticides in soil samples by gas chromatography. *Journal of Chromatography A*, 939, pp. 13-21.

Boyd-Boland, A.A.; Magdic, S.; Pawliszyn, J.B. (1996) Simultaneous determination of 60 pesticides in water using solid-phase microextraction and gas chromatography-mass spectrometry. *Analyst*, 121, July, pp. 929-938.

Boyd-Boland, A.A.; Pawliszyn, J.B. (1996) Solid-phase microextraction coupled with high-performance liquid chromatography for the determination of alkylphenol ethoxylate surfactants in water. *Analytical Chemistry*, 68, pp. 1521-1529.

Bozec, N.L.; Compère, C.; L'Her, M.; Laouenan, A.; Costa, D.; Marcus, P. (2001) Influence of stainless steel surface treatment on the oxygen reduction reaction in seawater. *Corrosion Science*, 43, pp. 765-786.

Brooks, A.; Westhorpe, D.; Bales, M. (1996) *The impacts of pesticides on riverine environments*. Department of Land and Water Conservation, Technical Services Directorate, Sydney, N.S.W.

Buchholz, K.D.; Pawliszyn, J. (1993) Determination of phenols by solid-phase microextraction and gas chromatographic analysis. *Environmental Science and Technology*, 27, pp. 2844-2848.

Burris, D.R.; Campbell, T.J.; Manoranjan, V.S. (1995) Sorption of trichloroethylene and tetrachloroethylene in a batch reactive metallic iron-water system. *Environmental Science and Technology*, 29, pp. 2850-2855.

Buxton, G.V.; Greenstock, C.L.; Helman, W.P.; Ross, A.B. (1988) Critical review of rate constants for reactions of hydrated electrons, hydrogen atoms and hydroxyl radicals in aqueous solution. *Journal of Physical and Chemical Reference Data*, 17, pp. 513-886.

Calvo, E.J.; Schiffrin, D.J. (1984) The reduction of hydrogen peroxide on passive iron in alkaline solutions. *Journal of Electroanalytical Chemistry*, 163, pp. 257-275.

Cantrell, K.J.; Kaplan, D.I. (1997) Zero-valent iron colloid emplacement in sand columns. *Journal of Environmental Engineering*, 123, pp. 499-505.

Cao, J.; Wei, L.; Huang, Q.; Wang, L.; Han, S. (1999) Reducing degradation of azo dyes by zero-valent iron in aqueous solution. *Chemosphere*, 38, pp. 565-571.

Capangpangan, M.B.; Suffet, I.H. (1996) Optimization of a drying method for filtered suspended solids from natural waters for supercritical fluid extraction analysis of hydrophobic organic compounds. *Journal of Chromatography A.*, 738, pp. 253-264.

Capangpangan, M.B.; Suffet, I.H. (1997) Validation studies for a new supercritical fluid extraction method for the isolation of hydrophobic organic compounds from filtered suspended solids. *Journal of Chromatography A.*, 782, pp. 247-256.

Cerejeira, M.J.; Viana, P.; Batista, S.; Pereira, T.; Silva, E.; Valério, M.J.; Silva, A.; Ferreira, M.; Silva-Fernandes, A.M. (2003) Pesticides in Portuguese surface and ground waters. *Water Research*, 37, pp. 1055-1063.

Charizopoulos, E.; Papadopoulou-Mourkidou, E. (1999) Occurrence of pesticides in rain of the Axios river basin, Greece. *Environmental Science and Technology*, 33, pp. 2363-2368.

Charlet, L.; Liger, E.; Gerasimo, P. (1998) Decontamination of TCE- and U-rich waters by granular iron: Role of sorbed Fe(II). *Journal of Environmental Engineering*, 124(1), pp. 25-30.

Chen, J.L.; Al-Abed, S.R.; Ryan, J.A.; Li, Z. (2001) Effects of pH on dechlorination of trichloroethylene by zero-valent iron. *Journal of Hazardous Materials*, 83(3), pp. 243-254.

Chen, R. Z.; Pignatello, J. J. (1997) Role of quinone intermediates as electron shuttles in Fenton and photoassisted Fenton oxidations of aromatic compounds. *Environmental Science and Technology*, 31(8), pp. 2399-2406.

Chew, C.F.; Zhang, T.C. (1999) Abiotic degradation of nitrites using zero-valent iron and electrokinetic processes. *Environmental Engineering Science*, 16(5), pp. 389-401.

Chiron, S.; Fernandez-Alba, A.; Rodriguez, A.; Garcia-Calvo, E. (2000) Pesticide chemical oxidation: state-of-the-art. *Water Research*, 34, pp. 366-377.

Choe, S.; Chang, Y.-Y.; Hwang, K.-Y.; Khim, J. (2000) Kinetics of reductive denitrification by nanoscale zero-valent iron. *Chemosphere*, 41, pp. 1307-1311.

Choe, S.; Lee, S.-H.; Chang, Y.-Y.; Hwang, K.-Y.; Khim, J. (2001) Rapid reductive destruction of hazardous organic compounds by nanoscale Fe⁰. *Chemosphere*, 42, pp. 367-372.

Cochran, R.C.; Kishiyama, J.; Aldous, C.; Carr, Jr, W.C. (1995) Chloripyrifos: hazard assessment based on a review of the effects of short-term and long-term exposure in animals and humans. *Food and Chemical Toxicology*, 33(2), pp. 165-172.

Coupe, R.H.; Thurman, E.M.; Zimmerman, L.R. (1998) Relation of usage to the occurrence of cotton and rice herbicides in three streams of the Mississippi Delta. *Environmental Science and Technology*, 32, pp. 3673-3680.

Crepeau, K.L.; Kuivila, K.M. (2000) Rice pesticide concentrations in the Colusa basin drain and the Sacramento River, California, 1990-1993. *Journal of Environmental Quality*, 29, pp. 926-935.

Crow, D.R. (1984) *Principles and applications of electrochemistry*. Chapman and Hall Ltd., USA.

Das, S.; Schuchmann, M.N.; Schuchmann, H.P.; Vonsonntag, C. (1987) The production of the superoxide radical-anion by the OH radical-induced oxidation of trimethylamine in oxygenated aqueous-solution-The kinetics of the hydrolysis of dimethylamine. *Chemische Berichte-Recueil*, 120(3), pp. 319-323.

Davenport, A.J.; Oblonsky, L.J.; Ryan, M.P.; Toney, M.F. (2000) The structure of the passive film that forms on iron in aqueous environments. *Journal of the Electrochemical Society*, 147, pp. 2162-2173.

Devlin, J.F.; Klausen, J.; Schwarzenbach, R.P. (1998) Kinetics of nitroaromatic reduction on granular iron in recirculating batch experiments. *Environmental Science and Technology*, 32, pp. 1941-1947.

Dombek, T.; Dolan, E.; Schultz, J.; Klarup, D. (2001) Rapid reductive dechlorination of atrazine by zero-valent iron under acidic conditions. *Environmental Pollution*, 111, pp. 21-27.

Donaldson, D.; Kiely, T.; Grube, A. (2002) *Pesticides industry sales and usage*. US EPA, Washington D.C.

Doong, R.; Chang, W. (1998) Photo-assisted iron compound catalytic degradation of organophosphorus pesticides with hydrogen peroxide. *Chemosphere*, 37(13), pp. 2563-2572.

Dorfman, L.M.; Buhler, R.E.; Taub, I.A. (1962) Pulse radiolysis studies. I. Transient spectra and reaction-rate constants in irradiated aqueous solutions of benzene. *The Journal of Chemical Physics*, 36(11), pp. 3051-3061.

Dowling, K.C.; Lemley, A.T. (1995) Organophosphate insecticide degradation by non-amended and cupric-amended Fenton's reagent in aqueous solution. *Journal of Environmental Science and Health B*, 30(5), pp. 585-604.

Dugay, J.; Miege, C.; Hennion, M.-C. (1998) Effect of the various parameters governing solid-phase microextraction for the trace-determination of pesticides in water. *Journal of Chromatography A*, 795, pp. 27-42.

Eberhardt, M.K.; Yoshida, M. (1973) Radiation-induced hemolytic aromatic substitution. I. Hydroxylation of nitrobenzene, chlorobenzene, and toluene. *The Journal of Physical Chemistry*, 77(5), pp. 589-597.

Eisert, R.; Levsen, K. (1995) Determination of pesticides in aqueous samples by solid-phase microextraction in-line coupled to gas chromatography-mass spectrometry. *Journal of the American Society for Mass Spectrometry*, 6, pp. 1119-1130.

Elliott, D.W.; Zhang, W.-X. (2001) Field assessment of nanoscale bimetallic particles for groundwater treatment. *Environmental Science and Technology*, 35, pp. 4922-4926.

Eykholt, G.; Davenport, D.T. (1998) Dechlorination of the chloroacetanilide herbicides alachlor and metolachlor by iron metal. *Environmental Science and Technology*, 32, pp. 1482-1487.

Farrell, J.; Wang, J.; O'Day, P.; Conklin, M. (2001) Electrochemical and spectroscopic study of arsenic removal from water using zero-valent iron media. *Environmental Science and Technology*, 35, pp. 2026-2032.

Fee, J.A.; DiCorleto, P.E. (1973) Observation on the oxidation-reduction properties of bovine erythrocyte superoxide dismutase. *Biochemistry*, 12, pp. 4893-4899.

Feitz, A.J.; Waite, T.D.; Joo, S.H.; Guan, J.; Biswas, T.K. (2002) *Development of nanosized zero-valent iron particles for organic contaminant degradation*. CRC WMPC report, Centre for Water and Waste Technology, UNSW, Sydney, Australia.

Feitz, A.J.; Waite, T.D. (2003) Kinetic modeling of TiO₂-catalyzed photodegradation of trace levels of microcystin-LR. *Environmental Science and Technology*, 37, pp. 561-568.

Felsot, A.S.; Racke, K.D.; Hamilton, D.J. (2003) Disposal and degradation of pesticide waste. *Reviews of Environmental Contamination and Toxicology*, 177, pp.123-200.

Ferrano, S.P.; Lee, H.; Smith, L.M.; Ozretich, R.J.; Specht, D.T. (1991) Accumulation factors for eleven polychlorinated biphenyl congeners. *Bulletin of Environmental Contamination and Toxicology*, 46(2), pp. 276-283.

Ferro, Y.; Allouche, A.; Marinell, F.; Brosset, C. (2004) Theoretical study of oxygen adsorption on boron-doped graphite. *Surface Science*, 559, pp. 158-168.

Ghauch, A. (2001) Degradation of benomyl, picloram, and dicamba in a conical apparatus by zero-valent iron powder. *Chemosphere*, 43, pp. 1109-1117.

Ghauch, A.; Gallet, C.; Charef, A.; Rima, J.; Martin-Bouyer, M. (2001) Reductive degradation of carbaryl in water by zero-valent iron. *Chemosphere*, 42, pp. 419-424.

Ghauch, A.; Suptil, J. (2000) Remediation of s-triazines contaminated water in a laboratory scale apparatus using zero-valent iron powder. *Chemosphere*, 41, pp. 1835-1843.

Gillham, R.W.; O'Hannesin, S.F. (1994) Enhanced degradation of halogenated aliphatics by zero-valent iron. *Ground Water*, 32(6), pp. 958-967.

Goody, D.C.; Chilton, P.J.; Harrison, I. (2002) A field study to assess the degradation and transport of diuron and its metabolites in a calcareous soil. *The Science of the Total Environment*, 297, pp. 67-83.

Green, J.M. (1996) A practical guide to analytical method validation. *Analytical Chemistry*, 68(9), pp. A305-A309.

Gu, B.; Phelps, T.J.; Liang, L.; Dickey, M.J.; Roh, Y.; Kinsall, B.L.; Palumbo, A.V.; Jacobs, G.K. (1999) Biogeochemical dynamics in zero-valent iron columns: implications for permeable reactive barriers. *Environmental Science and Technology*, 33, pp. 2170-2177.

Guerin, T.F.; Kimber, S.W.L.; Kennedy, I.R. (1992) Efficient one-step method for the extraction of cyclodiene pesticides from aqueous media and the analysis of their metabolites. *Journal of Agricultural and Food Chemistry*, 40, pp. 2309-2314.

Gunier, R.B.; Harnly, M.E.; Reynolds, P.; Hertz, A.; von Behren, J. (2001) Agricultural pesticide use in California: pesticide prioritization, use densities, and population distributions for a childhood cancer study. *Environmental Health Perspectives*, 109, pp. 1071-1078.

Gupta, P.K.; Salunkhe, D.K. (1985) *Modern toxicology, Vol III: Immuni and clinical toxicology*. Metropolitan book Co., New Delhi.

Harris, C.R.; Kennedy, I.R. (1996) *Pesticides in perspective*. Australian Cotton grower, Sydney.

Hartley, D.; Kidd, H. (1983) *The agrochemicals handbook*. The Royal Society of Chemistry, UK.

Hayon, E.; Ibata, T.; Lichtin, N.N.; Simic, M. (1970) Sites of attack of hydroxyl radicals on amides in aqueous solution. *Journal of American Chemical Society*, 92(13), pp. 3903-3998.

Hernandez, F.; Beltran, J.; Lopez, F.J.; Gaspar, J.V. (2000) Use of solid-phase microextraction for the quantitative determination of herbicides in soil and water samples. *Analytical Chemistry*, 72, pp. 2313-2322.

Ho, C.L.; Shebl, M.A.-A.; Watts, R.J. (1995) Development of an injection system for *in situ* catalyzed peroxide remediation of contaminated soil. *Hazardous waste & hazardous materials*, 12(1), pp. 15-25.

Hozalski, R.M.; Zhang, L.; Arnold, W.A. (2001) Reduction of haloacetic acids by Fe⁰: implications for treatment and fate. *Environmental Science and Technology*, 35, pp. 2258-2263.

Hsieh, Y.N.; Liu, L.F.; Wang, Y.S. (1998) Uptake, translocation and metabolism of the herbicide molinate in tobacco and rice. *Pesticide Science*, 53(2), pp. 149-154.

Hundal, L.S.; Singh, J.; Bier, E.L.; Shea, P.J.; Comfort, S.D.; Powers, W.L. (1997) Removal of TNT and RDX from water and soil using iron metal. *Environmental Pollution*, 97, pp. 55-64.

Hung, D.Q.; Thiemann, W. (2002) Contamination by selected chlorinated pesticides in surface waters in Hanoi, Vietnam. *Chemosphere*, 47, pp. 357-367.

Hutson, D.H.; Roberts, T.R. (1990) *Environmental fate of pesticides*. John Wiley & Sons Ltd., England.

Indian Pesticides Industry Scope Marketing & Information Solutions (IPISMIS, 2001) *Indian pesticides industry*. <http://www.researchmarkets.com>. Accessed in August 2004.

International Program on Chemical Safety (INCHEM) (1989) *Environmental health criteria 91*. <http://www.inchem.org>. Accessed in August 2004.

Ishikawa, T.; Kondo, Y.; Yasukawa, A.; Kandori, K. (1998) Formation of magnetite in the presence of ferric oxyhydroxides. *Corrosion Science*, 40(7), pp. 1239-1251.

Janda, V.; Vasek, P.; Bizova, J.; Belohlav, Z. (2004) Kinetic models for volatile chlorinated hydrocarbons removal by zero-valent iron. *Chemosphere*, 54, pp. 917-925.

Jayawardane, N.S.; Biswas, T.K.; Blackwell, J.; Cook, F.J. (2001) Management of salinity and sodicity in a land FILTER system for treating saline wastewater on a saline-sodic soil. *Australian Journal of Soil Research*, 39, pp. 1247-1258.

Joo, S.H.; Feitz, A.J.; Waite, T.D. (2002) Agrochemical degradation using nano-scale zero valent iron, ZVI/H₂O₂, and Fenton's reagent. *Proc. of the Second International Conference on Oxidation and Reduction Technologies for In-Situ Treatment of Soil and Groundwater*, 17-21 November, Toronto, Ontario, Canada.

Joo, S.H.; Feitz, A.J.; Waite, T.D. (2004) Oxidative degradation of the carbothioate herbicide, molinate, using nanoscale zero-valent iron. *Environmental Science and Technology*, 38, pp. 2242-2247.

Joo, S.H.; Feitz, A.J.; Waite, T.D. (2002) Agrochemical degradation using zero-valent iron.

Proc. 6th Annual Australian Environmental Engineering Research Event, Blackheath New South Wales Australia, CD-ROM; ISBN 0-9580158-1-3; EERE Organizing Committee.

Jovancicevic, V.; Bockris, J.O'M. (1986) The mechanism of oxygen reduction on iron in neutral solutions. *Journal of Electrochemical Society: Electrochemical Science and Technology*, 133(9), pp. 1797-1807.

Kamolpornwijit, W.; Liang, L.; West, O.R.; Moline, G.R.; Sullivan, A.B. (2003) Preferential flow path development and its influence on long-term PRB performance: column study. *Journal of Contaminant Hydrology*, 66(3-4), pp. 161-178.

Kanatharana, P.; Chindarasamee, C.; Kaewnarong, B. (1993) Extracting solvents for pesticide residues. *Journal of Environmental Science and Health part A – Environmental Science and Engineering & Toxic and Hazardous Substance Control*, 28(10), pp. 2323-2332.

Kaplan, D.I.; Catrell, K.J.; Wietsma, T.W.; Potter, M.A. (1996) Retention of zero-valent iron colloids by sand columns: Application to chemical barrier formation. *Journal of Environmental Quality*, 25, pp. 1086-1094.

Keene J.P. (1964) Pulse radiolysis of ferrous sulfate solution. *Radiation Research*, 22(1), p. 14.

Kelly, K.; Reed, N. (1996) *Pesticides for evaluation as candidate toxic air contaminants*. Sacramento, CA: California Department of Pesticide Regulation.

Kennedy, I.R.; Lee, A.; Wang, S.; Sanchez-Bayo, P. (1999) *ELISA Workshop: Training in the use of commercial test kits*. Department of Agricultural Chemistry & Soil Science, University of Sydney, Australia.

Kentucky Department of Agriculture Richie Farmer, Commissioner (KDARFC) (2004) *Guidelines for atrazine use and application for groundwater and surface water protection: Best management practices*. University of Kentucky College of Agriculture, Division of Conservation, and US Natural Resources Conservation Service Western Kentucky University, Kentucky State University, Syngenta, BMP-6.

Kim, Y.-H.; Carraway, E.R. (2000) Dechlorination of pentachlorophenol by zero-valent iron and modified zero-valent irons. *Environmental Science and Technology*, 34, pp. 2014-2017.

Kitajima, N.; Fukuzumi, S.; Ono, Y. (1978) Formation of superoxide ion during decomposition of hydrogen-peroxide on supported metal-oxides. *Journal of Physical Chemistry*, 82(13), pp. 1505-1509.

Klein, G.W.; Bhatla, K.; Madhavan, V.; Schuler, R.H. (1975) Reaction of hydroxyl radicals with benzoic acid: Isomer distribution in the radical intermediates. *Journal of Physical Chemistry*, 79, pp. 1767-1774.

Konstantinou, I.K.; Sakkas, V.A.; Albanis, T.A. (2001) Photocatalytic degradation of the herbicides propanil and molinate over aqueous TiO₂ suspensions: Identification of intermediates and the reaction pathway. *Applied Catalysis B: Environmental* 34, pp. 227-239.

Konstantinou, I.K.; Sakellarides, T.M.; Sakkas, V.A.; Albanis, T.A. (2001) Photocatalytic degradation of selected s-triazine herbicides and organophosphorus insecticides over aqueous TiO₂ suspensions. *Environmental Science and Technology*, 35, pp. 398-405.

Kormann, C.; Bahnemann, D.W.; Hoffmann, M.R. (1991) Photolysis of chloroform and other organic molecules in aqueous titanium dioxide suspensions. *Environmental Science and Technology*, 25, pp. 494-500.

Kremer, M.L. (1999) Mechanism of the Fenton reaction: evidence for a new intermediate. *Physical Chemistry Chemical Physics*, 1, pp. 3595-3605.

Lackovic, J.A.; Nikolaidis, N.P.; Dobbs, G.M. (2000) Inorganic arsenic removal by zero-valent iron. *Environmental Engineering Science*, 17, pp. 29-39.

Larson, R.; Weber, E. (1994) *Reactions Mechanisms in Environmental Organic Chemistry*, CRC Press, Inc., Boca Raton, FL, pp. 315-341.

Lee, S.; MaLaughlin, R.; Harnly, M.; Gunier, R.; Kreutzer, R. (2002) Community exposures to airborne agricultural pesticides in California: ranking of inhalation risks. *Environmental Health Perspectives*, 110, pp. 1175-1184.

Legrini, O.; Oliveros, E.; Braun, A.M. (1993) Photochemical processes for water treatment. *Chemical Reviews*, 93, pp. 671-698.

Li, Y.; Zhang, J. (1999) Agricultural diffuse pollution from fertilizers and pesticides in China. *Water Science and Technology*, 39(3), pp. 25-32.

Liang, L.; Korte, N.; Gu, B.; Puls, R.; Reeter, C. (2000) Geochemical and microbial reactions affecting the long-term performance of in situ 'iron barriers'. *Journal of Advances in Environmental Research*, 4, pp. 273-286.

Liang, L.; Sullivan, A.B.; West, O.R.; Moline, G.R.; Komolpoinwjjik, W. (2003) Predicting the precipitation of mineral phases in permeable reactive barriers. *Environmental Engineering Science*, 20(6), pp. 635-653.

Lin, S.; Gurol, M.D. (1998) Catalytic decomposition of hydrogen peroxide on iron oxide: kinetics, mechanism, and implications. *Environmental Science and Technology*, 32, pp. 1417-1423.

Lopez-Avila, V.; Young, R.; Tehrani, J.; Damian, J.; Hawthorne, S.; Dankers, J.; Heiden, C.V.D. (1994) Mini-round-robin study of a supercritical fluid extraction method for polynuclear aromatic hydrocarbons in soils with dichloromethane as a static modifier. *Journal of Chromatography A*, 672 (1-2), pp. 167-175.

Lücking, F.; Köser, H.; Ritter, A. (1998) Iron powder, graphite and activated carbon as catalysts for the oxidation of 4-chlorophenol with hydrogen peroxide in aqueous solution. *Water Research*, 32(9), pp. 2607-2614.

MacKenzie, P.D.; Baghel, S.S.; Eykholt, G.R.; Horney, D.P.; Salvo, J.J.; Sivavec, T.M. (1995) Pilot-scale demonstration of chlorinated ethane reduction by iron metal: Factors affecting iron lifetime. *ACS Extended Abstract*, Industrial and Engineering Chemistry Division, pp. 59-62.

Macounová, K.; Krýsová, H.; Ludvic, J.; Jirkovský, J. (2003) Kinetics of photocatalytic degradation of diuron in aqueous colloidal solutions of Q-TiO₂ particles. *Journal of Photochemistry and Photobiology A: Chemistry*, 156, pp. 273-282.

Magdic, S.; Pawliszyn, J.B. (1996) Analysis of organochlorine pesticides using solid-phase micro-extraction. *Journal of Chromatography A*, 723, pp. 111-122.

Magdic, S.; Boyd-Boland, A.; Jinno, K.; Pawliszyn, J.B. (1996) Analysis of organophosphorus insecticides. *Journal of Chromatography A.*, 736, pp. 219-228.

Mall, I.D.; Raju, K.; Kumar, N. (2003) Pesticide industry: impact on environment. *Chemical Engineering World*, 38(1), pp. 116-118, 121-123.

Matheson, L.J.; Tratnyek, P.G. (1994) Reductive dehalogenation of chlorinated methanes by iron metal. *Environmental Science and Technology*, 28(12), pp. 2045-2053.

Matin, M.A.; Malek, M.A.; Amin, M.R.; Rahman, S.; Khatoon, J.; Rahman, M.; Aminuddin, M.; Mian, A.J. (1998) Organochlorine insecticide residues in surface and underground water regions of Bangladesh. *Agriculture, Ecosystems and Environment*, 69, pp. 11-15.

Matisová, E.; Medved'ová, M.; Vraniaková, J.; Šimon, P. (2002) Optimisation of solid-phase microextraction of volatiles. *Journal of Chromatography A*, 960, pp. 159-164.

Mazellier, P.; Jirkovsky, J.; Bolte, M. (1997) Degradation of diuron photoinduced by iron (III) in aqueous solution. *Pesticide Science*, 49, pp. 259-267.

Mazellier, P.; Sulzberger, B. (2001) Diuron degradation in irradiated, heterogeneous iron/oxalate systems: The rate-determining step. *Environmental Science and Technology*, 35, pp. 3314-3320.

McKim, J.M. (1994) Physiological and biological mechanisms that regulate the accumulation and toxicity of environmental chemicals in fish. *Bioavailability: physical, chemical and biological interactions*. Hamelink, J.L.; Landrum, P.F.; Bergman, H.L.; Benson, W.H., eds., Lewis Publishers, Boca Raton, FL.

Mill, T.; Haag, W.R. (1989) Novel metal/peroxide systems for the treatment of organic compounds in drinking water. *Preprint Extended Abstract* presented before the Division of Environmental Chemistry, American Chemical Society, Miami Beach, Florida, September 10-15.

Mindbranch (2001) *Indian pesticides industry market report*.
[http:// www.mindbranch.com](http://www.mindbranch.com). Accessed in August 2004.

Mishra, R.; Shukla, S.P. (1997) Impact of endosulfan on lactate dehydrogenase from the freshwater catfish *clarias batrachus*. *Pesticide Biochemistry and Physiology*, 57, pp. 220-234.

Morrison, S.J.; Metzler, D.R.; Dwyer, B.P. (2002) Removal of As, Mn, Mo, Se, U, V and Zn from groundwater by zero-valent iron in a passive treatment cell: reaction progress modeling. *Journal of Contaminant Hydrology*, 56(1-2): pp. 99-116.

Muszkat, L. (1998) Photochemical processes. *Pesticide remediation in soils and water*, Kearney, P. C.; Roberts, T., eds, John Wiley & Sons Ltd., NY, pp. 307-337.

Nadezhdin, A. D.; Kozlov, Y. N.; Purmalis, A. (1976) Iron(3+) ion-catalyzed decomposition of hydrogen peroxide in the presence of tetranitromethane: determination of the chain prolongation reaction rate constant. *Zhurnal Fizicheskoi Khimii*, 50, pp. 910-912.

Nam, S.; Tratnyek, P.G. (2000) Reduction of azo dyes with zero-valent iron. *Water Research*, 34, pp. 1837-1845.

Naquvi, S.M.; Vaishnavi, C. (1993) Bioaccumulative potential and toxicity of endosulfan insecticide to non-target animals: A mini review. *Comparative Biochemistry and Physiology*, 105C, p 347.

Natangelo, M.; Tavazzi, S.; Benfenati, E. (2002) Evaluation of solid phase microextraction-gas chromatography in the analysis of some pesticides with different mass spectrometric techniques: application to environmental waters and food samples. *Analytical Letters*, 35(2), pp. 327-338.

National Center for Toxic and Persistent Substances (1995) *Pesticides in the aquatic environment*. Report of the National Rivers Authority, Water Quality Series No. 26, October, London:HMSO.

Naval Facilities Engineering Service Center (NFESC) (2004) *Permeable reactive barrier: remediation of chlorinated solvents in groundwater*.<http://enviro.nfesc.navy/>. Accessed in August 2004.

Nerín, C.; Batlle, R.; Sartaguda, M.; Pedrocchi, C. (2002) Supercritical fluid extraction of organochlorine pesticides and some metabolites in frogs from National Park of Ordesa and Monte Perdido. *Analytica Chimica Acta*, 464, pp. 303-312.

Nohara, S.; Hanazato, T.; Iwakuma, T. (1997) Pesticide residue flux from rainwater into Lake Nakanuma in the rainy season. *Rikusuigaku Zasshi*, 58(4), pp. 385-393.

Noordkamp, E.R.; Grotenhuis, J.T.C.; Rulkens, W.H. (1997) Selection of an efficient extraction method for the determination of polycyclic aromatic hydrocarbons in contaminated soil and sediment. *Chemosphere*, 35(9), pp. 1907-1917.

Noradoun, C.; Engelmann, M.D.; McLaughlin, M.; Hutcheson, R.; Breen, K.; Paszczynski, A.; Cheng, I.F. (2003) Destruction of chlorinated phenols by dioxygen activation under aqueous room temperature and pressure conditions. *Industrial & Engineering Chemistry Research*, 42, pp. 5024-5030.

Nowell, L.H.; Capel, P.D.; Dileanis, P.D. (1999) *Pesticides in stream sediment and aquatic biota: distribution, trends, and governing factors*. Lewis Publishers, Boca Raton, FL.

NRA (2000) *The NRA review of diazinon*. National Registration Authority for Agricultural and Veterinary Chemicals, Canberra, Australia.

Odziemkowski, M.S. (2000) The role of oxide films in the reduction of *n*-nitrosodimethylamine with reference to the iron groundwater remediation technology. *Oxide films proceedings of the international symposium*, Vol. 2000-4, The Electrochemical Society, Pennington, N.J., pp. 357-368.

O'Hannesin, S.F.; Gillham, R.W. (1998) Long-term performance of an in situ "iron wall" for remediation of VOCs. *Groundwater*, 36 (1), pp. 164-170.

Oliver, B.G. (1985) Bioconcentration factors of some halogenated organics for rainbow trout: limitations in their use for predictions of environmental residues. *Environmental Science and Technology*, 19, pp. 842-849.

Oros, D.R.; Jarman, W.M.; Lowe, T.; David, N.; Lowe, S.; David, J.A. (2003) Surveillance for previously unmonitored organic contaminants in the San Francisco Estuary. *Marine Pollution Bulletin*, 46, pp. 1102-1110.

Orth, W.S.; Gillham, R.W. (1996) Dechlorination of trichloroethene in aqueous solution using Fe-O. *Environmental Science and Technology*, 30, pp. 66-71.

Paldy, A.; Puskar, N.; Farkas, I. (1988) Pesticide use related to cancer incidence as studied in a rural district of Hungary. *Science Total Environment*, 73, pp. 224-229.

Paune, F.; Caixach, J.; Espadaler, I.; Om, J.; Rivera, J. (1998) Assessment on the removal of organic chemicals from raw and drinking water at a Liobregat River water works plant using GAC. *Water Research*, 32, pp. 3313-3324.

Pera-Titus, M.; Garcia-Molina, V.; Banos, M.A.; Gimenez, J.; Esplugas, S. (2004) Degradation of chlorophenols by means of advanced oxidation processes: a general review. *Applied Catalysis B: Environmental*, 47(4), pp. 219-256.

Pesticide Management Education Program (PMEP) (2003) *The pesticide management education program at Cornell University*. <http://pmep.cce.cornell.edu/>. Assessed in August 2004.

Pichat, P. (1997) Photocatalytic degradation of aromatic and alicyclic pollutants in water: By-products, pathways and mechanisms. *Water Science and Technology*, 35(4), pp. 73-78.

Pourbaix, M. (1966) *Atlas of electrochemical equilibria in aqueous solutions*, Pergamon, Oxford, p644.

Powell, R.M.; Puls, R.W.; Powell, P.O. (2002) Cost analysis of permeable reactive barriers for remediation of groundwater. Powell & Associates Science Services, Las Vegas, NV, USA, Gavaskar, A.R.; Chen, A.S.C., eds, Remediation of chlorinated and recalcitrant compounds, *Proceedings of the International Conference on Remediation of Chlorinated and Recalcitrant Compounds*, 3rd, Monterey, CA, US, May 20-23, pp. 104-111, Battelle Press, Columbus, Ohio.

Powell, R.M.; Puls, R.W.; Hightower, S.K.; Sabatini, D.A. (1995) Coupled iron corrosion and chromate reduction: mechanisms for subsurface remediation. *Environmental Science and Technology*, 29, pp. 1913-1922.

Powell, R.M.; Puls, R.W.; Blowes, D.W.; Vogan, J.L.; Gillham, R.W.; Powell, P.D.; Schultz, D.; Landis, R.; Sivavic, T. (1998) *Permeable reactive barrier technologies for contaminated remediation*. U.S. Environmental Protection Agency, EPA/600/R-98/125, Ada, OK.

Pratt, A.R.; Blowes, D.W.; Ptacek, C.J. (1997) Products of chromate reduction on proposed subsurface remediation material. *Environmental Science and Technology*, 31, pp. 2492-2498.

Puls, R.W.; Paul, C.J.; Powell, R.M. (1999) The application of in situ permeable reactive barrier technology for the remediation of chromate-contaminated groundwater: a field test. *Applied Geochemistry*, 14, pp. 989-1000.

Qiu, X.; Zhu, T.; Li, J.; Pan, H.; Li, Q.; Miao, G.; Gong, J. (2004) Organochlorine pesticides in the air around the Taihu Lake, China. *Environmental Science and Technology*, 38(5), pp. 1368-1374.

Råberg, S.; Nyström, M.; Erös, M.; Plantman, P. (2003) Impact of the herbicides 2,4-D and diuron on the metabolism of the coral porites cylindrical. *Marine Environmental Research*, 56, pp. 503-514.

Rahman, A.; Agrawal, A. (1997) Reduction of nitrate and nitrite by iron metal: implications for ground water remediation. *Preprint Extended Abstract*, 213th ACS National Meeting, American Chemical Society, Division of Environmental Chemistry, 37(1), pp. 157-159.

Ramamoorthy, S. (1997) *Chlorinated organic compounds in the environment: Regulatory and monitoring assessment*, Lewis Publishers, Boca Raton and New York.

Ramesh, A.; Ravi, P.E. (2001) Applications of solid-phase microextraction (SPME) in the determination of residues of certain herbicides at trace levels in environmental samples. *Journal of Environmental Monitoring*, 3, pp. 505-508.

Rao, P.S.; Hayon, E. (1975) Oxidation of aromatic amines and diamines by OH radicals: formation and ionization constants of amine cation radicals in water. *Journal of Physical Chemistry*, 79 (11), pp. 1063-1066.

Raupach, M.R.; Briggs, P.R.; Ford, P.W.; Leys, J.F.; Muschal, M.; Cooper, B.; Edge, V.E. (2001) Endosulfan transport: I. Integrative assessment of airborne and waterborne pathways. *Journal of Environmental Quality*, 30, pp. 714-728.

Redshaw, C.J. (1995) Ecotoxicological risk assessment of chemicals used in aquaculture: a regulation view point. *Aquaculture Research*, 26, pp. 629-637.

Reeter, C. (1997) *Permeable reactive wall: remediation of chlorinated hydrocarbons in ground water*. Technical Data Sheet, TDS-2047-ENV Port Hueneme, California: Naval Facilities Engineering Service Center.

Rivas, F.J.; Beltrán, F.J.; Frades, J.; Buxeda, P. (2001) Oxidation of *p*-hydroxybenzoic acid by Fenton's reagent. *Water Research*, 35, pp. 387-396.

Rochette, E.A.; Harsh, J.B.; Jr, H.H.H. (1993) Supercritical fluid extraction of 2,4-D from soils using derivatization and ionic modifiers. *Talanta*, 40(2), pp. 147-155.

Rock, M.L.; Kearney, P.C.; Helz, G.R. (1998) Innovative remediation technology. *Pesticide remediation in soils and water*, Kearney, P. C.; Roberts, T., eds, John Wiley & Sons Ltd., NY.

Roe, B.A.; Lemley, A.T. (1997) Treatment of two insecticides in an electrochemical Fenton system. *Journal of Environmental Science and Health B*, 32(2), pp. 261-281.

Rose, A.J.; Waite, T.D. (2002) Kinetic model for Fe(II) oxidation in seawater in the absence and presence of natural organic matter. *Environmental Science and Technology*, 36, pp. 433-444.

Sakai, M. (2003) Investigation of pesticides in rainwater at Isogo Ward of Yokohama. *Journal of Health Science*, 49(3), pp. 221-225.

Santos, F.J.; Galceran, M.T.; Fraisse, D. (1996) Application of solid-phase microextraction to the analysis of volatile organic compounds in water. *Journal of Chromatography A*, 742, pp. 181-189.

Sayles, G.D.; You, G.; Wang, M.; Kupferle, M.J. (1997) DDT, DDD and DDE dechlorination by zero-valent iron. *Environmental Science and Technology*, 31, pp. 3448-3454.

Scherer, M.M.; Balko, B.A.; Tratnyek, P.G. (1998) The role of oxides in reduction reactions at the metal-water interface. *Mineral-water interfacial reactions: kinetics and mechanisms*; Sparks, D.L.; Grudl, T.J., eds., ACS Symposium Series 715; American Chemical Society: Washington, DC, pp. 301-322.

Schneider, R.J. (1995) Evaluation of extraction method for triazine herbicides from soils for screening purposes. *Agribiological Research*, 48 (3-4), pp. 193-206.

Schnoor, J.L.; Licht, L.A.; McCutcheon, S.C.; Wolfe, N.L.; Carriera, L.H. (1995) Phytoremediation of organic and nutrient contaminants. *Environmental Science and Technology*, 29, pp. 318-323.

Simic, M.; Neta, P.; Hayon, E. (1971) Pulse radiolytic investigation of aliphatic amines in aqueous solution. *International Journal for Radiation Physics and Chemistry*, 3, pp. 309-320.

Sivakumar, M.; Gedanken, A. (2004) Insights into the sonochemical decomposition of Fe(CO)₅: theoretical and experimental understanding of the role of molar concentration and power density on the reaction yield. *Ultrasonics Sonochemistry*, 71, pp. 373-378.

Smith, A.G.; Gangolli, S.D. (2002) Organochlorine chemicals in seafood: occurrence and health concerns. *Food and Chemical Toxicology*, 40, pp. 767-779.

Steverson, E.M. (1998) Incineration as a pesticide remediation method. *Pesticide remediation in soils and water*, Kearney, P. C.; Roberts, T., eds., John Wiley & Sons Ltd., NY, pp. 85-103.

Steverson, D.E.; Walborg Jr, E.F.; North, D.W.; Sielken Jr, R.L.; Ross, C.E.; Wright, A.S.; Xu, Y.; Kamendulis, L.M.; Klaunig, J.E. (1999) Monograph: reassessment of human cancer risk of aldrin/dieldrin. *Toxicology Letters*, 109, pp. 123-186.

Stipp, S.L.S; Hansen, M.; Kristensen, R.; Hochella Jr., M.F.; Bennedsen, L.; Dideriksen, K.; Balic-Zunic, T.; Leonard, D.; Mathieu, H.-J. (2002) Behaviour of Fe-oxides relevant to contaminant uptake in the environment. *Chemical Geology*, 190, pp. 321-337.

Stumm, W.; Morgan, J.J. (1996) *Aquatic Chemistry: chemical equilibria and rates in natural waters*. 3rd ed.; John Wiley & Sons: New York. 780pp.

Su, C.; Puls, R.W. (2001) Arsenate and arsenite removal by zero-valent iron: kinetics, redox transformation, and implications for in situ groundwater remediation. *Environmental Science and Technology*, 35, pp. 1487-1492.

Sudo, M.; Kunitatsu, T.; Okubo, T. (2002) Concentration and loading of pesticide residues in Lake Biwa basin (Japan). *Water Research*, 36, pp. 315-329.

Sun, Y.; Pignatello, J.J. (1992) Chemical treatment of pesticide wastes-evaluation of Fe(III) chelates for catalytic hydrogen peroxide oxidation of 2,4-D at circumneutral pH. *Journal of Agricultural Food and Chemistry*, 40(2), pp. 322-327.

Suzuki, S.; Otani, T.; Iwasaki, S.; Ito, K.; Omura, H.; Tanaka, Y. (2003) Monitoring of 15 pesticides in rainwater in Utsunomiya, eastern Japan, 1999-2000. *Journal of Pesticide Science*, 28(1), pp. 1-7.

Sychev, A.Y.; Isak, V.G.; Pfannmeller, U. (1979) Determination of rate constants of hydroxyl radicals with organic and inorganic substances under conditions for the catalytic decomposition of hydrogen peroxide. *Zhurnal Fizicheskoi Khimii*, 53 (11), pp. 2790-2793.

Sychev, A.Y.; Isak, V.G. (deceased, 1995) Iron compounds and the mechanisms of the homogeneous catalysis of the activation of O₂ and H₂O₂ and of the oxidation of organic substrates. *Russian Chemical Reviews*, 64 (12), pp. 1105-1129.

Tang, W.Z.; Chen, R.Z. (1996) Decolorization kinetics and mechanisms of commercial dyes by H₂O₂/iron powder system. *Chemosphere*, 32(5), pp. 947-958.

Tratnyek, P. G.; Scherer, M. M.; Johnson, T. J.; Matheson, L. J. (2003) Permeable reactive barriers of iron and other zero-valent metals. *Chemical degradation methods for wastes and pollutants: environmental and industrial applications*, Tarr, M. A., ed., Marcel Dekker, New York, pp 371-421.

Tratnyek, P.G.; Johnson, T. L.; Schattauer, A. (1995) Interfacial phenomena affecting contaminant remediation with zero-valent iron metal. *Emerging technologies in hazardous waste management VII*, Kearney, P. C.; Roberts, T., eds., preprint extended abstract presented before the I&EC Special Symposium, ACS, Atlanta, GA, John Wiley & Sons Ltd., NY. pp. 589-592.

Troxler, W.L. (1998) Thermal desorption. *Pesticide remediation in soils and water*, Kearney, P. C.; Roberts, T., eds., John Wiley & Sons Ltd., NY.

Uhlig, H.H.; Revie, R.W. (1985) *Corrosion and corrosion control: an introduction to corrosion science and engineering*. 3rd ed., A Wiley-Interscience Publication, John Wiley & Sons, New York.

UNEP, ILO (1989) *Aldrin and dieldrin health and safety guide*. WHO, Geneva.

US Department of Energy Grand Junction Office (USDEGJO) (1989) *Permeable reactive barriers*. <http://www.gjo.doe.gov/perm-barr/>. Accessed in August 2004.

US EPA (2000) *chemicalWATCH Factsheet*. <http://www.beyondpesticides.org>. Accessed in August 2004.

Van Veen, J.A.; van Overbeek, L.S.; van Elsas, J.D. (1997) Fates and activity of microorganisms introduced into soil. *Microbiology and Molecular Biology Reviews*, 61, pp. 121-135.

Vereen, D.A.; McCall, J.P.; Butcher, D.J. (2000) Solid phase microextraction for the determination of volatile organics in the foliage of Fraser fir (*Abies fraser*). *Microchemical Journal*, 65, pp. 269-276.

Vidal, A.; Dinya, Z.; Jr, F.M.; Mogyorodi, F. (1999) Photocatalytic degradation of thiocarbamate herbicide active ingredients in water. *Applied Catalysis B: Environmental*, 21, pp. 259-267.

Voelker, B. (1994) *Iron redox cycling in surface waters: effects of humic substances and light*. Doctor of Natural Science Dissertation, Diss. ETH No.10901, Swiss Federal Institute of Technology, Zurich.

Wang, C.-B.; Zhang, W.-X. (1997) Synthesized nanoscale iron particles for rapid and complete dechlorination of TCE and PCBs. *Environmental Science and Technology*, 31 (7), pp. 2154-2156.

Warren, K.D.; Arnold, R.G.; Bishop, T.L.; Lindholm, L.C.; Betterton, E.A. (1995) Kinetics and mechanism of reductive dehalogenation of carbon tetrachloride using zero-valent metals. *Journal of Hazardous Materials*, 41, pp. 217-227.

Weber, J.B. (1994) Properties and behavior of pesticides in soil. *Mechanisms of pesticide movement into groundwater*, Honeycutt, R.C.; Schabacker, D.J., eds., Lewis Publishers, London.

Weber, E.J. (1996) Iron-mediated reductive transformations: investigation of reaction mechanism. *Journal of Environmental Science and Technology*, 30, pp. 716-719.

Wells, C.F.; Salam, M.A. (1968a) The effect of pH on the kinetics of the reaction of iron (II) with hydrogen peroxide in perchlorate media. *Journal of the Chemical Society [section] A: inorganic, physical, theoretical*, 1, pp. 24-29.

Wenzel, W.W.; Adriano, D.C.; Salt, D.; Smith, R. (1999) Phytoremediation: a plant-microbe-based remediation system. *Bioremediation of contaminated soils*, Adriano, D.C. et al., eds., Agron Monogr, vol. 37 Madison WI:ASA, CSSA and SSSA; pp. 457-508.

WHO (1989) *Aldrin and dieldrin health and safety guide*. No 21. World Health Organization, Geneva.

WHO (1988) *Thiocarbamate pesticides: A general introduction*. WHO, Geneva.

WHO (1998) *Diazinon*. World Health Organization, Geneva.

Worthing, C.R.; Hance, R.J. (1991) *The pesticide manual*. 9th ed., Surrey, UK: The British Crop Protection Council, pp. 243-244.

Yabusaki, S.; Cantrell, K.; Sass, B.; Steefel, C. (2001) Multicomponent reactive transport in an in situ zero-valent iron cell. *Environmental Science and Technology*, 35, pp. 1493-1503.

Young, R.; Lopez-Avila, V. (1996) On-line determination of organochlorine pesticides in water by solid-phase microextraction and gas chromatography with electron capture detection. *Journal of High Resolution Chromatography*, 19, May, pp. 247-256.

Zablotowicz, R.M.; Hoagland, R.E.; Locke, M.A. (1998) Biostimulation: enhancement of cometabolic processes to remediate pesticide-contaminated soils. *Pesticide remediation in soils and water*, Kearney, P. C.; Roberts, T., eds., John Wiley & Sons Ltd., NY.

Zečević, S.; Drazic, D.M.; Gojkovic, S. (1989) Oxygen reduction on iron: part III. an analysis of the rotating disk-ring electrode measurements in near neutral solutions. *Journal of the Electrochemical Society*, 265 (1-2), pp. 179-193.

Zečević, S.; Drazic, D.M.; Gojkovic, S. (1991) Oxygen reduction on iron-IV: the reduction of hydrogen peroxide as the intermediate in oxygen reduction reaction in alkaline solutions. *Electrochimica Acta*, 36(1), pp. 5-14.

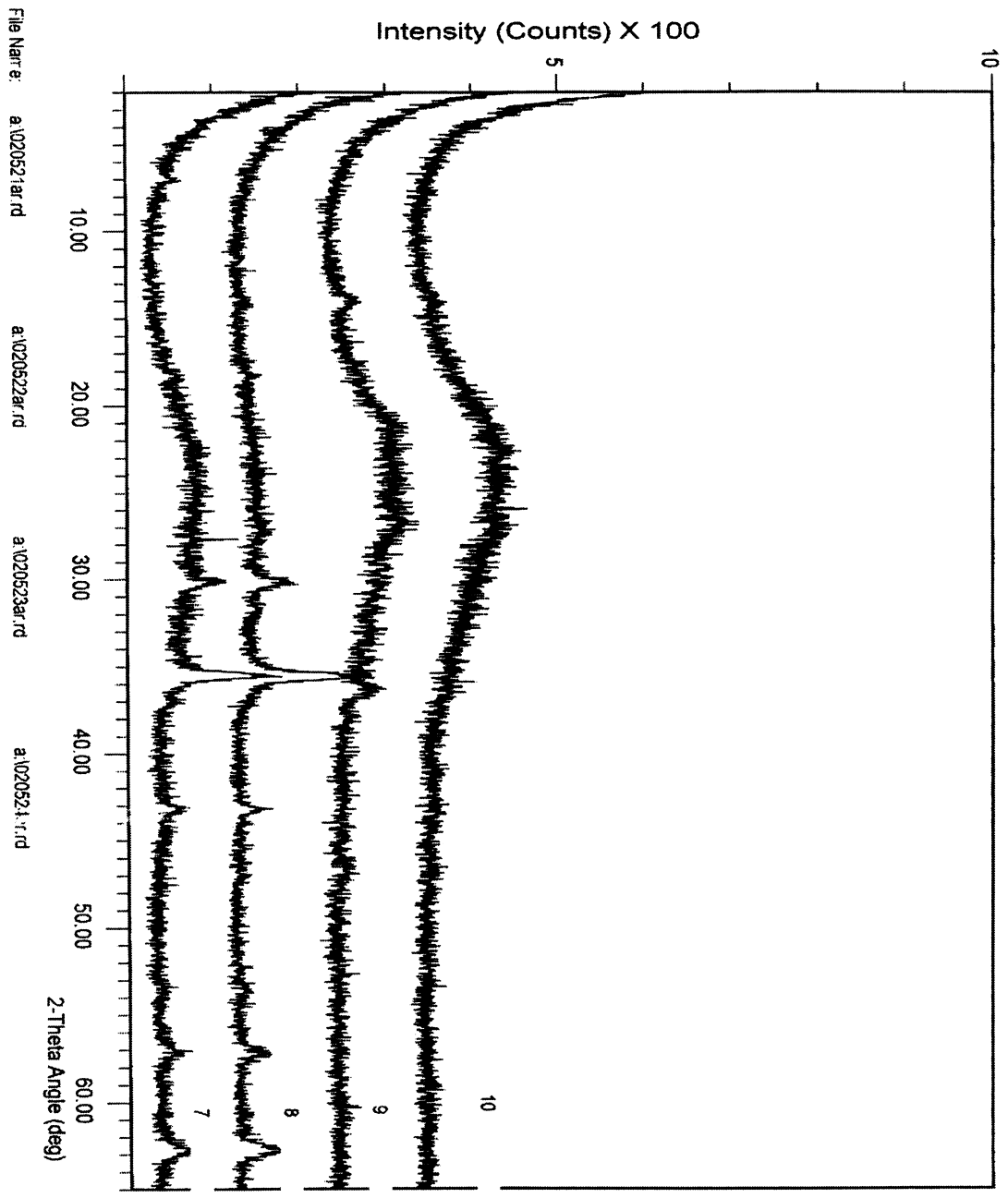
Zhang, W.-X.; Wang, C.-B.; Lien, H.-L. (1998) Treatment of chlorinated organic contaminants with nanoscale bimetallic particles. *Catalysis Today*, 40, pp. 387-395.

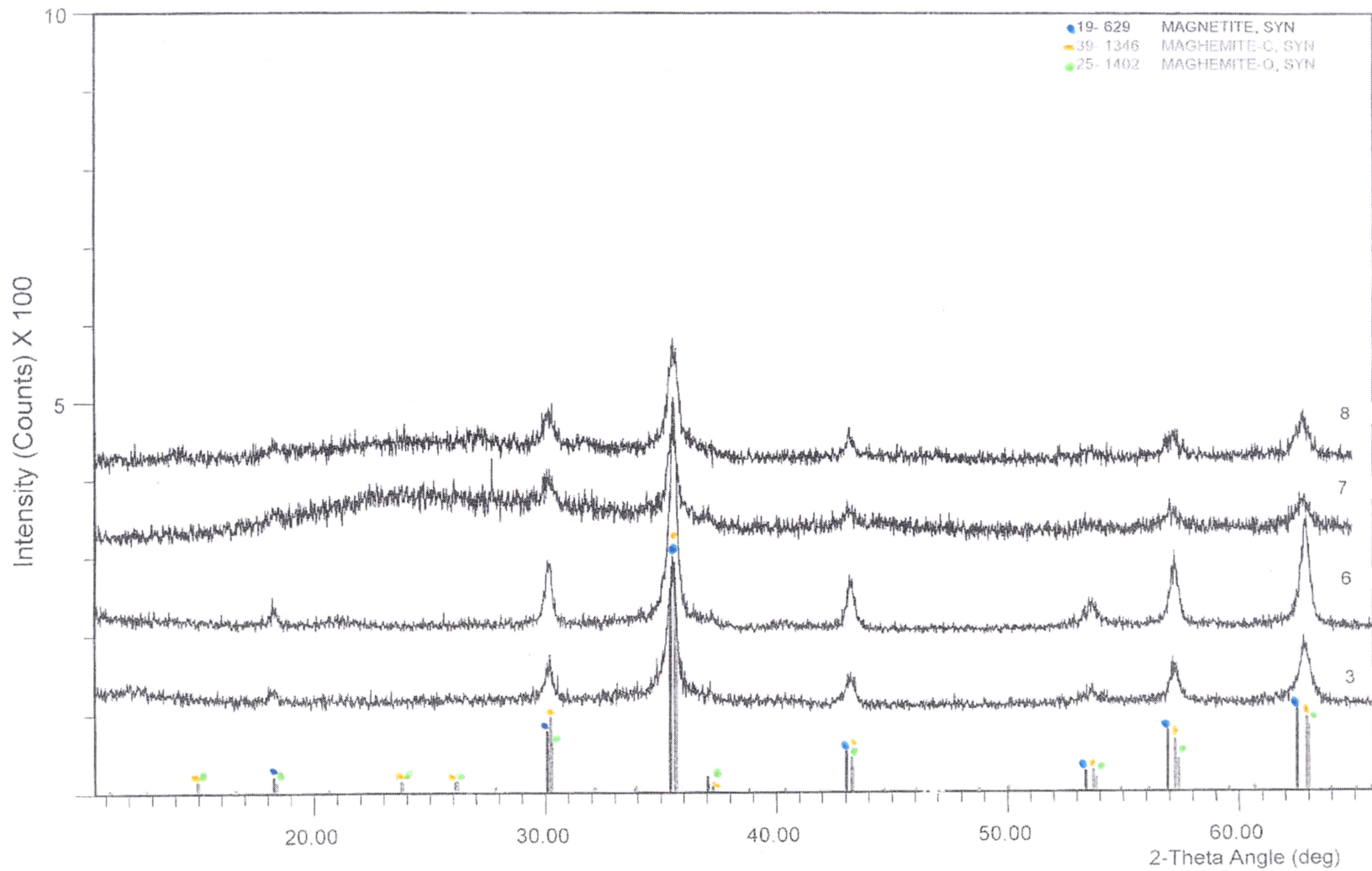
Zhang, W.-X. (2003) Nanoscale iron particles for environmental remediation. *Journal of Nanoparticle Research*, 5, pp. 323-332.

Zhou, X.; Mopper, K. (1990) Determination of photochemically produced hydroxyl radicals in seawater and freshwater. *Marine Chemistry*, 30, pp. 71-88.

Appendix A – XRD analysis of ZVI collected from 4 different samples
(In the presence of molinate).

SAMPLE 7: ZVI (1.79mM) + H₂O₂ (0.33mM) in Milli-Q water
SAMPLE 8: ZVI in Milli-Q water
SAMPLE 9: ZVI in Bicarbonate
SAMPLE 10: ZVI + H₂O₂ in Bicarbonate



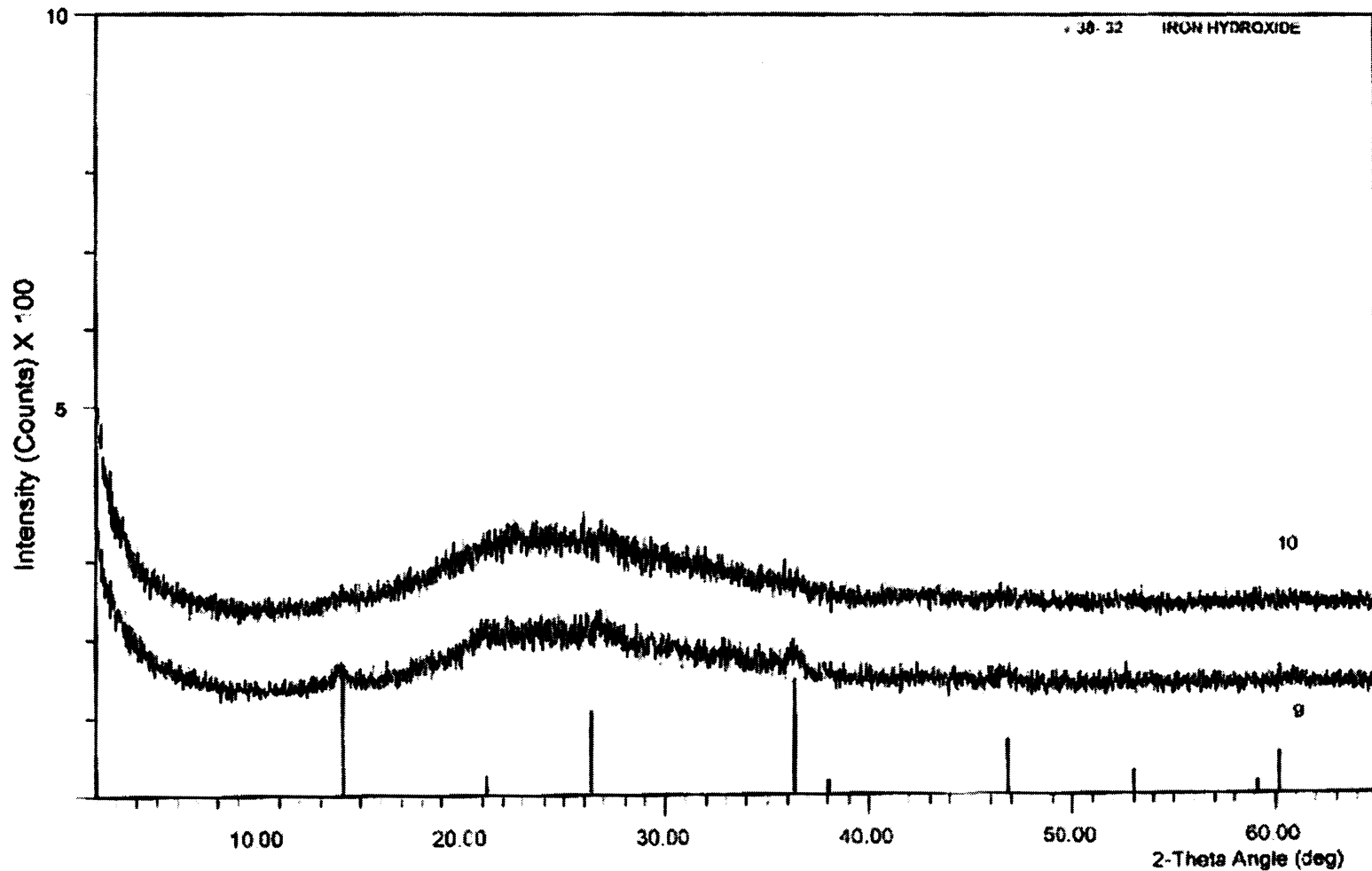


File Name: a:\020508ar.rd

a:\020511ar.rd

a:\020521ar.rd

a:\020521ar.rd

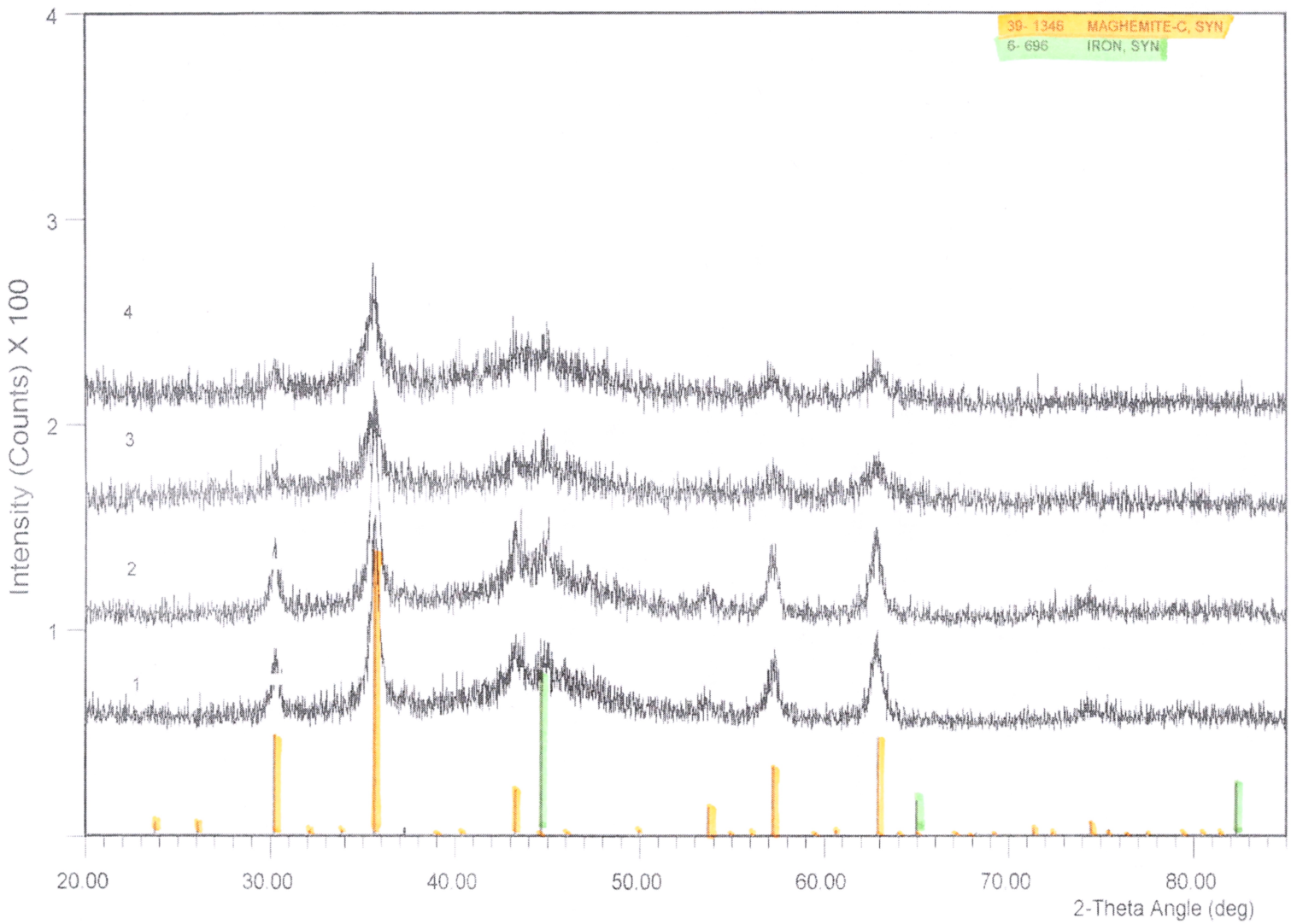


File Name: a\020523a.rd

a\020524a.rd

Appendix B – XRD analysis of ZVI collected from 4 different samples
(In the absence of molinate).

Sample No. 1 - 4



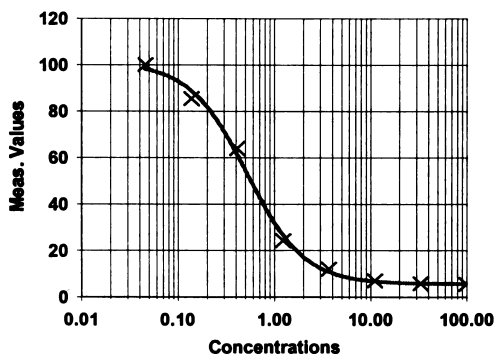
Appendix C – ELISA analysis methodology

Commercial Enzyme-Linked Immuno-Sorbent Assay (ELISA) kits were used for molinate, chlorpyrifos and diazinon analysis. Antibody and enzyme conjugates used for the cyclodiene insecticides and diuron analyses were provided by the Department of Agricultural Chemistry & Soil Science, University of Sydney.

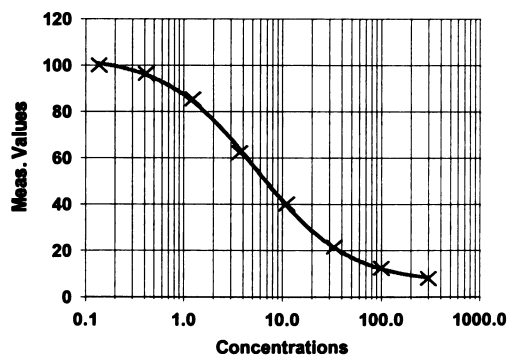
A. Procedures for cyclodiene insecticides (e.g. endosulfan, endosulfan sulfate, aldrin, chlordane, dieldrin, heptachlor) were as follows:

1. Dilute purified antibody stock ($R_{ab} \propto$ ENDO II-KLH, 12.4 mg/mL) to 10 μ g/mL in coating solutions, mix well but avoiding frothing
2. Add 100 μ L to each well and incubate overnight at room temperature
3. Wash three times with washing solution and tap dry on absorbent paper
4. Add 200 μ L of blocking solution (3% skim milk in phosphate buffer saline (PBS)) to each well and incubate for one hour at room temperature
5. Wash three times with washing solution and use immediately
6. Prepare a standard curve

A standard curve is obtained by plotting either % of control absorbance, % of inhibition of antibody binding or absorbance on Y axis in linear scale and the concentration of pesticide on X axis in log scale (Examples are shown below).



a. chlorpyrifos



b. molinate

The % of control absorbance is determined by equation 1. The % inhibition is the reverse of the % of control and calculated as equation 2.

$$\% B/B_0 = \frac{A - A_{blank}}{A_{control} - A_{blank}} \times 100 \quad \text{Eq.1}$$

$$\% \text{ Inhibition} = \left[1 - \frac{A - A_{blank}}{A_{control} - A_{blank}} \right] \times 100 \quad \text{Eq.2}$$

A = absorbance

$A_{CONTROL}$ = absorbance of pesticide at zero concentration

A_{BLANK} = absorbance of blank wells

$A_{CONTROL} - A_{BLANK}$ = absorbance of negative control

(The inhibition values range from 100% (absence of the hapten) to n% (hapten saturated antibodies))

7. Prepare enzyme conjugate (For working stock, add 1 μ L of stock enzyme conjugate (ENDO III-HRP; diuron-HRP) in 500 μ L of 0.2% Bovine Serum Albumin (BSA)-PBS);

8. For working solution, add 88 μ L of working stock to 11 mL of 0.2% BSA-PBS (use this solution in the immunoassay). Enzyme conjugate solution should be prepared freshly each experiment

9. Bring all assay reagents including sample extracts to room temperature before use. Steps 10 and 11 should be performed within 15minutes. Do not expose substrate to direct sunlight pipetting or while incubating in the test wells

10. Add 100 μ L of standards and samples to their respective wells. Add 100 μ L of purified water to control and blank wells

11. Add 100 μ L of enzyme conjugate to each well and thoroughly mix by moving in a circular motion on the benchtop. Incubate plate at room temperature for one hour

12. Wash six times with washing solution. Sit plates for 1-2minutes between each wash. Tap dry on absorbent paper

13. Mix 480 μ L of substrate solution B and 15.52 mL of substrate solution A. Add 150 μ L of substrate mix to each well

14. Incubate plate at room temperature for 30 minutes. Blue color should develop

15. Add 50µL of stop solution to each well and mix thoroughly. This will turn the well contents yellow. Read as soon as possible (within 30 minutes) in a plate reader with a 450 nm filter. (NOTE: Before reading the microplates, ensure that there are no bubbles in any of the wells and no condensation on the bottom of the microplates. If necessary, rupture any bubbles with a clean pipette tip and wipe the bottom of the plate clean with a soft cloth.)

B. Procedures using commercial ELISA kits for the compounds of molinate, chlorpyrifos, diazinon.

B-I. Molinate

A molinate plate kit (EnviroGard™ Test Kit), which was purchased from Strategic Diagnostics Inc., was used for ELISA analysis of molinate. It contained a molinate stock solution (3µg/mL), coated strip microwells, enzyme conjugate, substrate and stop solution (13mL of 1N HCl).

1. Prepare a standard curve
2. Add 200µL of blank and 100µL of negative control (purified water), standards and sample to separate wells
3. Add 100µL of enzyme conjugate to wells (except blank)
4. Mix contents in a circular motion and incubate at room temperature for one hour
5. Empty contents into a sink and wash plate under cool running water five times
6. Add 100µL of substrate using a multi-channel pipette and mix in a circular motion, before incubating at room temperature for 30min
7. Add stop solution of 100µL (1N HCl) using a multi-channel pipette and mix in a circular motion
8. Read developed colour as soon as possible (within 30 minutes) in a plate reader at the absorbance of 650nm - 450 nm

B-2. Chlorpyrifos

The chlorpyrifos plate kit (EnviroGard™ Test Kit), purchased from Strategic Diagnostics Inc., contained a chlorpyrifos stock solution (1µg/mL), coated strip microwells, enzyme conjugate, substrate and stop solution (13mL of 1N HCl).

Analytical procedures are the same as for molinate (B1).

B-3. Diazinon

The diazinon plate kit (EnviroGard™ Test Kit), also purchased from Strategic Diagnostics Inc., contained diazinon stock solution (100ng/mL), coated strip microwells, enzyme conjugate, substrate and stop solution (1N HCl). Analytical procedures are the same as for molinate (B1).

Appendix D – Oven programs for GC/MS analysis of pesticides

ATRAZINE				
Oven Ramp	°C/min	Next, °C	Hold min	Run Time
Initial		50	1	1
Ramp 1	15	150	0.5	8.17
Ramp 2	4	180 (210)	1	16.67 (24.17)
Ramp 3	0			
Post run				16.67 (24.17)
MOLINATE (for quantitative analysis)				
To achieve satisfactory limits of detection of target compounds, the SIM mode was used				
Oven Ramp	°C/min	Next, °C	Hold min	Run Time
Initial		80	1	1
Ramp 1	30	178	3	7.27
Ramp 2	30	250	5	14.67
Ramp 3	0			
Post run				14.67
MOLINATE (for qualitative analysis)				
Oven Ramp	°C/min	Next, °C	Hold min	Run Time
Initial		80	0	0
Ramp 1	5	200	0	24
Ramp 2	5	210	3	29
Ramp 3	20	270	3	35
Post run				35
ENDOSULFAN				
Oven Ramp	°C/min	Next, °C	Hold min	Run Time
Initial		140	1	1
Ramp 1	30	180	0	2.33
Ramp 2	10	250	6	15.33
Ramp 3				
Post run				15.33
CHLORPYRIFOS				
Oven Ramp	°C/min	Next, °C	Hold min	Run Time
Initial		50	1	1
Ramp 1	15	150	0.5	8.17
Ramp 2	4	210	1	24.17
Ramp 3				
Post run				24.17

- Inlet: injection volume - 2µL, inlet front - EPC split-splitless inlet, mode - splitless, gas: He, heater (°C) - 260, pressure (psi) - 10.7 (atrazine, chlorpyrifos), 10.4 (endosulfan, chlorpyrifos), 9.3 (molinate), 12.8 (endosulfan), total flow (mL/min) - 4.5 (atrazine, chlorpyrifos), 4.2 (molinate, endosulfan), purge flow to split vent - 1mL/min@0.9min.

- Washes: Pre-injection - 2 times in sample, 3 times in solvents, 3 times in pumps, post-injection - 4 times in solvents.

- Mode: const flow, He flow - pressure 10.8psi (atrazine, chlorpyrifos), 9.4psi (molinate), 12.8psi (endosulfan), flow - 1.3mL/min (atrazine, chlorpyrifos), 1mL/min (molinate, endosulfan), average velocity - 42cm/sec (atrazine, chlorpyrifos), 37cm/sec (molinate), 38cm/sec (endosulfan), installed column - inventory #, 29.8m × 250µm × 0.25µm calibrated.

- Manufacturer’s specifications: model no. - HP 19091S - 433, 325°C max, HP – 5MS; 5% phenyl methyl siloxane, capillary; 30m × 250µm × 0.25µm nominal, aux, heater - 280 °C, oven configuration - maximum (300°C), equilibrium (0.5min).

Appendix E –

Experimental conditions for pesticides and preliminary screening studies using nanoscale ZVI

Experiments were conducted using two analytical techniques, SPME GC/MS and ELISA. Samples in ELISA methods were analysed without filtration as this enabled confirmation that the agrochemicals were indeed degraded and not removed from solution by adsorption. Control were undertaken to confirm that ELISA tests were unaffected by the presence of the nZVI particles as shown in the following Figure.

Big Wig and its sensitivity to Endo I-HRP(10)

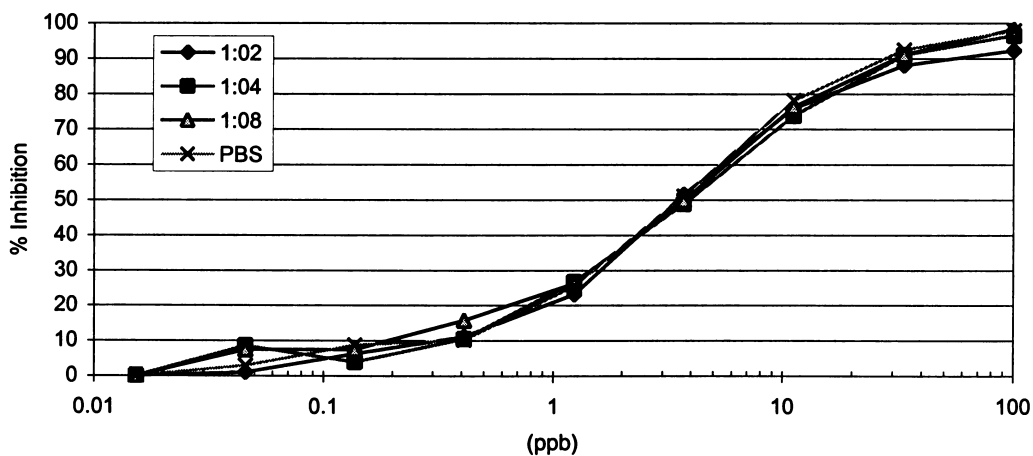


Figure-Appendix D: test of ZVI particles for the inhibition from antibody in ELISA analysis (concentration of ZVI particles: 1.8mM).

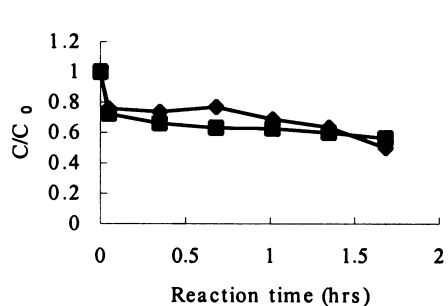
Experimental conditions for pesticides.

Compounds	Analysis	Initial Concentration (µg/L)	ZVI (mM)	Other Conditions	pH
α-, β-Endosulfan	ELISA	10	8.9	O ₂ , NF	6.8
Endosulfan sulfate	ELISA	50 ⁽¹⁾ 10 ⁽²⁾	1 ⁽¹⁾ 8.9 ⁽²⁾	O ₂ , NF ⁽¹⁾ O ₂ , NF ⁽²⁾	4 ⁽¹⁾ 4, 6.8 ⁽²⁾
	GC/MS	50 ⁽¹⁾	1 ⁽¹⁾	N ₂ , F ⁽¹⁾	4 ⁽¹⁾
Aldrin	ELISA	20 ⁽³⁾ 10 ⁽⁴⁾	5.36 ⁽³⁾ 8.9 ⁽⁴⁾	O ₂ , After 3hr NF ⁽³⁾ O ₂ , After 5hr NF ⁽⁴⁾	6.8 ⁽³⁾ 6.8 ⁽⁴⁾
		Dieldrin, Heptachlor, Chlordane	10	8.9	O ₂ , NF
Atrazine	GC/MS	1000	8.9, 35.7	N ₂ , F	6.8
Molinate	ELISA ⁽⁵⁾	10	31.3	O ₂ , NF	-
	GC/MS ⁽⁶⁾	100	10.7	O ₂ , F	-
Chlorpyrifos	ELISA	10	25	O ₂ , NF	-
Diazinon	ELISA	0.1	5.36, 10.7	O ₂ , NF	-
Diuron	ELISA	100	17.9	O ₂ , NF	6.8

(Note that pH 4 was adjusted with 10⁻⁴M HCl while pH 6.8 was adjusted with 0.02M phosphate buffered solution. NF: No Filtering, F: Filtering)

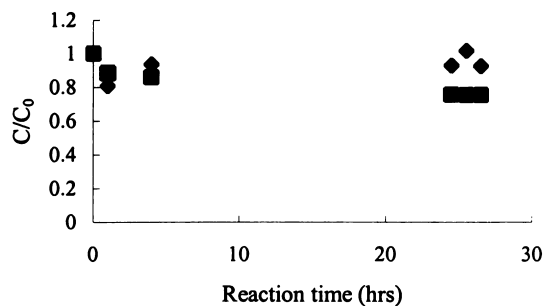
< Results of pesticides >

(1) Endosulfan sulfate



◆ ELISA ■ SPME GC/MS

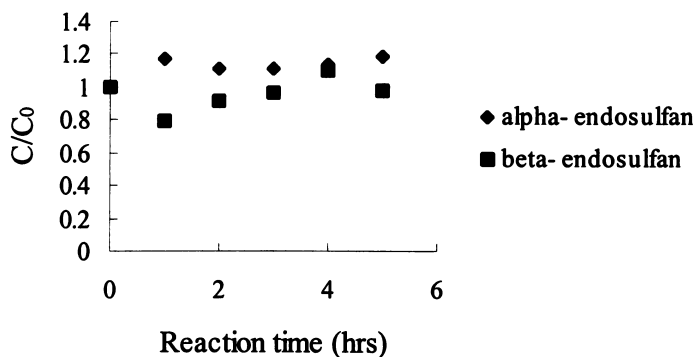
(Exp. Condition 1)



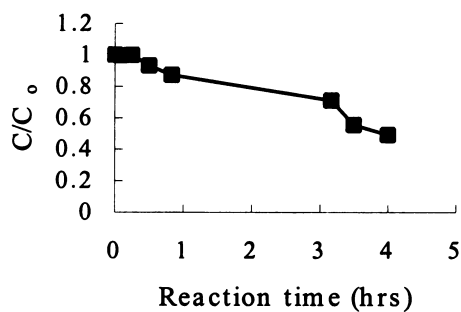
◆ pH 4.0 ■ pH 6.8

(Exp. Condition 2)

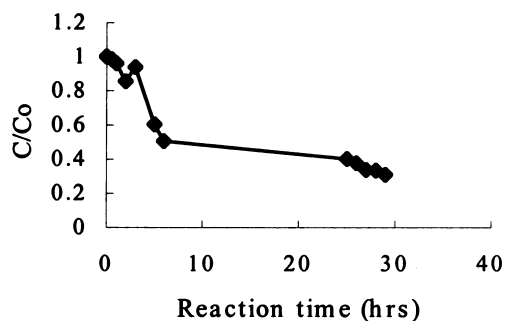
(2) α -, β - Endosulfan



(3) Aldrin

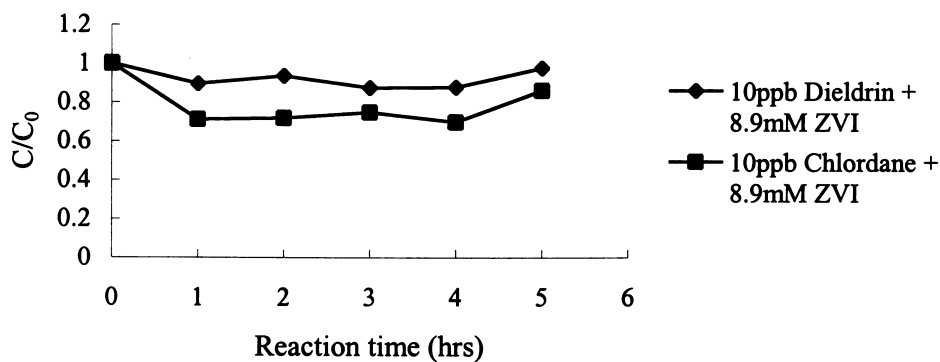


(Exp. Condition 3)

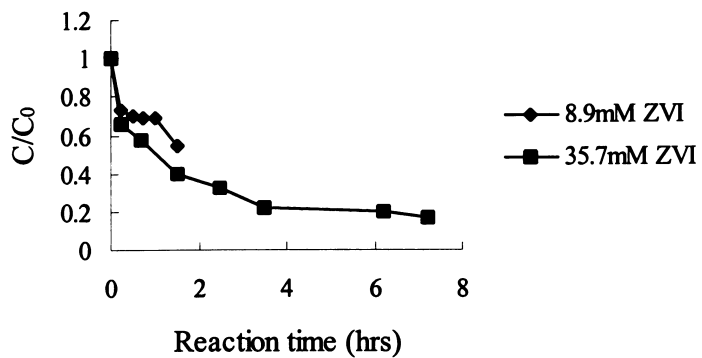


(Exp. Condition 4)

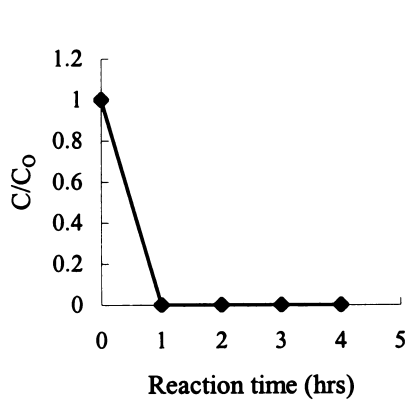
(4) Dieldrin, Chlordane



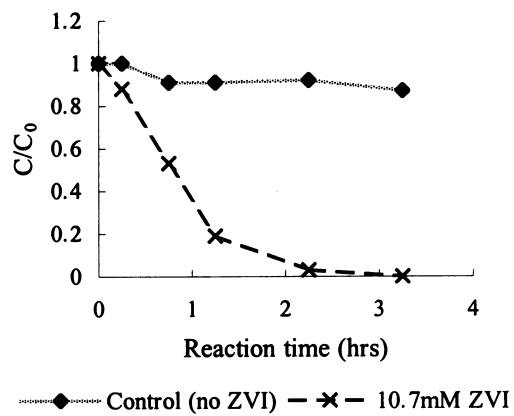
(5) Atrazine



(6) Molinate

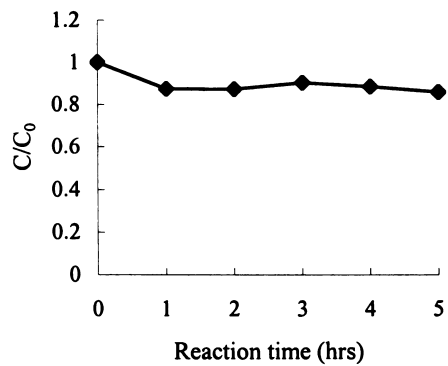


(Exp. Condition 5)

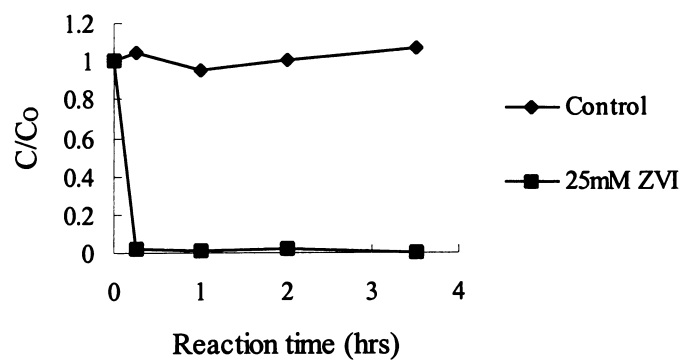


(Exp. Condition 6)

(7) Diuron



(8) Chlorpyrifos



(9) Diazinon

